THE SYNTHESIS AND STRUCTURAL CHARACTERIZATION OF MAIN GROUP AND TRANSITION METAL COMPLEXES SUPPORTED BY NITROGEN BASED LIGANDS

by

LESLIE ANNE LESIKAR

Bachelor of Science, May 2005
Texas Christian University
Fort Worth, Texas

Submitted to the Graduate Faculty of the
College of Science and Engineering
Texas Christian University
in partial fulfillment of the requirements
for the degree of

Doctorate of Philosophy

December, 2008

THE SYNTHESIS AND STRUCTURAL CHARACTERIZATION OF MAIN GROUP AND TRANSITION METAL COMPLEXES SUPPORTED BY NITROGEN BASED LIGANDS

by

Leslie Anne Lesikar

Dissertation approved:

Anne F. Richards

Major Professor

Robert H Neilson

Mary A. Hanner

For the College of Science and Engineering

ACKNOWLEDGEMENTS

To begin, I would like to thank my graduate research advisor Dr. Anne F. Richards for her extensive patience and encouragement. She has truly been an inspirational figure in my life offering a profound knowledge of chemistry that I admire. Her assistance helping me to achieve independent critical thinking involving my research has exceeded my expectations, and I know will guide me to success and help me to become the person I am destined for. I am extremely blessed to have been a part of this research group.

I also want to express my appreciation to the Texas Christian University Chemistry faculty for their never ending support and help. Specifically, I would like to say thank you to Dr. Jean-Luc Montchamp for the advice he always generously offered on my research. Additionally, I would like to thank my fellow graduate students that I have been so fortunate to work with in the Richards group and the department, always available for insightful scientific discussions.

Finally, I would like to thank my family for supporting me throughout my graduate studies. My dad and mom for encouraging me to never give up on my goals and dreams, which has molded me into who I am today and the success I have accomplished with my education. Finally, to my brother who has always been there for me and been a persistent friend outside of my chemistry world.

I would also like to thank TCU–RCAF and the Robert A Welch Foundation for their financial support.

TABLE OF CONTENTS

LIST OF ABBREVIATIONS

Ad	1-Adamantyl
Ar	Aryl
Bn	Benzyl
n-Bu	Butyl
t-Bu	Tertiary Butyl
Cy	Cyclohexyl
DCM	Dichloromethane
Dipp	2,6-diisopropylphenyl
DMF	N,N′-Dimethylformamide
EGEE	Ethylene glycol ethyl ether
Et	Ethyl
Et_2O	Diethyl Ether
EtOH	Ethanol
HMPT	Hexamethylphosphoric triamide
^{i}Pr	isopropyl
IR	Infrared
Me	Methyl
MeOH	Methanol
Mes	$C_6H_2Me_3$-2,4,6
nacnac	β-diketiminato, $[\{N(R^3)C(R^2)\}_2C(R^1)]^-$
NMR	Nuclear Magnetic Resonance
Ph	Phenyl

PySe	Pyridineselenolate, C_5H_4NSe
Pyz	Pyrazine, $C_4H_4N_2$
Pyza	Pyrazinecarboxamide, $C_5H_5N_3O$
rt	Room temperature
THF	Tetrahydrofuran
TMSOTf	Trimethylsilyl trifluoromethanesulfonate
UV	Ultraviolet

LIST OF EQUATIONS

LIST OF FIGURES

LIST OF SCHEMES

LIST OF TABLES

CHAPTER I

Literature Review

1.1 β-Diketiminato Ligands

1.1.1 β-Diketimines, a Useful Bidentate Ligand

Nitrogen based bidentate chelating ligands have captured a significant interest due to their ability to coordinate to a wide variety of elements. The search began for a group of ligands that could offer more accessible tunability in order to replace the widely used cyclopentadienyl ligand class.[1] A variety of ligands have been discovered that meet this criteria including β-diketiminates, chelating nitrogen and oxygen ligands, and amidinates (Figure 1).[2] Since the 1990's, an increasing amount of attention has focused on the bidentate β-diketiminates creating an explosive field. As a result, these ligands, and the related β-diketonato and β-enaminoketonato ligands, have evolved into one of the most versatile ligand families associated with their chelating, monoanionic, and π-conjugated N-donor abilities.[3a] The substituents R^1, R^2, and R^3 typically consist of hydrogen, silyl, alkyl, or aryl groups.

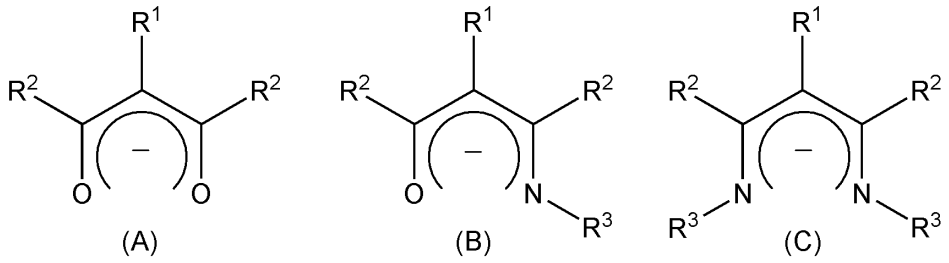

Figure 1. (A) β-Diketonato ligand, (B) β-Enaminoketonato ligand, and (C) β-Diketiminato ligand

Further alterations targeting the carbon backbone of the β-diketimines has offered an additional platform in developing derivatives of the parent ligand, such as 1,3,5-triazapentadienes[3], formazans[3], and 3-sila-β-diketiminato ligands[4] (Figure 2).

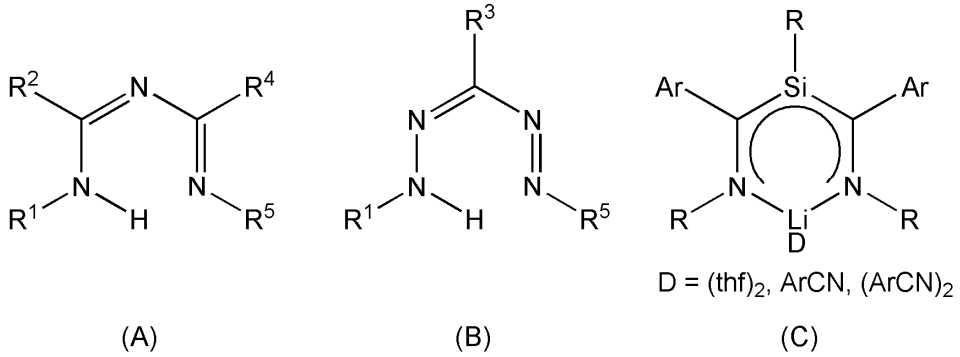

Figure 2. (A) 1,3,5-Triazapentadienes, (B) Formazans, and (C) 3-Sila-β-diketiminato ligands

β-Diketiminato ligands of formula $[\{N(R^3)C(R^2)\}_2C(R^1)]^-$, where most commonly R^3 = aryl, R^2 = Me, R^1 = H, are frequently referred to as nacnac,[2] due to its correspondence with $acac^-$. These ligands have been studied extensively since the mid-1990's forming an array of complexes with transition metals,[5] main group metals,[6] and lanthanides.[7] The β-diketiminato ligands are characterized by their function as N,N'-centered nucleophiles.[4c] Thus, they offer various coordination modes proving to be beneficial for stabilizing metals of low oxidation states.[2,8] Further advantages of the ligand are their facile, high yielding syntheses, ability to crystallize easily and easy manipulation of their R groups allowing for a variation of the steric and electronic properties of the ligand.[8,9] β-Diketiminate complexes have shown pivotal applications in catalytic activity. The metal β-diketiminate systems can undergo a number of catalytic processes due to the formation of coordinated unsaturated complexes as well as other key features.[2] These particular complexes, including those stabilized in unusually low metal oxidation states, cations, and those multiply bonded to metal coligands, have proven to be useful catalysts for olefin polymerization,[2,5d-f,6b-c,10] polymerization of lactide,[2,11]

copolymerization of epoxides and carbon dioxide,[2,12] and enzyme mimics.[2] In addition to their catalytic behavior, β-diketiminate systems offer other applications, including modeling metal active sites in metalloproteins,[5l-m,13] intra- and intermolecular C–H activation reactions, electrophilic activation of the NCCCN γ-C, cross-metathesis involving the imine functionality of the ligand, and C–N bond cleavage of the NCCCN backbone.[14]

Among the copious nacnac complexes synthesized, it has been pivotal in its role of stabilizing metals in low oxidation states. Groundbreaking examples include a dippnacnac gallium(I) carbene analogue,[8k] a cationic germanium complex,[8j] and the first stable monomeric imides of the heavier group 13 elements employing the metal(I) dippnacnac monomers with the azide.[8i] Similarly, Holland and co-workers have used dippnacnac to stabilize low coordinate Fe(I) and Fe(II) complexes where it was observed that lower coordination plays a more significant role in π-donor ability.[8b,8d-e] Recently in 2007, Jones et al. synthesized a stable magnesium(I) dippnacnac complex containing magnesium–magnesium bonds by the reduction of a magnesium(II) iodide nacnac complex with potassium metal.[8l]

1.1.2 Synthesis of β-Diketiminates

Numerous procedures have been reported in the preparation of the β-diketiminate ligand. Among the more predominant methods, the most typical synthesis, and that which is relevant to the current research, occurs by the use of a β-diketone or β-diacetal and offer numerous advantages including good yields, inexpensive materials, and easy to

synthesize reagents.[2] The first synthesis of a β-diketimine ligand from a β-diketone was reported in 1968 (Scheme 1).[15]

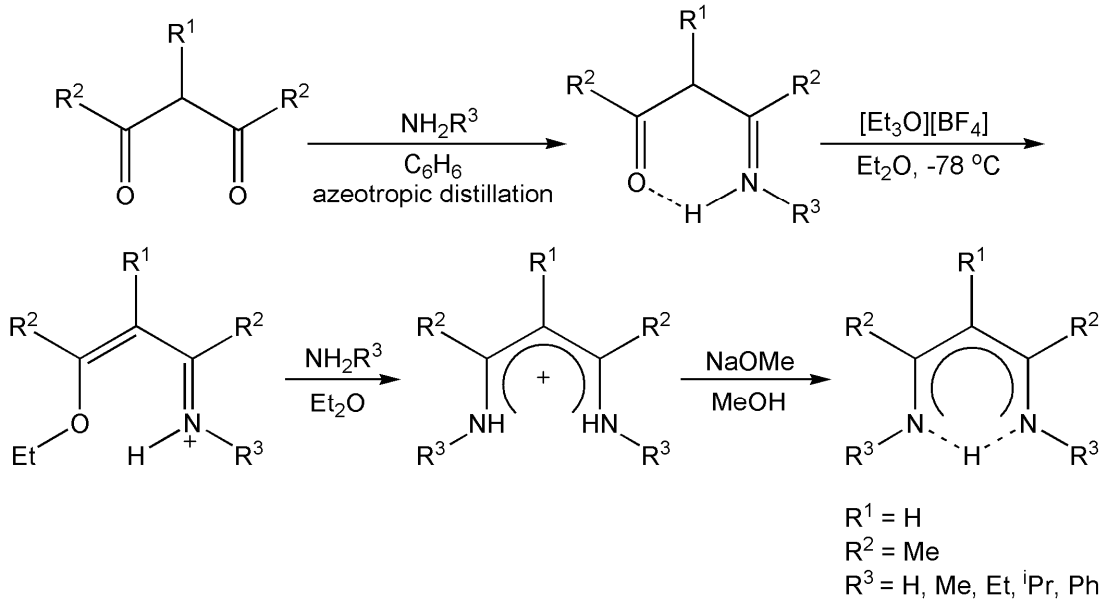

Scheme 1. Preparation of β-diketimine from β-diketone

The β-diketimine can also be prepared by the formation of a ketoketal from the β-diketone, and then continuing to the final ligand (Eq. 1.1).[16] The reaction conditions can further be altered by reacting 2,4-pentanedione in the presence of HCl, ethanol, and aqueous Na_2CO_3 respectively (Eq. 1.2).[10,17] Additionally, 1,1,3,3-tetraethoxypropane, a β-diacetal, is an alternative precursor in the formation of the β-diketimine ligand while under similar conditions as for the 2,4-pentanedione (Eq. 1.3).[12,18]

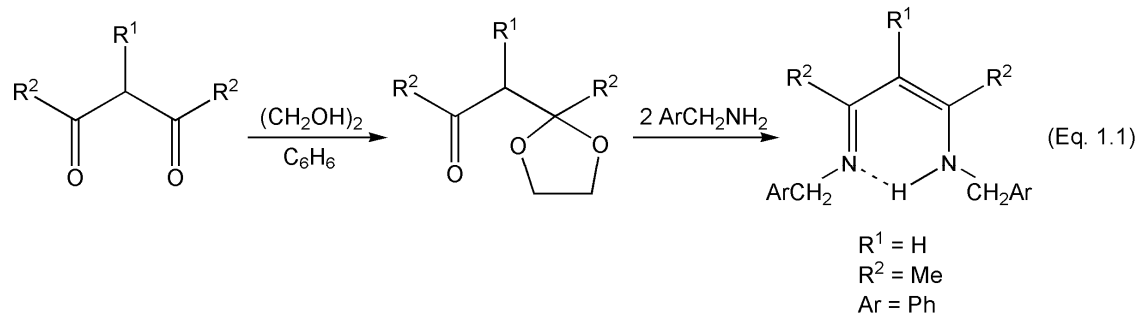

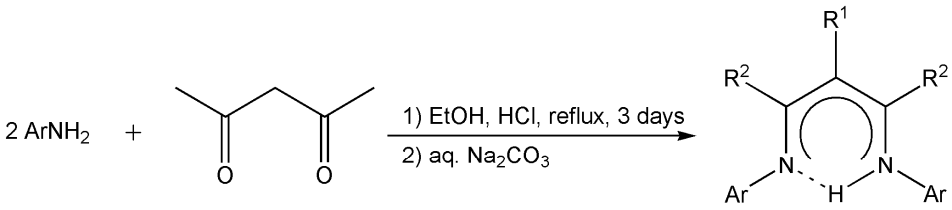

(Eq. 1.2)

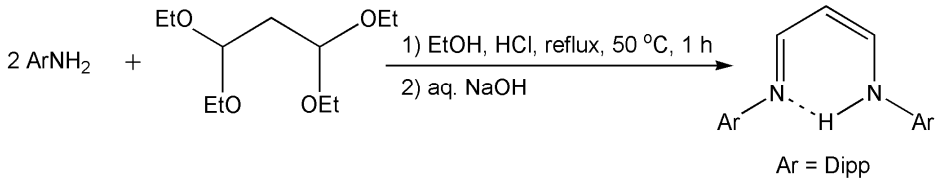

(Eq. 1.3)

1.1.3 Formation of Lithium and Sodium Derivatives

In 1994, the first crystalline alkali metal β-diketiminate, $[Li\{N(R^1)C(R))_2CH\}]_2$ where R = $SiMe_3$ and R^1 = Ph, was characterized and reported.[19] These results, as well as many others since, are synthesized from $LiCHR^1_2$ and the appropriate nitrile RCN (Eq. 1.4). Despite the success of the formerly mentioned lithiation, a majority of lithium β-diketiminates are synthesized from the diketimine and ^{n}BuLi (Eq. 1.5).

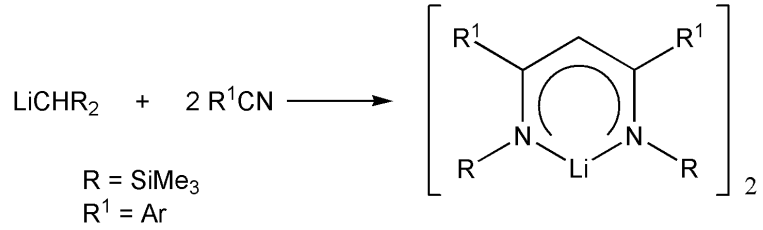

(Eq. 1.4)

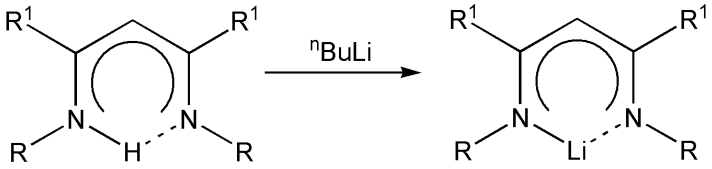

(Eq. 1.5)

Many of the β-diketiminato metal complexes reported have been derived from the alkali metal β-diketiminates.[20] Typically, coordination occurs by means of a base, such as ethers, amines, or nitriles, due to the highly Lewis acidic property of the alkali metal. X-ray analysis has shown that the base-free complexes exist as dimers, oligomers, or polymers and no reports of a solid-state base-free complex in monomeric form have been reported. The alkali metal β-diketiminates are most commonly used as ligand transfer reagents in the presence of a metal halide.[2,17] The resulting side product is the alkali metal halide which can be easily removed from the reaction in order to isolate the metal complex. Reactions utilizing the lithium derivative are more widely used.[2] Yet, it is the sodium and potassium derivatives which offer a more simplistic route due to the heavier alkali metal halide side product which can be removed more easily than the lithium halide.

1.2 β-Enaminoketonato Ligands

1.2.1 β-Ketoiminato Ligands

The β-enaminoketonato ligands (Figure 3) have also attracted much attention due to their similar comparisons to the β-diketiminates and prominent success as catalysts.[21]

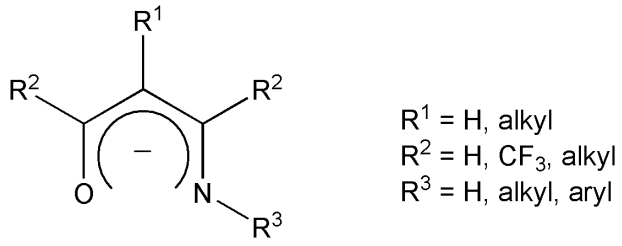

Figure 3. General structure of the β-ketoiminato ligand

Early contributions in 1949 by Cromwell and co-workers, focused on the characterization of β-ketoiminato ligands specifically by infrared spectroscopy.[22] Later in the 1950's, Witkop,[23] Holtzclaw et al.,[24] and Weinstein and Wyman[25] reported a series of α,β-unsaturated-β-ketoamines utilizing infrared spectra in order to characterize these complexes. In the 1960's, Dudek et al. examined the proton resonance on a variety of β-ketoamines.[26] As a result, it can be concluded that the α,β-unsaturated-β-ketoamines can exist as three forms A, B, and C (Figure 4), where it has been observed that the tautomeric equilibrium lies between forms A and B.[24d,26b]

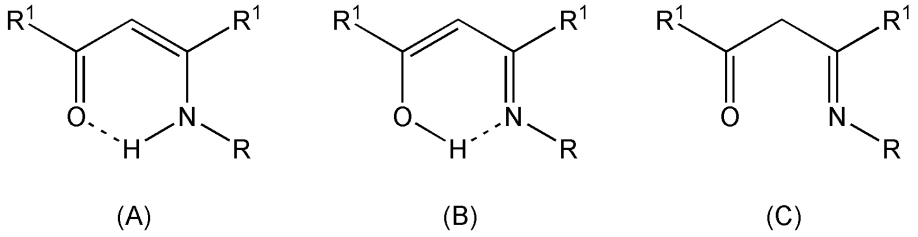

Figure 4. (A) Ketamine form (B) Enimine form (C) Schiff base form

Further investigation continued throughout the 1960's, providing numerous examples of metal complexes of β-ketoamines which were reported and structurally characterized by spectral, proton resonance, and magnetic measurements.[24-27]

1.2.2 Advantages and Applications

The attractive features of the β-ketoiminato ligand family are ease of preparation, high yielding syntheses, and strong coordination ability to metal centers as monovalent and divalent ligands.[21,28] The principal advantage of the ligand lies in the ability to alter steric and electronic properties through manipulation of the R groups attached to the backbone or the nitrogen.[21,29,30] Furthermore, as the substituents attached to the nitrogen

of either β-ketoiminato or β-diketiminato ligands become more bulky, the π-bonding tendencies to the same metal center become stronger as compared to the Schiff-base system.[29,31] As a result, the ketoiminato ligand lies between the Schiff-base ligand and the β-diketiminato ligand in their coordination ability (Scheme 2).[21,28-31]

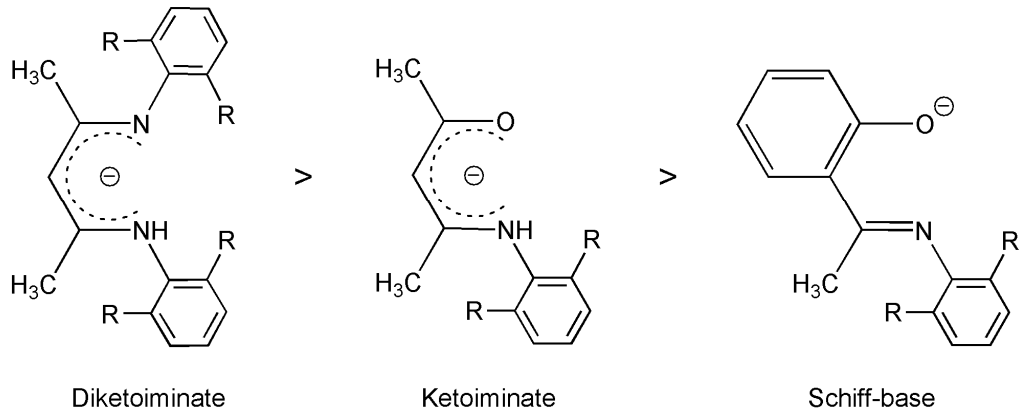

Scheme 2. Order of coordination ability

Due to the unique array of properties, metal β-ketoiminato complexes have been successfully employed in several catalytic cycles,[28-30,32-38] for example reduction of ketones,[30] cyclizations,[30] olefin polymerization,[28-30,32,33] and ring-opening polymerization,[29,34-36] to name a few. In addition to the extensive catalytic behavior that has been observed, metal β-ketoiminate complexes have also become useful precursors for chemical vapor deposition (CVD).[39,40]

1.2.3 Synthesis of β-Ketiminates

A variety of β-ketimine ligands can be prepared due to the availability of altering the R groups attached to the backbone and nitrogen of the ligand. A ligand of specific steric hindrance can be prepared through manipulation of the substituent attached to the

nitrogen from an aryl to an alkyl. Only a select number of procedures have been reported for the preparation of β-ketoiminate ligands that are dependent on the nitrogen substituent attached. The formation of β-ketimines incorporating an aryl group typically follows one of the described methods, or a slight variation of these (Eq. 1.6). The more classic method consists of a condensation reaction of the β-diketone and the corresponding primary amine.[27a,27d,31] A 1:1.5 mole ratio of the β-diketone and primary amine, respectively, is heated for several hours at 100 ^{o}C in the presence of calcium sulfate. The product is then recovered either by vacuum distillation or crystallization. Another method very similar occurs by reacting a 1:1 ratio of the β-diketone and aniline in methanol using a catalytic amount of formic acid.[34] The third method for preparation of the β-ketimine occurs by a toluene solution of a 1:2 mole ratio of the β-diketone and aniline, respectively, in the presence of a catalytic amount of *p*-toluene sulfonic acid hydrate.[30] The reaction is refluxed using a Dean–Stark apparatus for 24 hours and following workup results in the ketiminato ligand.

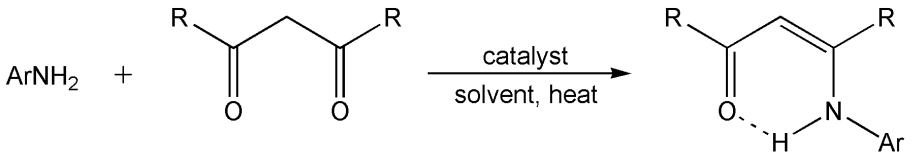

(Eq. 1.6)

On the other hand, it is possible to alter the steric bulk of the ligand by attaching an alkyl group to the nitrogen, which, in 1982, proved to be useful in producing tetradentate non-symmetrical Schiff bases (Scheme 3A).[41] Later in 1987, Costes continued to exemplify the enormous possibilities of the β-ketimine ligand in its ability to form additional acyclic ligands (Scheme 3B-E), macrocyclic, and homo and heterodinuclear nickel complexes.[42] Different synthetic methods had previously been

reported for ligands **B**[43] and **E**[41e] shown in Scheme 3, as well as for ligand **C**[44] which had been prepared *in situ* and used in the formation of nickel complexes.

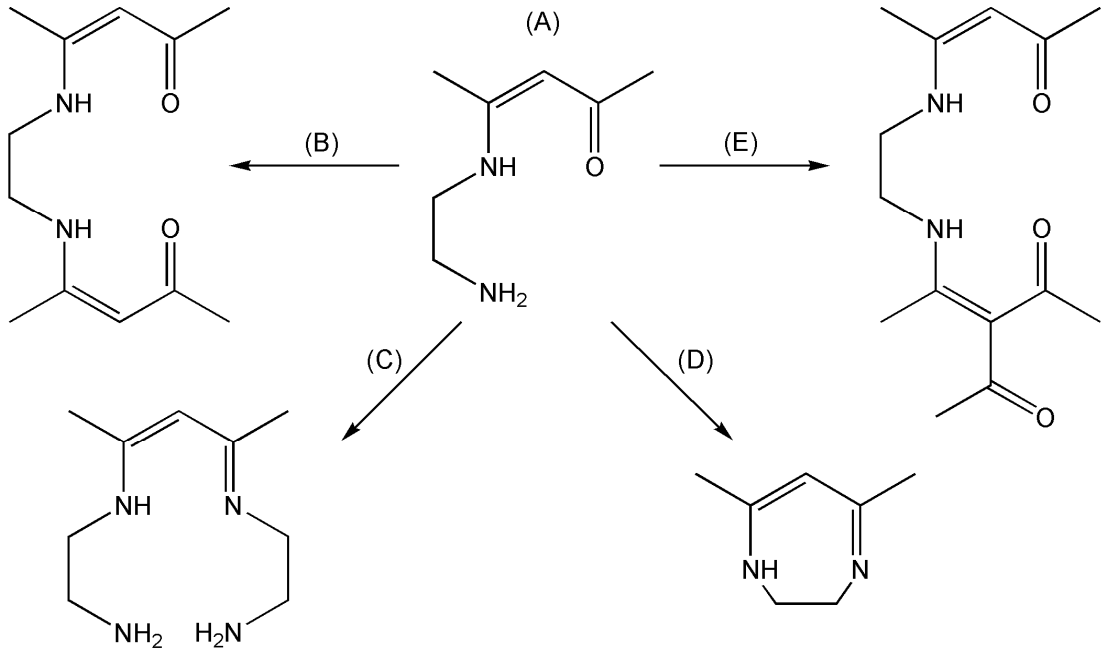

Scheme 3. β-Ketimine ligands containing pendant arm

To further fine tune steric constraints of the ligand, alterations to the steric bulk of the pendant arm can be made, as was exemplified by Roesky and co-workers who reported the synthesis and isolation of a new β-diketiminato ligand (Eq. 1.7).[45] The β-ketiminato ligand, consisting of the same bulky pendant arm, is synthesized as an intermediate and isolated prior to the formation of the final β-diketiminato ligand.

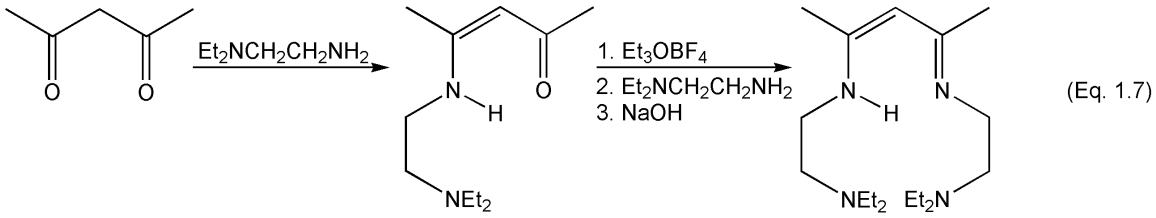

(Eq. 1.7)

Roesky et al. successfully used this β-diketiminato arms ligand for the synthesis and characterization of several lanthanide, transition, and main group metal complexes.[46] The success of the β-diketiminato arms ligand, [RN(H)C(Me)CHC(Me)NR] where R = $C_2H_4NEt_2$, lies in its ability to form solvent-free, monomeric, neutral, nonmetallocene complexes. Since the synthesis of this ligand, a number of similar β-ketiminato and ketoimine ligands incorporating the arm substituent have been reported (Figure 5).[36,39,47-51]

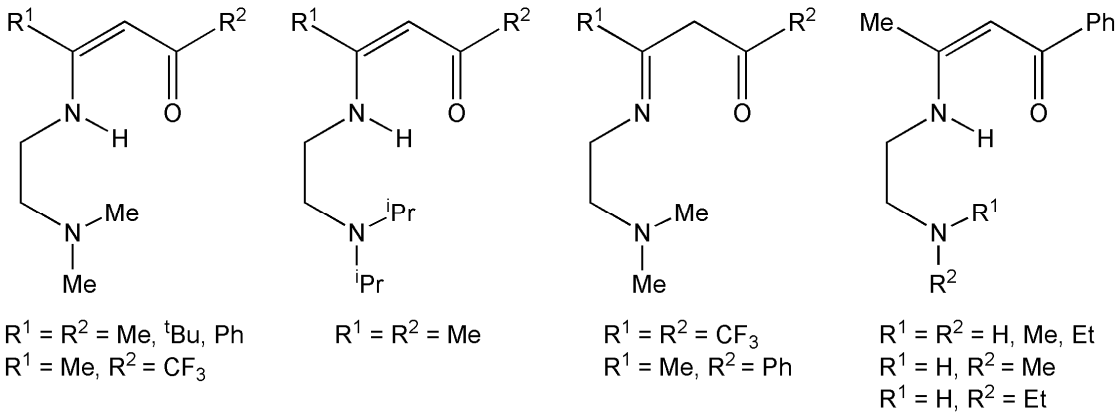

Figure 5. Different examples of β-ketiminato and ketoimine ligands

Several synthetic methods have been used in the preparation of the β-ketiminato arm ligand with only slight variations observed. For example, the condensation reaction between a 1:1 mole ratio of the desired diketone and the corresponding amine is often observed.[47,50,51] The reaction mixture is typically refluxed in methanol for 1.5-3 hours. Another method of synthesis for the β-ketiminato arm ligand involves the reaction of the diketone and the desired amine in a 1:1 mole ratio in toluene with drops of concentrated H_2SO_4.[48] The reaction mixture is then refluxed using a Dean–Stark apparatus for several hours, in order to remove water as an azeotrope, and distilled. A final example for the

synthetic procedure of the arm ligand involves a simple reflux of the diketone and amine for 1 day[36] in EtOH or Et_2O with a slight excess of the aniline.

1.3 Amidine Ligands

1.3.1 Introduction

In 1858, the first amidine was synthesized by reacting N-phenylbenzimidyl chloride with aniline.[52] Since then, the amidine family of ligands has provided a rich collection of complexes from elements across the periodic table.[53] The ligand can exist in its neutral state, $R^1NCR^2N(H)R^3$, as the amidinate anion $[R^1NCR^2NR^3]^-$, or as the cationic amidinium salt (Figure 6).[54]

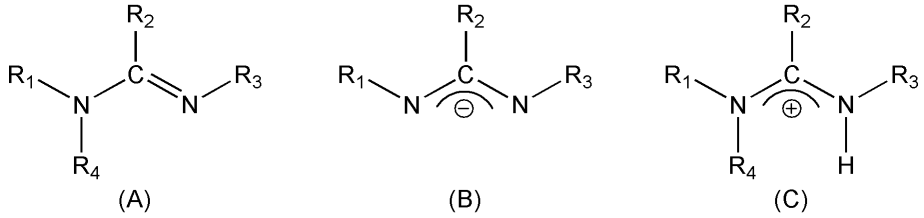

Figure 6. (A) Neutral amidine (B) Amidinate anion (C) Amidinium cation

More specifically, amidines are commonly known as formamidine, when R_2 = H, acetamidine, when $R_2 = CH_3$, butyramidine, when $R_2 = C_4H_9$, and benzamidine, when $R_2 = C_6H_5$ (Figure 7).[53b]

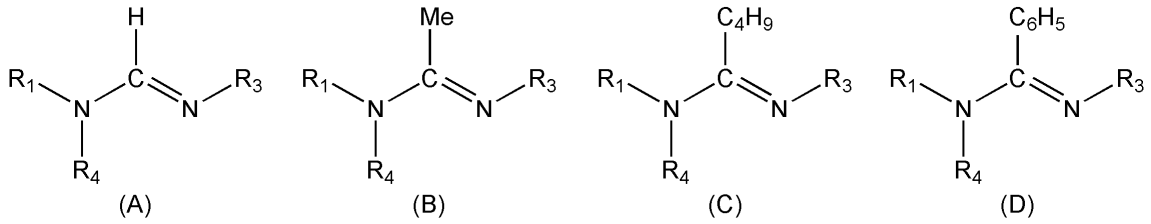

Figure 7. (A) Formamidine (B) Acetamidine (C) Butyramidine (D) Benzamidine

Typically, the anionic amidinate is employed due to its preference to form four membered N,N'-chelated metallocyclic complexes.[55] The ability of the ligand to undergo steric and electronic alterations is readily accomplished upon modifying the substituents attached to the carbon and nitrogen atoms of the backbone.[52,56] It has been shown that the steric demand can be altered depending upon the substituent attached at the nitrogen atoms, ultimately effecting the NMN coordination plane.[56]

Metal amidinate complexes have been discovered to be relatively useful for a variety of catalytic applications including olefin polymerization and organic transformations.[57,58] Aside from the catalytic behavior that has been observed, the amidinate complexes have also become useful precursors for chemical vapor deposition (CVD)[59] and atomic layer deposition (ALD).[60]

1.3.2 Metal Amidinate Coordination Modes and Structural Forms

Eight coordination modes are possible among metal amidinate complexes (Figure 8).[57]

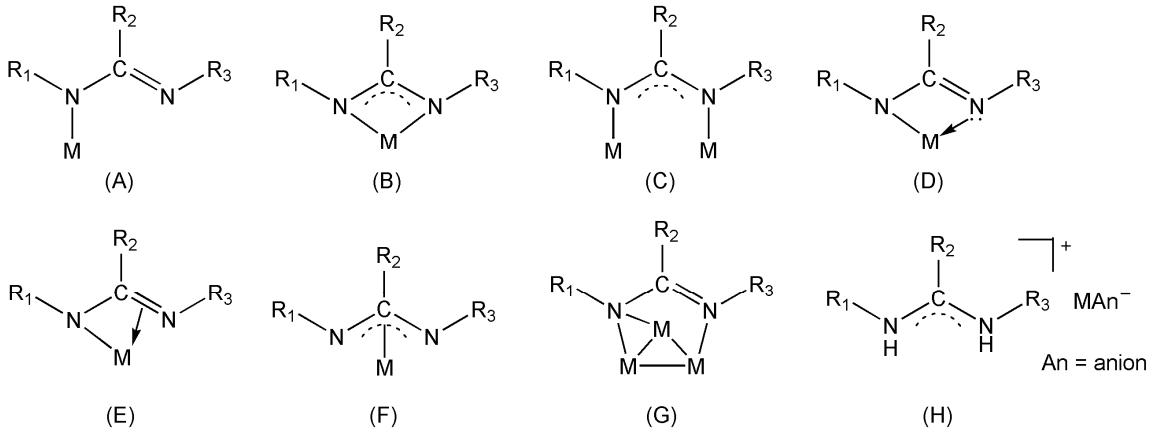

Figure 8. Amidinate coordination modes

Relatively few examples have been reported of the monodentate binding mode (η^1) (Figure 8A).[61] The most common structural types reported include the bidentate chelating (η^2) (Figure 8B) and bimetallic bridging (μ-η^1:η^1) (Figure 8C).[57] The non-symmetrical coordination mode (Figure 8D) is a variation of type B with a discrete M-N σ bond and coordination by the imine nitrogen lone electron pair.[61] Another variation of type B involves coordination occurring from the imino C=N electron donation (Figure 8E). No examples of this structural type have been reported to date. Nagashima and co-workers have reported the only example of the π-bonded (η^3) binding mode (Figure 8F) in a ruthenium amidinate complex.[62] The last two binding modes are fairly uncommon and found only in cluster complexes (Figure 8G) or existing as the protonated amidinate cation with no bonding between the amidinate and the metal atom (Figure 8H).[57]

Different isomeric or tautomeric forms of amidines can exist depending on the substituents present and their position (Scheme 4).[54] Boeré et al. reported different isomers and tautomers of the amidinate by varying steric and electronic properties of the substituents attached to the nitrogens and the carbon.[63,64] Other reports suggest that steric factors also influence specific coordination modes of the ligands to the metal centers.[65]

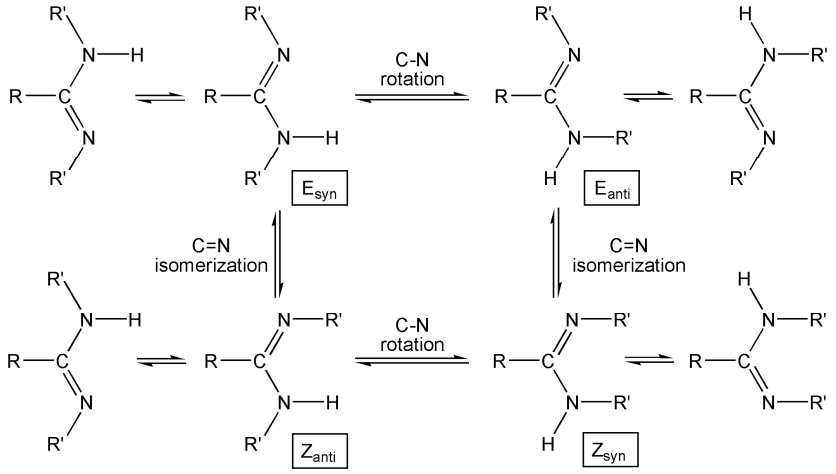

Scheme 4. Amidinate isomeric and tautomeric forms

1.3.3 Synthesis of Amidines

Amidinate complexes can be prepared according to a number of different synthetic routes. One approach involves a silyl migration pathway.[54] In 1973, Sanger reported the synthesis of the first N,N'-disilyated benzamidine compounds by reacting benzonitrile with lithium bis(trimethylsilyl)amide (Eq. 1.8).[65]

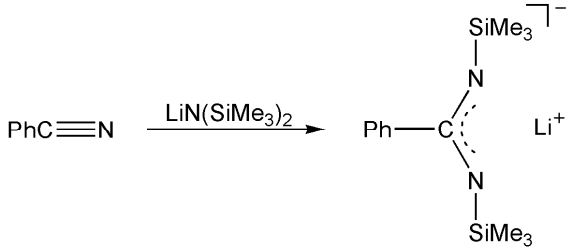

(Eq. 1.8)

Based upon these results, 1,3-bis(trimethylsilyl)amidinate complexes can be prepared by reacting metal bis(trimethylsilyl)amide in the presence of an alkyl or aryl cyanide (Eq. 1.9).[57] The lithium amidinate species produced can be reacted in the presence of a metal halide to give the N,N'-chelated benzamidinate metal complex.[54]

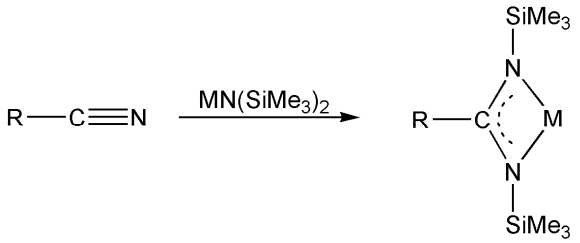

(Eq. 1.9)

A second method of preparation involves the insertion of a metal alkyl into the C=N double bond of a carbodiimide, $R_1N{=}C{=}NR_3$ (Eq. 1.10).[54,57] This route is commonly used due to its high yields and mild conditions.[57]

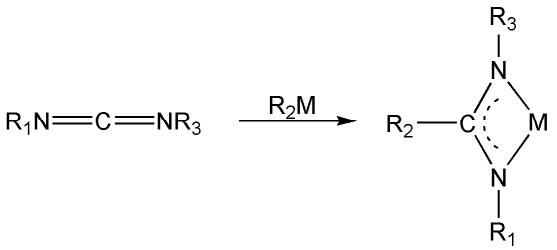

(Eq. 1.10)

More specifically, a direct synthesis can be employed to exclusively prepare and isolate the neutral amidine ligand incorporating an aryl group (Eq. 1.11).[66]

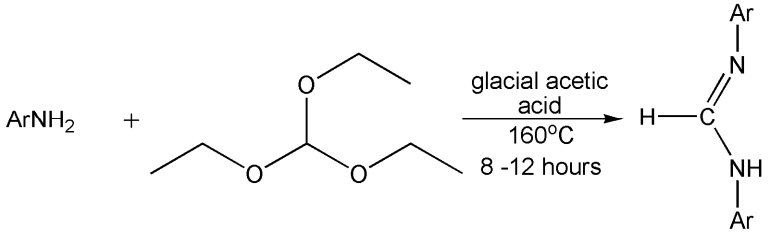

(Eq. 1.11)

Employing the isolated free ligand allows for another synthetic approach involving the deprotonation of the neutral amidine in the reaction with metal alkyl (M–R) or metal amide (M–NR_2) groups (Eq. 1.12).[57]

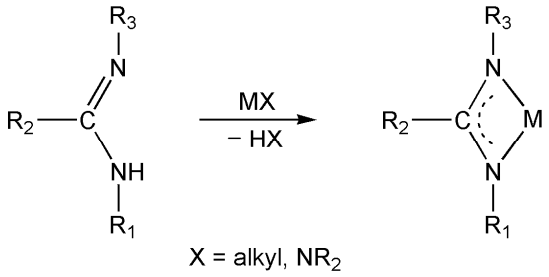

(Eq. 1.12)

Finally, the method used most often entails the metathesis of an anionic amidinate alkali salt with a metal halide (Eq. 1.13).[57]

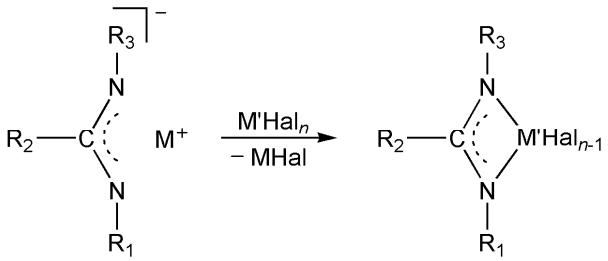

(Eq. 1.13)

1.4 Pyridineselenolate and Pyrazinamide Ligands

1.4.1 Pyridineselenolate

1.4.1.1 Introduction

Extensive studies have focused on organoselenium compounds due to their efficacy in organic synthesis.[67] The majority of chalcogenolate chemistry incorporates very bulky organic ligands, which are used to prevent the formation of polymeric structures as well as neutral donor coordination, and thus augment the compounds' solubility and volatility.[68] On the other hand, anionic or neutral bifunctional chalcogenolate ligands that incorporate both selenium and nitrogen donors are lacking.[67c] One such ligand, the pyridineselenolates, can exist as three different forms: pyridineselenol (A), selenobispyridine (B), or dipyridyl diselenide (C), (Figure 9) each consisting of varied isomers. For purposes related to the current research, 2-selenopyridines are shown.

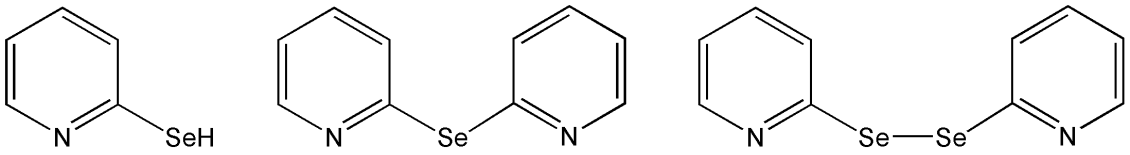

(A) (B) (C)

Figure 9. (A) Pyridine-2-selenol (B) 2,2'-Selenobispyridine (C) 2,2'-Dipyridyl Diselenide

Although pyridineselenolate ligands have been known since the early 1960's,[69] their coordination chemistry remained unexplored until the mid 1990's.[70-74] Since then, several other examples of transition,[75-83] main group,[83-85] and lanthanide[86] metal complexes have been reported. Interest for further investigating these ligands lies in the

competitive coordination behavior that exists between the nitrogen and selenium present as hard and soft Lewis bases, respectively.[69,70] Additionally, pyridine selenolates (PySeH) are not very stable as a monomeric species which is governed by resonance contributions that play a role in stability of the metal pyridineselenolate complexes, $M(SePy)_x$.[68,74] Complexes can exist as metal-chalcogenolate compounds with attached pyridine donors, or as a metal amido complex with a C=Se functional group.

Pyridine-2-selenolate complexes, with an appropriate metal center, are potential precursors for the synthesis of thin metal selenide layers[85] and the low temperature production of semi-conducting materials.[68,70,74,76] Specifically, the formation of chalcogenide complexes with metals such as tin and lead yields the formation of narrow-band gap semiconductors, with applications ranging from sensor and laser materials, thin film polarizers, and thermoelectric cooling materials.[68] Likewise, pyridinechalcogenolate compounds are potential precursors for chemical vapor deposition (CVD).[74] Pyridineselenolate complexes, with metals such as platinum, can also have medicinal applications such as cytostatic drugs.[70]

1.4.1.2 Synthesis of Pyridineselenolates

A number of procedures have been reported for the preparation of pyridineselenolates. In 1962, Mautner and co-workers reported the synthesis of 2-selenopyridine and 2,2'-dipyridyl diselenide.[69a] The 2-selenopyridine was prepared by refluxing hydrogen selenide and 2-bromopyridine in ethylene glycol monoethyl ether for 19 hours (Eq. 1.14).

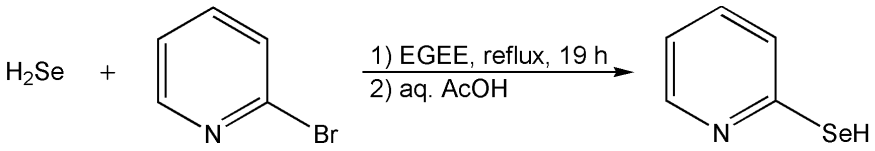

(Eq. 1.14)

After workup, the desired product formed as yellow needles in 61% yield as the monomer. However, during recrystallization in benzene, it was found that 2-selenopyridine existed as the dimmer, 2,2'-dipyridyl diselenide. The 2,2'-dipyridyl diselenide ligand was also obtained, by reacting an aqueous solution of 2-selenopyridine with 30% hydrogen peroxide, in 75% yield. However, further attempts to reproduce these ligands following the described methods[69a,87] proved to be unsuccessful. As a result, variations to the preparations were investigated. In 1984, Toshimitsu et al. synthesized 2,2'-dipyridyl diselenide by refluxing sodium hydrogen selenide, as prepared by the method of Klayman and Griffin,[88] and 2-bromopyridine in ethanol for 96 hours, after which oxygen gas was bubbled through the reaction. Following an aqueous/CH_2Cl_2 workup, the product was obtained by column chromatography in 83% yield (Eq. 1.15).[89]

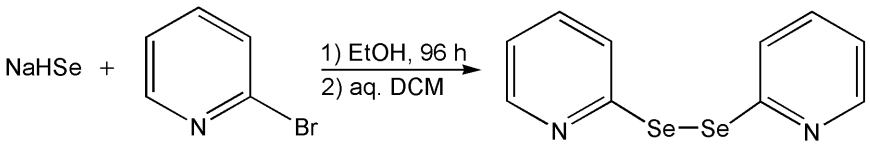

(Eq. 1.15)

In 1988, Syper and Mlochowski synthesized 2,2'-selenobispyridine and 2,2'-dipyridyl diselenide by reacting 2-bromopyridine with lithium diselenide in the presence of hexamethylphosphoric triamide (Eq. 1.16).[90] In conjunction with the long reaction time and low yield of the desired product, the 2,2'-selenobispyridine formed only as a minor side product.

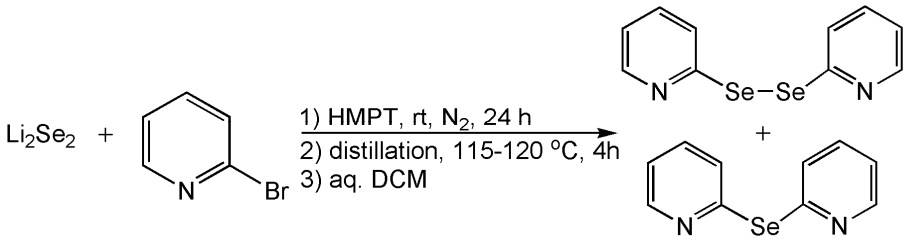

(Eq. 1.16)

The 2,2'-selenodipyridine ligand was first prepared by Grant and Summers in 1978 by a condensation reaction of 2-selenopyridine and 2-bromopyridine (Eq. 1.17). The product was isolated as a yellow oil in 80% yield.[91] Prior to Syper and Mlochowski isolating the ligand as a minor side product, 2,2'-selenodipyridine has only been obtained one other time, similarly as a by-product in 20% yield.[92]

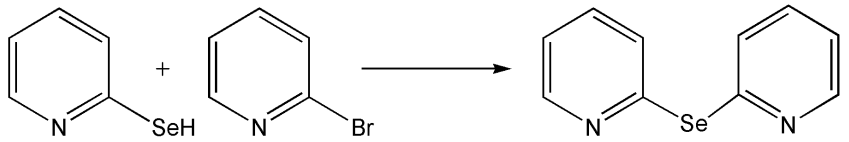

(Eq. 1.17)

In 1994, Brennan et al. reported the synthesis, similar to Toshimitsu et al., of pyridine-2-selenol by reacting sodium hydrogen selenide,[88] ammonium chloride, and 2-bromopyridine in DMF at 85 °C for 15 hours.[72] Following an aqueous/methanolic workup, yellow crystals were obtained in 56% yield (Eq. 1.18).

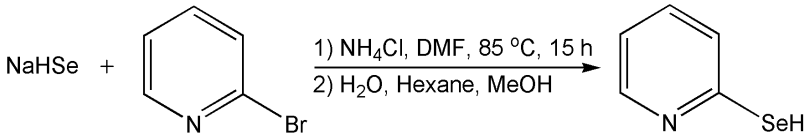

(Eq. 1.18)

Following these reports, a variety of similar methods for the preparation of pyridine-2-selenol,[70,93] 2,2'-selenobispyridine,[93-95] and 2,2'-dipyridyl diselenide[70,96-98] have been reported. Among the synthetic methods discussed, the most ubiquitous pathway involves a metathesis reaction between the alkali-metal selenide and the halopyridine.[93] One example different from the standard procedure involves the reaction of elemental selenium with lithiopyridines at -78 °C to produce 2,2'-dipyridyl

diselenide.[97] This reaction is advantageous over existing metathesis methods as the reaction time is a short 2 hours compared to 15-96 hours, as well as eluding the evolution of toxic hydrogen selenide gas. A second methodology involves a bromine-magnesium exchange reaction.[93] Here the reaction occurs between 2-bromopyridine, or various methyl substituted 2-bromopyridines, and isopropylmagnesium chloride in a 1:1 stoichiometric amount. Addition of elemental selenium and an additional equivalent of either 2-bromopyridine or alkylhalide lead to the desired products in good yield (Scheme 5).

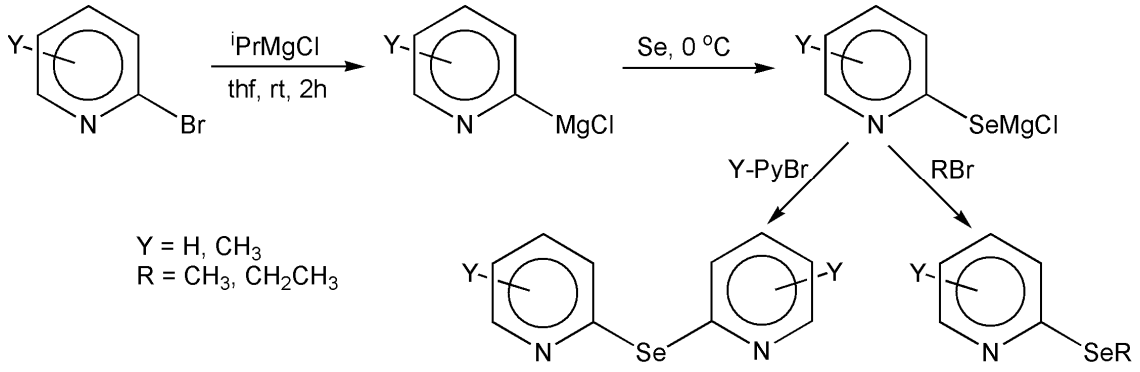

Scheme 5. Synthesis of pyridineselenolates via bromine-magnesium exchange

1.4.1.3 Metal Pyridineselenolate Binding Modes

Each of the three structural forms of 2-selenopyridines (Figure 9) contains multiple ways of binding to metal centers. The most complex system, and therefore the system with the greatest variety of coordination modes, is 2,2'-dipyridyl diselenide. The coordination possibilities increase as a result of two pairs of nitrogen (hard) and selenium (soft) donors present (Scheme 6).[70] Additionally, 2,2'-dipyridyl diselenide has the potential to cleave in reactions as the Se–Se bond is fairly weak, therefore acting as a reactive source of PySe.

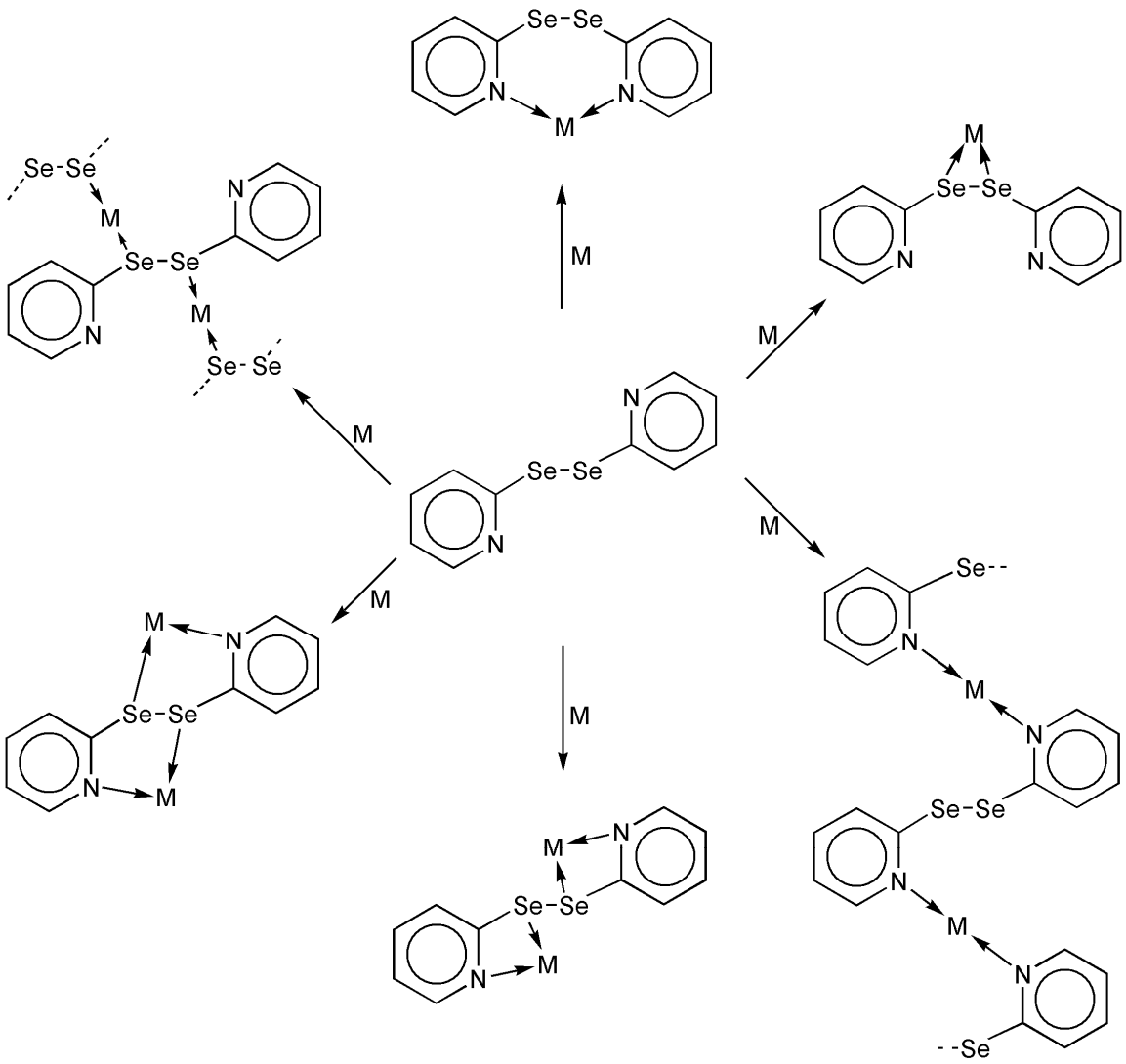

Scheme 6. Possible coordination modes of 2,2'-dipyridyl diselenide

1.4.2 Pyrazinamide

1.4.2.1 Introduction

The pyrazine ligand has been known since the late 1870's.[99] The basic parent ligand consists of an aromatic ring, similar to benzene, with nitrogen atoms in a para oriented position.[100] A significant interest of pyrazines is due to their prevalent occurrence in nature including insects, terrestrial vertebrates, plants, and food sources.

Related pyrazine analogs include pyrimidine and pyridazine, where the nitrogen atoms are in the 1 and 3 or 1 and 2 positions, respectively (Figure 10).

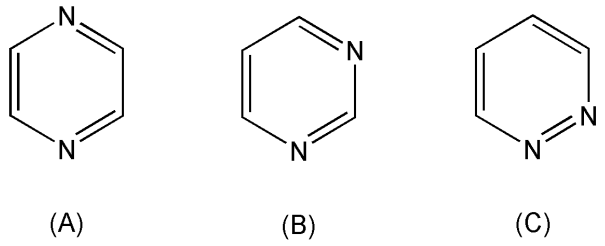

Figure 10. (A) Pyrazine (B) Pyrimidine (C) Pyridazine

Pyrazines and substituted pyrazines typically act as multidentate ligands that can bridge metal ions in a linear fashion, thus producing oligomeric and polymeric metal complexes affording unique structures such as infinite-chain, pleated-sheet, double or triple interpenetrating frameworks, and interwoven honeycomb like designs.[101] Pyrazines can consist of one to four substituents attached on the aromatic ring. Specifically, pyrazinecarboxamide consists of one amide group attached ortho to one of the nitrogen atoms (Figure 11). Interest focusing on the pyrazinecarboxamide resides in the desire to synthesize five membered chelate compounds by means of one of the nitrogen atoms of the ring and either the oxygen or the nitrogen atom of the amide group.[102]

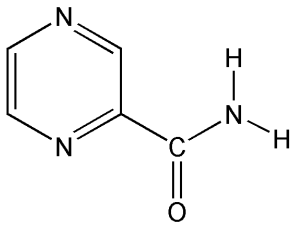

Figure 11. Pyrazinecarboxamide ligand

The pyrazinecarboxamide ligand has been a key drug in the treatment of tuberculosis for about fifty years.[103-105] However, the ligand system applied as a drug is known to have various side effects including hepatic damage, uric acid retention, gastrointestinal disturbances, and joint pains.[104] In order to overcome these side effects, numerous studies have focused on the synthesis of pyrazinamide metal complexes which offer antimicrobial properties.[105] Due to the substituted ligands' ability to form inorganic polymers, the metal complexes formed are also potential precursors for solid-state electro-optical systems, primarily found in sensors and detectors.[106] The applications of the ligand system range farther proving useful in catalysis, such as polymerization of ethylene and photochemistry processes.[107-109]

1.4.2.2 Synthesis of Pyrazinecarboxamides

The syntheses of pyrazines[99] and substituted pyrazines,[110] such as the pyrazinecarboxamide, have been reported since as early as 1876. However, the ease of synthesis of these ligands has resulted in a range of commercially available derivatives that are relatively inexpensive.

1.4.2.3 Metal Pyrazinecarboxamide Binding Modes

Pyrazinecarboxamide is a multidentate ligand which incorporates a variety of binding modes, arising from four coordination sites, two nitrogen atoms in the aromatic ring, as well as the oxygen and nitrogen atom of the amide group (Scheme 7).[102,103,106,111]

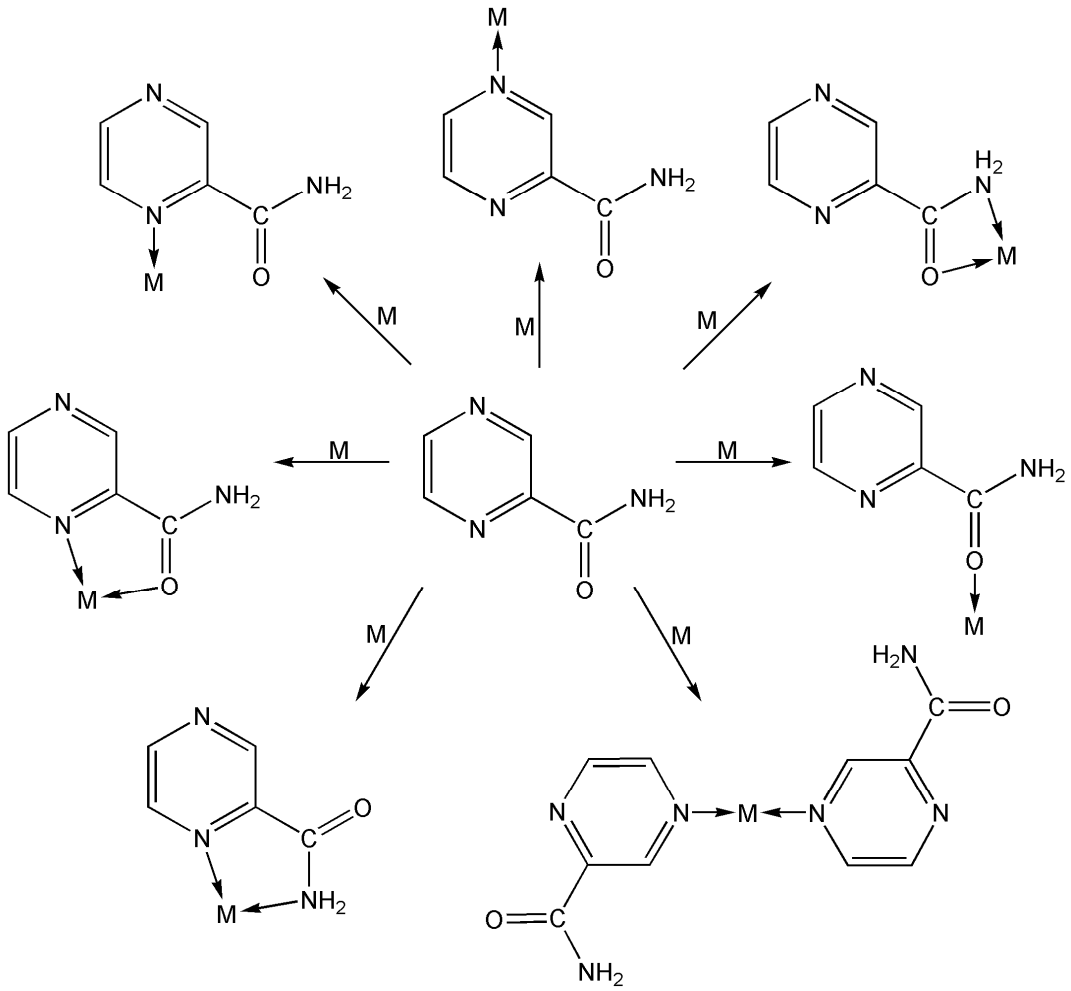

Scheme 7. Examples of pyrazinecarboxamide binding modes

CHAPTER II

Synthesis and Characterization of β-Diketiminato Complexes Containing Sb(III) and As(III) Halides

2.1 Introduction

β-Diketiminato complexes have been reported for virtually every group within the periodic table. However, until recently group 15 and 16 were lagging, if not absent, in results.

Previous attempts to react group 15 precursors with nacnac resulted in a variety of unique results. In 2001, Igua and Majoral reported a novel N-phosphino-β-diketiminate ligand where phosphorus moieties were attached to the imino nitrogen atoms (Figure 12A).[112] In the same year, Scheer and Schiffer reported a complex of a phosphorus diketiminate heterocycle (Figure 12B)[113] which, until recently, was the only example of an N,N'-chelated phosphorus compound.

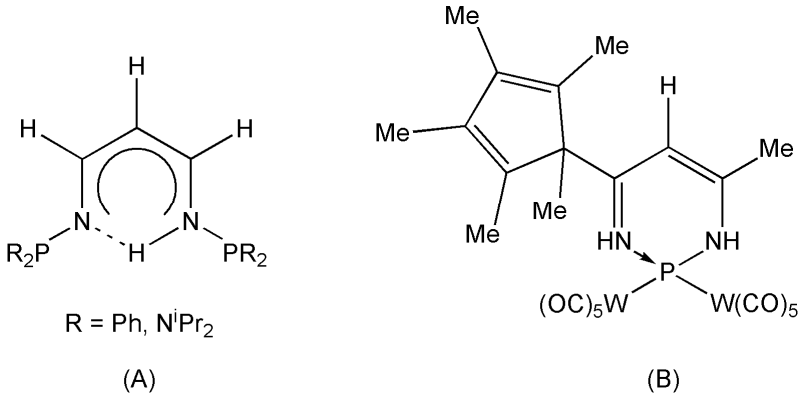

Figure 12. (A) N-phosphino-β-diketiminate ligand (B) Phosphorus diketiminate heterocycle

Almost simultaneously the research groups of Burford[114] and Lappert[115] revealed that the electron rich group 15 β-diketiminato complexes preferred to react at the γ-carbon rather than the usual N,N'-chelation.[114,115] Burford showed that upon treatment of the β-diketimine with ^{n}BuLi and Ph_2PCl, the phosphine preferentially coordinates at the γ-position (Figure 13A).[114a] The reaction of the γ-phosphino-β-diketiminate complex with

ECl_3 (E = As, Sb) resulted in a cyclization reaction with the group 15 metal rather than N,N'-chelation (Figure 13C).[114a-b] Additionally, Lappert showed similar results undergoing the same reaction but with $PhPCl_2$ (Figure 13B).[115] Furthermore, after dechlorination of the γ-phosphino-β-diketiminate complex, cyclization occurred and a heterocycle formed (Figure 13D). The ensuing γ-phosphino-β-diketiminate complexes were proposed to form as a result of the very bulky Dipp substituent and the incompatible bite angle of the 6 membered β-diketiminate ring.[114a] These results have thus prompted further investigation into the pnictogen elements in order to isolate N,N'-chelated β-diketiminate complexes from these electron rich elements.

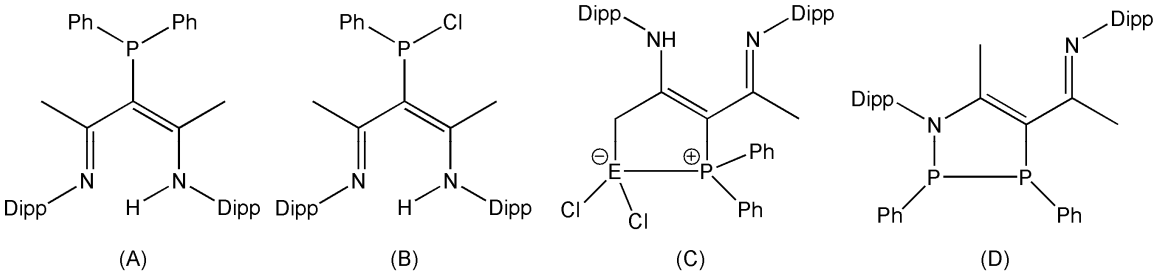

Figure 13. (A) Burford's γ-phosphino-β-diketiminate (B) Lappert's γ-phosphino-β-diketiminate (C) Burford's group 15 heterocycle (D) Lappert's heterocycle

As for the remaining pnictogen elements, there are no reports of β-diketiminato complexes containing antimony and arsenic. Twamley and Power reported a dihydridoaluminum nacnac complex formed from an *in situ* reaction of $DippnacnacBiCl_2$ and $LiAlH_4$ in diethyl ether (Eq 2.1).[116]

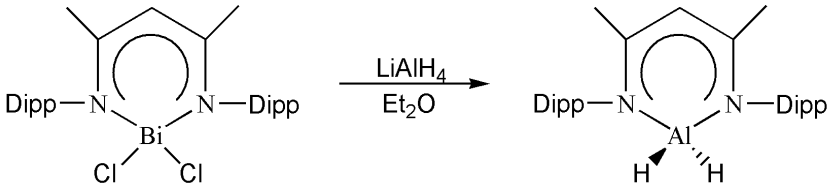

(Eq. 2.1)

In this chapter, we report the synthesis of antimony(III) and arsenic(III) β-diketiminato complexes and the investigation into further reactivity and chemistry of these compounds as precursors for organometallic syntheses. Exploration of these pnictogen compounds were desirable since examples of low valent antimony complexes are less common than their phosphorus counterparts, thus preventing structural comparisons to related main group structures.[117] Furthermore, the preparation of such complexes can offer further insight into the potential applications of group 15 heterocyclic compounds that have already been observed.[118] Specifically, the research focuses on the individual synthetic methods for the preparation of antimony and arsenic complexes. Structural data were acquired by single-crystal X-ray diffraction experiments for each complex in parallel with other spectroscopic techniques and their geometrical parameters compared to related pertinent compounds from the literature.

2.2 Results and Discussion

2.2.1 Discussion of [(DippnacnacH)SbBr]$_2$(μ-Br)$_2$, 1[119]

The crystalline compound **1** was prepared from the metathesis reaction of DippnacnacLi with $SbBr_3$ in a 1:1 ratio (Scheme 8). Storage of the saturated toluene solution of **1** at –5 ^oC for 1 day resulted in crystalline yellow plates suitable for X-ray structural analysis.

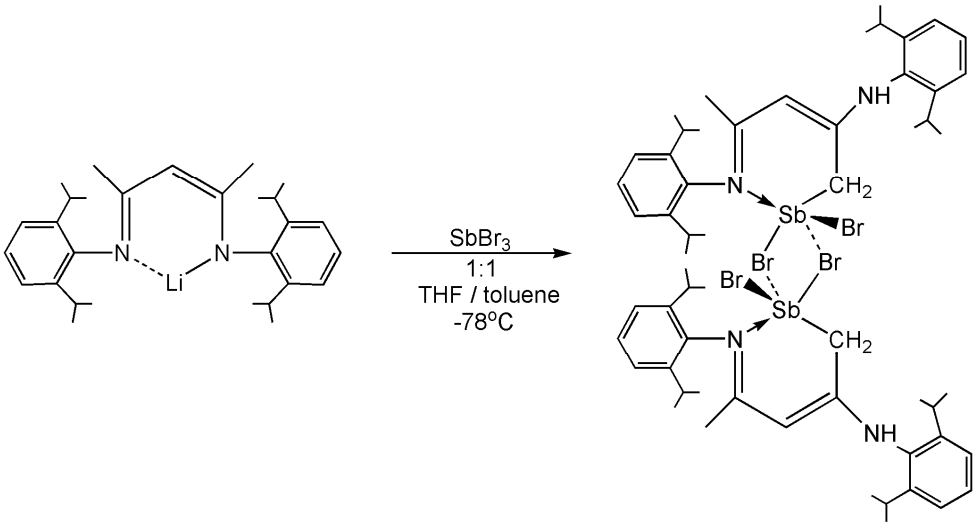

Scheme 8. Synthesis of compound **1**.

Compound **1** crystallizes in the triclinic space group $P\bar{1}$, and the crystallographic study revealed that the backbone of the Dippnacnac ligand had undergone intramolecular C–H activation. C–H activation or ligand rearrangement is not a new phenomenon for these ligands but is usually associated with more reactive species, for example the early transition metals and the β-diketiminato compounds of the alkaline earth metals.[6t,120] Intramolecular C–H activation is most likely the result of the SbX_3 (X = halide) reacting with the anionic enamine form of the ligand rather than the imine form,[121] and the

reaction conditions. In order to observe C–H activation, the addition of DippnacnacLi to the antimony halide must proceed rapidly and the reaction mixture brought quickly to room temperature. Compound **1** was isolated as a yellow crystalline solid and is a bridged Sb(III) compound (Figure 14).

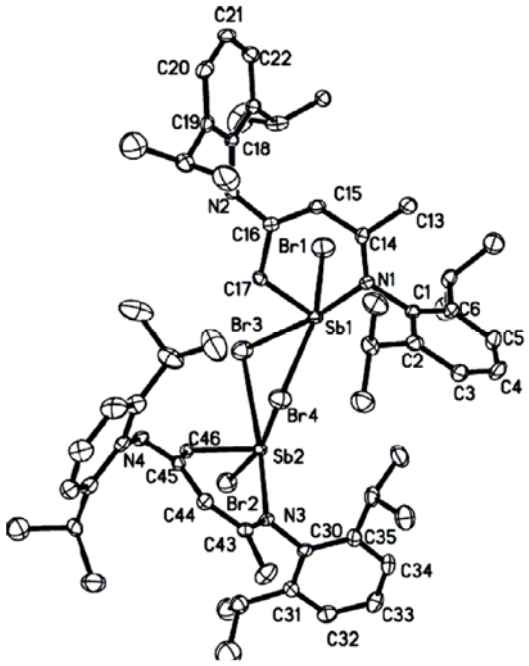

Figure 14. Molecular structure of $[(DippnacnacH)SbBr]_2(\mu\text{-}Br)_2$, **1**. Thermal ellipsoids at 50% probability level, hydrogen atoms are omitted for clarity. Selected bond lengths(Å) and angles(^{o}): Sb(1)-Br(1) 2.446(16), Sb(1)-Br(3) 2.791(16), Sb(1)-Br(4) 2.911(16), Sb(2)-Br(2) 2.531(17), Sb(2)-Br(3) 2.981(15), Sb(2)-Br(4) 2.723(16), Sb(1)-C(17) 2.143(6), Sb(1)-N(1) 2.272(5), Sb(2)-C(46) 2.141(6), Sb(2)-N(3) 2.188(4), N(1)-C(14) 1.305(7), C(14)-C(15) 1.421(8), C(15)-C(16) 1.359(8), C(16)-C(17) 1.502(7), C(17)-Sb(1)-N(1) 81.96(19), C(17)-Sb(1)-Br(1) 90.05(15), N(1)-Sb(1)-Br(1) 92.54(12), Br(1)-Sb(1)-Br(3) 89.52(5), N(1)-Sb(1)-Br(3) 169.0(11).

The bond lengths in **1** compare well to those of the optimized C–H activated Dippnacnac^{2-} ion as predicted by ab initio calculations.[6t] Both antimony atoms are N,C–bonded and consist of a terminal and bridged bromide. The Sb–Br bond lengths vary from 2.446(16) Å, Sb(1)–Br(1), to 2.981(15) Å, Sb(2)–Br(3), and highlight the lack of symmetry in the bridged Sb–Br conformation. These values are not unusual for Sb–Br bonds,[122,123] and this asymmetry appears to be a common characteristic in the 32 reported Sb–Br bridged structures.[123] Each Sb center can be viewed as having distorted see-saw geometry with the vacant coordination site presumably occupied by the Sb lone pair which is observed by bond angles of 81.96(19)^{o}, 90.05(15)^{o}, 92.54(12)^{o}, 89.52(5)^{o}, and 169.0(11)^{o} for C(17)-Sb(1)-N(1), C(17)-Sb(1)-Br(1), N(1)-Sb(1)-Br(1), Br(1)-Sb(1)-Br(3), and N(1)-Sb(1)-Br(3) respectively. The NCCCC backbone exhibits distinctive double bonds for N(1)-C(14) and C(15)-C(16) at 1.305(7) and 1.359(8) Å, respectively. Additionally, the ^{1}H NMR spectrum displays a characteristic singlet peak at 4.86 ppm representing the N–H proton resulting from the C–H activation and ligand rearrangement.

2.2.2 Discussion of [(DippnacnacHSbCl$_2$)SbCl]$^{+}$[Cl]$^{-}$, 2[119]

Compound **2** can be isolated when a slight excess of $SbCl_3$ is present in the reaction (Scheme 9).

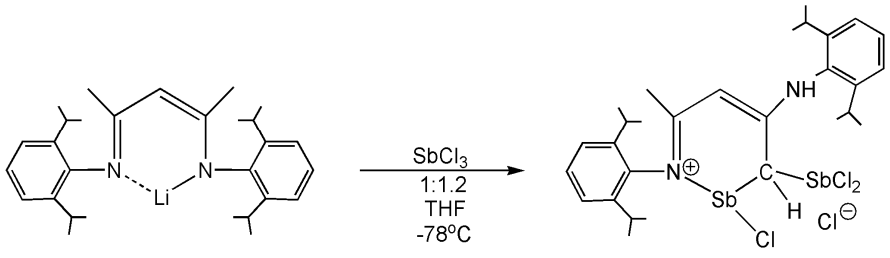

Scheme 9. Synthesis of compound **2**.

Compound **2** was isolated serendipitously in low yield from the reaction of DippnacnacLi, which was prepared *in situ* from DippnacnacH, with $SbCl_3$ at –78 ^oC in THF. Upon completion of the reaction, the mixture was filtered from the LiCl precipitate and after several weeks afforded crystalline **2** (Figure 15).

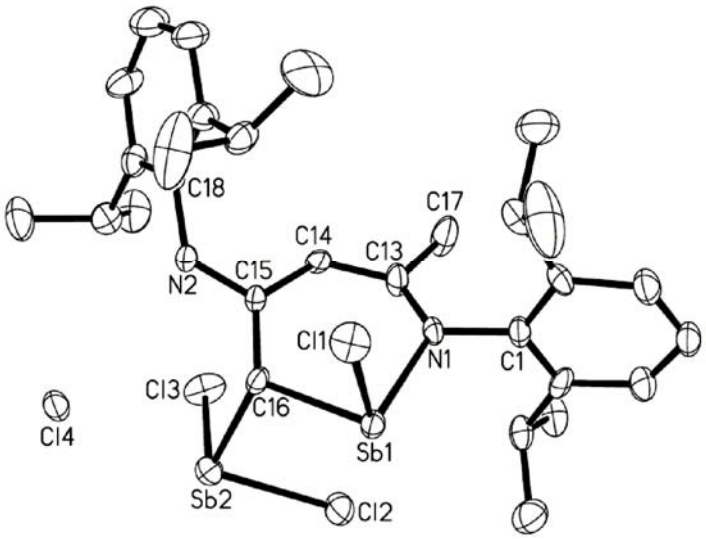

Figure 15. Molecular structure of $[(DippnacnacHSbCl_2)SbCl]^+[Cl]^-$, **2**. Thermal ellipsoids at 30% probability level, hydrogen atoms and a THF molecule are omitted for clarity. Selected bond lengths(Å) and angles(^{o}): Sb(1)-Cl(1) 2.407(4), Sb(1)-N(1) 2.113(9), Sb(1)-C(16) 2.151(10), Sb(2)-Cl(2) 2.452(3), Sb(2)-Cl(3) 2.381(3), Sb(2)-C(16) 2.452(3), N(1)-C(13) 1.326(15), C(13)-C(14) 1.401(15), C(14)-C(15) 1.418(14), C(15)-C(16) 1.456(15), N(2)-C(15) 1.359(13), N(1)-Sb(1)-C(16) 92.20(4), C(16)-Sb(1)-Cl(1) 88.00(3), N(1)-Sb(1)-Cl(1) 96.00(3), C(16)-Sb(2)-Cl(2) 89.40(3), C(16)-Sb(2)-Cl(3) 96.50(3), Cl(3)-Sb(2)-Cl(2) 91.41(14).

This complex is somewhat unusual as both C–H activation and a subsequent deprotonation has occurred. LiCl is displaced and Sb(1) sits in the C–N pocket. The geometry around Sb(1) is distorted trigonal pyramidal where the Sb lone pair occupies

the vacant coordination site. The distorted trigonal pyramidal geometry is observed by the bond angles 92.20(4)°, N(1)-Sb(1)-C(16), 88.00(3)°, C(16)-Sb(1)-Cl(1), and 96.00(3)°, N(1)-Sb(1)-Cl(1). The excess $SbCl_3$ from the reaction mixture is coordinated as a $SbCl_2$ fragment to the adjacent carbon atom in the nacnac backbone. The +1 charge on N(1) is balanced by a chloride ion that sits in close proximity to a Dipp group at a distance of ~2.96 Å from the $SbCl_2$ fragment. While the exact mechanism for the formation of **2** is unclear, it appears from the isolation of compound **1** that this is the primary product formed. It is envisaged that the reaction proceeds in a similar manner as observed in the formation of [(DippnacnacH)(PPh_2)(ECl_2)] (E = As, Sb),[114] nucleophilic displacement of the chloride on the excess $SbCl_3$ present in the reaction and inter- or intramolecular tautomerism that gives access to the carbon for coordination. The crystal structure of **2** reveals a normal Sb–N bond length of 2.113(9) Å (covalent radii ~2.11 Å) as well as normal Sb–Cl bond lengths[117] (2.407(4), 2.452(3), and 2.381(4) Å) and bond angles and are similar to other previously reported examples.

2.2.3 Discussion of [(Mesnacnac)$SbCl_2$], 3[119]

In our continuing efforts to isolate the N,N'-chelated antimony species, the equimolar reaction of MesnacnacLi with $SbCl_3$ in THF at –78 °C was carried out (Scheme 10).

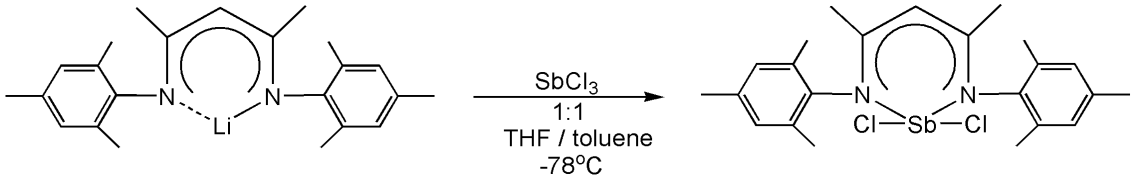

Scheme 10. Synthesis of compound **3**.

Compound **3** was successfully isolated in a moderate yield. Examination of the solid-state structure revealed it as monomeric MesnacnacSbCl$_2$ (Figure 16).

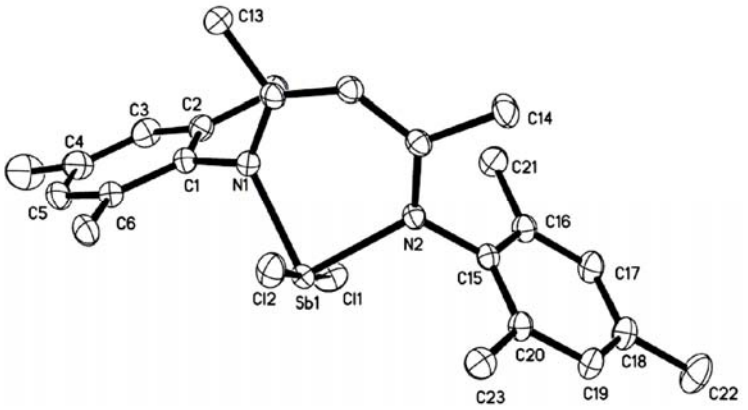

Figure 16. Molecular structure of [(Mesnacnac)SbCl$_2$], **3**. Thermal ellipsoids at 50% probability level, hydrogen atoms are omitted for clarity. Selected bond lengths(Å) and angles(^{o}): Sb(1)-Cl(1) 2.575(8), Sb(1)-Cl(2) 2.565(7), Sb(1)-N(1) 2.092(2), Sb(1)-N(2) 2.084(18), N(1)-C(10) 1.340(3), N(2)-C(12) 1.332(3), C(10)-C(11) 1.399(3), C(11)-C(12) 1.391(4), N(2)-Sb(1)-N(1) 88.34(8), N(1)-Sb(1)-Cl(1) 90.51(6), N(2)-Sb(1)-Cl(1) 91.07(6), N(1)-Sb(1)-Cl(2) 87.81(6), N(2)-Sb(1)-Cl(2) 88.01(6), Cl(2)-Sb(1)-Cl(1) 178.1(2).

The crystallographic analysis revealed no unexceptional features of **3** with all bond lengths and angles comparable to reported structures.[117] The coordination geometry of the Sb is as predicted by VSEPR for an AX$_4$E structure. Within the 'see-saw' structure the Cl(1)–Sb(1)–Cl(2) arrangement is almost linear with an angle of 178.1(2)^o. An angle of 88.34(8)^o for N(2)–Sb(1)–N(1) is also close to the 90^o angle expected. These small deviations from the predicted values are associated with the sterics of the bulky ligand and the possibility of lone pair delocalization, which is also responsible for the asymmetry of the molecule. The bond lengths from the chelating nitrogen atoms and C–C

atoms in the Mesnacnac backbone are similar lengths and reinforce the probability of delocalization within the ligand.

2.2.4 Discussion of Further Chemistry, Compounds 4–7

To further explore the chemistry of complexes **1**–**3**, we attempted to reduce the halide precursors to obtain low valent species. To this end a variety of reducing agents were employed. One example involves the reaction between MesnacnacSbCl$_2$, **3**, and 2 equiv. of the soft reducing agent 'GaI' affording compound **4** (Scheme 11).[119]

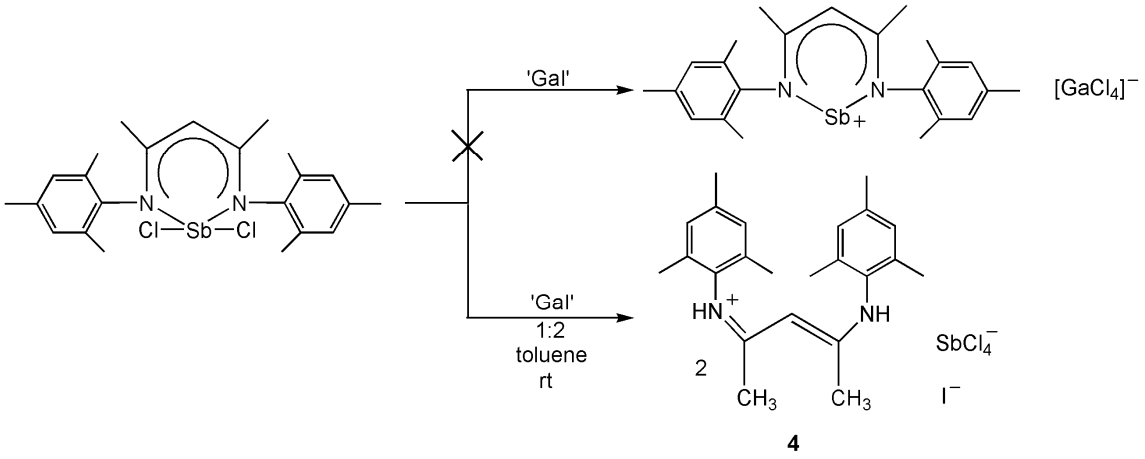

Scheme 11. Synthesis of compound **4**.

A representative crystal structure of complex **4** is depicted in order to display the common solid-state structure obtained for compounds **4**–**7** (Figure 17). From the X-ray analysis of **4** it can be seen that the Mesnacnac ligand opens up where both mesityl groups are parallel to each other, forming a highly symmetrical structure that is protonated at both nitrogen atoms. The cationic structure is balanced by the presence of an $SbCl_4^-$ anion. Within the asymmetric unit there are two Mesnacnac cations with an iodide ion from the 'GaI' as the anion for the second cation in the lattice. The bond

lengths across the N(1)–C(2)–C(3)–C(2a)–N(1a) chain exhibit delocalization of the π-bonding. The infrared spectra of **4** exhibited a characteristic N–H stretch at 3172 cm^{-1}, which was confirmed by ^{1}H NMR with a resonance observed at 3.72 ppm.[124,125] Unfortunately, despite numerous attempts all reactions gave similar products, the results of which are summarized in Table 1.

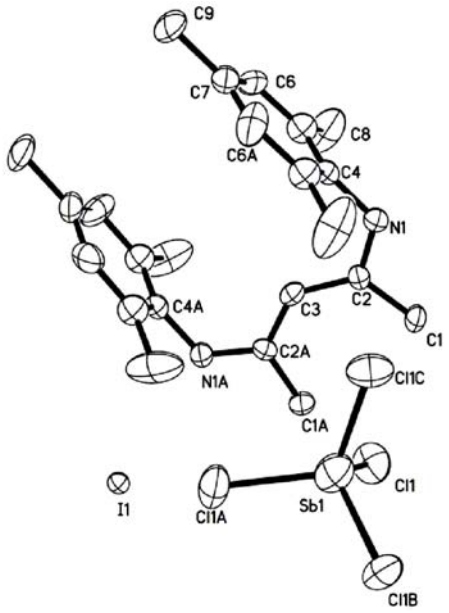

Figure 17. Molecular structure of $2[MesnacnacH_2]^+[SbCl_4]^-[I]^-$, **4**. Thermal ellipsoids at 30% probability level, second $MesnacnacH_2^+$ and hydrogen atoms are omitted for clarity. Selected bond lengths(Å) and angles(°): Sb(1)-Cl(1) 2.166(2), N(1)-C(2) 1.312(9), C(1)-C(2) 1.497(8), C(2)-C(3) 1.398(8), Cl(1)-Sb(1)-Cl(1) 113.5(15), Cl(1)-Sb(1)-Cl(1) 107.5(7).

Table 1. Reduction reactions yielding compounds **5**–**7**.

Reactant	Reducing Agent	Desired Outcome	Actual Outcome
$MesnacnacSbCl_2$	GaI	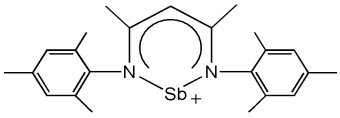	$[MesnacnacH_2]^+[GaHCl_3]^-$ [**5**]
$MesnacnacSbCl_2$	$NaBH_4$	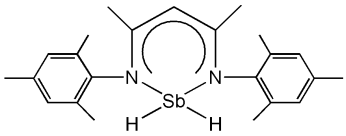	$2[MesnacnacH_2]^+2[SbCl_4]^-$ [**6**]
$DippnacnacSbCl_2$	GaI	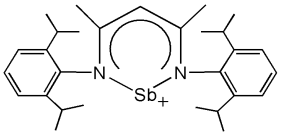	$[DippnacnacH_2]^+[GaCl_4]^-$ [**7**]

The remaining compounds **5**–**7** exhibit features similar to those observed in compound **4**. The solid-state analysis for all complexes reveals that the ligand is protonated at each nitrogen atom**.** In addition, the ligand in each compound shows delocalization of the double bond across the backbone. Lastly, each X-ray crystallographic structure displays an anion to counterbalance the protonated ligand cation.

2.2.5 Discussion of $[(Dippnacnac)AsCl]^+[As_2Cl_4(\mu\text{-}O)][Cl]^-$, 8

In an attempt to isolate crystals of $DippnacnacAsCl_2$, the reaction of DippnacnacLi with a 1.2 equiv. of $AsCl_3$ at –78 ^oC was performed and yielded colorless crystals of **8** (Scheme 12).

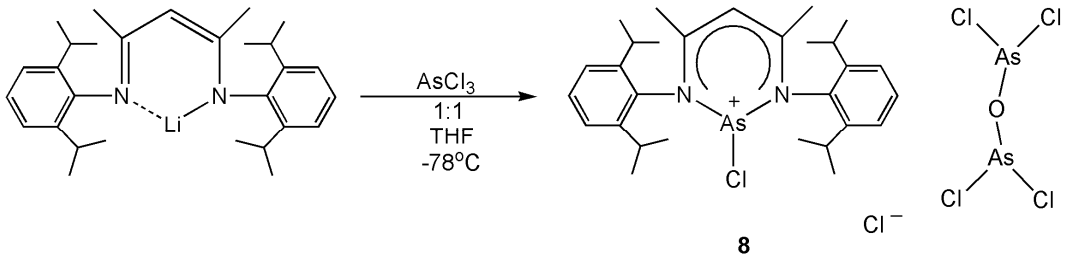

8

Scheme 12. Synthesis of compound **8**.

The X-ray crystal structure of **8** reveals a chloroarsenic cation which is balanced by a chlorine anion, also present is a $[As_2Cl_4(\mu\text{-}O)]$ compound. The source of the oxygen contamination is not confirmed, but likely from atmospheric oxygen/water moisture during the reaction (Figure 18). While there is no doubt about the atom connectivity (R factor ~5%), the thin crystalline needles resulted in large thermal ellipsoids, preventing a publishable structure. The arsenic center, As(1), is N,N'-chelated to the dippnacnac ligand. The distance between the chloroarsenic cation and the chlorine anion lies at ~6.7 Å, from As(1) to Cl(4). The bond distances observed throughout the NCCCN backbone suggest the double bond to be delocalized. Additionally, the bond distance of 1.862(7) Å observed for N(1)–As(1) lies within the appropriate range and has been similarly observed in other arsenic N,N'-chelated systems, for example 1.823(10) Å and 1.831(11) Å observed in $[MesDADAs]^+$, where MesDAD = (Mes)NC(H)C(H)N(Mes)[126] and 1.839(3) Å and 1.857(4) Å observed in $[Dipp\text{-}BIANAs]^+$, where Dipp-BIAN = 1,2-bis(dipp-imino)acenaphthene.[127] Complex **8** is structurally similar to the N,N'-phosphenium cation reported by Cowley and co-workers[128] in that the chloride attached to As(1) lies orthogonal to the AsN_2C_3 six-membered ring due to the stereochemically active lone pair of electrons on the arsenic center. Bond angles of 95.70(5)° and 98.40(2)° are observed for N(1)#1–As(1)–N(1) and N(1)–As(1)–Cl(1) respectively.

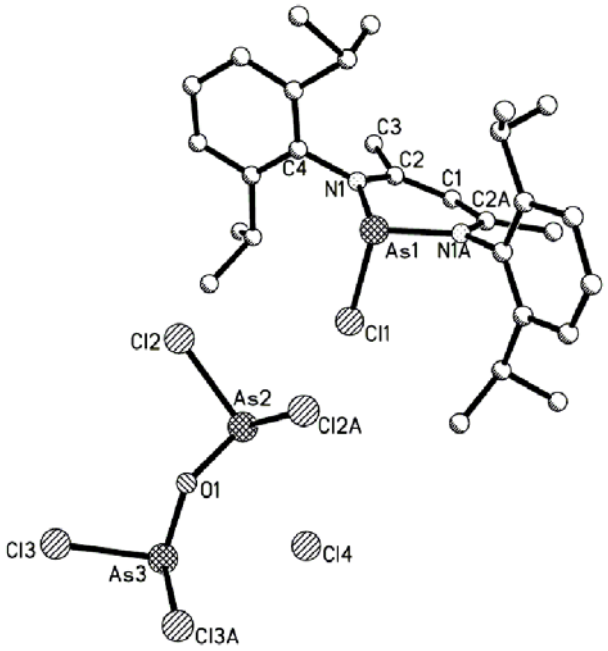

Figure 18. Molecular structure of $[(Dippnacnac)AsCl]^{+}[As_2Cl_4(\mu\text{-}O)][Cl]^{-}$, **8**. Hydrogen atoms are omitted for clarity. Selected bond lengths(Å) and angles(^{o}): As(1)-Cl(1) 2.193(3), As(1)-N(1) 1.862(7), As(2)-Cl(2) 2.242(4), As(2)-O(1) 1.773(8), As(3)-Cl(3) 2.198(3), As(3)-O(1) 1.768(8), N(1)-C(2) 1.348(12), C(1)-C(2) 1.379(15), N(1)#1-As(1)-N(4) 95.70(5), N(1)-As(1)-Cl(1) 98.40(2), O(1)-As(2)-Cl(2) 92.70(2), Cl(2)#1-As(2)-Cl(2) 92.00(3), O(1)-As(3)-Cl(3) 94.50(2), As(3)-O(1)-As(2) 123.0(5).

2.2.6 Discussion of Further Chemistry, Compounds 9–11

To further explore the chemistry of complex **8**, we wished to try and reproduce the arsenic cation complex with the Mesnacnac ligand or attempt the formation of $MesnacnacAsCl_2$. Additionally, we sought to reduce the halide precursors to obtain low valent arsenic species. To this end a few reducing agents were employed. One example involves the investigation of the further chemistry of $MesnacnacAsCl_2$, **9**, in which the crystalline structure could never be obtained but spectroscopy confirmed the desired

product. In order to try to form a derivative of compound **4** incorporating the arsenic center for structural characterization, the reaction of MesnacnacAsCl$_2$ with 2 equiv. of 'GaI' was performed affording complex **10** (Scheme 13).[119]

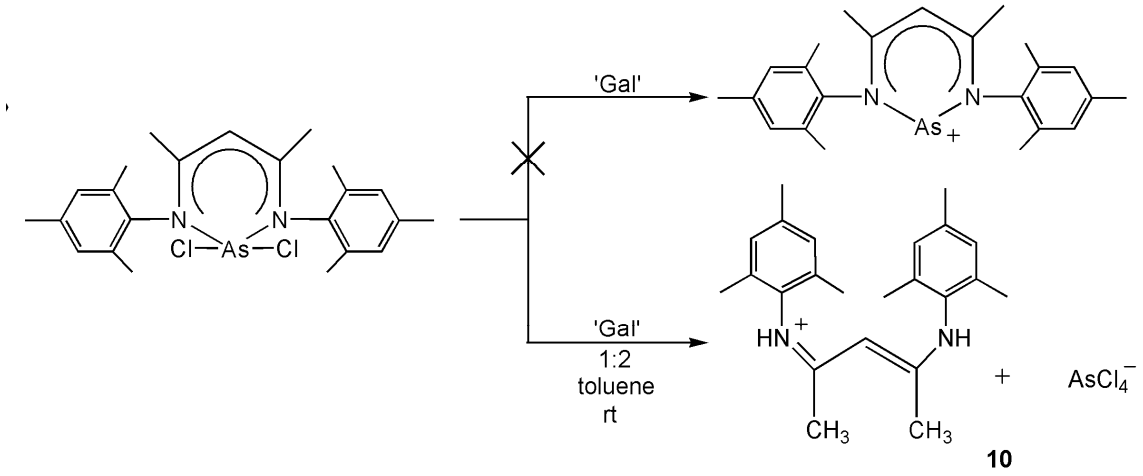

Scheme 13. Synthesis of compound **10**.

A representative crystal structure of complex **10** is depicted in order to display the common solid-state structure additionally obtained for compound **11** (Figure 19). The X-ray crystal structure of **10** reveals that the reaction outcome shows similarity with that of the Sb reaction, complex **4**. The Mesnacnac ligand has opened up where both Mes aryl groups are parallel to each other, as well as being protonated at both nitrogen atoms. The arsenic atom is displaced from the ligand and within the asymmetric unit there are two cationic [MesnacnacH$_2$]$^+$ molecules which are balanced by the presence of two $AsCl_4^-$ anions. Complex **10** exhibits that π-bonding is delocalized across the N(1)–C(2)–C(3)–C(4)–N(2) chain. The solid-state analysis is confirmed by the infrared spectra which exhibits a characteristic N–H stretch at 3152 cm^{-1} and solution NMR where the ^{1}H NMR spectrum exhibits an indicative single peak associated with the N–H proton at 3.75 ppm.

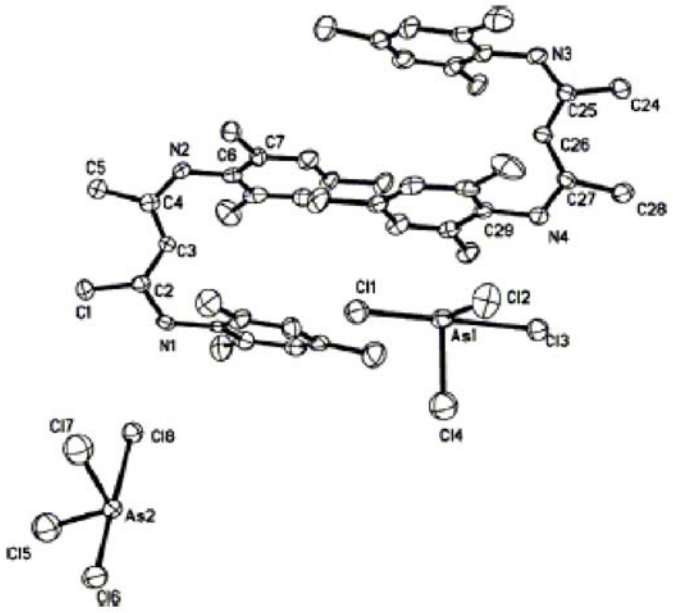

Figure 19. Molecular structure of $2[MesnacnacH_2]^+2[AsCl_4]^-$, **10**. Thermal ellipsoids at 50% probability level, hydrogen atoms are omitted for clarity. Selected bond lengths(Å) and angles(°): As(1)-Cl(1) 2.308(3), As(1)-Cl(2) 2.181(4), As(1)-Cl(3) 2.679(3), As(1)-Cl(4) 2.184(4), N(1)-C(2) 1.337(14), N(2)-C(4) 1.362(15), C(1)-C(2) 1.514(15), C(2)-C(3) 1.379(15), C(3)-C(4) 1.367(16), C(4)-C(5) 1.494(17), Cl(2)-As(1)-Cl(1) 92.28(15), Cl(2)-As(1)-Cl(3) 87.32(12), Cl(2)-As(1)-Cl(4) 97.79(17), Cl(4)-As(1)-Cl(1) 93.68(14), Cl(4)-As(1)-Cl(3) 85.55(12), Cl(1)-As(1)-Cl(3) 179.1(12), Cl(5)-As(2)-Cl(6) 93.30(17), Cl(5)-As(2)-Cl(7) 100.9(18), Cl(5)-As(2)-Cl(8) 87.62(15), Cl(7)-As(2)-Cl(6) 93.88(16), Cl(7)-As(2)-Cl(8) 86.14(14), Cl(6)-As(2)-Cl(8) 179.2(14).

Unfortunately, despite numerous attempts all reactions gave similar products, the results of which are summarized in Table 2. The remaining compounds, **9** and **11**, exhibit similar features that are seen for the previous Sb examples **4**–**7** and the As example **10**. The solid-state analysis for all of the complexes reveals that the ligand is protonated at each nitrogen atom and exhibits delocalization of the double bond across the backbone.

Lastly, each X-ray crystallographic structure displays an anion to counterbalance the protonated ligand cation.

Table 2. Further chemistry yielding compounds **9**–**11**.

Reactant 1	**Reactant 2**	**Desired Outcome**	**Actual Outcome**
MesnacancLi	$AsCl_3$	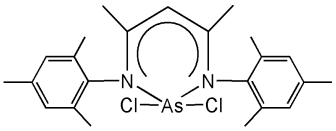	$[MesnacnacH_2]^+[Cl]^-$(thf) [**9**]
$MesnacnacAsCl_2$	GaI	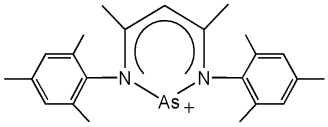	$2[MesnacnacH_2]^+2[AsCl_4]^-$ [**10**]
$DippnacnacAsCl^+$	$AgSbF_6$	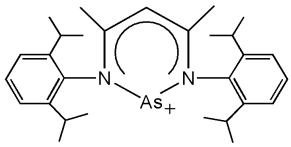	$[DippnacnacH_2]^+[SbF_6]^-$ [**11**]

2.3 Summary

Compounds **1**–**11** are a variety of β-diketiminato antimony and arsenic complexes and show that through manipulation of the halide precursor, reaction stoichiometry, and the R substituent on the nacnac different reaction outcomes can be achieved. The reactions involving the salt elimination using [(Ar)NC(Me)CHC(Me)N(Ar)]Li·OEt_2 (Ar = Dipp, Mes) provided novel antimony and arsenic complexes. Reactions using DippnacnacLi with $SbBr_3$ and $SbCl_3$ proceed rapidly with C–H activation observed. Using the MesnacnacLi with $SbCl_3$ results in the isolation of the monomeric Mesnacnac antimony(III) chloride. Likewise, by controlling the reaction conditions the reaction of DippnacnacLi with $AsCl_3$ results in the formation of the mono-chloroarsenic cation. Further exploration into the N,N'-chelated and N,C'-chelated complexes suggests that the reaction pathway in the formation of complexes **1** and **2** occur by the reaction of SbX_3 with the anionic enamine form of the ligand, while complexes **3** and **8** result from the reaction of SbX_3 or AsX_3 with the imine. Further work on additional reactions exploring the chemistry of **1**–**3** and **8** was investigated resulting in a series of complexes discussed throughout this chapter. Additionally, these complexes prompted the investigation into the preparation of the remaining congeners of the group 15 elements, phosphorus and bismuth.

2.4 Experimental

2.4.1 General Procedures

The THF was dried over potassium, toluene over sodium, and CH_2Cl_2 over calcium hydride and degassed before use. All solid reagents were handled in a nitrogen filled M-Braun drybox. All manipulations were performed under anaerobic conditions using standard Schlenk techniques. The reagents *n*-BuLi (1.6 M in hexanes), $SbCl_3$, $SbBr_3$, $AsCl_3$, $NaBH_4$, and $AgSbF_6$ were purchased from Aldrich and used as received. DippnacnacH, MesnacnacH and their corresponding lithium salts were prepared according to published procedures.[17] 'GaI' was also prepared according to published procedures.[129]

2.4.2 Spectroscopy Measurements

The ^1H and ^{13}C NMR spectra were recorded on a Varian Mercury 300 spectrometer (^1H 300.05 MHz and ^{13}C 75.45 MHz). NMR spectra were collected on crystalline products and observed spectras included either pure or crude compounds. IR analysis was conducted as Nujol Mulls with NaCl plates on a MIDAC M4000 Fourier transform infrared (FT IR) spectrometer. Melting points were determined in capillaries under a nitrogen atmosphere and are uncorrected.

2.4.3 X-Ray Crystallography

Crystal data for all compounds in Chapters 2–6 were collected with a Bruker SMART 1000 diffractometer, using graphite monochromated molybdenum radiation (λ =

0.7107 Å). Crystals were mounted on glass fibers using paratone oil to minimize exposure to oxygen. The data were corrected for absorption. Structures were solved by direct methods[130] and refined[130] via full-matrix least squares.

2.4.4 Experimental Procedures and Spectroscopic Data

Preparation of [(DippnacnacH)SbBr]$_2$(μ-Br)$_2$, 1: A 30 mL THF solution of DippnacnacLi (0.5 g, 1.2 mmol) was added rapidly by cannula to a stirred 20 mL THF solution of $SbBr_3$ (0.29 g, 1.2 mmol) at –78 ^oC. The resultant yellow colored reaction mixture was immediately removed from the dry-ice bath and allowed to reach ambient temperature. Stirring was maintained for a further 12 h, after which time the THF was removed *in vacuo* and the yellow solid extracted into toluene. Concentration of the toluene solution and storage at –5 ^oC for 1 day afforded **1** as crystalline yellow plates in moderate yield. Yield: 1.49 g, 48% yield. M.p. 103–108 ^oC. ^1H NMR (d^8 PhMe, 25 ^oC): δ (ppm) 1.08, 1.11, 1.13, 1.14 (4 doublets, 48H, $^1J_{H\text{-}H}$ = 6.6 Hz, CH(CH_3)$_2$), 1.38 (s, 6H, C*Me*), 1.99 (s, 4H, CH_2), 2.36–3.02 (m, 8H, C*H*(CH$_3$)$_2$), 4.59 (br. s, 2H, γ–C*H*), 4.86 (s, 2H, N–H), 6.75 (d, *m*–H$_{aryl}$, 8H, $^1J_{H\text{-}H}$ = 6.2 Hz), 6.92 (t, *p*–H$_{aryl}$, 4H, $^1J_{H\text{-}H}$ = 6.2 Hz); ^{13}C NMR (d^8 PhMe, 25 ^oC): δ (ppm) 23.3 (CH(*C*H$_3$)$_2$), 24.7 (*C*H(CH$_3$)$_2$), 27.9 (backbone CH$_3$), 121.7, 122.2, 123.9, 124.5, 124.7, 127.2 (Ar–C), 141.4 (C-backbone N–*C*CN), 160.1 (Sb–C).

Preparation of [(DippnacnacHSbCl$_2$)SbCl]$^+$[Cl]$^-$, 2: A –78 ^oC THF (30 mL) solution of DippnacnacH (0.5 g, 1.22 mmol) had 1 equiv. of *n*-BuLi (0.76 mL of a 1.6 M solution) added dropwise. The solution was slowly warmed to room temperature and stirred for 4

h, after which time it was rapidly added to a stirred THF (20 mL) solution of $SbCl_3$ (0.33 g, 1.44 mmol) at –78 ^oC. An immediate color change was observed and the resultant amber colored reaction mixture was removed from the dry-ice bath and allowed to warm to ambient temperature. Stirring was maintained for an additional 12 h, after which time the reaction mixture was filtered from the LiCl precipitate. Repeated filtration and concentration over a period of weeks afforded **2** in low yield. M.p. 122–125 ^oC. Due to the low yield, no spectroscopic data were obtained.

Preparation of [(Mesnacnac)$SbCl_2$], 3: A 100 mL Schlenk flask was charged with 0.3361 g of $SbCl_3$ (1.47 mmol) and 20 mL of THF. MesnacnacLi (0.5 g, 1.46 mmol) was dissolved in 30 mL of THF and added dropwise to a stirred THF solution of $SbCl_3$ at –78 ^oC. The clear yellow solution was stirred overnight. Following removal of the THF under vacuum, 20 mL of toluene was added and stirred. The clear dark yellow solution was filtered, concentrated under reduced pressure, and placed in a –30 ^oC freezer to obtain crystals. Yield: 0.31 g, 34%. M.p. 149–151 ^oC. ^1H NMR (d^8 PhMe, 25 ^oC): δ 1.45 (s, 6H, C*Me*), 1.71 (s, 9H, Mes CH_3), 1.85 (s, 9H, Mes CH_3), 4.72 (s, 1H, γ–C*H*), 6.45 (s, 4H, H_{aryl}); ^{13}C NMR (d^8 PhMe, 25 ^oC): δ 17.1 (Mes CH_3), 22.3 (Mes CH_3), 25.9 (C*Me*), 92.8(γ–C), 126.3–127.9 (br, *m*–ArC and *p*–ArC), 136.1 (*o*–ArC), 140.5 (C–N), 166.2 (C_α).

Preparation of 2[MesnacnacH_2]$^+$[$SbCl_4$]$^-$[I]$^-$, 4, and [MesnacnacH_2]$^+$[$GaHCl_3$]$^-$, 5: To a flask charged with 0.14 g (0.72 mmol) of 'GaI' in 20 mL of toluene a solution of 0.19 g (0.36 mmol) of **3** in 20 mL of toluene were added dropwise at room temperature.

The resulting dark green solution was stirred overnight, filtered and the reaction mixture concentrated under reduced pressure. Storage of the solution at room temperature for 5 days afforded green crystals of **4** and **5**. Due to **5** being a minor product, the separation of the crystals was unsuccessful. Yield of **4** and **5**: 0.16 g, 42%, M.p. 124–126 ^{o}C. ^{1}H NMR (C_6D_6, 25 ^{o}C): δ 1.13 (s, 6H, C*Me*), 1.76 (s, 9H, Mes CH_3), 2.06 (s, 9H, Mes CH_3), 3.72 (s, 2H, NH), 4.48 (s, 1H, γ–C*H*), 6.13 (s, 2H, H_{aryl}), 6.50 (s, 2H, H_{aryl}); ^{13}C NMR (C_6D_6, 25 ^{o}C): δ 17.6 (Mes CH_3), 19.4 (Mes CH_3), 21.5 (C*Me*), 95.1 (γ–C), 128.7 (*m*–ArC), 132.2 (*p*–ArC), 135.3 (*o*–ArC), 140.6 (C–N), 169.8 (C_α); IR (Nujol Mull): ν (cm^{-1}) 3172 (shoulder, N–H stretch), 1608 (w), 1550 (m), 1205 (m), 874.2 (m).

Preparation of $2[MesnacnacH_2]^+2[SbCl_4]^-$, 6: A 20 mL THF solution of $MesnacnacSbCl_2$ (0.30 g, 0.57 mmol) was added drop-wise to a 20 mL THF suspension of $NaBH_4$ (0.21 g, 5.7 mmol) at –78 ^{o}C. The resulting dark orange solution was removed from the dry-ice bath and allowed to warm to ambient temperature. Stirring was maintained for 1 h, resulting in a dark forest green solution. The THF was removed *in vacuo* and the tannish green solid was extracted into toluene. Subsequent concentration and filtration of the toluene solution and storage at –30 ^{o}C afforded **6** as crystalline colorless plates. No further characterization was performed.

Preparation of $[DippnacnacH_2]^+[GaCl_4]^-$, 7: A 20 mL toluene solution of $DippnacnacSbCl_2$ (0.25 g, 0.28 mmol) was added dropwise at –78 ^{o}C to a 20 mL toluene solution of 'GaI' (0.16 g, 0.81 mmol). The solution was slowly warmed to room temperature and stirred overnight, after which time the resulting pale yellow reaction was

filtered and concentrated under reduced pressure. Storage of the solution at –30 ^{o}C over a period of weeks afforded colorless plate crystals of **8**. Yield: 0.21 g, 77%. M.p. 131–134 ^{o}C. ^{1}H NMR (C_6D_6, 25 ^{o}C): δ (ppm) 0.52 (d, 12H, $^{1}J_{H\text{-}H}$ = 7.2 Hz, CH(CH_3)$_2$), 0.81 (d, 12H, $^{1}J_{H\text{-}H}$ = 6.9 Hz, CH(CH_3)$_2$), 1.67 (s, 3H, C*Me*), 1.81 (s, 3H, *CMe*), 2.29–2.42 (septet, 4H, C*H*(CH$_3$)$_2$), 4.01 (s, 2H, N–H), 4.06 (s, 1H, γ–C*H*), 6.48 (d, 4H, $^{1}J_{H\text{-}H}$ = 7.8 Hz, *m*–H$_{aryl}$), 6.57–6.68 (m, 2H, *p*–H$_{aryl}$); ^{13}C NMR (C_6D_6, 25 ^{o}C): δ (ppm) 21.5 (CH(*C*H$_3$)$_2$), 23.3 (C*Me*), 27.2 (*C*H(CH$_3$)$_2$), 92.9 (γ–C), 122.9 (*m*–ArC), 128.7 (*p*–ArC), 129.4 (*o*–ArC), 144.2 (C–N), 171.8 (C$_α$).

Preparation of [(Dippnacnac)AsCl]$^{+}$[As$_2$Cl$_4$(μ-O)][Cl]$^{-}$, 8: A 30 mL THF solution of DippnacnacLi (0.50 g, 1.2 mmol) was added drop-wise to a 20 mL THF solution of $AsCl_3$ (0.12 mL, 1.4 mmol) at –78 ^{o}C. The resulting yellowish orange solution was removed from the dry-ice bath and allowed to warm to ambient temperature. Stirring was maintained overnight, after which time the THF was removed *in vacuo* and the pale orange solid was extracted into toluene. Subsequent concentration and filtration of the toluene solution and storage at –30 ^{o}C afforded **8** as crystalline colorless plates. Due to the low yield no further characterization was obtained.

Preparation of [MesnacnacH$_2$]$^{+}$[Cl]$^{-}$(THF), 9: A 30 mL THF solution of MesnacnacLi (0.50 g, 1.4 mmol) was added dropwise at –78 ^{o}C to a stirred THF (20 mL) solution of $AsCl_3$ (0.12 mL, 1.4 mmol). The resulting yellowish orange solution was immediately removed from the dry-ice bath and allowed to warm to ambient temperature. Stirring was maintained overnight. Following the removal of THF *in vacuo*, the brown solid was

extracted into toluene, filtered, and concentrated under reduced pressure. After several attempts concentrating, toluene was removed *in vacuo* and the brown solid was extracted into THF, filtered, concentrated under reduced pressure, and placed in a –30 ^{o}C freezer for several days affording colorless crystals of **9**. Yield: 0.34 g, 29%. M.p. 136–139 ^{o}C. ^{1}H NMR (C_6D_6, 25 ^{o}C): δ 1.23 (s, 6H, C*Me*), 1.67 (s, 6H, Mes CH_3), 1.71 (s, 6H, Mes CH_3), 1.75 (s, 6H, Mes CH_3), 1.82 (s, 3H, Mes CH_3), 3.91 (s, 2H, NH), 4.68 (br. s, 1H, γ–C*H*), 6.28 (s, 2H, H_{aryl}), 6.42 (s, 2H, H_{aryl}); ^{13}C NMR (C_6D_6, 25 ^{o}C): δ 18.1 (Mes CH_3), 18.5 (Mes CH_3), 19.0 (Mes CH_3), 19.6 (Mes CH_3), 21.6 (C*Me*), 93.2 (γ–C), 128.4 (*m*–ArC), 128.9 (*m*–ArC), 133.3 (*p*–ArC), 133.7 (*p*–ArC), 137.1 (*o*–ArC), 137.6 (*o*–ArC), 138.1 (C–N), 165.6 ($C_α$), 168.1 ($C_α$).

Preparation of 2[MesnacnacH$_2$]$^+$2[AsCl$_4$]$^-$, 10: To a stirred toluene (20 mL) suspension of 'GaI' (0.28 g, 14.3 mmol) was added a toluene (20 mL) solution of MesnacnacAsCl_2 (0.4 g, 7.0 mmol) at room temperature. No immediate color change was observed. After stirring for 16 h, a metallic precipitate with a brown solution was observed. The solution was decanted and placed at –30 ^{o}C for 2 days to yield compound **10**. Yield: 0.29 g, 36%. M.p. 145–146 ^{o}C. ^{1}H NMR (C_6D_6, 25 ^{o}C): δ 1.18 (s, 6H, C*Me*), 2.10 (s, 18H, Mes CH_3), 3.75 (s, 2H, NH), 4.52 (br. s, 1H, γ–C*H*), 6.21 (s, 2H, H_{aryl}), 6.55 (s, 2H, H_{aryl}); ^{13}C NMR (C_6D_6, 25 ^{o}C): δ 18.2 (Mes CH_3), 22.5 (Mes CH_3), 24.6 (C*Me*), 94.4 (γ–C), 127.9 (*m*–ArC), 128.2 (*p*–ArC), 130.1 (*o*–ArC), 139.0 (C–N); IR (Nujol Mull): ν (cm^{-1}) 3152 (shoulder, N–H stretch), 2853 (w), 1608 (m), 1560 (m) 1215 (m).

Preparation of $[MesnacnacH_2]^+[SbF_6]^-$, 11: To a stirred CH_2Cl_2 (20 mL) solution of $AgSbF_6$ (0.32 g, 0.94 mmol) in a foil covered Schlenk was added a CH_2Cl_2 (20 mL) solution of $MesnacnacAsCl_2$ (0.4 g, 0.94 mmol) at room temperature. No immediate color change was observed. After stirring overnight, the resulting solution was filtered through celite. The CH_2Cl_2 was removed *in vacuo* from the resulting orange solution and toluene added. The brown solution was concentrated under reduced pressure, filtered, and stored at room temperature to yield crystalline colorless plates of compound **11**. No further characterization was pursued.

CHAPTER III

The Reactions of P(III) and Bi(III) Halides with β-Diketiminato Ligands

3.1 Introduction

The electron rich p-block elements are of particular interest due to a continued search for improved scientific applications such as better catalysts and cocatalysts in chemical reactions, as well as novel structures, bonding arrangements, and unusual reactivity patterns.[131] Ultimately, the reactivity of these complexes is what draws attention to them for further chemistry. Isolation of the pnictogenium cations, $[\{R^2C(C(Me)N(R^1))_2\}M]^+$ (Figure 20), are of particular interest as they exhibit bonding and structure similarities with carbenes which have found a plethora of applications.[132]

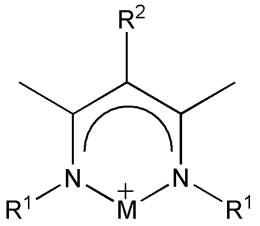

R^1 = aryl
R^2 = H, Me
M = P, As, Sb, Bi

Figure 20. Structure of a pnictogenium cation

In 2006, we[133] and Cowley[128,134] reported examples of N,N'-chelated and N,C-bonded phosphenium cations employing the β-diketiminate ligand. Cowley et al. altered both reaction conditions and ligand substituents, for example by replacing the hydrogen in the γ-carbon position with an alkyl, exchanging the aryl groups attached to the nitrogen's, and using different chloride ion abstraction agents. Firstly, the reaction of PCl_3 with $[MeC(CMeNDipp)_2]Li$ or $[HC(CMeNC_6F_5)_2]Na$ resulted in a mixture of the bis-imine derivative and the iminoamine isomer (Figure 21).[128]

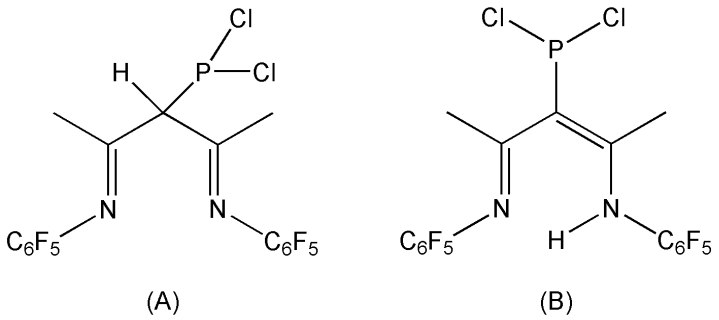

Figure 21. (A) Phosphorus bis-imine (B) Phosphorus iminoamine

When the phosphorus bis-imine, (A), is further treated with TMSOTf in CH_2Cl_2, the N,N'-chelated chlorophosphenium salt is formed and Me_3SiCl is eliminated (Eq. 3.1).[128]

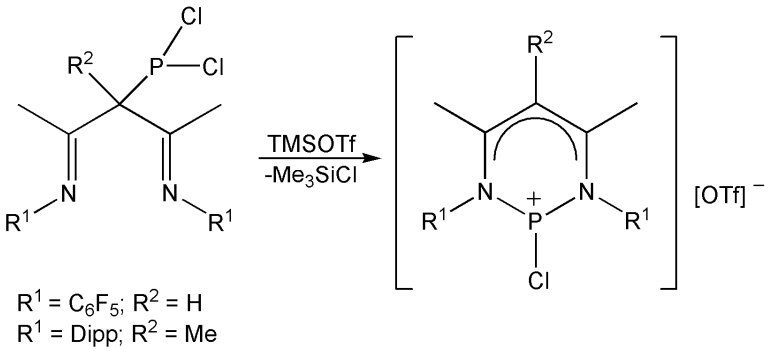

(Eq. 3.1)

Depending on the substituents of the β-diketiminate ligand, intramolecular C-H activation can occur. For example, by removing the methyl group from the γ-carbon position and reacting $[HC(CMeNDipp)_2]Li$ with PCl_3 and TMSOTf, the N,C-bonded phosphenium cation is produced (Eq. 3.2).[134] Similarly, the N,C-bonding occurs upon reacting $[MeC(CMeNDipp)_2]Li$, where methyl is present in the γ-carbon position, with $PhPCl_2$ and $AlCl_3$ (Eq. 3.3).

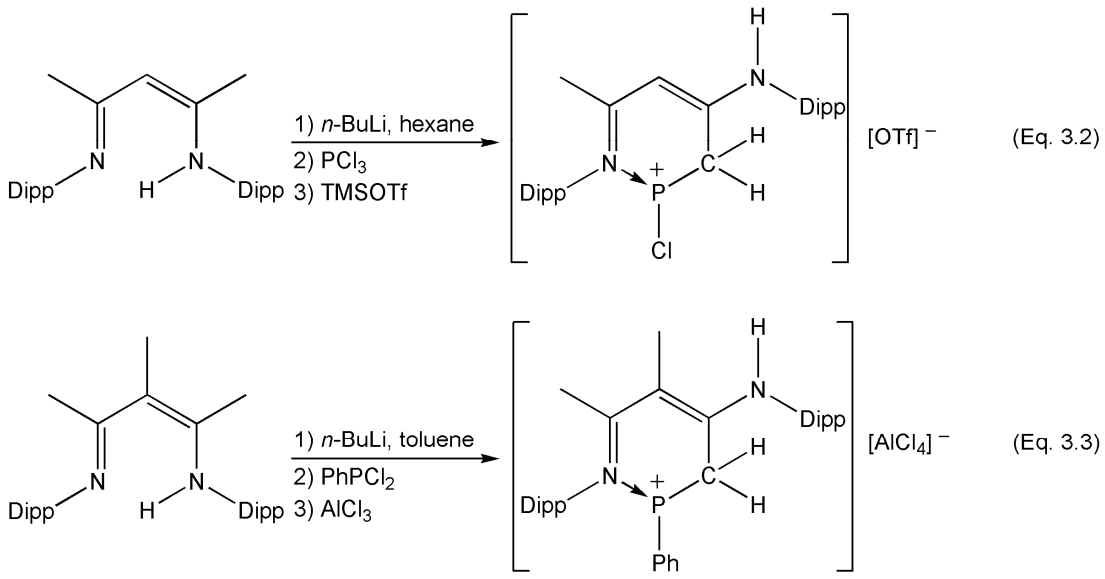

The N,N'-chelated halopnictogenium salts have the potential to undergo reduction and act as precursors in the formation of phosphinidenes, arsinidenes, stibinidenes, and bismuthinidenes. Yet, attempts at reduction of the chlorophosphenium cation with potassium resulted in a 1,2-azaphospholine derivative from the triplet β-diketiminato phosphinidene rather than the desired product (Scheme 14).[135] The 1,2-azaphospholine complex is the result of C-H activation of the methyl in the β-carbon position and NCCCN ligand backbone cleavage.

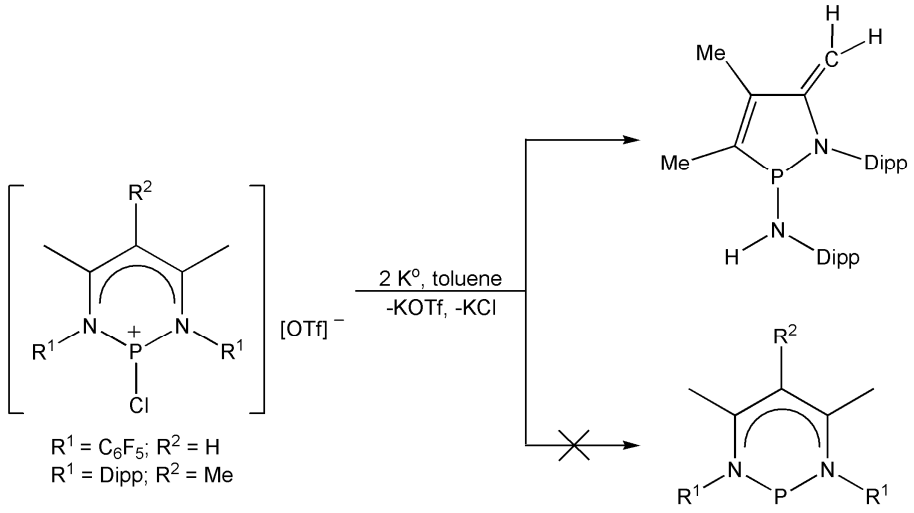

Scheme 14. Formation of a phosphinidene valence isomer: obtained and expected

In addition to the formation of phosphinidenes, β-diketiminato halophosphenium cations also possess the ability to undergo nucleophilic substitution reactions. Cowley and co-workers additionally investigated the reaction of the bromophosphenium salt, [{MeC(CMeNDipp)$_2$}PBr][OTf], with NaOH in order to accomplish this type of reaction.[136] The hydroxyphosphenium cation (Figure 22A), the hydrophosphoryl tautomer (Figure 22B), or a mixture of both were all possible outcomes. However, upon treatment with an equimolar amount of NaOH, the bromophosphenium salt affords the hydroxyphosphenium cation structure (Figure 22A).

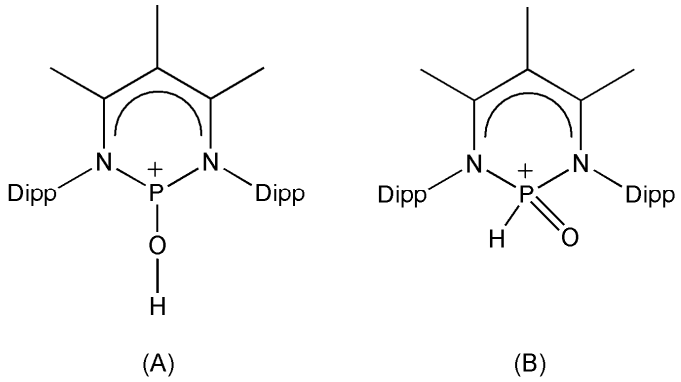

Figure 22. (A) Hydroxyphosphenium cation (B) Hydrophosphoryl tautomer

Lappert et al. also reported similar results of a N,N'-chelated phosphenium cation by reacting the potassium β-diiminate ligand [PhC(CHNDipp)$_2$]K with PI_3.[137] Attempts at reacting [PhC(CHNDipp)$_2$]K with PCl_3 or PBr_3 led to a mixture of phosphorus containing products of which could not be isolated. However, upon reacting the ligand with PI_3, the β-dialdiminatophosphenium triiodide species was produced (Eq. 3.4).

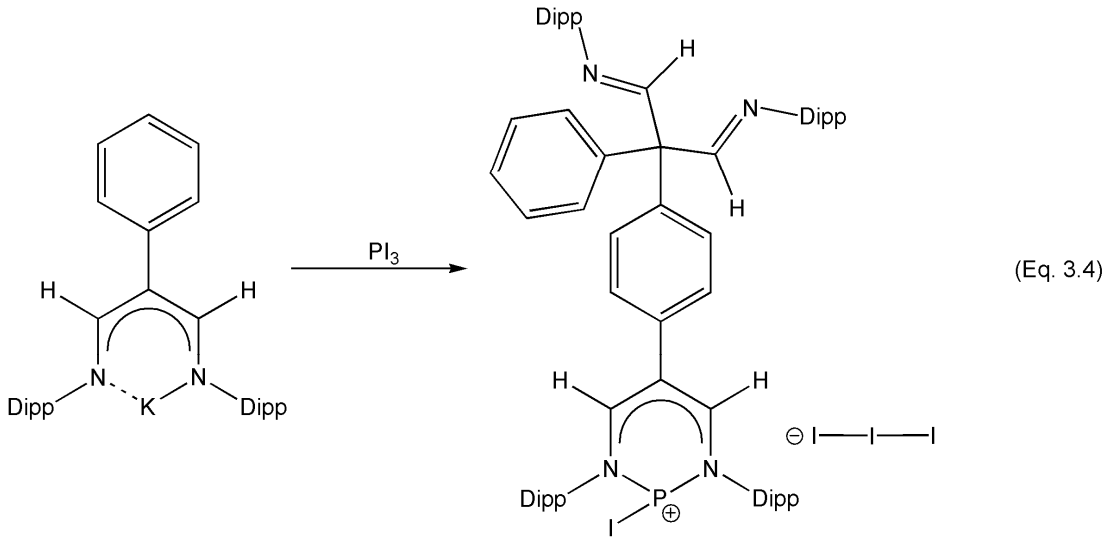

(Eq. 3.4)

The current chapter focuses on the synthesis and characterization of phosphorus(III) and bismuth(III) nacnac complexes and their relation to other similar reports in the literature. Again, the descriptive synthetic procedures are examined as reaction conditions alter the crystalline compounds produced. The isolation of two N, C bonded phosphenium ions, **12** and **13**, an N,N' coordinated phosphenium ion with an anionic arsenic counter-ion, **14**, and a non coordinated bismuth chloride complex, **16**, are observed. The compounds **12** and **14** are prepared by a facile one pot synthesis that can be compared to earlier more sophisticated methods. Compound **13** is isolated in low yield but exhibits previously unobserved coordination of a rearranged β-diketiminato ligand with phosphorus(III) bromide. Finally, complex **15** unusually shows no signs of ligand coordination, ultimately resulting in the cationic ligand, $[HC(CMeNHDipp)_2]^+$, three cationic aniline molecules, $[DippNH_3]^+$, probably the result of ligand decomposition, and anionic $[Bi_2Cl_{10}]^{4-}$.

3.2 Results and Discussion

3.2.1 Discussion of [(DippnacnacH)PBr]$^{+}$[Br]$^{-}$, 12[133]

The reaction of the sodium salt, DippnacnacNa, with PBr_3 at –78 ^{o}C afforded colorless needles of complex **12** following work-up of the reaction mixture in hexanes (Scheme 15). The colorless chunks crystallize in the orthorhombic space group *Pbca* in moderate yield.

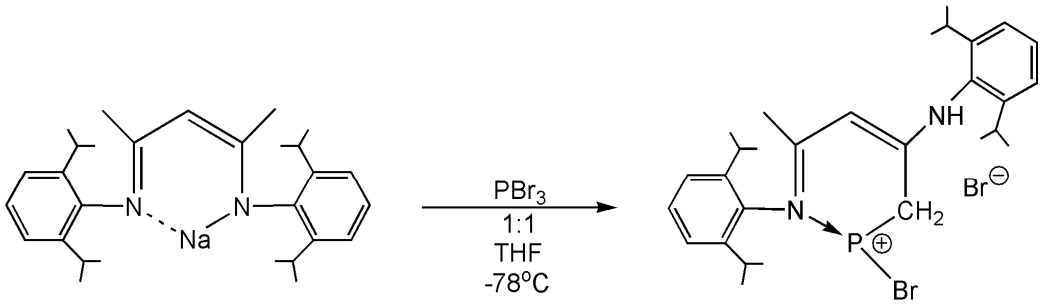

12

Scheme 15. Synthesis of compound **12**.

Single crystal X-ray analysis revealed that the backbone of the nacnac ligand in compound **12** had undergone intramolecular C–H activation (Figure 23). This phenomenon was previously observed in complexes **1**–**2** in chapter 2, but, as already stated, usually is associated with more reactive species, such as the early transition elements and the nacnac compounds of the alkaline earth metals.[6t,120] Again, the intramolecular C–H activation is likely the result of the PX_3 (X = halide) reacting with the anionic enamine form of the ligand rather than the imine form.[121] Compound **12** is structurally related to the reported N,C-chelated and N,N'-chelated β-diketiminato

phosphenium cations reported by Cowley et al.,[128,134] shown in Eq. 2.1,3.1,3.2, with remarkably similar bond lengths and angles.

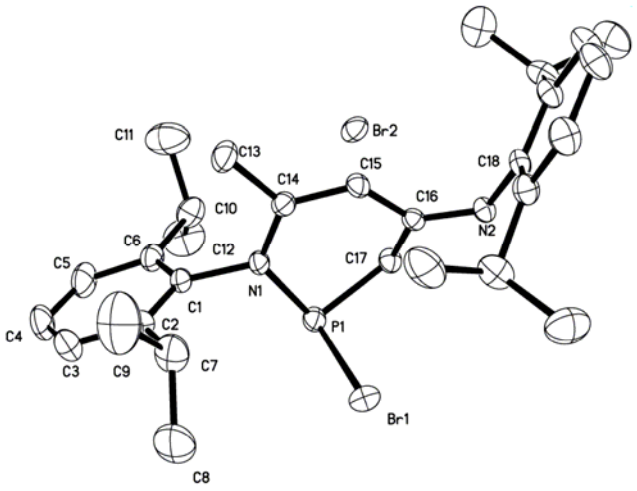

Figure 23. Molecular structure of $[(DippnacnacH)PBr]^{+}[Br]^{-}$, **12**. Thermal ellipsoids at 30% probability level, hydrogen atoms are omitted for clarity. Selected bond lengths(Å) and angles(°): P(1)-N(1) 1.716(2), P(1)-Br(1) 2.264(9), P(1)-C(17) 1.819(2), N(1)-C(14) 1.376(3), N(2)-C(16) 1.303(3), C(14)-C(15) 1.362(3), C(15)-C(16) 1.415(3), C(16)-C(17) 1.479(3), N(1)-P(1)-C(17) 98.98(10), N(1)-P(1)-Br(1) 103.3(7), C(17)-P(1)-Br(1) 97.69(8).

The difference between the phosphenium cations reported by Cowley et al. and **12** is the bromide counter-ion that sits 4.675 Å from the cationic phosphorus center. The closest interaction is ~3.9 Å with the isopropyl group of the aryl group. The P(1)–N(1) and P(1)–C(17) bond lengths of 1.716(2) Å and 1.819(2) Å respectively, are nearly identical to the P–N and P–C bond lengths observed for $[(DippnacnacH)PCl]^{+}[OTf]^{-}$ at 1.718(3) Å and 1.821(4) Å.[134] The P(1)–N(1) bond distance corresponds well to the expected range for the N→P donor-acceptor bonding. Additionally, the P(1)–Br(1) bond distance, 2.264(9) Å, is nearly identical to the P–Br bond length, 2.204(10) Å, found in

[(Dippnacnac)PBr]$^{+}$[OTf]$^{-}$, which was recently reported in 2008 by Cowley et al.[136] The infrared spectra of **12** exhibited a characteristic N–H stretch at 3192 cm^{-1}, which was confirmed by ^{1}H NMR with a resonance observed at 8.01 ppm. The P–CH_2 carbon is confirmed by ^{13}C NMR with a peak at 192.4 ppm, while the ^{31}P NMR displayed a characteristic peak at 139.3 ppm that is comparable to 149.3 ppm for [(DippnacnacH)PCl]$^{+}$[OTf]$^{-}$.[134]

3.2.2 Discussion of [(MeDippnacnacH)PBr]$^{+}$[Br]$^{-}$, 13

In order to observe further the reaction yielding complex **12**, the ligand MeDippnacnac, where a methyl group is present at the γ-carbon, was employed. The reaction of the lithium salt, MeDippnacnacLi, with PBr_3 at –78 ^{o}C afforded colorless plates of complex **13** following work-up of the reaction mixture in toluene (Scheme 16). The colorless plates crystallize in the triclinic space group $P\bar{1}$ in moderate yield.

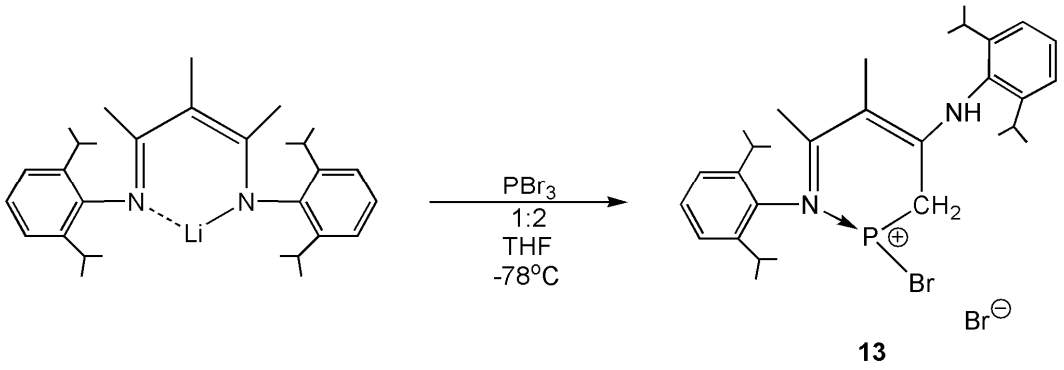

Scheme 16. Synthesis of compound **13**.

The X-ray analysis revealed that the backbone of the nacnac ligand in compound **13** had undergone intramolecular C–H activation as similarly observed for complex **12** (Figure 24). Increasing the steric hindrance of the γ-carbon with a methyl group, rather

than a hydrogen, does not prevent the rearrangement from occurring and is likely the result of the PX_3 (X = halide) reacting with the anionic enamine form of the ligand rather than the imine form.[121]

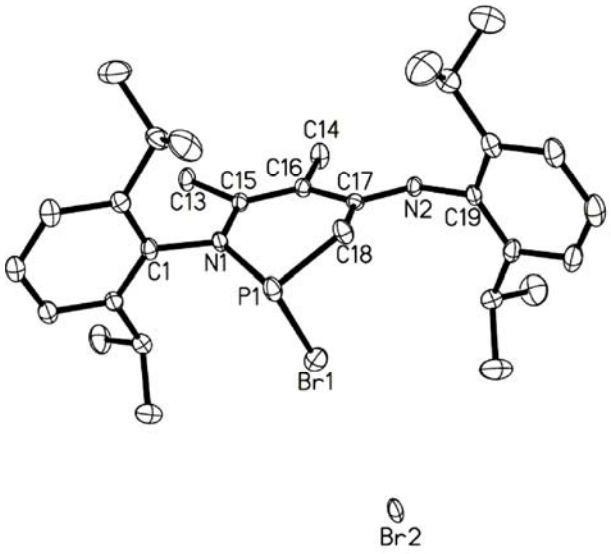

Figure 24. Molecular structure of $[(MeDippnacnacH)PBr]^{+}[Br]^{-}$, **13**. Thermal ellipsoids at 30% probability level, PhMe molecule and hydrogen atoms are omitted for clarity. Selected bond lengths(Å) and angles(°): P(1)-N(1) 1.705(4), Br(1)-P(1) 2.293(17), P(1)-C(18) 1.797(5), N(1)-C(15) 1.386(6), N(2)-C(17) 1.308(6), C(15)-C(16) 1.380(6), C(17)-C(16) 1.434(6), C(17)-C(18) 1.490(6), N(1)-P(1)-C(18) 97.30(2), N(1)-P(1)-Br(1) 104.0(15), C(18)-P(1)-Br(1) 95.65(18).

Compound **13** is structurally related to the reported N,C-chelated and N,N'-chelated β-diketiminato phosphenium cations reported by Cowley et al.,[128,134] shown in Eq. 2.1,3.1,3.2, with remarkably similar bond lengths and angles. The bromide counter-ion sits ~10.7 Å from the cationic phosphorus center. The closest interaction is ~5.6 Å with the toluene solvent molecule present in the asymmetric unit. The bond lengths of

1.705(4) Å and 1.797(5) Å, for P(1)–N(1) and P(1)–C(18) respectively, are nearly identical to the P–N and P–C bond lengths observed for complex **12** at 1.716(2) Å and 1.819(2) Å,[133] as well as $[(DippnacnacH)PCl]^{+}[OTf]^{-}$ at 1.718(3) Å and 1.821(4) Å.[134] Additionally, the P(1)–Br(1) bond distance, 2.293(17) Å, is nearly identical to the P–Br bond length, 2.264(9) Å, found in complex **12**, and 2.204(10) Å, found in $[(Dippnacnac)PBr]^{+}[OTf]^{-}$, which was recently reported in 2008 by Cowley et al.[136] The infrared spectra of **13** exhibited a characteristic N–H stretch at 3176 cm^{-1}, which was confirmed by ^{1}H NMR with a resonance observed at 4.05 ppm. The P–CH_2 carbon is confirmed by ^{13}C NMR with a peak at 198.4 ppm, while the ^{31}P NMR displayed a characteristic peak at 98.93 ppm.

3.2.3 Discussion of $[(DippnacnacPBr)_2PBr]$, 14[133]

In the course of experimental work leading to the formation of **12**, compound **14** was isolated in low yield and the solid-state analysis revealed a complex with interesting structural features (Scheme 17). Complex **14** was formed from the addition of 1.1 equiv. of neat PBr_3 to DippnacnacLi in the dry-box. On addition of PBr_3 an obvious color change from yellow to orange was observed concomitant with evolution of a gas (HBr) indicating an immediate reaction. Toluene was added to the yellow/orange solid affording a yellow colored solution that was stirred overnight. The yellow solution was filtered from the LiBr precipitate, concentrated, and stored overnight yielding large yellow crystals of **14**.

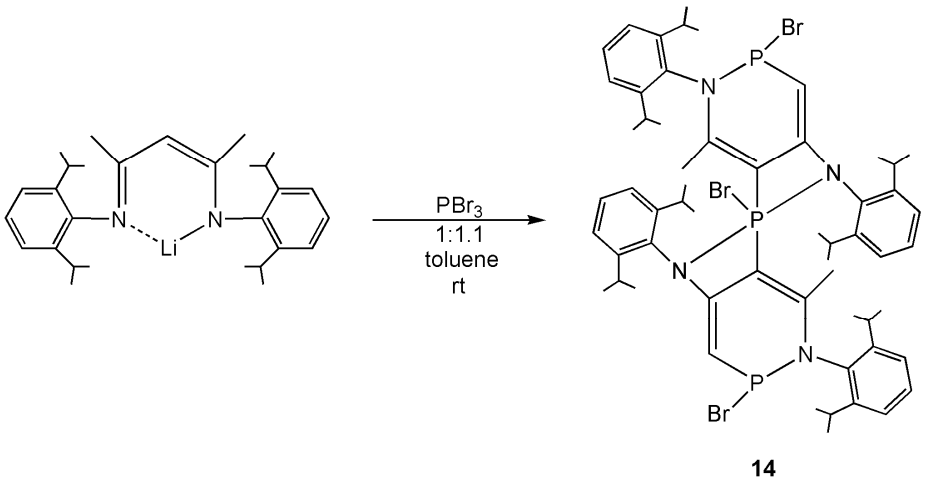

Scheme 17. Synthesis of compound **14**.

The X-ray analysis of **14** is depicted (Figure 25), and the formation of **14** is tentatively attributed to initial intramolecular C–H activation followed by activation of the γ carbon. The P–N and P–C bond lengths are similar to those observed in **12** and **13**, and indicate single bonds around the phosphorus center. The P–Br bonds, 2.297(9) Å and 2.348(8) Å, show no noteworthy discrepancies and are similar to the P–Br bond lengths, 2.264(9) Å and 2.293(17) Å, observed in complexes **12** and **13**, respectively. The bond lengths of 1.339(3) Å and 1.343(3) Å between C(1)–C(2) and C(4)–C(17), respectively, are indicative of double bond character in the NCCCC backbone. The geometry around the P(III) center is distorted trigonal pyramidal with bond angles ranging from 99.20(8)^{o} to 102.5(7)^{o}. The remaining central phosphorus center, P(1), represents a distorted trigonal bipyramidal geometry with a C(1)–P(1)–C(1A) bond angle of 171.5(14)^{o}, which lies close to the expected 180^{o}, while the remaining bond angles range from 94.22(7)^{o} to 130.9(13)^{o}. Complex **14** was determined to be rather thermally stable, however, due to the exceedingly low yield no further spectroscopic data was obtained. Despite numerous

attempts to reproduce this compound, all were unsuccessful affording the N–C bonded phosphenium cation.

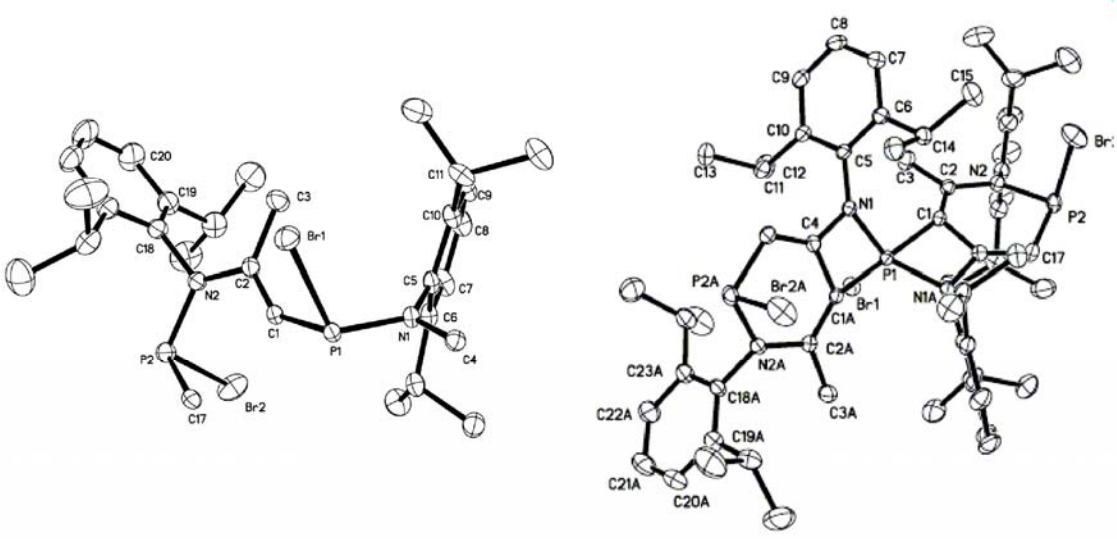

Figure 25. Molecular structure of [(DippnacnacPBr)$_2$PBr], **14**. The left hand side is the asymmetric unit and the right hand side is the full molecule. Thermal ellipsoids at 30% probability level, two toluene molecules and hydrogen atoms are omitted for clarity. Selected bond lengths(Å) and angles(^{o}): P(1)-N(1) 1.723(17), P(1)-Br(1) 2.297(9), P(1)-C(1) 1.872(2), P(2)-N(2) 1.703(2), P(2)-Br(2) 2.348(8), P(2)-C(17) 1.764(8), N(1)-C(4) 1.407(3), N(2)-C(2) 1.407(3), C(1)-C(2) 1.339(3), C(1)-C(4) 1.435(3), C(4)-C(17) 1.343(3), C(1)-P(1)-Br(1) 94.22(7), N(1)-P(1)-C(1) 102.4(9), N(1)-P(1)-Br(1) 114.5(7), N(1)-P(1)-N(1A) 130.9(13), C(1)-P(1)-C(1A) 171.5(14), C(17)-P(2)-Br(2) 99.20(8), N(2)-P(2)-C(17) 100.9(10), N(2)-P(2)-Br(2) 102.5(7), C(4)-N(1)-P(1) 96.90(13), P(2)-N(2)-C(2) 126.6(15).

3.2.4 Discussion of 2[(DippnacnacH)PCl]$^+$[As$_2$Br$_6$(μ-Br)]$^-$[Br]$^-$, 15[133]

In order to observe further the results of complex **14** incorporating both intramolecular C–H activation and attack at the γ carbon, the reaction of DippnacnacLi

with PCl_3 was performed in a similar manner as described for **14**. However, following the addition of THF, the reaction mixture was cooled to –78 ^oC and 1.2 equiv. of $AsBr_3$ were added drop-wise (Scheme 18). The reaction yielded colorless blocks in 67% yield that crystallize in the triclinic space group $P\bar{1}$.

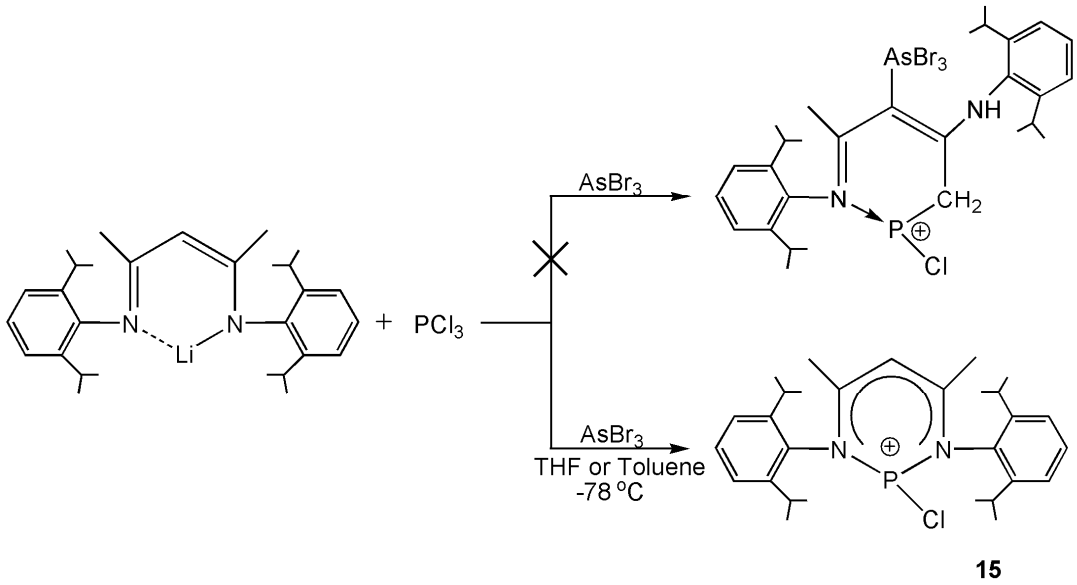

Scheme 18. Synthesis of compound **15**.

It was anticipated that addition of $AsBr_3$ would lead to a product similar to that shown in Scheme 18, instead compound **15** was isolated in moderate to high yield and could be obtained whether the initial reaction was performed in toluene or THF (Figure 26). Complex **15** shows structural similarity to the N,N'-chelated phosphenium cation discussed earlier reported by Cowley and co-workers.[128] Within the asymmetric unit there are two phosphenium cations present. The cationic charge is counterbalanced by the presence of an arsenic anion, $[As_2Br_7]^-$, and a free bromide ion located between the anion and two neutral $AsBr_3$ molecules. The phosphorus atom sits in the N,N pocket and is coordinated to two nitrogen atoms. The P–N bonds are very similar in length to those for

compounds **12–14**, as well as to the $[(Dippnacnac)PCl]^{+}[OTf]^{-}$ reported by Cowley et al.[134]

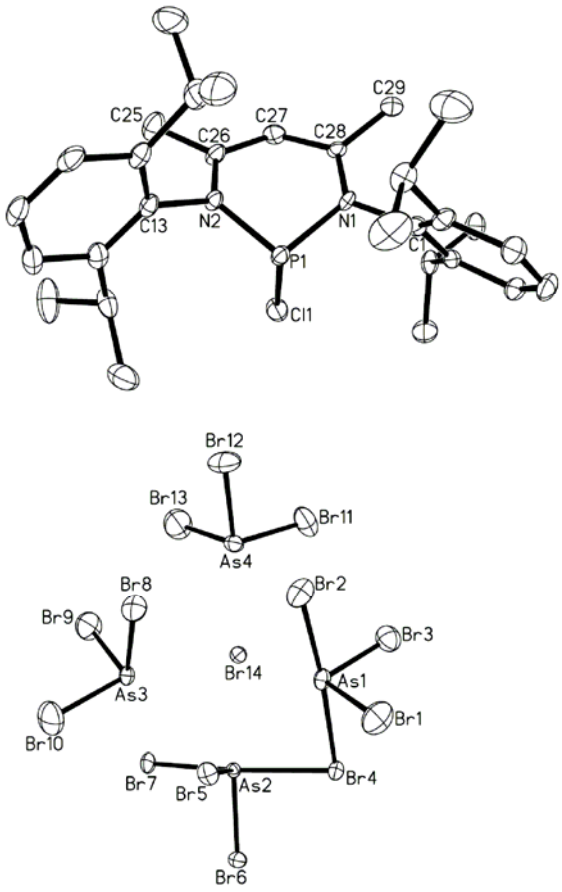

Figure 26. Molecular structure of $2[(DippnacnacH)PCl]^{+}[As_2Br_6(\mu\text{-}Br)]^{-}[Br]^{-}$, **15**. Thermal ellipsoids at 30% probability level, hydrogen atoms are omitted for clarity. Selected bond lengths(Å) and angles(^{o}): P(1)-N(1) 1.742(9), P(1)-N(2) 1.691(8), P(1)-Cl(1) 2.072(4), N(1)-C(28) 1.338(12), N(2)-C(26) 1.381(13), C(26)-C(27) 1.372(15), C(27)-C(28) 1.406(14), N(1)-P(1)-Cl(1) 97.60(3), N(2)-P(1)-N(1) 98.90(4), N(2)-P(1)-Cl(1) 101.2(3).

As seen in **12**, the chlorine atom attached to the phosphorus center in complex **15** is orthogonal to the PNCCCN ring due to the lone pair of electrons on the phosphorus,

with N(1)–P(1)–Cl(1), N(2)–P(1)–N(1), and N(2)–P(1)–Cl(1) bond angles at 97.60(3)°, 98.90(4)°, and 101.2(3)° respectively. The bond distances observed across the NCCCN backbone exhibit delocalization of the double bond with distances at 1.381(13) Å (N(2)–C(26)), 1.372(15) Å (C(26)–C(27)), 1.406(14) Å (C(27)–C(28)), and 1.338(12) Å (N(1)–C(28)). The solid-state analysis is confirmed by solution NMR where the ^{31}P NMR spectrum exhibits an indicative single peak at 130.2 ppm, which is similar to other closely related examples.[128,134]

3.2.5 Discussion of $[DippnacnacH_2]^+3[DippNH_3]^+[Bi_2Cl_9(\mu\text{-}Cl)]^{4-}$, 16

In continuation with our interest of the pnictogen metals, the reaction of DippnacnacLi with $BiCl_3$ in a 1:1 ratio was performed in THF at –78 °C in an attempt at forming the Dippnacnac$BiCl_2$ complex (Scheme 19). The resulting pale yellow solution was then allowed to stir at room temperature overnight. Following workup of the reaction mixture in toluene, compound **16** was isolated as colorless cube crystals in low yield.

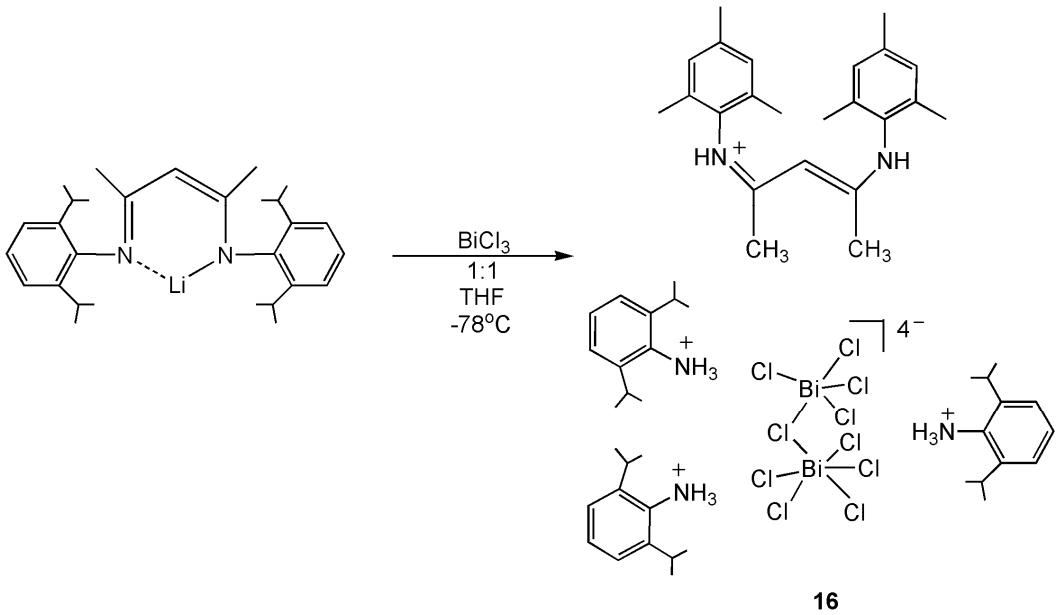

Scheme 19. Synthesis of compound **16**.

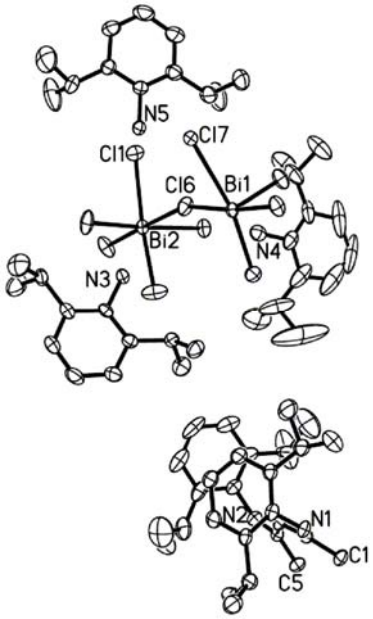

Figure 27. Molecular structure of $[DippnacnacH_2]^+3[DippNH_3]^+[Bi_2Cl_9(\mu\text{-}Cl)]^{4-}$, **16**. Thermal ellipsoids at 30% probability level, hydrogen atoms are omitted for clarity. Selected bond lengths(Å) and angles(°): N(1)-C(2) 1.334(5), N(2)-C(4) 1.333(5), C(1)-C(2) 1.511(5), C(2)-C(3) 1.395(6), C(3)-C(4) 1.392(6), C(4)-C(5) 1.494(5), Bi(1)-Cl(7) 2.984(10), Bi(1)-Cl(9) 2.569(12), Bi(1)-Cl(10) 2.527(12), Bi(2)-Cl(3) 2.539(13), Bi(2)-Cl(5) 2.893(12), Bi(2)-Cl(6) 2.929(12), Cl(8)-Bi(1)-Cl(9) 91.89(4), Cl(9)-Bi(1)-Cl(7) 92.19(4), Cl(9)-Bi(1)-Cl(6) 174.3(4), Cl(2)-Bi(2)-Cl(4) 90.18(5), Cl(3)-Bi(2)-Cl(2) 91.18(5), Bi(1)-Cl(6)-Bi(2) 161.8(6), Bi(1)#1-Cl(7)-Bi(1) 99.40(3).

From the X-ray analysis of **16** it can be seen that the Dippnacnac ligand opens up where both Dipp aryl groups are parallel to each other and both nitrogen atoms are protonated (Figure 27). The cationic $[DippnacnacH_2]^+$ is accompanied by three cationic 2,6-diisopropylaniline groups which are balanced by a $[Bi_2Cl_{10}]^{4-}$ anion that is located within the center of the cationic aniline groups. Strong hydrogen bonding is observed between the $-NH_3$ hydrogens of the aniline molecules and the chlorine atoms. The

polychlorinated anion, $[Bi_2Cl_{10}]^{4-}$, has been previously observed and reported.[138] The bond lengths 1.334(5) Å, 1.395(6) Å, 1.392(6) Å, and 1.333(5) Å for N(1)–C(2), C(2)–C(3), C(3)–C(4), and N(2)–C(4), respectively, are suggestive of delocalized π-bonding across the N(1)–C(2)–C(3)–C(4)–N(2) chain. The hydrogen atoms on the 2,6-diisopropylaniline cations were confirmed using the electron difference map from the X-ray data. The Bi–Cl bond distances range from 2.527(12)–2.984(10) Å (Figure 28) and are similar to other $[Bi_2Cl_{10}]^{4-}$ examples (2.564–2.945 Å).[138a] The longer bond lengths 2.836(11) Å, 2.837(12) Å, 2.893(12) Å, 2.929(12) Å, and 2.984(10) Å observed for Bi(1)–Cl(6), Bi(2)–Cl(1), Bi(2)–Cl(5), Bi(2)–Cl(6), and Bi(1)–Cl(7), respectively, are due to the lone electron pair on the Bi centers.[138a] Unfortunately, the DippnacnacBiCl_2 complex was not isolated and has yet to be structurally characterized, but rather only prepared *in situ* to further react with $LiAlH_4$ in the formation of DippnacnacAlH_2.[116] As a result of the uncoordinated bismuth compound **16**, no further structural characterization was executed.

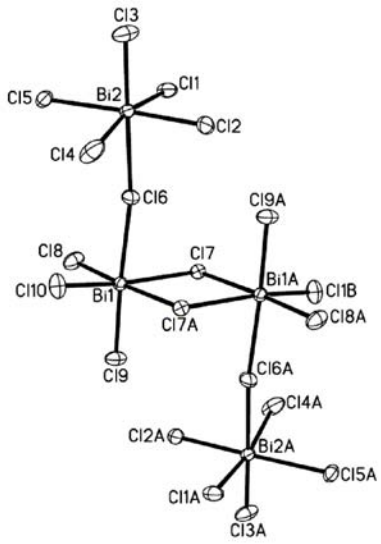

Figure 28. Molecular structure of $[Bi_4Cl_{20}]^{8-}$ anion. Thermal ellipsoids at 30% probability level.

3.3 Summary

Five group 15 complexes have been derived from reactions with β-diketiminato ligands and are described. The reported phosphorus structures **12**, **13**, and **15** complement the existing published work of Cowley et al.,[128,134] while compound **14** reveals a novel arrangement of the C–H activated nacnac ligand. These complexes highlight how different outcomes can be achieved by manipulating the halide precursor and reaction stoichiometry. Reaction of the sodium or lithium salts, [HC{DippNC(Me)}$_2$]Na or [MeC{DippNC(Me)}$_2$]Li, with PBr_3 in a 1:1 and 1:2 ratio, respectively, provided **12** and **13** which are similar to the antimony complexes **1** and **2,** where intramolecular C–H activation occurred. Conversely, the lithium salt elimination with [HC{DippNC(Me)}$_2$]Li and a slight excess of PBr_3 resulted in the novel compound **14**, resulting from intramolecular C–H activation followed by subsequent activation of the γ carbon. However, reaction of the lithium salt in the presence of PCl_3 and a slight excess of $AsBr_3$, resulted in the N,N'-chelated phosphenium cation, **15**. The isolation of complex **15** is attributed to the presence of the $AsBr_3$ blocking the γ carbon from undergoing attack by the phosphorus, thus allowing the ligand to have the opportunity to undergo N,N'-chelation. In numerous attempts to obtain DippnacnacBiCl_2, a variety of reaction conditions were employed, but no coordination complexes were isolated, and compound **16** was produced. Therefore, it can be concluded that the preferred reaction outcomes with the group 15 metals and the β-diketiminate ligand depend on the reaction conditions. Further work exploring the chemistry forming the six-membered pnictogen ring complexes prompted the investigation into the related β-ketiminato ligand with main group and transition metals and to further examine the role of reaction conditions.

3.4 Experimental

3.4.1 General Procedures

The solvents used were dried over sodium or potassium and degassed before use. The reagents were handled in a nitrogen filled M-Braun drybox. All manipulations were performed under anaerobic conditions using standard Schlenk techniques. The reagents PBr_3, $AsBr_3$, and $BiCl_3$ were purchased from Aldrich and used as received. The reagent PCl_3 was purchased from Aldrich and distilled prior to use. DippnacnacH, MeDippnacnacH, and the corresponding lithium and sodium salts were prepared according to published procedures.[17]

3.4.2 Spectroscopy Measurements

The ^{1}H, ^{13}C, and ^{31}P NMR spectra were recorded on a Varian Mercury 300 spectrometer (^{1}H 300.05 MHz, ^{13}C 75.45 MHz, and ^{31}P 121.47 MHz). IR analysis was conducted as Nujol Mulls with NaCl plates on a MIDAC M4000 Fourier transform infrared (FT IR) spectrometer. Melting points were determined in capillaries under a nitrogen atmosphere and are uncorrected.

3.4.3 Experimental Procedures and Spectroscopic Data

Preparation of $[(DippnacnacH)PBr]^{+}[Br]^{-}$, 12: A THF (30 mL) solution of DippnacnacNa (0.5 g, 1.13 mmol) was added dropwise at –78 ^{o}C to a stirred THF solution (20 mL) of PBr_3 (0.11 mL, 1.13 mmol). The resulting yellow solution was immediately removed from the dry-ice bath, allowed to warm to ambient temperature, and stirred overnight. Following the removal of THF *in vacuo*, the pale yellow solid was

extracted in hexanes, filtered, and concentrated under reduced pressure. Storage at 25 ^{o}C afforded **12** in moderate yield. Yield: 0.85 g, 52%. M.p. 135–137 ^{o}C. ^{1}H NMR (C_6D_6, 25 ^{o}C): δ (ppm) 0.65–1.27 (m, 24H, CH(C*H*$_3$)$_2$), 1.64 (s, 3H, C*Me*), 3.25–3.38 (septet, 2H, C*H*(CH$_3$)$_2$), 3.48 (s, 2H, C*H*$_2$), 3.71–3.86 (septet, 2H, C*H*(CH$_3$)$_2$), 4.69 (s, 1H, γ–C*H*), 6.57–6.92 (m, 6H, H$_{aryl}$) 8.01 (s, 1H, N–H); ^{13}C NMR (C_6D_6, 25 ^{o}C): δ (ppm) 21.6 (CH(*C*H$_3$)$_2$), 22.2 (CH(*C*H$_3$)$_2$), 22.4 (CH(*C*H$_3$)$_2$), 22.9 (CH(*C*H$_3$)$_2$), 23.2 (CH(*C*H$_3$)$_2$), 23.3 (CH(*C*H$_3$)$_2$), 23.9 (CH(*C*H$_3$)$_2$), 24.7 (CH(*C*H$_3$)$_2$), 25.7 (C*Me*), 27.1 (*C*H(CH$_3$)$_2$), 27.3 (*C*H(CH$_3$)$_2$), 27.7 (*C*H(CH$_3$)$_2$), 28.0 (*C*H(CH$_3$)$_2$), 98.2 (γ–C), 123.2 (*m*–ArC), 124.0 (*m*–ArC), 124.2 (*m*–ArC), 124.7 (*m*–ArC), 128.4 (*p*–ArC), 129.0 (*p*–ArC), 144.4 (*o*–ArC), 145.3 (*o*–ArC), 146.1 (*o*–ArC), 146.5 (*o*–ArC), 147.7 (C–N), 148.6 (C–N), 167.9 (C$_α$), 179.4 (CH$_2$*C*NH), 192.4 (P*C*H$_2$); ^{31}P{^{1}H} NMR (121 MHz, C_6D_6, 25 ^{o}C): δ (ppm) 139.3; IR (Nujol Mull): ν (cm^{-1}) 3192 (shoulder, N–H stretch).

Preparation of [(MeDippnacnacH)PBr]$^{+}$[Br]$^{–}$, 13: A THF (30 mL) solution of MeDippnacnacH (0.40 g, 0.92 mmol) had 1 equiv. of *n*-BuLi (0.37 mL of a 2.5 M solution, 0.92 mmol) added drop-wise at 0 ^{o}C. The solution was allowed to warm to room temperature slowly and stirred for 2 h, after which time it was rapidly added to a stirred THF (20 mL) suspension of PBr_3 (0.16 g, 1.8 mmol) at –78 ^{o}C. The resulting brownish orange solution was immediately removed from the dry-ice bath, allowed to warm to ambient temperature, and stirred overnight. A color change to cloudy neon orange was observed and following the removal of THF *in vacuo*, the orange solid was extracted in toluene, filtered, and concentrated under reduced pressure. Storage at 25 ^{o}C afforded **13** in moderate yield. Yield: 0.36 g, 55%. M.p. 221–224 ^{o}C. ^{1}H NMR (C_6D_6, 25 ^{o}C): δ (ppm)

1.16–1.38 (m, 18H, CH(CH_3)$_2$), 1.37 (d, 6H, $^1J_{H\text{-}H}$ = 6.3 Hz, CH(CH_3)$_2$), 1.97 (br. s, 3H, C*Me*), 2.28 (s, 3H, C*Me*), 2.73 (s, 2H, CH_2), 3.35–3.39 (m, 4H, C*H*(CH$_3$)$_2$), 4.05 (s, 1H, N–H), 7.29–7.40 (m, 6H, H_{aryl}); ^{13}C NMR (C_6D_6, 25 ^{o}C): δ (ppm) 20.7 (CH(*C*H$_3$)$_2$), 22.3(CH(*C*H$_3$)$_2$), 22.8 (CH(*C*H$_3$)$_2$), 23.5 (CH(*C*H$_3$)$_2$), 27.9 (C*Me*), 28.1 (C*Me*), 28.5 (*C*H(CH$_3$)$_2$), 30.1 (*C*H(CH$_3$)$_2$), 31.7 (*C*H(CH$_3$)$_2$), 32.1 (*C*H(CH$_3$)$_2$), 98.3 (γ–C), 123.7 (*m*–ArC), 123.9 (*m*–ArC), 124.1 (*m*–ArC), 124.5 (*m*–ArC), 127.4 (*p*–ArC), 128.2 (*p*–ArC), 128.5 (*o*–ArC), 129.8 (*o*–ArC), 136.9 (*o*–ArC), 140.6 (*o*–ArC), 141.9 (C–N), 143.4 (C–N), 171.6 (C_α), 187.8 (CH$_2$*C*NH), 198.4 (P*C*H$_2$); ^{31}P{^{1}H} NMR (121 MHz, C_6D_6, 25 ^{o}C): δ (ppm) 98.93; IR (Nujol Mull): ν (cm^{-1}) 3176 (shoulder, N–H stretch), 1589 (w), 1561 (w), 1228 (m), 934 (m).

Preparation of [(DippnacnacPBr)$_2$PBr], 14: DippnacnacLi (0.5 g, 1.18 mmol) had 1.1 equiv. of PBr_3 (0.11 mL, 1.3 mmol) added neat in the dry-box. An immediate reaction was observed. The yellow colored solid was dissolved in 30 mL of toluene and stirred overnight. The reaction mixture was filtered from the LiBr precipitate. Concentration to ~5 mL followed by storage at room temperature for 5 days, yielded large yellow crystals of **14**. M.p. 144–148 ^{o}C, due to low yield no further spectroscopic data were obtained.

Preparation of [(DippnacnacH)PCl]$^+$[As$_2$Br$_6$(μ-Br)]$^-$, 15: DippnacnacLi (0.5 g, 1.18 mmol) had 1.1 equiv. of PCl_3 (0.11 mL, 1.3 mmol) added neat in the dry-box. An immediate reaction was observed. The yellow colored solid was dissolved in 30 mL of THF and cooled to –78 ^{o}C. $AsBr_3$ (0.37 g, 1.18 mmol), dissolved in 10 mL of THF, was added dropwise. There was no observable color change and the resulting yellow colored

solution was brought to ambient temperature and stirred overnight. Following removal of THF *in vacuo*, the yellow solid was extracted in toluene. Concentration of the solution and storage at –5 ^{o}C afforded compound **15** in moderate yield. Yield: 1.00 g, 67% (based on PCl_3). M.p. 96–99 ^{o}C. ^{1}H NMR (C_6D_6, 25 ^{o}C): δ (ppm) 0.72 (d, 12H, $^{1}J_{H\text{-}H}$ = 6.8 Hz, $CH(CH_3)_2$), 0.77 (d, 12H, $^{1}J_{H\text{-}H}$ = 6.6 Hz, $CH(CH_3)_2$), 1.05 (m, 4H, $CH(CH_3)_2$), 1.49 (s, 6H, C*Me*), 5.74 (s, 1H, γ–C*H*), 6.78 (m, 6H, H_{aryl}); ^{13}C NMR (C_6D_6, 25 ^{o}C): δ (ppm) 21.7 ($CH(CH_3)_2$), 23.4 ($CH(CH_3)_2$), 26.9 (C*Me*), 28.8 ($CH(CH_3)_2$), 92.9 (γ–C), 117.9 (*m*–ArC), 118.4 (*p*–ArC), 139.0 (*o*–ArC), 147.4 (C–N), 197.5 (C_α); ^{31}P{^{1}H} NMR (121 MHz, C_6D_6, 25 ^{o}C): δ (ppm) 130 and 243.

Preparation of $[DippnacnacH_2]^{+}3[DippNH_3]^{+}[Bi_2Cl_9(\mu\text{-}Cl)]^{-}$, 16: A THF (30 mL) solution of DippnacnacLi (0.5 g, 1.18 mmol) was added dropwise to a THF (20 mL) solution of $BiCl_3$ (0.37 g, 1.18 mmol) at –78 ^{o}C. The resulting pale yellow solution was removed from the dry-ice bath and allowed to warm to ambient temperature. Stirring was maintained overnight, after which time the THF was removed *in vacuo* and the yellow solid was extracted in toluene, concentrated, and filtered. Storage at –30 ^{o}C resulted in colorless cube crystals of complex **16**. Due to the low yield and the unacceptable results no further characterization was pursued.

CHAPTER IV

Synthesis, Characterization, and Steric Hindrance Comparisons of Selected Transition and Main Group Metal β-Ketiminato Complexes

4.1 Introduction

β-Ketiminato complexes, [RN(H)(C(Me))$_2$C(Me)=O] where R = aryl, have been reported for elements across the periodic table (Figure 29).

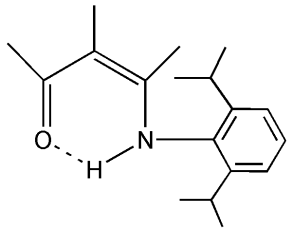

Figure 29. Structure of β-ketoiminato aryl ligand

Throughout the 1960's, numerous reports of β-ketiminato transition metal complexes were reported consisting mostly of nickel, copper, and cobalt.[27] Since then, nickel β-ketiminato complexes continue to be reported due to their large success as catalysts.[29,31-33,37,139] Likewise, a variety of other transition[28,30,31,140-144] and main group[34,145-150] metal complexes have been synthesized. Of those reported, tin and zinc β-ketiminato complexes are related to the current research. Due to their successful catalytic activity and living polymerization characteristics, zinc complexes with β-diketoiminato ligands have been extensively examined.[5i,13,30,139] Despite their structural similarities, zinc β-ketiminato complexes have been rather neglected. In 2003, Coates et al. reported the structure of a zinc alkyl complex with a similar ligand, β-oxo-δ-diiminate (Figure 30A).[140] In 2006, Liu and co-workers reported six zinc β-ketiminato complexes that were prepared as catalysts for the copolymerization of cyclohexene oxide and carbon dioxide (Figure 30B-D),[30] however they were not isolated or structurally characterized.

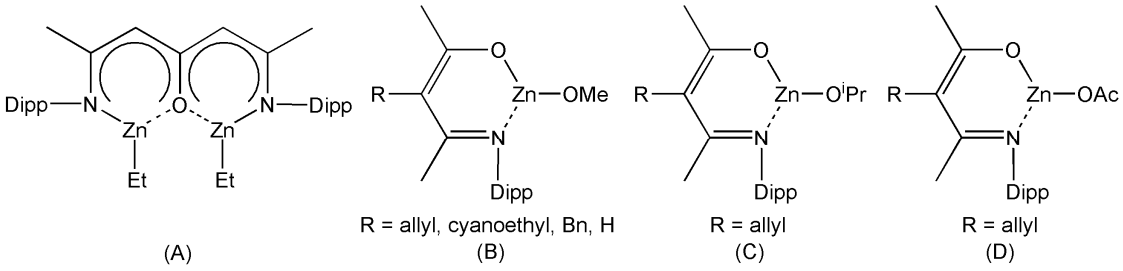

Figure 30. Examples of zinc β-ketiminato complexes

Similarly to the limited number of zinc complexes reported are the small collection of aluminum and magnesium ketiminate complexes. Huang and co-workers have reported a variety of aluminum and magnesium complexes containing the bidentate monoanionic ketiminate ligand, for example [OCMeCHCMeNDipp], and some have found to be active catalysts in the ring opening polymerization of ε-caprolactones.[34,145-147] Although aluminum and magnesium complexes are not examined in this research, magnesium and zinc are typically investigated together due to their periodic similarities and their wide reaching potential in a variety of chemical disciplines.[150] More recently in 2008, Huang and co-workers reported the synthesis of tin(II) and tin(IV) compounds incorporating the ketiminate ligand, [OCMeCHCMeNDipp] (Scheme 20).[149] The resulting divalent and tetravalent tin compounds were characterized by X-ray crystallography and NMR. The significance of organotin compounds lies in their variety of applications including organic synthesis, catalysis, and medicinal applications.[151] For example, in vitro studies have shown tin(II) complexes to actively fight against tumor cell lines.[151d-g]

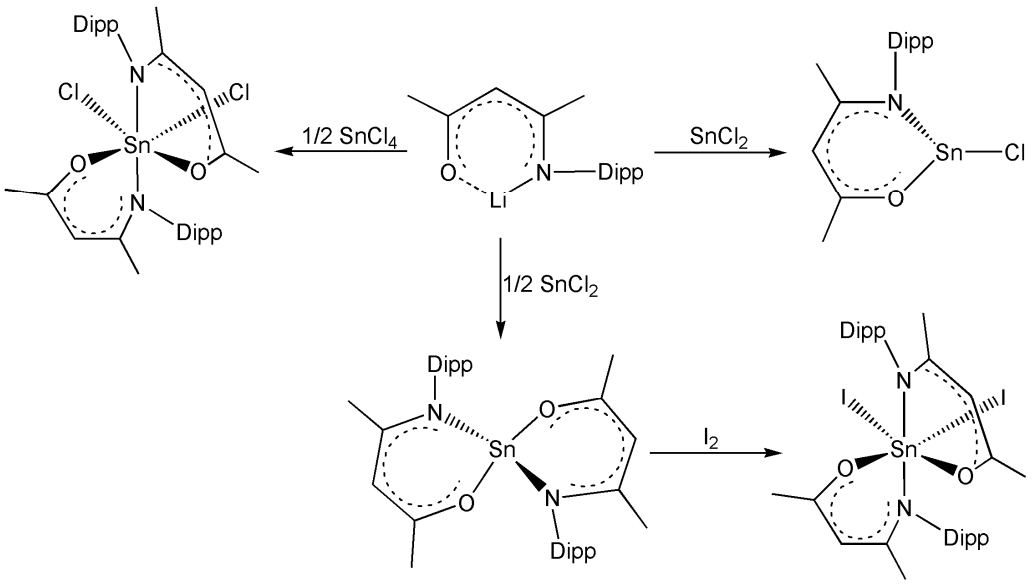

Scheme 20. Tin(II) and tin(IV) ketiminate complexes

Related to β-ketiminato ligands are those that have a pendant arm group attached to the nitrogen atom, [RN(H)C(Me)CHC(Me)=O] where R = $C_2H_4NH_2$, $C_2H_4N(alkyl)_2$ (Figure 31).

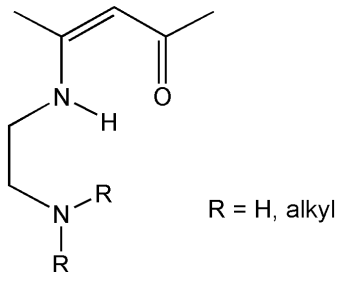

Figure 31. Structure of β-ketoiminato arm ligand

These ligands have been used to support several transition metals particularly for exploration of their magnetic properties,[43,48,50-51,152-159] while main group counterparts are less well studied. A common feature of the β-ketoiminato arm ligand are the $–NH_2$, $–NMe_2$, –NHMe, or –NHEt pendant arm groups.[43,48,50-51,152-156] Only two examples

featuring the $-NEt_2$ group, which are pertinent to the current research, have been described (Figure 32).[51,158]

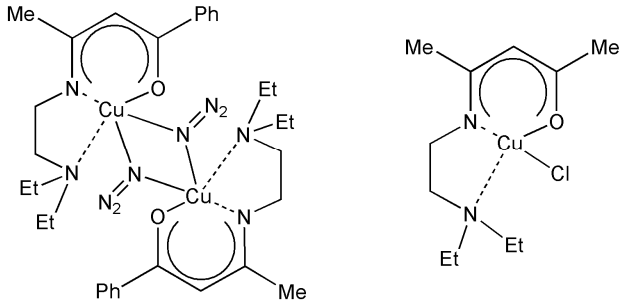

Figure 32. Examples of $-NEt_2$ arm β-ketiminato complexes

The remaining transition and main group β-ketiminato arm complexes are more rare including reports with zinc, cobalt, manganese, indium, and alkaline earth metals.[35,36,39,48,157] These structures consist only of $-NMe_2$ and $-N^iPr_2$ groups on the pending arm,[35,36,39,48] those of Zn, Mn, and In pertaining to the discussed research.[35,39,157] Of particular interest is the indium complex reported by Chi, Carty, and co-workers as a precursor for metal-organic chemical vapor deposition (MOCVD) of indium oxide thin films (Figure 33).[39]

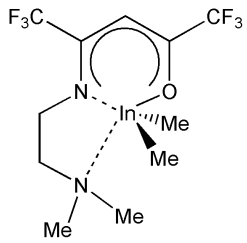

Figure 33. Indium β-ketiminato arm complex

In 1996, Tsubomura et al. reported a manganese ketiminate complex (Figure 34).[157] The tripodal β-ketoimine moiety coordinated to the manganese atom in a monodentate fashion affording a monomeric octahedral coordinated complex.

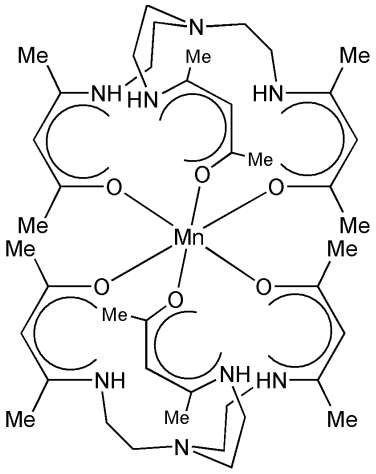

Figure 34. Tripodal manganese β-ketoimine complex

In the same year, Tsubomura and co-workers reported a zinc ketiminate complex supported by a tripodal ketoimine (Figure 35),[157] resulting in N,O coordination to the zinc center.

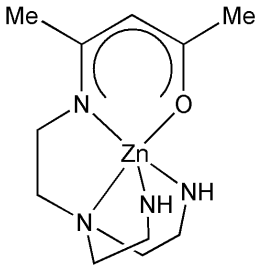

Figure 35. Tripodal zinc β-ketoimine complex

In 2008, Chen and co-workers reported a unique set of zinc β-ketoiminato structures resembling crown-like macrocycles (Scheme 21).[35] Of these, the zinc alkoxide complex (Scheme 21B) was shown to act as an initiator in ring-opening polymerization.

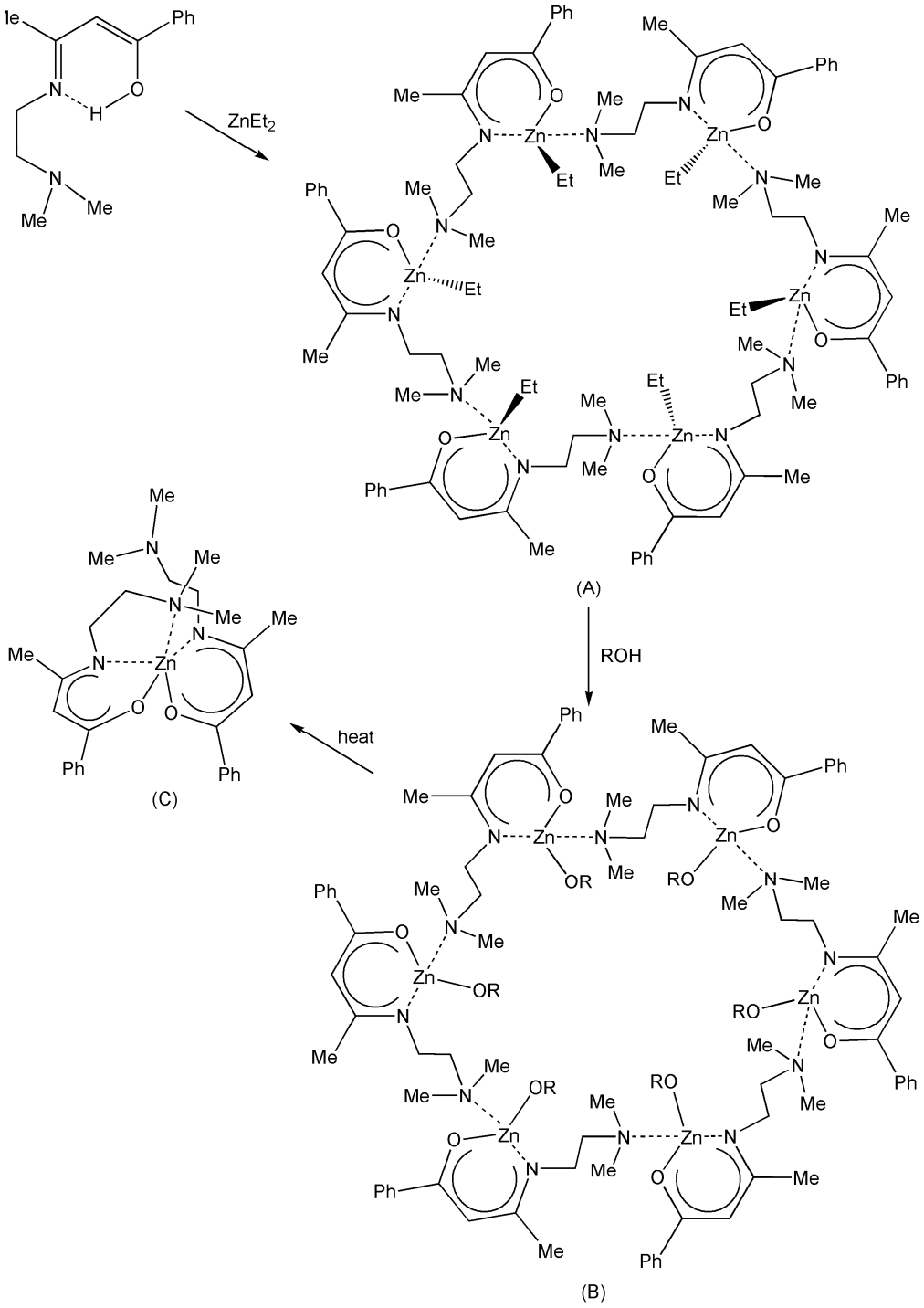

Scheme 21. A variety of zinc β-ketoiminato structures

In this chapter, the coordination preference of the ketoiminato ligands, $RN(H)(C(Me))_2C(Me)=O$, (R = Dipp), L^1 and $RN(H)C(Me)CHC(Me)=O$, (R =

$C_2H_4NEt_2$), L^2 (Figure 36), have been investigated with a range of d and p block metal halides and alkyls, to compare and contrast the outcome obtained from the bulky ketoiminato ligand, L^1, versus the more flexible, but multi-dentate, L^2.

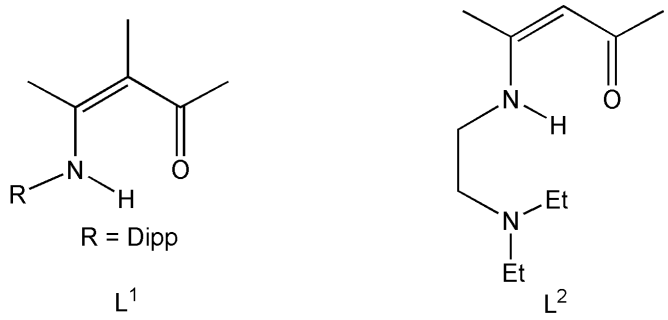

Figure 36. Chemical representation of the ketiminato ligands L^1 and L^2.

In particular, we chose to target elements that have proved successful with nacnac and have garnered useful biological or technological applications.[159] The bidentate ligand, L^1, with a bulky substituent on one side can protect the metal center while keeping the other side open to increase activity of the metal complexes. The pendant arm of ligand L^2 is postulated to be advantageous as can tether and protect metal centers because of the NNO tridentate system and can overcome problems associated with the single sided support of ketoiminato ligands. The complexes obtained have been characterized by X-ray crystallography along with other spectroscopic techniques, including NMR, IR, UV/Vis, and M/S, and show how the preferred metal geometry remains constant for products with either ligand, but the steric protection offered by the individual ligands governs the nuclearity of the products, affording monomers, dimers and tetramers. Herein we compare and contrast the coordination preferences of L^1 and L^2 with $MnCl_2$, Et_2Zn, $InCl_3$, $GaCl_3$, $SnCl_2$, and $SbCl_3$ affording products ranging from tetrameric cages to simple adducts.

4.2 Results and Discussion

4.2.1 Discussion of [DippN(H){C(Me)}$_2$C(Me)O]SnCl$_2$, 17

The equimolar reaction of the lithiated ligand, L[1], with $SnCl_2$ in THF was performed at –78 ^oC (Scheme 22).

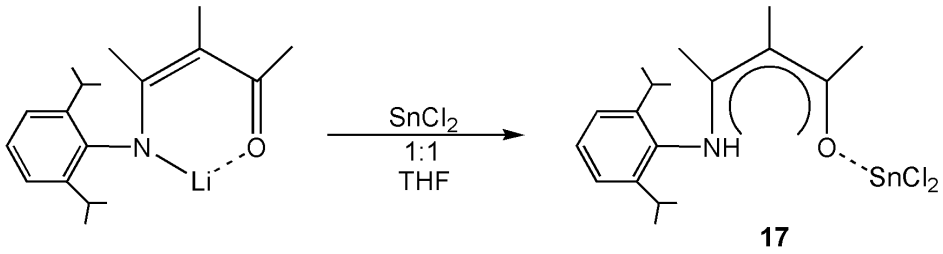

Scheme 22. Synthesis of compound **17**.

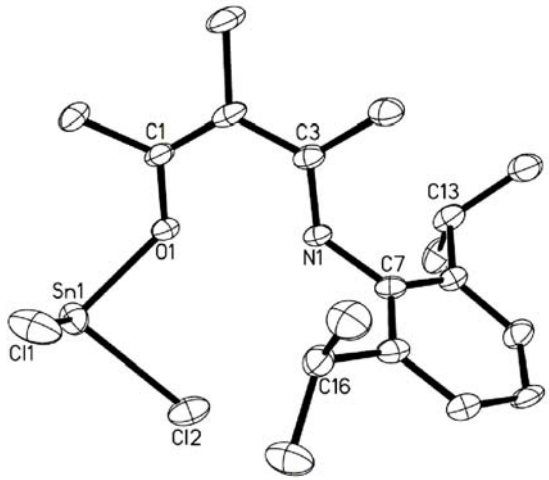

Figure 37. Molecular structure of [DippN(H){C(Me)}$_2$C(Me)O]SnCl$_2$, **17**. Thermal ellipsoids at 30% probability level, hydrogen atoms are omitted for clarity. Selected bond lengths(Å) and angles(^{o}): Sn(1)-O(1) 2.186(5), Sn(1)-Cl(1) 2.446(2), Sn(1)-Cl(2) 2.474(2), O(1)-C(1) 1.332(7), N(1)-C(3) 1.343(8), C(1)-C(2) 1.390(10), C(2)-C(3) 1.457(9), O(1)-Sn(1)-Cl(1) 87.89(14), O(1)-Sn(1)-Cl(2) 83.55(13), Cl(1)-Sn(1)-Cl(2) 96.38(9).

Colorless crystalline blocks were obtained from the reaction in low yield and determined by X-ray crystallography as compound **17** (Figure 37). Despite employing the lithiated reagent, no LiCl displacement was observed in the crystallographic analysis. The isolation of **17** is most likely from an incomplete lithiation reaction. Complex **17** was additionally isolated in higher yield from repeating the reaction of L^1H with $SnCl_2$. The structural features of **17** are unremarkable. The infrared spectra of **17** exhibits a characteristic N–H stretch at 3177 cm^{-1}, which was confirmed by ^1H NMR with a resonance observed at 13.06 ppm.

4.2.2 Discussion of [DippN(H){C(Me)}$_2$C(Me)O]SbCl$_3$, 18[160]

As a continuation of the antimony work with the β-diketiminato ligand,[119] the reaction of the lithiated ligand L^1 with 1.5 equiv. of $SbCl_3$ was performed (Scheme 23).

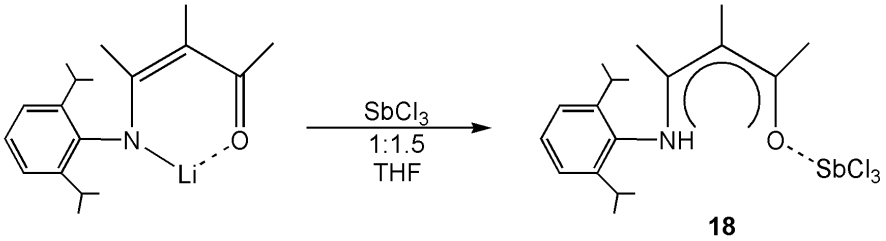

Scheme 23. Synthesis of compound **18**.

As similarly observed in **17**, complex **18** shows no signs of LiCl displacement but rather the solid-state analysis reveals a simple adduct in low yield (Figure 38). Again, the isolation of **18** is likely due to the incomplete lithiation reaction, and indeed a higher yield of the product can be obtained from the direct reaction of L^1H with $SbCl_3$ in THF. Structural parameters of **18** show no exceptional features. The infrared spectra of **18** exhibits a characteristic N–H stretch at 3185 cm^{-1}, which is confirmed by ^1H NMR with a

resonance observed at 12.84 ppm.[161] Isolation of the [L^1SbCl_2] product with concomitant loss of LiCl could not be achieved despite the facile syntheses of the related analogues nacnacSb complexes.[119]

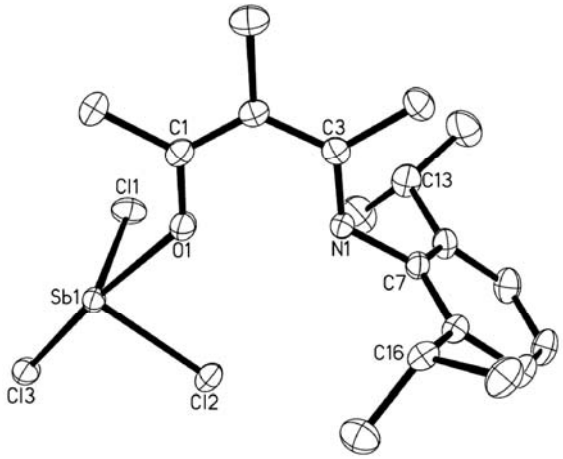

Figure 38. Molecular structure of [DippN(H){C(Me)}$_2$C(Me)O]$SbCl_3$, **18**. Thermal ellipsoids at 30% probability level, hydrogen atoms are omitted for clarity. Selected bond lengths(Å) and angles(^{o}): Sb(1)-O(1) 2.329(2), Sb(1)-Cl(1) 2.349(8), Sb(1)-Cl(2) 2.375(8), Sb(1)-Cl(3) 2.508(8), O(1)-C(1) 1.296(4), N(1)-C(3) 1.327(4), C(1)-C(2) 1.394(4), C(3)-C(2) 1.416(4), O(1)-Sb(1)-Cl(1) 84.84(7), O(1)-Sb(1)-Cl(2) 81.35(6), O(1)-Sb(1)-Cl(3) 170.2(6), Cl(1)-Sb(1)-Cl(2) 95.76(3), Cl(1)-Sb(1)-Cl(3) 88.96(3), Cl(2)-Sb(1)-Cl(3) 91.76(3).

4.2.3 Discussion of [$Et_2NC_2H_4NC(Me)CHC(Me)O]SbCl_2$, 19[160]

By contrast to complex **18**, the *in situ* lithiation of L^2 and subsequent reaction with $SbCl_3$, yields complex **19**, [L^2SbCl_2] (Scheme 24). Following work up of the reaction mixture, the THF solution resulted in colorless chunk crystals isolated in low yield.

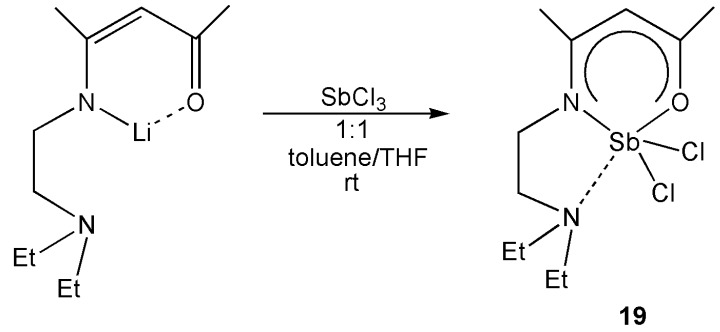

Scheme 24. Synthesis of compound **19**.

The solid-state analysis revealed complex **19** crystallizes in the monoclinic space group $P2_1/c$ (Figure 39). The geometry around the antimony center is square pyramidal, with the lone pair occupying the vacant site. In complex **19**, the nitrogen atom on the pendant arm forms a dative bond to the Sb center, with a Sb–N bond length of 2.481(2) Å, which is longer the Sb–N bond lengths of 2.084(18) Å and 2.092(2) Å observed in [(Mesnacnac)$SbCl_2$], complex **3**, as well as the covalent radii, 2.1 Å, but shorter than the sum of the van der waals radii, 3.55 Å.[162] The O(1)–C(1), N(1)–C(3), C(1)–C(2), and C(2)–C(3) bond distances, 1.296(3) Å, 1.316(3) Å, 1.362(4) Å, and 1.408(4) Å respectively, are indicative of delocalization across the NCCCO backbone. Additionally, the bond angles around the antimony center exhibit the distorted square pyramidal geometry and selected bond angles can be observed for complex **19**. Solution ^{1}H and ^{13}C NMR confirmed the X-ray crystal structure, and infrared spectroscopy shows characteristic CO and CN stretching bands at 1613 and 1521 cm^{-1}.

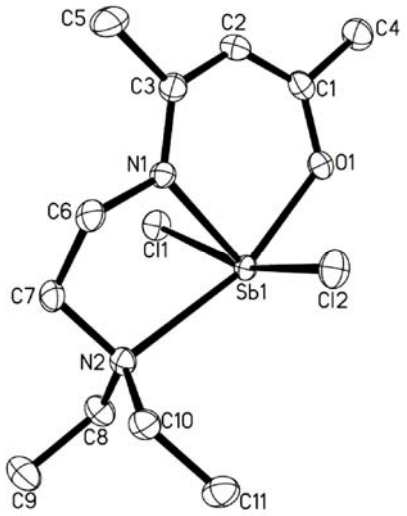

Figure 39. Molecular structure of $[Et_2NC_2H_4NC(Me)CHC(Me)O]SbCl_2$, **19**. Thermal ellipsoids at 30% probability level, hydrogen atoms are omitted for clarity. Selected bond lengths(Å) and angles(°): Sb(1)-O(1) 2.093(18), Sb(1)-N(1) 2.144(2), Sb(1)-N(2) 2.481(2), Sb(1)-Cl(1) 2.588(7), Sb(1)-Cl(2) 2.564(7), O(1)-C(1) 1.296(3), N(1)-C(3) 1.316(3), C(1)-C(2) 1.362(4), C(2)-C(3) 1.408(4), O(1)-Sb(1)-N(1) 87.23(8), O(1)-Sb(1)-N(2) 163.2(7), O(1)-Sb(1)-Cl(2) 87.15(6), N(2)-Sb(1)-Cl(2) 93.03(5), N(2)-Sb(1)-Cl(1) 89.65(5).

4.2.4 Discussion of $[DippN\{C(Me)\}_2C(Me)O]_2InCl$, 20[160]

To further examine the coordination preferences of the ligand L^1 with metal halides, $InCl_3$ was selected for reaction. There is increasing interest in organoindium complexes because of their potential use as CVD precursors for the production of III–V and III–VI composite semiconductors.[39,163] More recently, work has been focused on indium complexes supported by oxygen ligands as these are potentially useful for the preparation of In_2O_3 thin films, which are used as transparent conductors in applications such as display panels and solar cell windows.[164] Since homoleptic β-diketonates have

been successfully employed for this purpose,[165] we deemed that L^1 might also prove a useful precursor. The THF reaction of L^1Li with $InCl_3$ in a 1:1 ratio was performed at room temperature (Scheme 24). However, upon the failure to acquire the $[L^1SnCl_2]$ and $[L^1SbCl_3]$ products due to isolation of the incomplete lithiated ligand, L^1 was lithiated *in situ* at 0 ^oC and added to $InCl_3$ after stirring for 2 h.

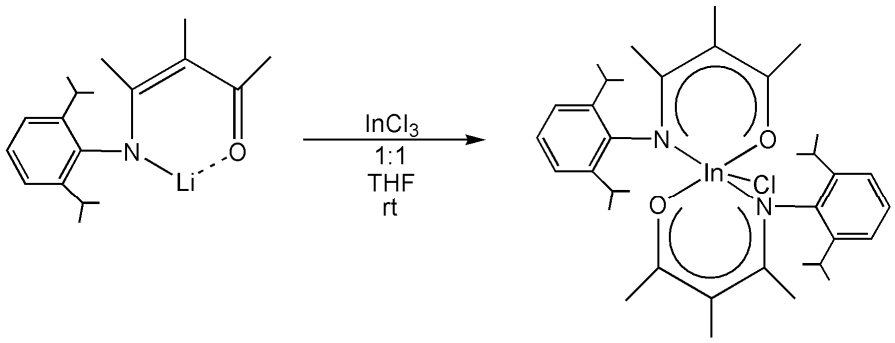

20

Scheme 25. Synthesis of compound **20**.

Colorless crystalline blocks of **20** were isolated in moderate yield, and the molecular structure was determined by X-ray crystallography (Figure 40). The reaction of L^1Li with $InCl_3$ at room temperature or low temperature affords an In(III) structure featuring two ligand molecules on one indium center and a terminal halide. The indium center is found to adopt distorted trigonal bipyramidal geometry which is typical for five coordinate indium derivatives.[166] In **20**, the nitrogen and oxygen bond lengths to the In metal center lie at 2.177(2) Å, 2.184(2) Å, 2.087(2) Å, and 2.090(2) Å for In(1)–N(1), In(1)–N(2), In(1)–O(1), and In(1)–O(2) respectively, and are similar to the covalent radii of 2.19 Å for In–N and 2.08 Å for In–O.[162] The bond lengths across the NCCCO backbones range from 1.294(4)–1.431(4) Å and again indicate charge delocalization. The distorted trigonal bipyramidal geometry around the In(III) center can be observed from

the bond angles which range from 83.96(8)° to 127.3(9)°. The positive-mode LRMS spectrum of **20** exhibits a parent peak at *m/z* = 695.2. The solid-state structure is further confirmed by the IR spectra of complex **20** which displays the characteristic peaks expected.[39,167,168] The NMR suggests that the structure is the same in the solid-state as in solution as no metal decomposition is observed in solution, as is also true for other N–N and N–O coordinated complexes discussed here. This is likely due to the N–O or N–N chelation which is strong enough to maintain structural integrity in solution.

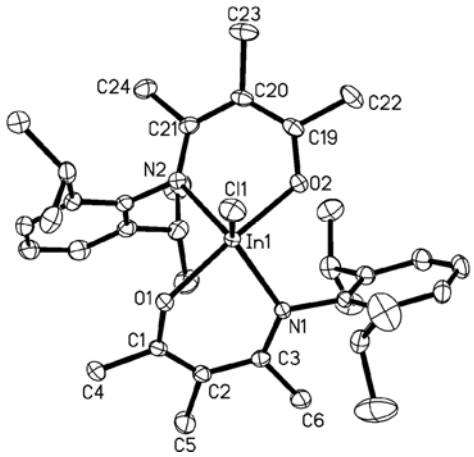

Figure 40. Molecular structure of [DippN{C(Me)}$_2$C(Me)O]$_2$InCl, **20**. Thermal ellipsoids at 30% probability level, hydrogen atoms are omitted for clarity. Selected bond lengths(Å) and angles(°): In(1)-O(1) 2.087(2), In(1)-O(2) 2.090(2), In(1)-N(1) 2.177(2), In(1)-N(2) 2.184(2), In(1)-Cl(1) 2.378(9), O(1)-C(1) 1.296(3), N(1)-C(3) 1.333(4), C(1)-C(2) 1.386(4), C(3)-C(2) 1.427(4), O(2)-C(19) 1.294(4), N(2)-C(21) 1.327(4), C(20)-C(19) 1.382(5), C(21)-C(20) 1.431(4), O(1)-In(1)-O(2) 167.4(9), O(1)-In(1)-N(1) 83.96(8), O(1)-In(1)-N(2) 92.83(9), O(2)-In(1)-N(1) 88.78(8), O(2)-In(1)-N(2) 83.45(9), O(1)-In(1)-Cl(1) 95.73(6), O(2)-In(1)-Cl(1) 96.80(7), N(1)-In(1)-Cl(1) 123.6(7), N(2)-In(1)-Cl(1) 109.0(7), N(1)-In(1)-N(2) 127.3(9).

4.2.5 Discussion of $[Et_2NC_2H_4NC(Me)CHC(Me)O]InCl_2$, 21[160]

In addition to the formation of complex **20**, we aimed to synthesize the analogous indium complex with L^2. Thus, *in situ* lithiation of L^2 and subsequent reaction with $InCl_3$ in THF at room temperature led to complex **21**, $[L^2InCl_2]$ (Scheme 26). Following work up of the reaction mixture in toluene, colorless plates were isolated in moderate yield and crystallize in the monoclinic space group C_c.

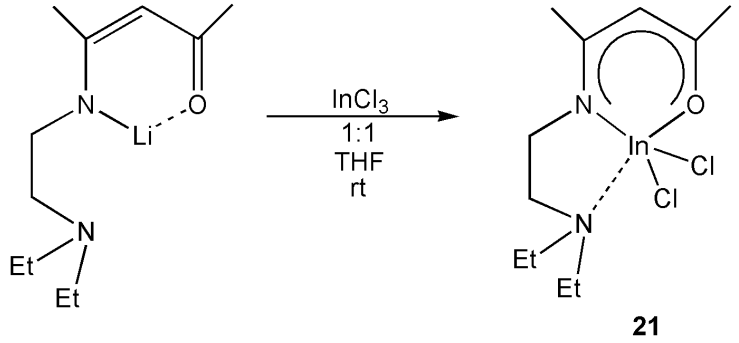

Scheme 26. Synthesis of compound **21**.

The molecular structure of **21** was determined by X-ray crystallography (Figure 41). The indium atom adopts a distorted trigonal bipyramidal geometry, which was also observed for the analogous complex **20**, $[DippN\{C(Me)\}_2C(Me)O]_2InCl$, and is typical for five coordinate indium derivatives.[166] In comparing both **20** and **21**, similar molecular geometries in the structures can be observed. The solid-state analysis for complex **21** reveals that the resultant product has one ligand molecule and two terminal halides. The formation of **21** can in part be attributed to the preferred trigonal bipyramidal geometry of the indium atom, and by the presence of the coordinating 'arm', which is able to occupy vacant coordination sites and prevent further ligand coordination.

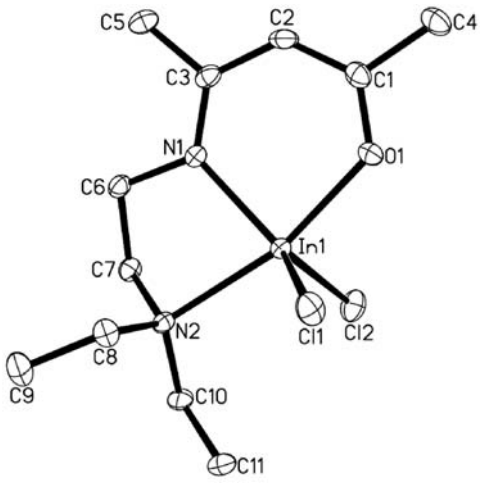

Figure 41. Molecular structure of $[Et_2NC_2H_4NC(Me)CHC(Me)O]InCl_2$, **21**. Thermal ellipsoids at 30% probability level, hydrogen atoms are omitted for clarity. Selected bond lengths(Å) and angles(°): In(1)-O(1) 2.119(2), In(1)-N(1) 2.152(3), In(1)-N(2) 2.337(3), In(1)-Cl(1) 2.381(11), In(1)-Cl(2) 2.381(10), O(1)-C(1) 1.288(5), N(1)-C(3) 1.331(5), C(1)-C(2) 1.373(6), C(3)-C(2) 1.419(6), O(1)-In(1)-N(1) 87.64(11), O(1)-In(1)-N(2) 165.9(13), N(1)-In(1)-N(2) 78.31(13), O(1)-In(1)-Cl(1) 91.82(9), O(1)-In(1)-Cl(2) 92.56(9), N(1)-In(1)-Cl(2) 118.8(9).

In complex **21** the nitrogen atom on the pendant arm forms a dative bond to the In center, with a In–N bond length of 2.337(3) Å, which is slightly longer than the N→In interaction of 2.466(1) Å in $[In(Me)_2(amak)]_2$ where amak = $OC(CF_3)_2CH_2NHR$, R = $(CH_2)_2OMe$ or $Me_2In(C_6H_4CH_2NMe_2)$ of 2.38(1) Å.[39] This bond length is also longer than the sum of the covalent radii, 2.19 Å, of N(sp^3) and O.[169] Complex **21** is structurally similar to that of $[InMe_2(keim)]$ where keimH is a tridentate ketoimine ligand of structural formula $OC(CF_3)CHC(CF_3)=NCH_2CH_2NMe_2$, which also has a long interaction of 2.428(2) Å from the pendant nitrogen atom to the trigonal bipyramidal

indium atom.[167] The IR spectra of complex **21** displays the characteristic peaks expected for C=O, C=C, C–N at 1577, 1557, and 1520 cm^{-1}, respectively.[39,167,168]

4.2.6 Discussion of $[Et_2NC_2H_4NC(Me)CHC(Me)O]GaCl_2$, 22

Additionally within group 13, we aimed to synthesize the analogous gallium complex with L^2. Therefore *in situ* lithiation of L^2 and subsequent reaction with $GaCl_3$ in THF at room temperature led to complex **22**, $[L^2GaCl_2]$ (Scheme 27). Following work up of the reaction mixture in toluene, pale yellow plates were isolated and crystallize in the monoclinic space group $P2_1/c$.

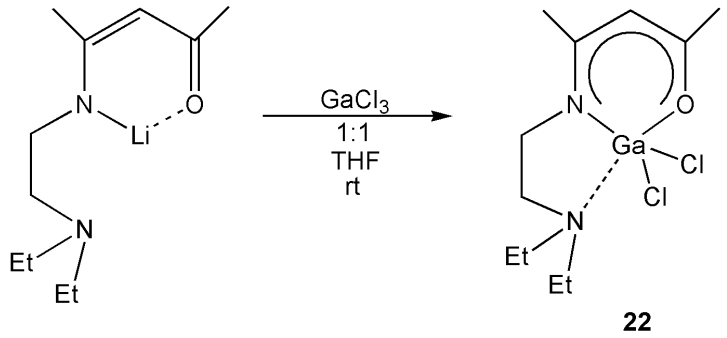

Scheme 27. Synthesis of compound **22**.

The molecular structure of complex **22** was determined by X-ray crystallography and revealed a Ga(III) center coordinated in an analogous manner to **19** and **21** (Figure 42). The geometry around the gallium center adopts distorted trigonal bipyramidal geometry where one ligand molecule is present as well as two terminal chlorides displaying the loss of LiCl during the reaction. The coordinating 'arm' is occupying the vacant coordination site preventing further ligand coordination. A dative bond is formed from the nitrogen atom of the pendant arm to the Ga center, with a Ga–N bond length of 2.229(5) Å, which is longer than the sum of the covalent radii, 1.9 Å, but shorter than the

sum of the van der waals radii, 3.42 Å.[162] The O(1)–C(1), C(2)–C(1), C(3)–C(2), and N(1)–C(3) bond distances, 1.291(7) Å, 1.376(9) Å, 1.396(9) Å, and 1.334(7) Å respectively, indicate delocalized π bonding across the NCCCO backbone. Additionally, the bond angles around the gallium center exhibit the distorted trigonal bipyramidal geometry where the O(1)–Ga(1)–N(2) bond angle lies at 171.2(18)^{o} as compared to the expected 180^{o}, while the remaining bond angles range from 80.56(19)^{o} to 124.6(14)^{o}.

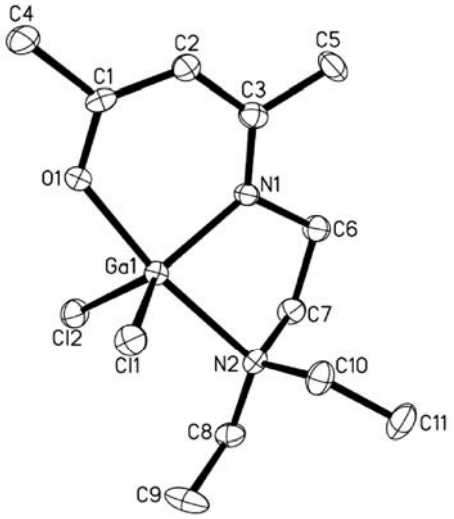

Figure 42. Molecular structure of $[Et_2NC_2H_4NC(Me)CHC(Me)O]GaCl_2$, **22**. Thermal ellipsoids at 30% probability level, hydrogen atoms are omitted for clarity. Selected bond lengths(Å) and angles(^{o}): Ga(1)-O(1) 1.954(4), Ga(1)-N(1) 1.966(5), Ga(1)-N(2) 2.229(5), Ga(1)-Cl(1) 2.216(16), Ga(1)-Cl(2) 2.210(17), O(1)-C(1) 1.291(7), N(1)-C(3) 1.334(7), C(2)-C(1) 1.376(9), C(3)-C(2) 1.396(9), O(1)-Ga(1)-N(1) 90.71(18), O(1)-Ga(1)-N(2) 171.2(18), N(1)-Ga(1)-N(2) 80.56(19), O(1)-Ga(1)-Cl(1) 91.44(14), O(1)-Ga(1)-Cl(2) 91.70(14), N(1)–Ga(1)–Cl(1) 124.6(14), N(1)-Ga(1)-Cl(2) 121.4(14).

Solution ^{1}H and ^{13}C NMR confirmed the X-ray crystal structure of complex **22**, along with the IR spectra displaying characteristic peaks for C=O, C=C and C–N

stretching bands at 1610, 1572, and 1531 cm^{-1}. The UV/Vis of **22** is characteristic of the oxidation state of the gallium complex; with λ_{max} observed at 230 (ε = 2756 cm^{-1} mol^{-1} dm^3) and 318 nm (ε = 7940 cm^{-1} mol^{-1} dm^3) comparing well to the corresponding gallium(III)/L complex species, where L = 4-(N),10-(N)-bis[2-(3-hydroxo-2-oxo-2-*H*-pyridine-1-yl)acetamido]-1,7-dimethyl-1,4,7,10-tetraazacyclododecan.[170] The lower energy level bands are attributed to the n→π* electronic transitions.

4.2.7 Discussion of $[Et_2NC_2H_4NC(Me)CHC(Me)O]ZnEt$, 23[160]

Moving across the periodic table, the reaction of L^2 with diethyl zinc was performed. β-Diketoiminato complexes with zinc[169] have been studied extensively for their catalytic ability and, as a result, has extended the investigation to ketoiminato ligands.[140,171] The equimolar, neat addition of $ZnEt_2$ to L^2H in toluene at room temperature afforded colorless needles of complex **23** which was determined by X-ray crystallography to crystallize in the tetragonal space group I–4 (Scheme 28).

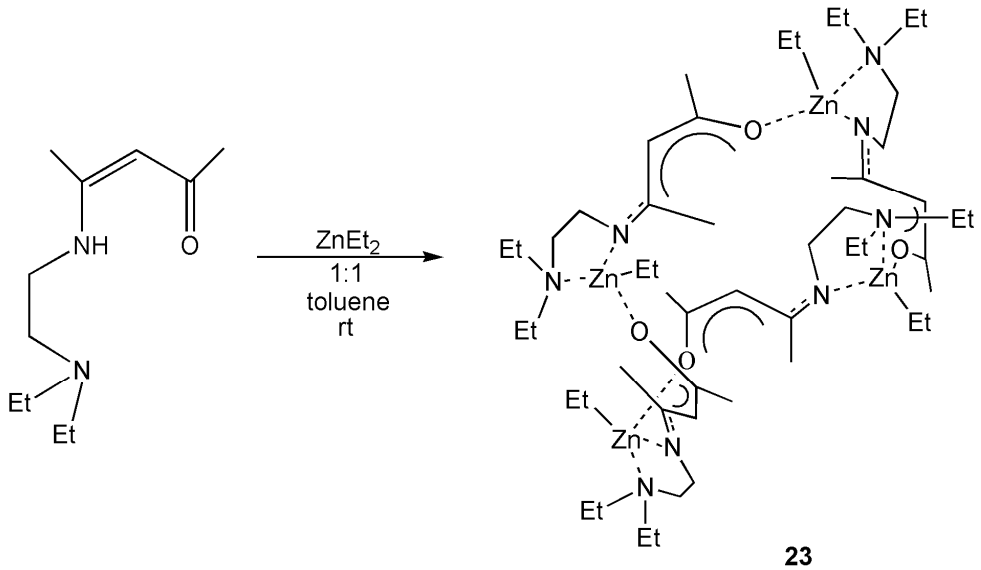

Scheme 28. Synthesis of compound **23**.

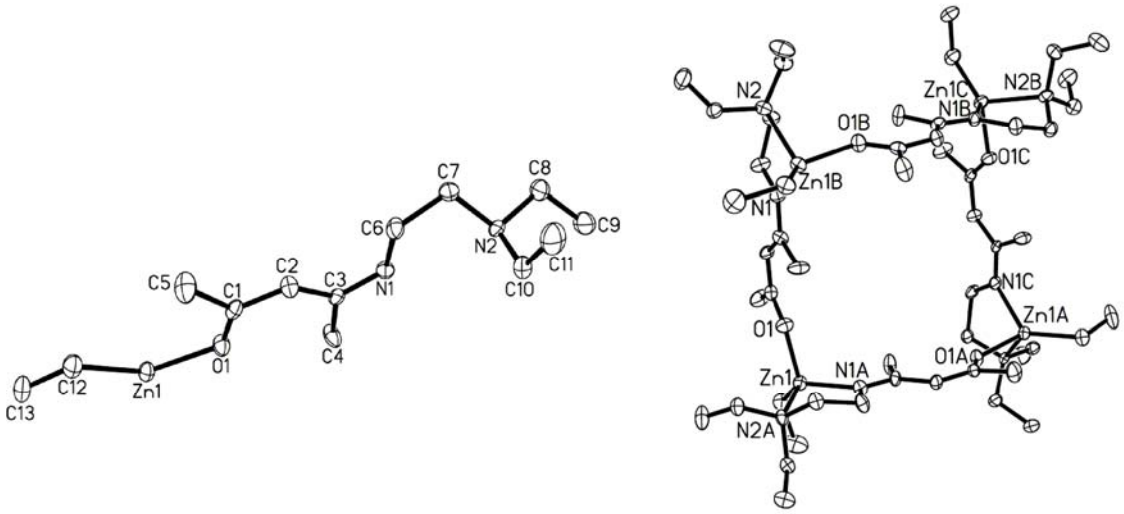

Figure 43. Molecular structure of $[Et_2NC_2H_4NC(Me)CHC(Me)O]ZnEt$, **23**. Displayed on the left side is the asymmetric unit and on the right side the tetrameric product. Thermal ellipsoids at 30% probability level, hydrogen atoms are omitted for clarity. Selected bond lengths(Å) and angles(^{o}): Zn(1)-O(1) 2.024(3), Zn(1)-N(1)#1 2.055(4), Zn(1)-N(2)#1 2.156(4), N(1)-C(3) 1.321(4), N(1)-C(6) 1.443(6), N(2)-C(7) 1.488(5), O(1)-C(1) 1.268(5), C(2)-C(1) 1.395(5), C(3)-C(2) 1.428(6), C(3)-C(4) 1.481(7), C(12)-Zn(1)-O(1) 124.1(17).

Structural analysis revealed that the zinc atom is able to achieve a coordination number of four giving rise to distorted tetrahedral geometry around the zinc center (Figure 43). As has been previously observed in reactions of nacnac,[119,121,133,137,172] ligand rearrangement has occurred, which is believed to arise from the presence of additional donor atoms that become involved in intramolecular coordination affording complex structures. The solid-state analysis of **23** revealed four Zn^{2+} cations that occupy the corners of a molecular square or wheel with each ligand acting as a bridge between the metal centers to form an edge. Within the asymmetric unit of **23** are one Zn^{2+} and one

molecule of rearranged ligand. An ethyl group retained on the zinc atom balances the cationic charge along with a -1 charge associated with the ligand. Two nitrogen atoms and a dative oxygen interaction occupy the remaining tetrahedral coordination sites around each zinc atom. Examination of the bond lengths and angles in **23** suggests delocalization of the negative charge over the ligand backbone. The Zn–O bonds are within normal values, 2.028(5)–2.076(6) Å,[173] and correspond to dative bonds.[174,175] The Zn–N bonds vary from 2.055(4)–2.156(4) Å and are comparable to reported Zn–N bonds.[6l,140,171,176] The solid-state analysis is confirmed by solution NMR where the ^{1}H NMR spectrum exhibits an indicative single peak associated with the C–H on the backbone at 4.89 ppm. This value can be similarly compared to a slightly downfield C–H backbone shift of 5.45 ppm that was observed in a related zinc β-ketoiminato complex where a macrocycle structure of six units formed.[35] The IR bands of **23** are also similar to those previously reported[6l,22,24d,42,139,169,175] occurring at 1585 (C=O), 1509 (C=C), and 1412 cm^{-1} (C–N). The tetrameric outcome of the reaction of L^2 with $ZnEt_2$ is not too surprising given that zinc alkoxides readily give rise to zinc tetramers that often feature a distorted cubic Zn_4O_4.[175] The degree of association is dependent on ligand size and decreases with increasing bulk resulting in dimers, trimers, or monomers.[177] Thus, the bulkier ligand L^1 can stabilize a monomeric species, whereas the less bulky ligand L^2, yields a tetramer as observed by complex **23**. The distances within the core from each zinc atom are ~7.77 Å. These distances can be compared to related documented systems of 11.11 Å or 8.6 Å as observed in the tetramers, $[Zn_4H_8L^1{}_4][PF_6]_5[NO_3]_2\cdot S$ and $[Zn_4H_8L^2{}_4][PF_6]_6[NO_3]_2\cdot S$ (L = bistridentate Schiff base ligands, S = solvent).[178] Within the tetrameric core are channels that are estimated to be about 494.6 Å^3, that correlates to

about 14.3% of the crystal volume, calculated by PLATON.[179] The identity of a solvent within the channel could not be resolved by X-ray crystallography and was omitted from the final refinement by SQUEEZE.[179] The unidentified solvent is believed to be a disordered water molecule which was confirmed by spectroscopic techniques.[180] Confirmatory evidence that water is the unresolved solvent molecule in the channels of **23** is observed by solution NMR where ^{1}H NMR exhibited a distinctive singlet peak at 1.86 ppm that integrated to two protons. The positive-mode mass spectrum of **23** further confirmed the presence of the water molecule with a peak at *m/z* = 309.3 followed by sequential loss of the water molecule to give a peak at *m/z* = 292 representing the asymmetric unit of **23**. The cause of water contamination is not confirmed but is most likely from atmospheric water contamination during the reaction, as has been seen with related zinc systems.[181-183] Attempts to achieve elimination of two ethane molecules through the 2:1 reaction were unsuccessful and resulted in an oily residue. Crystals of complex **23** decompose rapidly on exposure to air.

4.2.8 Discussion of $[Et_2NC_2H_4NC(Me)CHC(Me)O]MnCl–ClLi(thf)_2$, 24[160]

In keeping with our original goal of targeting specific elements, manganese coordination chemistry has become increasingly interesting,[184,185] stemming from the involvement of Mn in several biological redox active systems. Of particular interest is the oxygen evolving complex of photosystem II which is believed to be a tetranuclear Mn aggregate with NO donors.[184] The equimolar, room temperature reaction of L^2Li with $MnCl_2$ afforded complex **24**, a monomeric Mn^{2+} complex in moderate yield (Scheme 29).

The resulting pale yellow chunks crystallize in the monoclinic space group $P2_1/n$ (Figure 44).

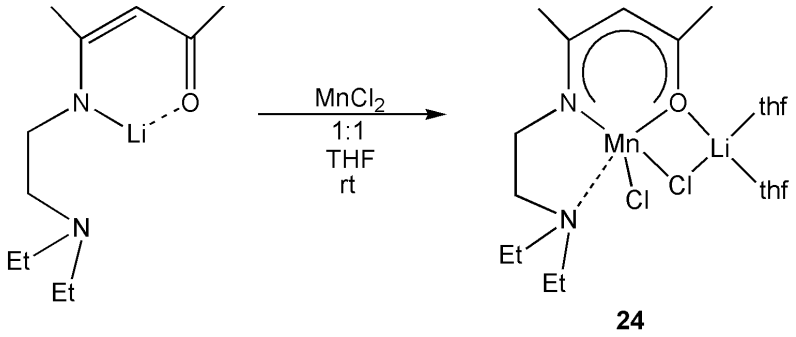

Scheme 29. Synthesis of compound **24**.

Due to employing the lithiated salt as the reactant, crystallographic analysis revealed incorporation of LiCl in the final product; a common occurrence in transition metal chemistry.[186] In complex **24**, the manganese atom adopts five coordinate, trigonal bipyramidal geometry, with Mn–Cl bonds of 2.370(9) Å and 2.453(9) Å which are comparable to related Mn–Cl systems. The latter, longer, Mn–Cl distance is associated with the bridged Cl, coordinated to the Li center. The bond lengths 2.144(2) Å and 2.154(2) Å for Mn(1)–O(1) and Mn(1)–N(1) are within the appropriate values for normal bonds, and similar to other manganese(II) examples, i.e. Mn–N bond lengths of 2.050(1) Å and 2.096(1) Å,[187b] as well as with the covalent radii for Mn–O and Mn–N to be 2.12 Å and 2.14 Å, respectively.[162] The Mn(1)–N(2) bond distance of 2.337(2) Å indicates a dative bond interaction, as similarly observed for the M–N(2) (where M = Sb, In) in complexes **19** and **21**.

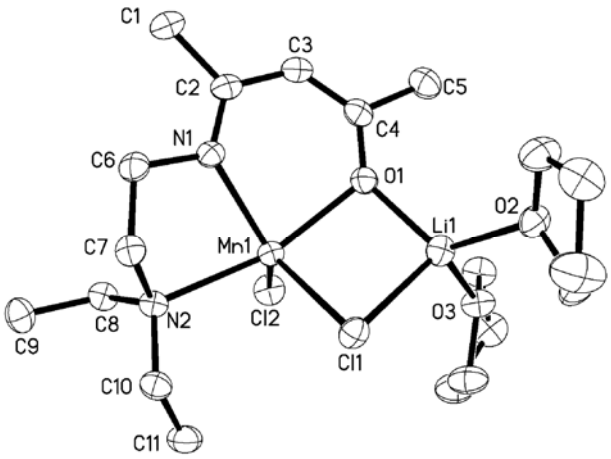

Figure 44. Molecular structure of $[Et_2NC_2H_4NC(Me)CHC(Me)O]MnCl–ClLi(thf)_2$, **24**. Thermal ellipsoids at 30% probability level, hydrogen atoms are omitted for clarity. Selected bond lengths(Å) and angles(°): Mn(1)-O(1) 2.144(2), Mn(1)-N(1) 2.154(2), Mn(1)-N(2) 2.337(2), Mn(1)-Cl(1) 2.453(9), Mn(1)-Cl(2) 2.370(9), Cl(1)-Li(1) 2.398(5), Li(1)-O(1) 1.895(6), N(1)-C(2) 1.306(4), O(1)-C(4) 1.294(4), C(2)-C(3) 1.428(4), C(3)-C(4) 1.360(5), O(1)-Mn(1)-N(1) 83.53(8), O(1)-Mn(1)-N(2) 159.0(8), N(1)-Mn(1)-N(2) 77.95(9), O(1)-Mn(1)-Cl(1) 85.47(6), N(2)-Mn(1)-Cl(1) 96.37(6), N(1)-Mn(1)-Cl(2) 122.1(7).

The UV/Vis of **24** is characteristic of the oxidation state of the manganese complex; with λ_{max} observed at 230 and 310 nm which compares well to the corresponding manganese(II) β-diketoiminato complex values of 231 and 376 nm.[187b] The significantly high ε value of 17,400 is indicative of a charge transfer transition.[22,24d,42,169] By comparison, the maxima observed for manganese(III) complexes have been reported in the range of 321–328 nm for examples including $[DippN\{C(Me)\}_2C(Me)O]_2MnCl$[160] and three (pyrrolidine salen)Mn(III) complexes (also of the formula $[(RNO)_2MnCl]$).[187a]

4.3 Summary

A series of metal complexes have been prepared using two similar ketoiminato ligands, $RN(H)(C(Me))_2C(Me)=O$, (R = Dipp), L^1 and the less bulky, multidentate molecule $RN(H)C(Me)CHC(Me)=O$, ($R = C_2H_4NEt_2$), L^2. The X-ray crystallographic analysis on complexes **17**–**24** revealed that the preferred metal geometry predominates in the solid-state; however it is the steric preferences of the ligand that govern the nuclearity of the product. This can be exemplified by the variety of products synthesized ranging from adducts for tin and antimony complexes **17** and **18**; monomers for antimony, indium, gallium, and manganese complexes **20**, **21**, **22**, and **24**; dimers for the indium complex **19**; and a tetrameric cage for the zinc complex **23**. Reaction conditions including stoichiometry, temperature, and ligand lithiation were selected and observed throughout each particular reaction.

4.4 Experimental

4.4.1 General Procedures

THF was dried over potassium and degassed before use, while toluene was dried using an MBraun-SPS solvent purification system. The reagents were handled in a nitrogen filled M-Braun drybox. All manipulations were performed under anaerobic conditions using standard Schlenk techniques. The reagents *n*-BuLi (2.5 M in hexanes), $MnCl_2$, $ZnEt_2$ (1.0 M in hexanes), $InCl_3$, $GaCl_3$, and $SbCl_3$ were purchased from Aldrich and $SnCl_2$ was purchased from Acros Organics and used as received. The ligands $RN(H)(C(Me))_2C(Me)=O$, (R = Dipp), L^1, and $RN(H)(C(Me)CHC(Me)=O$, (R = $C_2H_4NEt_2$), L^2, and the corresponding lithium salts were prepared according to published procedures.[34,45]

4.4.2 Spectroscopy Measurements

The ^1H and ^{13}C NMR spectra were recorded on a Varian Mercury 300 spectrometer (^1H 300.05 MHz and ^{13}C 75.45 MHz). IR analysis was conducted as Nujol Mulls with NaCl plates on a MIDAC M4000 Fourier transform infrared (FT IR) spectrometer. Ultraviolet-visible absorption spectra were recorded on an Agilent 8453 UV/Vis spectrometer. Mass spectrometry analysis was carried out using a Bruker Esquire 6000 Mass Spectrometer. Melting points were determined in capillaries under a nitrogen atmosphere and are uncorrected.

4.4.3 Experimental Procedures and Spectroscopic Data

Preparation of [DippN(H){C(Me)}$_2$C(Me)OSnCl$_2$], 17: A 20 mL THF solution of L^{1}Li (0.25 g, 0.90 mmol) was added dropwise at –78 ^{o}C to a stirred 20 mL THF solution of $SnCl_2$ (0.17 g, 0.90 mmol). The resulting pale yellow solution was immediately removed from the dry-ice bath and allowed to warm to ambient temperature. Stirring was maintained overnight. Following the removal of THF *in vacuo*, the pale yellow solid was extracted into toluene and filtered. Concentration under reduced pressure of the toluene solution and storage at room temperature afforded colorless blocks of **17**. Yield: 0.12 g, 29%. M.p. 132–137 ^{o}C (decomp). ^{1}H NMR ($CDCl_3$, 25 ^{o}C): δ (ppm) 1.06–1.12 (m, 12H, CH(C*H*$_3$)$_2$), 1.65 (s, 3H, C*Me*), 1.85 (s, 3H, C*Me*), 2.19 (s, 3H, C*Me*), 2.91 (septet, 2H, $^1J_{H\text{-}H}$ = 6.8 Hz, C*H*(CH$_3$)$_2$), 7.10 (d, 2H, J = 7.2 Hz, *m*–H$_{aryl}$), 7.21 (t, 1H, $^1J_{H\text{-}H}$ = 7.8 Hz, *p*–H$_{aryl}$), 13.06 (s, 1H, NH); ^{13}C NMR ($CDCl_3$, 25 ^{o}C): δ (ppm) 13.7 (C*Me*), 15.8 (C*Me*), 21.7 (CH(*C*H$_3$)$_2$), 23.5 (CH(*C*H$_3$)$_2$), 27.0 (*C*H(CH$_3$)$_2$), 27.4 (C*Me*), 97.9 (γ-*C*), 122.5 (C$_m$), 126.9 (C$_p$), 133.0 (C$_o$), 145.0 (Ar*C*–N), 162.2 (*C*N), 193.7 (*C*O); IR (υ cm^{-1}, Nujol mull): 3177 (shoulder, N–H stretch), 1602 m, 1560 m; MS (*m/z*; (found (calcd)): 464.4 (463.0) M$^+$; 434.5 (433.0) M – 2Me; 420.3 (418.0) M – 3Me; 280.2 (276.2) M – 2Me – 2^{i}Pr – 2Cl.

Preparation of [DippN(H){C(Me)}$_2$C(Me)O]SbCl$_3$, 18: A 20 mL THF solution of L^{1}Li (0.25 g, 0.90 mmol) was added dropwise at –78 ^{o}C to a stirred 20 mL THF solution of $SbCl_3$ (0.31 g, 1.3 mmol). The resulting yellow solution was immediately removed from the dry-ice bath and allowed to warm to ambient temperature. Stirring was maintained overnight. Following the removal of THF *in vacuo*, the pale orange solid was extracted

into toluene and filtered. Repeated filtration, concentration, and storage at room temperature for two weeks afforded colorless plate crystals of **18** in moderate yield. Yield: 0.30 g, 67%. M.p. 149–152 ^{o}C. ^{1}H NMR ($CDCl_3$, 25 ^{o}C): δ (ppm) 1.02–1.23 (m, 12H, CH(CH_3)$_2$), 1.78 (s, 3H, C*Me*), 1.88 (s, 3H, C*Me*), 2.27 (s, 3H, C*Me*), 2.83 (septet, 2H, $^{1}J_{H\text{-}H}$ = 6.8 Hz, C*H*(CH_3)$_2$), 7.14–7.31 (m, 3H, H$_{aryl}$), 12.84 (s, 1H, NH); ^{13}C NMR ($CDCl_3$, 25 ^{o}C): δ (ppm) 13.6 (C*Me*), 16.8 (C*Me*), 21.8 (CH(*C*H_3)$_2$), 23.5 (CH(*C*H_3)$_2$), 25.4 (*C*H(CH_3)$_2$), 27.6 (C*Me*), 99.1 (γ-*C*), 122.9 (C_m), 127.9 (C_p), 131.7 (C_o), 144.4 (Ar*C*–N), 167.7 (*C*N), 189.9 (*C*O); IR (Nujol Mull): ν (cm^{-1}) 3185 (shoulder, N-H stretch), 1575 (m), 1170 (m); MS (*m/z*; (found (calcd)): 500.4 (501.5) M^+; 380.4 (380.1) M – 3Cl – Me; 274.3 (273.4) M – $SbCl_3$.

Preparation of [$Et_2NC_2H_4$NC(Me)CHC(Me)O]$SbCl_2$, 19: A –78 ^{o}C diethyl ether (20 mL) solution of L^{2}H (1.5 g, 7.5 mmol) had 1 equiv. of *n*-BuLi (3.0 mL of a 2.5 M solution, 7.5 mmol) added drop-wise. After stirring for 2 h at –78 ^{o}C, the reaction was allowed to warm to room temperature slowly and stirred overnight. The solvent was then removed and 30 mL of toluene added. The toluene solution was then slowly added by cannula to a stirred suspension of $SbCl_3$ (1.7 g, 7.5 mmol) in a 30 mL toluene-THF mixture at room temperature. The initial yellow reaction gradually turned dark orange and was allowed to stir overnight. Following the removal of solvent *in vacuo*, the dark orange-red solid was extracted into THF and filtered. Concentration under reduced pressure and storage at –30 ^{o}C afforded colorless crystalline chunks of **19**. Yield: 0.55 g, 19%. M.p. 108–112 ^{o}C (decomp). ^{1}H NMR ($CDCl_3$, 25 ^{o}C): δ (ppm) 1.25 (t, 6H, $^{1}J_{H\text{-}H}$ = 7.3 Hz, C$H_3$$CH_2$N), 1.94 (s, 3H, NC*Me*), 1.96 (s, 3H, OC*Me*), 2.90–2.97 (m, 4H,

NCH_2CH_2N), 3.66–3.75 (m, 4H, CH_3CH_2N), 4.97 (s, 1H, γ-C*H*); ^{13}C NMR ($CDCl_3$, 25 ^oC): δ (ppm) 7.6 (NC*Me*), 18.1 (OC*Me*), 24.6 (CH_3CH_2N), 27.9 (CH_3CH_2N), 42.9 (CH_3CH_2N), 45.9 (CH_3CH_2N), 50.8 (NCH_2CH_2N), 66.9 (NCH_2CH_2N), 100.9 (γ-*C*H), 161.7 (*C*N), 190.5 (*C*O); IR (Nujol Mull): ν (cm^{-1}) 1613 (w), 1580 (m), 1521 (m); MS (*m/z*; (found (calcd)): 391.2 (389.9) M^+; 361.4 (360.9) M – Et; 199.2 (198.2) $Et_2NCH_2CH_2N(H)C(Me)CHC(Me)O$.

Preparation of [DippN{C(Me)}$_2$C(Me)O]$_2$InCl, 20: A 20 mL THF solution of L^1H (0.50 g, 1.8 mmol) had 1 equiv. of *n*-BuLi (0.73 mL of a 2.5 M solution, 1.8 mmol) added drop-wise at 0 ^oC. The solution was allowed to warm to room temperature slowly and stirred for 2 h, after which time it was rapidly added to a stirred 20 mL THF suspension of $InCl_3$ (0.40 g, 1.8 mmol) at room temperature. The resulting bright yellow solution was allowed to stir overnight, after which time the THF was removed *in vacuo*. The pale orange solid was extracted into toluene (20 mL), filtered, and concentrated until saturated. Overnight storage of the solution at 5 ^oC afforded colorless crystalline blocks of **20**. Yield: 0.52 g, 41%. M.p. 191–196 ^oC (decomp). ^1H NMR ($CDCl_3$, 25 ^oC): δ (ppm) 0.98–1.11 (m, 12H, $CH(CH_3)_2$), 1.22 (d, 3H, $^1J_{H\text{-}H}$ = 6.3 Hz, $CH(CH_3)_2$), 1.38 (s, 6H, C*Me*), 1.67 (d, 9H, $^1J_{H\text{-}H}$ = 9.9 Hz, $CH(CH_3)_2$), 1.84 (s, 6H, C*Me*), 2.23 (s, 6H, C*Me*), 2.92 (septet, 4H, $^1J_{H\text{-}H}$ = 6.8 Hz, $CH(CH_3)_2$), 7.00–7.17 (m, 6H, H_{aryl}); ^{13}C NMR ($CDCl_3$, 25 ^oC): δ (ppm) 13.8 (C*Me*), 16.2 (C*Me*), 21.8, 22.2, 22.3, 23.0, 23.4, 23.7, 23.8, 23.8 ($CH(CH_3)_2$), 25.3, 26.8 ($CH(CH_3)_2$), 27.4 (C*Me*), 99.4 (γ-*C*), 121.9, 122.5, 122.9, 124.8 (C_m), 127.0 128.0 (C_p), 140.8, 141.1, 141.9, 142.2 (C_o), 144.9 (Ar*C*–N), 177.4 (*C*N), 182.4 (*C*O); IR (Nujol Mull): ν (cm^{-1}) 3424 (br), 1561 (m), 1139 (w); MS (*m/z*; (found

(calcd)): 695.2 (695.1) M^+; 553.4 (553.4) M – Cl – ^{i}Pr – 4Me – 3H; 498.3 (498.3) M – Cl – Dipp; 323.9 (322.3) M – Cl – 2Dipp – Me; 280.2 (277.3) M – Cl – 2Dipp – 4Me.

Preparation of $[Et_2NC_2H_4NC(Me)CHC(Me)O]InCl_2$, 21: A –78 ^{o}C diethyl ether (30 mL) solution of L^2H (0.35 g, 1.8 mmol) had 1 equiv. of *n*-BuLi (1.1 mL of a 1.6 M solution, 1.8 mmol) added drop-wise. After stirring for 2 h at –78 ^{o}C, the reaction was allowed to warm to room temperature slowly and stirred overnight. The solvent was then removed and 20 mL of THF added. The THF solution was then added rapidly to a stirred 20 mL THF suspension of $InCl_3$ (0.39 g, 1.8 mmol) at room temperature. The resulting bright yellow solution was allowed to stir for 12 h, after which time the THF was removed *in vacuo* and the yellow solid extracted into toluene. Concentration of the toluene solution and storage at room temperature afforded **21** as colorless plate crystals. Yield: 0.36 g, 53%. M.p. 201–204 ^{o}C. ^{1}H NMR (C_6D_6, 25 ^{o}C): δ (ppm) 0.37 (t, 6H, $^1J_{H\text{-}H}$ = 7.2 Hz, C*H*$_3$CH$_2$N), 0.95 (s, 3H, NC*Me*), 1.52 (s, 3H, OC*Me*), 1.70–1.82 (m, 6H, CH$_3$C*H*$_2$N, NC*H*$_2$CH$_2$N), 1.99 (quartet, 2H, $^1J_{H\text{-}H}$ = 6.2 Hz, CH$_3$C*H*$_2$N), 4.40 (s, 1H, γ-C*H*); ^{13}C NMR (C_6D_6, 25 ^{o}C): δ (ppm) 6.4 (NC*Me*), 21.9 (OC*Me*), 28.8 (*C*H$_3$CH$_2$N), 42.2 (CH$_3$*C*H$_2$N), 48.8 (N*C*H$_2$CH$_2$N), 66.6 (NCH$_2$*C*H$_2$N), 96.4 (γ-*C*H), 166.7 (*C*N), 187.4 (*C*O); IR (Nujol Mull): ν (cm^{-1}) 3391 (br), 1577 (w), 1557 (w), 1520 (m), 942 (m); MS (*m/z*; (found (calcd)): 381.4 (382.8) M^+; 199.2 (198.2) $Et_2NCH_2CH_2N(H)C(Me)CHC(Me)O$.

Preparation of $[Et_2NC_2H_4NC(Me)CHC(Me)O]GaCl_2$, 22: To a solution of L^2H (0.35 g, 1.7 mmol) in 20 mL of THF was added 1 equiv. of *n*-BuLi (0.71 mL of a 2.5 M

solution, 1.7 mmol) drop-wise at –78 ^{o}C. The solution was slowly warmed to room temperature and stirred for 2 h, after which time it was rapidly added to a stirred 20 mL THF suspension of $GaCl_3$ (0.31 g, 1.7 mmol) at room temperature. Stirring of the pale orange solution was maintained overnight after which THF was removed *in vacuo* and the pale orange solid was extracted into toluene and filtered. Concentration under reduced pressure of the toluene solution and storage at room temperature afforded pale yellow plate crystals of **22**. Yield: 0.14 g, 23.2%. M.p. 123–126 ^{o}C. ^{1}H NMR ($CDCl_3$, 25 ^{o}C): δ (ppm) 1.06 (t, 6H, $^{1}J_{H\text{-}H}$ = 7.2 Hz, C*H*$_3$CH$_2$N), 1.33 (t, 6H, $^{1}J_{H\text{-}H}$ = 7.1 Hz, C*H*$_3$CH$_2$N), 1.95 (s, 6H, NC*Me*), 1.99 (s, 6H, OC*Me*), 2.85 (t, 6H, $^{1}J_{H\text{-}H}$ = 6.3 Hz, NC*H*$_2$CH$_2$N), 3.06 (br. m, 8H, CH$_3$C*H*$_2$N), 3.33 (t, 2H, $^{1}J_{H\text{-}H}$ = 6.3 Hz, NC*H*$_2$CH$_2$N), 5.00 (s, 1H, γ-C*H*), 5.08 (s, 1H, γ-C*H*), 10.8 (s, 1H, NH); ^{13}C NMR ($CDCl_3$, 25 ^{o}C): δ (ppm) 7.0 (NC*Me*), 22.4 (OC*Me*), 25.8 (*C*H$_3$CH$_2$N), 42.7 (CH$_3$*C*H$_2$N), 47.2 (N*C*H$_2$CH$_2$N), 66.3 (NCH$_2$*C*H$_2$N), 97.4 (γ-*C*H), 160.4 (*C*N), 186.3 (*C*O); IR (Nujol Mull): ν (cm^{-1}) 1610 (w), 1572 (m), 1531 (m), 1345 (m), 949 (m), 868 (w); UV/Vis (CH_2Cl_2, 25^{o}C): λ (nm) 230, 318.

Preparation of [Et$_2$NC$_2$H$_4$NC(Me)CHC(Me)O]ZnEt, 23: $ZnEt_2$ (1.8 mL of a 1.0 M solution in hexane, 1.8 mmol) was added neat to a solution of L^{2}H (0.35 g, 1.8 mmol) in 30 mL of toluene at room temperature. An immediate color change was observed and the resultant bright yellow reaction mixture was stirred for 3 h. The solvent was then removed *in vacuo* and the yellow solid was extracted into hexane. Concentration of the toluene solution and storage at –30 ^{o}C overnight, afforded colorless needles of **23**. Yield: 0.16 g, 30%. M.p. 176–181 ^{o}C. ^{1}H NMR ($CDCl_3$, 25 ^{o}C): δ (ppm) 0.97 (t, 9H, $^{1}J_{H\text{-}H}$ = 7.0

Hz, C*H*$_3$CH$_2$Zn, C*H*$_3$CH$_2$N), 1.18 (s, 3H, NC*Me*), 1.87 (s, 2H, H$_2$O), 1.93 (s, 3H, OC*Me*), 2.45–2.57 (m, 8H, CH$_3$C*H*$_2$N, NC*H*$_2$CH$_2$N), 3.23 (q, 2H, $^1J_{H\text{-}H}$ = 6.5 Hz, CH$_3$C*H*$_2$Zn), 4.89 (s, 1H, γ-C*H*); ^{13}C NMR (C$_6$D$_6$, 25 ^{o}C): δ (ppm) 10.9 (CH$_3$*C*H$_2$Zn), 13.1 (NC*Me*), 18.1 (OC*Me*), 27.8 (*C*H$_3$CH$_2$Zn), 28.7 (*C*H$_3$CH$_2$N), 40.6 (CH$_3$*C*H$_2$N), 46.2 (N*C*H$_2$CH$_2$N), 51.5 (NCH$_2$*C*H$_2$N), 94.2 (γ-*C*H), 161.7 (*C*N), 193.7 (*C*O); IR (Nujol Mull): ν (cm^{-1}) 1585 (m), 1509 (m), 1412 (m), 938 (m); MS (*m/z*; (found (calcd)): 309.3 (309.7) M$^+$; 292 (291.7) M – H$_2$O; 260.0 (262.6) M – H$_2$O – Et; 250.1 (251.5) M – 2Et; 205.3 (204.5) M – H$_2$O – 3Et; 177.0 (175.7) M – H$_2$O – Et – Me – NEt$_2$; 143.0 (142.1) M – 3Et – Zn – Me; 122.2 (124.0) M – H$_2$O – 3Et – Zn – Me.

Preparation of [Et$_2$NC$_2$H$_4$NC(Me)CHC(Me)O]MnCl–ClLi(thf)$_2$, 24: To a solution of L^{2}H (0.50 g, 2.5 mmol) in 20 mL of THF was added 1 equiv. of *n*-BuLi (1.01 mL of a 2.5 M solution, 2.5 mmol) drop-wise at –78 ^{o}C. The solution was slowly warmed to room temperature and stirred for 2 h, after which time it was rapidly added to a stirred THF (20 mL) suspension of MnCl$_2$ (0.32 g, 2.5 mmol) at room temperature. The initial cloudy yellow solution gradually turned to a clear golden orange upon stirring for 45 min and stirring was maintained overnight. After concentrating, filtering, and storage at 5 ^{o}C overnight, pale yellow chunk crystals of **24** were obtained. Yield: 0.52 g, 43%. M.p. 99–104 ^{o}C (decomp). IR (Nujol Mull): ν (cm^{-1}) 1595 (m), 1510 (m), 1304 (w), 1155 (w), 1136 (w) 1045 (m), 939 (m), 918 (m), 891 (m), 753 (w), 736 (w); UV/Vis (CH$_2$Cl$_2$, 25^{o}C): λ (nm) 230, 310; MS (*m/z*; (found (calcd)): 328.2 (329.8) M – 2(thf); 252.1 (252.2) M – 2(thf) – LiCl$_2$; 199.1 (198.2) Et$_2$NCH$_2$CH$_2$N(H)C(Me)CHC(Me)O.

CHAPTER V

The Synthesis and Characterization of Bulky Amidinato Complexes Containing Al and Zn

5.1 Introduction

The amidinate complexes consisting of main group, transition, and lanthanide metals have been extensively explored.[53] In particular, these ligands with zinc and aluminum metal centers have provided a number of successful examples. Amidinate aluminum complexes are significantly important due to their potential as precursors in chemical vapor[59] and thin film deposition,[60] as well as their ability to act as catalysts in olefin polymerization,[57,58f,58i-j] polymerization of ethylene,[58j] and C-H bond activation.[58l] As a result, numerous monoamidinate (Figure 45) and bisamidinate (Figure 46) aluminum complexes have been reported.[58f,58i-l,188-191]

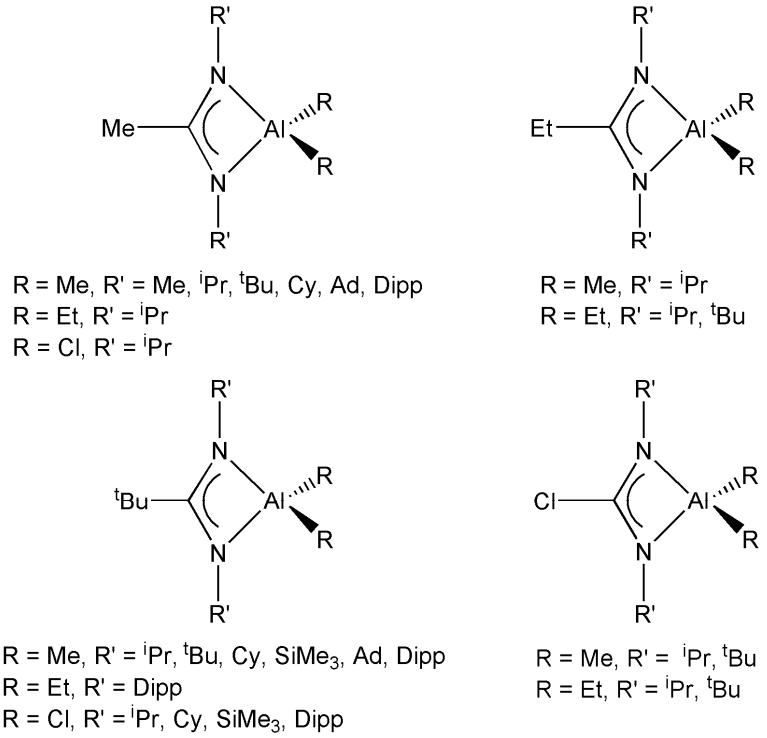

Figure 45. Selection of monoamidinate aluminum complexes

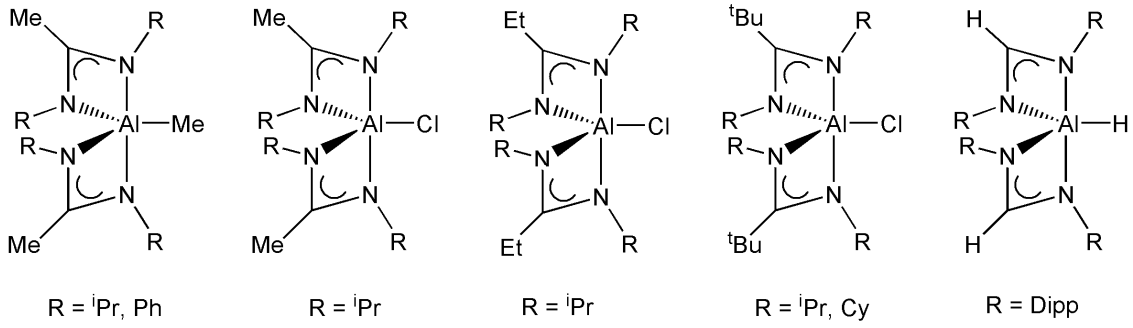

Figure 46. Examples of bisamidinate aluminum complexes

In the 1990's, Jordan and co-workers synthesized a series of amidinate complexes by reacting aluminum halides with bulky lithium amidinates and aluminum alkyls with carbodiimides (Scheme 30).[58h,i] The results revealed diverse structural motifs of the amidinate which are dependent on the size of substituents attached to the ligand, for example monoamidinate, bis(amidinate), and dinuclear cationic complexes.[58h,i]

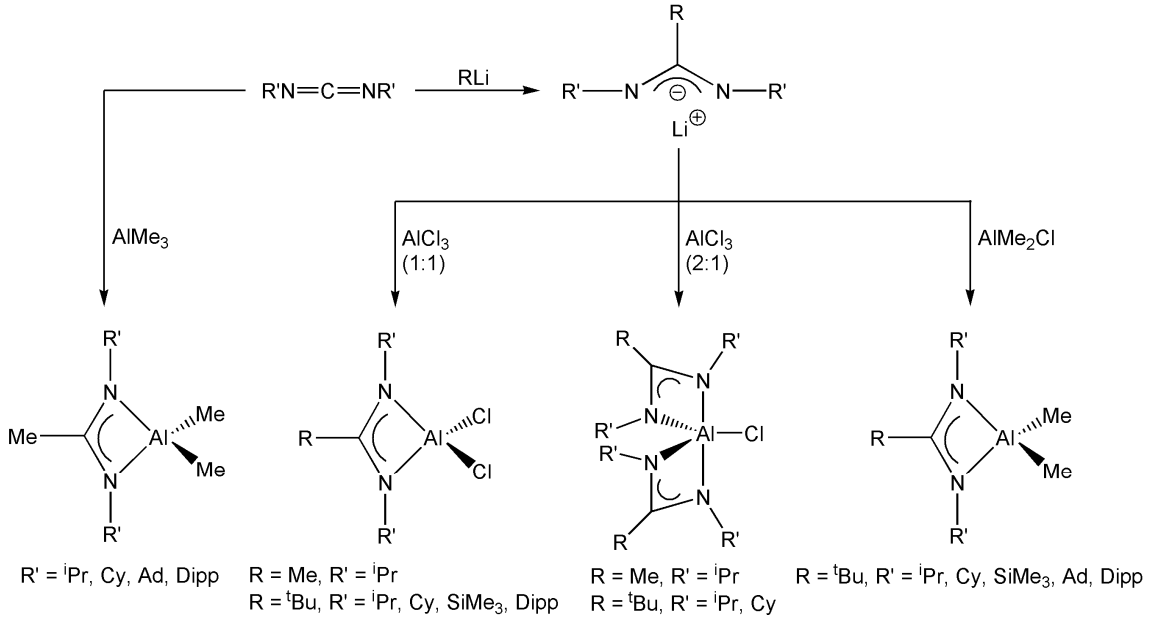

Scheme 30. Aluminum methyl and chloride amidinates

Typically, when the substituents attached to the nitrogen or carbon atoms of the amidinate backbone are sterically large, the chelating bonding mode is favored, while small substituents at these positions favor the bridging bonding mode.[55,192,193] The preferred bonding mode depending on substituent size is further exemplified by reacting exceedingly bulky neutral amidines with aluminum alkyls (Scheme 31).[188,192]

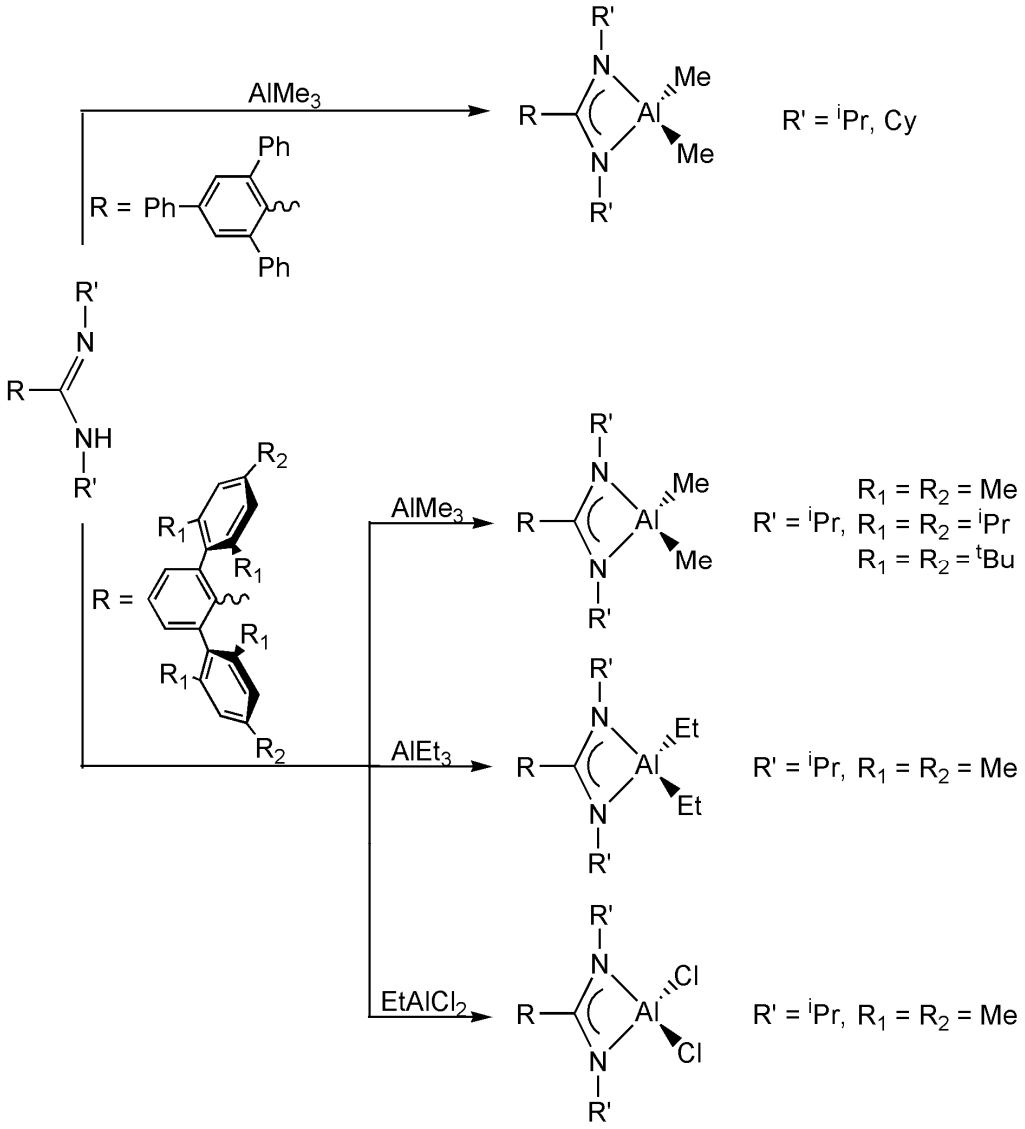

Scheme 31. Aluminum complexes from neutral amidine

When compared to the aluminum amidinate complexes reported, zinc amidinate complexes reported are much more scarce yet have potential catalytic applications,[194] since the related zinc guanidinate complexes have been found to act as catalysts in ring-opening polymerization (ROP) of lactides.[195] Additionally, similar zinc complexes with N,N'-chelating ligands, such as the β-diketiminate ligand, have also shown to act as catalysts in ROP of lactides and the copolymerization of CO_2 with a variety of epoxides.[194] However, the application potential of zinc amidinates is still unexplored due to their fairly recent discovery.

In 1975, Bonati et al. described a $ZnBr_2L_2$ adduct where L = N,N'-di-*p*-tolylformamidine.[53b,194] Later in 1991, Edelmann and co-workers synthesized the first benzamidinate zinc complex (Figure 47).[53a,181] By reacting zinc(II) chloride with two equivalents of $Na[PhC(NSiMe_3)_2] \cdot 0.5Et_2O$, the bis-chelating complex was produced.

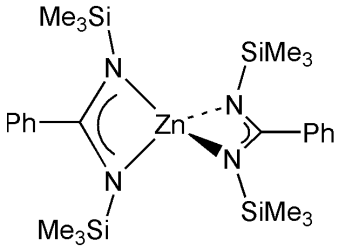

Figure 47. Zinc amidinate complex

Since then, a diminutive variety of zinc amidinate complexes have been reported including oxygenated tetranuclear zinc clusters (Figure 48A),[182,183,196] mixed Li/Zn amidinate oxide oligomers,[196] bisamidinate (Figure 48B-C),[53a,181,196] monoamidinate (Figure 48D-F),[196] and polynuclear zinc structures.[194]

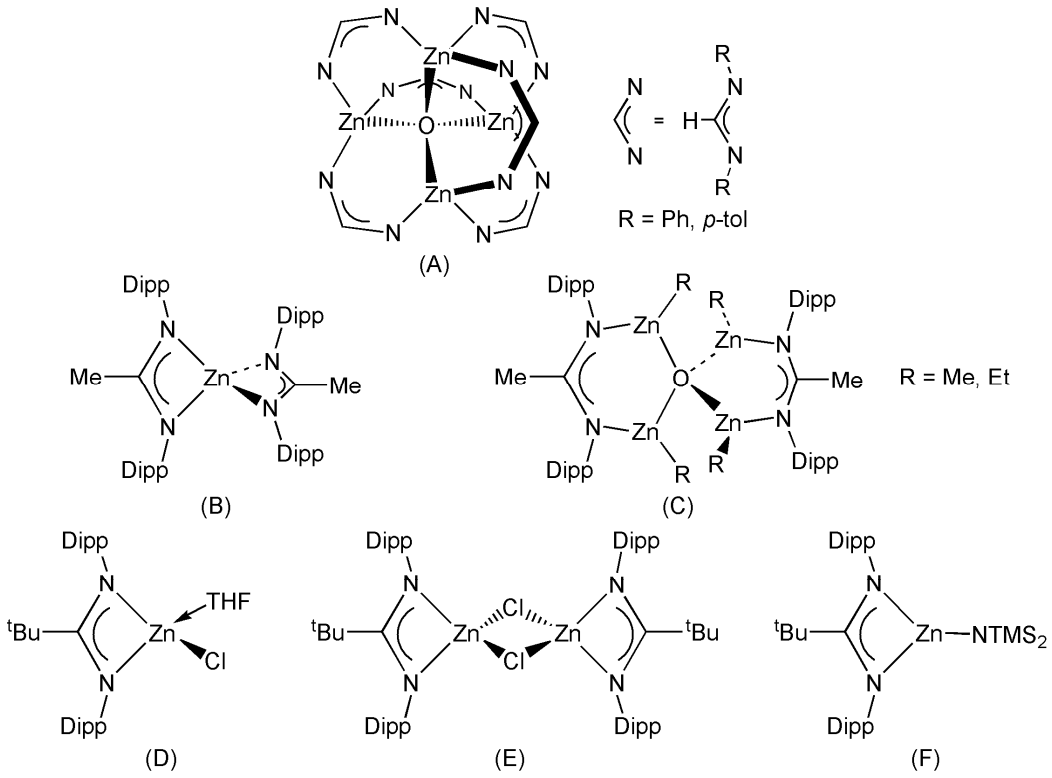

Figure 48. Selected examples of zinc amidinate complexes

Similarly, steric effects play a role on the mode of chelation adopted in the zinc complexes. Results show that the mono-chelate zinc structure is formed when the size of the substituent attached to the carbon of the backbone increases.[196] Therefore, when the substituent is not bulky, bis(amidinate) complexes are formed.

In this chapter, the N,N'-chelating formamidinate ligand RN(H)C(H)NR, (R = Dipp), L^H, has been employed for the synthesis and characterization of a series of Al and Zn complexes as potential catalysts and for stabilizing low valent zinc and aluminum complexes. Coordination preferences for the smaller ligand backbone (NCN) are emphasized in relation to the β-diketiminato and β-ketiminato (NCCCN) ligands. Specifically, we wished to focus on the affect of stoichiometric ratio of L^H to the metal alkyl. To this end, we report on the synthesis and characterization of a series of aluminum

and zinc amidinate complexes using RN(H)C(H)NR (R = Dipp = 2,6-diisopropylphenyl), where we observed varied coordination modes including monodentate, bidentate, and bridging ligands. The products have been characterized by X-ray crystallography and other spectroscopic techniques to exemplify the variety of coordination modes that exist.

5.2 Results and Discussion

5.2.1 Discussion of [{HC(NDipp)$_2$}$_2$AlMe], 25[197]

The room temperature, 2:1 reaction of L^H with $AlMe_3$ in toluene afforded colorless crystals of an Al(III) bisformamidinate complex, **25**, that crystallized in the monoclinic space group $P2_1/n$ (Scheme 32).

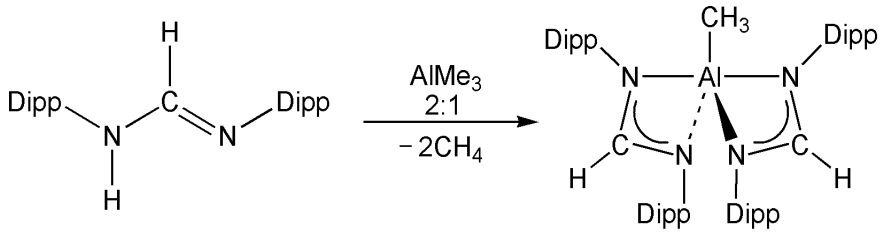

25

Scheme 32. Synthesis of compound **25**.

Structural analysis revealed that the aluminum atom adopts distorted trigonal bipyramidal geometry (Figure 49). The equatorial positions are occupied by the nitrogen and carbon atoms N1, N3, and C51 and, as expected, result in shorter Al–N bond distances as compared to the Al–N distances from the N2 and N4 atoms in the axial positions. These distances can be compared to related systems 1.925(12) Å and 2.096(12) Å as observed for N_{eq}–Al and N_{ax}–Al respectively, in [{MeC(N^{i}Pr)$_2$}$_2$AlCH$_3$],[190] as well as 1.914(2) Å and 2.041(2) Å observed in [{MeC(N^{i}Pr)$_2$}$_2$AlCl].[58i] The bond angles of 119.1(16)^o, 119.6(16)^o, and 121.1(12)^o for N(3)–Al(1)–C(51), N(1)–Al(1)–C(51), and N(3)–Al(1)–N(1) respectively, are close to the 120^o expected for trigonal bipyramidal geometry. Similarly to the related aluminum systems [{MeC(N^{i}Pr)$_2$}$_2$AlCl],[58i] [{MeC(N^{i}Pr)$_2$}$_2$AlCH$_3$],[190] [{PhC(NSiMe$_3$)$_2$}$_2$AlH],[58l] and [{HC(NDipp)$_2$}$_2$AlH],[188] the

bond angle N(2)-Al(1)-N(4), 156.3(12)^{o}, shows a distortion from the expected 180^{o} which can be attributed to the rather acute bite angles of 65.80(11)^{o} and 66.22(11)^{o} for N(1)–Al(1)–N(2) and N(3)–Al(1)–N(4) respectively.

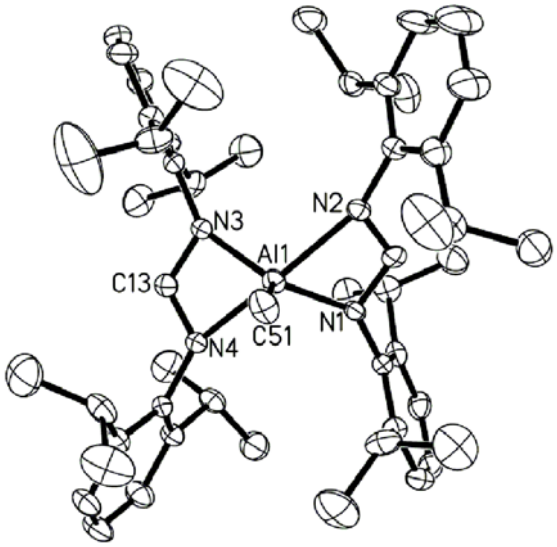

Figure 49. Molecular structure of [{HC(NDipp)$_2$}$_2$AlMe], **25**. Thermal ellipsoids at 30% probability level, hydrogen atoms have been omitted for clarity. Selected bond lengths(Å) and angles(^{o}): Al1-N1 1.926(3), Al1-N2 2.095(3), Al1-N3 1.925(3), Al1-N4 2.112(3), Al1-C51 1.959(4), N1-C38 1.336(4), N2-C38 1.308(4), N3-C13 1.352 (4), N4-C13 1.298(4), Al1-C38 2.4245(4), Al1-C13 2.420(4), N2-C38-N1 111.7(3), N4-C13-N3 113.1(3), N1-Al1-N2 65.80(11), N3-Al1-N4 66.22(11), N3-Al1-N2 102.7(12), N3-Al1-N1 121.1(12), N2-Al1-N4 156.3(12), N3-Al1-C51 119.1(16), N1-Al1-C51 119.6(16).

Spectroscopic data confirmed the solid-state analysis. The ^{1}H NMR displays a distinctive singlet peak at -0.36 ppm characteristic of the methyl group attached to the aluminum, which is typically observed in this region.[58f,58h-i,193,190] The IR spectra of **25** displays the characteristic peaks at 1666, 1635 (C=N), 1553 (C=C), and 1324 cm^{-1} (C–

N), while the LRMS gave the parent ion peak at m/z = 769.4 compared to the calculated m/z = 769.1.

5.2.2 Discussion of [{HC(NDipp)$_2$H}AlMeCl$_2$], 26[197]

For comparison with the product obtained from the trimethyl aluminum reaction, the reaction of L^H with dimethyl aluminum chloride was performed. Unlike the bisamidinate complex **25**, the room temperature reaction of L^H with a 1.2 equiv. of $AlMe_2Cl$ afforded the monodentate complex **26** in moderate yield (Scheme 33).

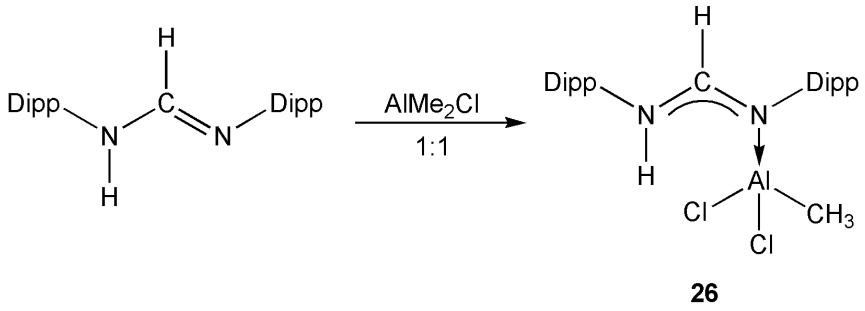

26

Scheme 33. Synthesis of compound **26**.

Complex **26** is interesting since despite numerous literature reports of amidinate complexes, only a handful exhibit the monodentate coordination mode, with examples of aluminum fairly rare.[198] The crystal structure of **26** indicates that the metal complex crystallizes preferentially as the *E* isomer with respect to the N(1)–C(13) bond (Figure 50). The formation of the geometric isomer is predicted to be a result of the hydrogen attached to the NCN backbone, rather than a more bulky alkyl group. For example, the formamidinate gallium complex, [{HC(NDipp)$_2$H}GaCl$_3$], crystallizes as the *E* isomer,[198] whereas the acetamidinate aluminum[198] and molybdenum[63] complexes, [{MeC(NDipp)$_2$H}AlI$_3$] and [{MeC(NDipp)$_2$H}Mo(CO)$_5$], crystallize in the *Z* form.

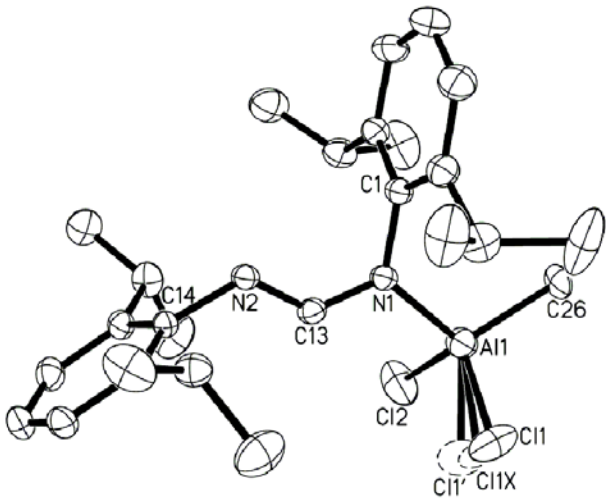

Figure 50. Molecular structure of [{HC(NDipp)$_2$H}AlMeCl$_2$], **26**. Thermal ellipsoids at 30% probability level, hydrogen atoms have been omitted for clarity. Selected bond lengths(Å) and angles(^{o}): Al1-Cl1 2.147(2), Al1-Cl2 2.137(2), Al1-C26 1.964(4), Al1-N1 1.918(3), N1-C13 1.302(5), N2-C13 1.319(5), C26-Al1-Cl1 115.9(18), C26-Al1-Cl2 116.0(16), Cl2-Al1-Cl1 104.7(11), N1-Al1-Cl1 102.9(13), N1-Al1-Cl2 104.7(13), N1-Al1-C26 110.9(17), N1-C13-N2 128.8(4).

The aluminum center in **26** has distorted tetrahedral geometry with the Al(1)–N(1) bond length of 1.918(3) Å in the normal range.[53] Comparison of the N(1)–C(13) and N(2)–C(13) bond lengths, 1.302(5) Å and 1.319(5) Å respectively, suggests delocalization of the double bond. A methyl group and a chlorine atom occupy two of the four tetrahedral coordination sites and are refined at full occupancy, while the remaining sites consist of a dative nitrogen bond and a chlorine atom which is disordered over 3 positions, each at 1/3 occupancy. The attachment of the second chlorine, rather than a methyl group, is most likely as a result from the reaction conditions, employing a slight excess of AlMe$_2$Cl to L^H at room temperature. The ^{1}H NMR spectroscopy confirmed the

N–H proton with a resonance peak at 8.46 ppm which corresponds well with 8.98 and 8.67 ppm reported for the aluminum acetamidinate and gallium formamidinate examples [{MeC(NDipp)$_2$H}AlI$_3$] and [{HC(NDipp)$_2$H}GaCl$_3$], respectively.[198] Similarly, the ^{1}H NMR and ^{13}C NMR confirm the presence of only one methyl group attached to the aluminum metal center and is additionally confirmed by mass spectral analysis.

5.2.3 Discussion of [{HC(NDipp)$_2$H}AlCl$_{1.4}$I$_{1.6}$], 27[197]

In an attempt to examine the chemistry of this system, we wished to synthesize [{HC(NDipp)$_2$H}AlClI$_2$] for further reactions. To this end, the reaction of [{HC(NDipp)$_2$H}AlClMe$_2$] with I$_2$ was performed (Scheme 34). Colorless crystals of **27** were isolated in 58% yield and found to crystallize in the monoclinic space group P2$_1$/*c* (Figure 51).

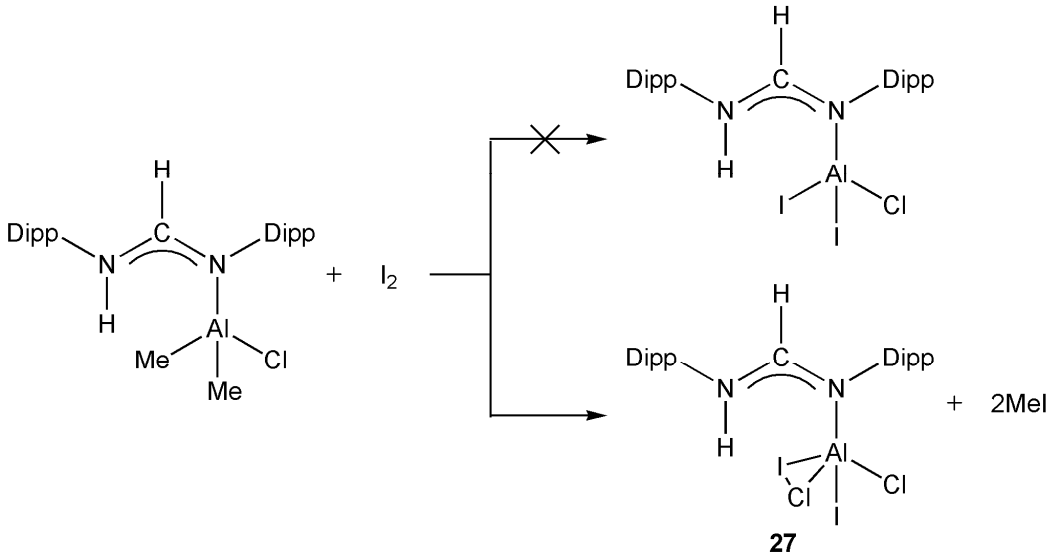

Scheme 34. Synthesis of compound **27**.

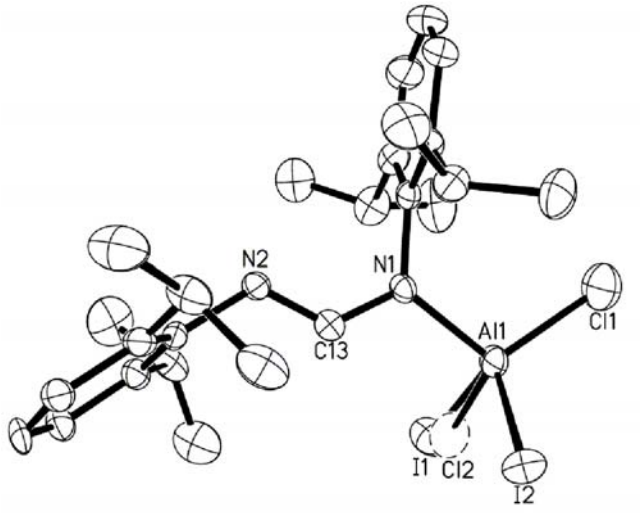

Figure 51. Molecular structure of [{HC(NDipp)$_2$H}AlCl$_{1.4}$I$_{1.6}$], **27**. Thermal ellipsoids at 30% probability level, hydrogen atoms have been omitted for clarity. Selected bond lengths(Å) and angles(^{o}): Cl1-Al1 2.146(4), Al1-Cl2 2.050(12), I1-Al1 2.550(4), I2-Al1 2.506(3), Al1-N1 1.908(7), N1-C13 1.316(9), N2-C13 1.306(10), Cl2-Al1-Cl1 117.1(5), Cl1-Al1-I1 116.0(17), Cl1-Al1-I2 111.9(5), Cl2-Al1-I2 104.5(5), I1-Al1-I2 110.7(14), N1-Al1-Cl1 109.6(2), N1-Al1-Cl2 109.3(5), N1-Al1-I1 104.0(2), N1-Al1-I2 103.4(2), N2-C13-N1 127.0(7).

Like complex **26**, the Al atom has distorted tetrahedral geometry. The Al(1)–N(1) bond length of 1.908(7) Å and aluminum–halide distances are within normal values,[53] such as the Al(III)Cl amidinate structure examples [{MeC(N^{i}Pr)$_2$}AlCl$_2$],[58i] [{EtC(N^{i}Pr)$_2$}$_2$AlCl],[189] and [{^{t}BuC(NCy)$_2$}AlCl$_2$].[58i] The Al(1)–I(2) bond length of 2.506(3) Å falls in the expected range of Al(III)I distances, for example the monodentate acetamidinate compound [{MeC(NDipp)$_2$}AlI$_3$] has Al–I bond lengths of 2.530 Å, 2.531 Å, and 2.473 Å.[198] X-ray crystallographic analysis revealed that complex **27** has an iodine and chlorine atom sharing a position with partial occupancy at 60/40 (I:Cl), which is

probably the result of the *in situ* reaction containing an excess of both iodine and dimethyl aluminum chloride competing to replace the second methyl group.[6i,8f,199] The bond lengths of 2.050(12) Å for Al(1)–Cl(2) and 2.550(4) Å for Al(1)–I(2) did not have to be fixed during refinement. The adduct of the neutral formamidine shows delocalization across the NCN backbone (N(1)–C(13): 1.316(9) Å, N(2)–C(13): 1.306(10) Å). The solid-state analysis is confirmed by the infrared spectra exhibiting a characteristic N–H stretch at 3302 cm^{-1}, which was also confirmed by ^{1}H NMR with a resonance observed at 12.05 ppm. The positive-mode mass spectrum of the aluminum adduct complex gave the parent ion peak at *m/z* = 644.1 as compared to the calculated *m/z* = 644.2, which confirms the I and Cl at 60:40 partial occupancy. The parent peak is followed by sequential loss of an iPr, I, Cl, and Cl (partial occupancy) to give a peak at *m/z* = 422.3.

5.2.4 Discussion of [{HC(NDipp)$_2$}$_2$Zn], 28[197]

In order to compare the coordination preferences and products obtained from the aluminum alkyl reactions with L^H, the reactions with $ZnEt_2$ were performed under varying conditions. Colorless crystals of complex **28** were obtained by reacting 1 equiv. of $ZnEt_2$ with 2 equiv. of L^H at room temperature (Scheme 35).

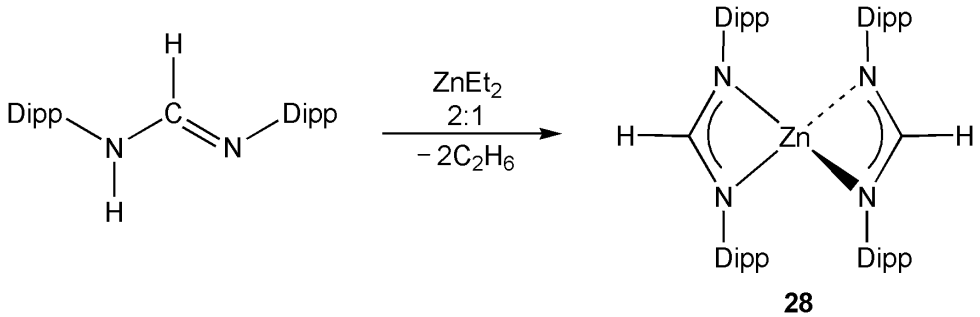

28

Scheme 35. Synthesis of compound **28**.

As observed in complex **25**, the reaction resulted in a homoleptic zinc complex through elimination of both ethyl groups (Figure 52). Similar bisformamidinate zinc complexes have been reported, examples including $[\{PhC(NSiMe_3)_2\}_2Zn]$[200] and $[\{MeC(NDipp)_2\}_2Zn]$.[183]

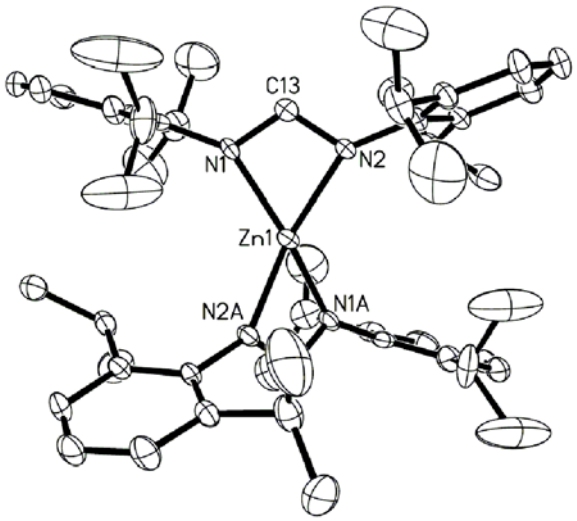

Figure 52. Molecular structure of $[\{HC(NDipp)_2\}_2Zn]$, **28**. Thermal ellipsoids at 30% probability level, hydrogen atoms have been omitted for clarity. Selected bond lengths(Å) and angles(°): Zn1-N1 2.013(3), Zn1-N2 2.036(3), Zn1-C13 2.430(4), N1-C13 1.323(5), N2-C13 1.320(5), N1-Zn1-N2 65.88(12), N1-Zn1-N2#1 123.8(12), N1#1-Zn1-N2 123.8(12), N1#1-Zn1-N1 150.3(18), N2-Zn1-N2#1 146.4(18), N2-C13-N1 112.8(3).

Structural analysis of complex **28** shows the zinc atom achieves a coordination number of four with bond angles between 123.8(12)°–150.3(18)° which can be attributed to the rather acute bite angle 65.88(12)° of the formamidinate ligand. The bond lengths within the ligand backbone N(1)–C(13) and N(2)–C(13) are nearly identical at 1.323(5) Å and 1.320(5) Å and are indicative of delocalization over the NCN backbone. The Zn–N bond distances of 2.013(3) Å and 2.036(3) Å are similar to the Zn–N bond distances that

have been reported for similar structures, for example; the acetamidinate zinc(II) complex $[\{MeC(NDipp)_2\}_2Zn]$[183] has Zn–N bond distances of 2.031(5) Å and 2.038(4) Å. Mass spectra analysis of crystalline **26** displayed the parent ion peak at *m/z* = 793.4, while infrared analysis displayed the characteristic peaks of 1667, 1634 (C=N), 1557 (C=C), and 1319 cm^{-1} (C–N).

5.2.5 Discussion of $[\{HC(NDipp)_2\}Zn_2Et_2]_2O$, 29[197]

Continuing with the reactions of L^H and $ZnEt_2$ with the aim of isolating a heteroleptic Zn(II) complex, the reaction stoichiometry was altered. From the 1:1 reaction of L^H with $ZnEt_2$ colorless crystals of complex **29** were isolated in low yield and found to crystallize in the triclinic space group $P\bar{1}$ (Scheme 36).

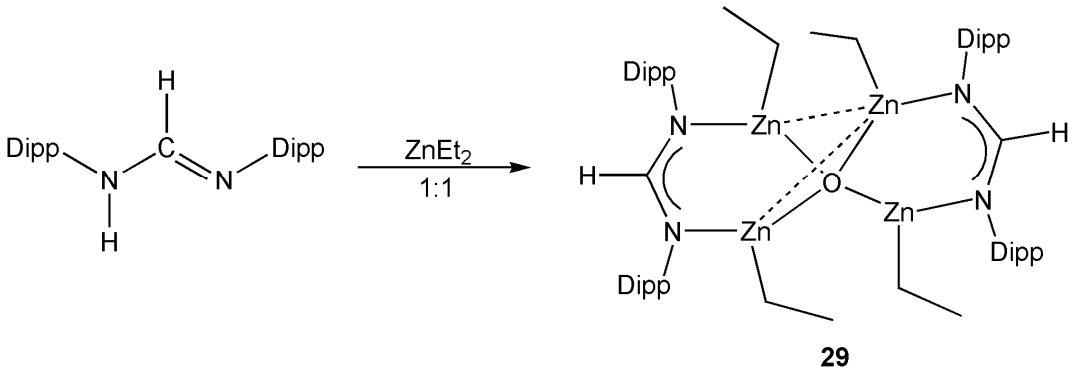

Scheme 36. Synthesis of compound **29**.

Single crystal X-ray analysis of complex **29** revealed a four-coordinate central oxygen atom surrounded by four zinc atoms (Figure 53), and the formamidinate ligand, L^H, exhibiting a bimetallic bridging coordination with the four N–Zn covalent bonds.

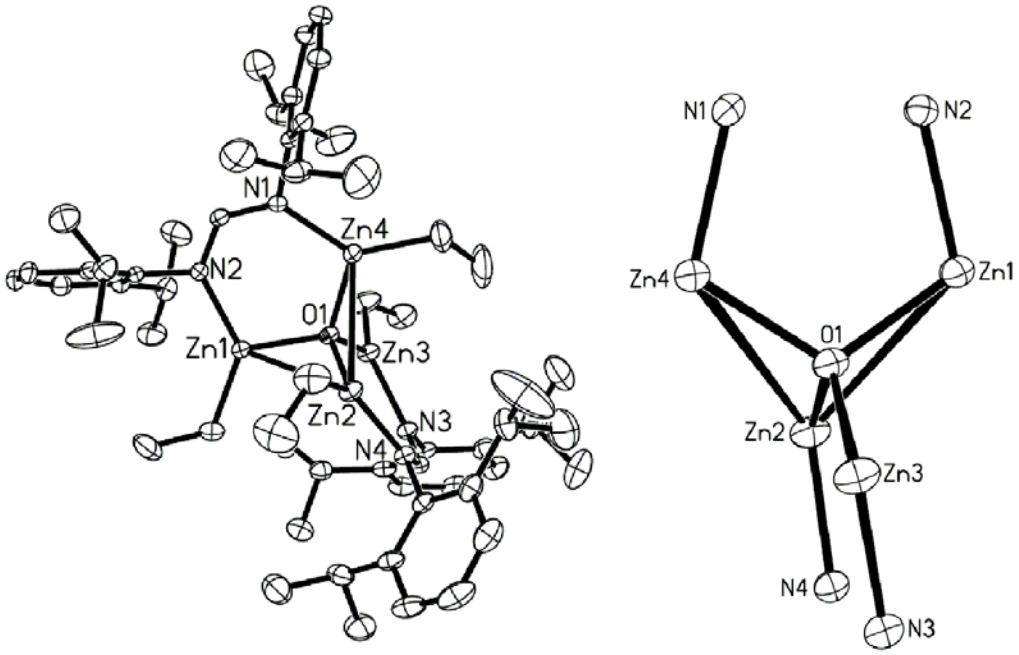

Figure 53. Molecular structure of $[\{HC(NDipp)_2\}Zn_2Et_2]_2O$, **29**. On the left hand side is the asymmetric unit and on the right hand side is the central Zn_4O core of the molecule. Thermal ellipsoids at 30% probability level, hydrogen atoms have been omitted for clarity. Selected bond lengths(Å) and angles(^{o}): Zn1-N2 1.965(2), Zn2-N4 1.966(2), Zn3-N3 1.988(2), Zn4-N1 1.969(2), Zn1-O1 1.966(2), Zn2-O1 1.965(2), Zn3-O1 1.948(2), Zn4-O1 1.960(2), Zn1-Zn2 2.983(5), Zn2-Zn4 3.108(6), N1-C13 1.317(4), N2-C13 1.323(4), Zn2-O1-Zn1 98.74(9), Zn3-O1-Zn4 109.7(10), Zn4-O1-Zn1 114.4(9), Zn3-O1-Zn2 114.6(10), O1-Zn1-C28 119.1(13), O1-Zn2-C57 119.3(16), O1-Zn3-C55 123.4(14), C26-Zn4-O1 118.2(16).

The overall +8 charge of the zinc cations is balanced by a –1 charge observed for each NCN ligand, (–2), as well as a –2 charge on the central oxygen atom and a –1 charge for each ethyl group, (–4). The central oxygen atom O(1) adopts distorted tetrahedral geometry with O–Zn bond angles ranging from 98.74(9)^o to 114.6(10)^o and

bond lengths in the range of 1.948(2) Å to 1.966(2) Å for O–Zn and 1.965(2) Å to 1.988(2) Å for N–Zn. These bond lengths compare well to three related tetrahedral Zn_4O cluster amidinate compounds which exhibit bond lengths in the range of 1.912(4)–1.927(3) Å (O–Zn) and 2.023(5)–2.045(4) Å (N–Zn) for $[\{HC(NPh)_2\}_6Zn_4](O)$,[181] 1.923(15) Å (O–Zn) and 2.015(6) Å (N–Zn) for $[\{HC(N\textit{p}\text{-Tol})_2\}_6Zn_4](O)$,[182] and 1.948(13)–1.953(14) Å (O–Zn) and 1.962(17)–1.974(18) Å (N–Zn) for $[\{MeC(NDipp)_2\}Zn_2R_2]_2(O)$ (R = Me, Et).[183] Each zinc center exhibits distorted trigonal planar geometry which can be observed by the selected bond lengths and angles listed in Figure 53. Complex **29** exhibits Zn(1)···Zn(2) and Zn(2)···Zn(4) distances of 2.983(5) Å and 3.108(6) Å respectively, which correspond closely to the $[\{HC(NPh)_2\}_6Zn_4](O)$ and $[\{HC(N\textit{p}\text{-Tol})_2\}_6Zn_4](O)$ complexes with distances at 3.135 Å (mean average) and 3.145(25) Å respectively,[181,182] and are slightly longer than the sum of van der Waals radii for Zn–Zn, 2.78 Å.[162] Additionally, the observed Zn–Zn separation is longer than the single-bond metallic radius, 2.50 Å.[162] Distances shorter than that are rarely observed but have been reported, including the Zn(I) complexes Cp*Zn–ZnCp* (Cp* = C_5Me_5)[201] where the Zn–Zn separation was found at 2.305(3) Å, and RZn–ZnR (R = $[\{N(Dipp)C(Me)\}_2CH]$)[202] where the Zn–Zn separation was found at 2.358(7) Å. Spectroscopic data confirmed the structure of **29**. Infrared spectroscopy gave distinctive peaks for C=N, C=C, and C–N with stretching bands at 1667, 1597, 1557, and 1320 cm^{-1}, respectively.

5.2.6 Discussion of [{HC(NDipp)$_2$}$_2$Zn$_3$Et$_2$](OEt)$_2$, 30[197]

In an attempt to eliminate oxygen contamination, the reaction was performed numerous times and it was found that **29** was reproducibly isolated. However, on one attempt complex **30** was isolated as colorless needles in low yield (Scheme 37).

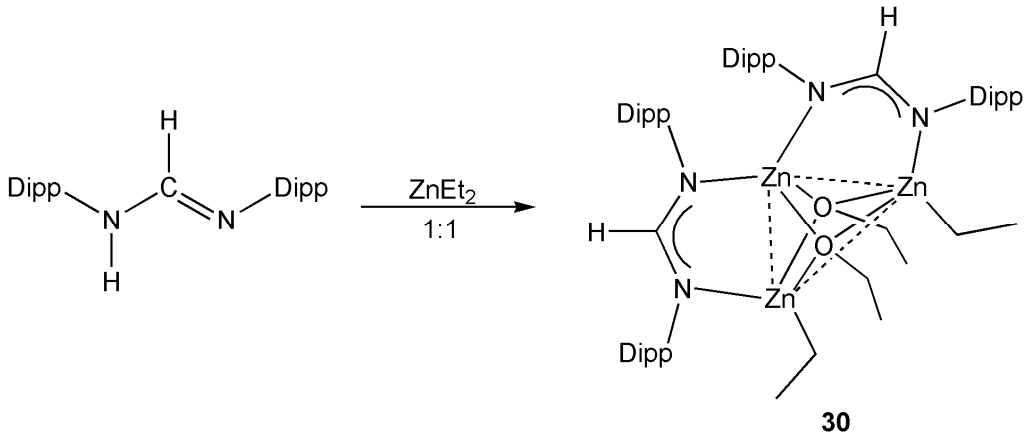

Scheme 37. Synthesis of compound **30**.

X-ray analysis revealed that **30** similarly crystallized in the triclinic space group $P\bar{1}$ (Figure 54). In the asymmetric unit of complex **30** there are two compounds that differ only slightly in bond lengths and angles. No higher symmetry space group could be determined by PLATON.[179] In comparison with **29**, the crystal structure of **30** reveals a bimetallic bridging binding mode, however, in contrast complex **30** contains two four-coordinate oxygen atoms within the central core, each with a distorted tetrahedral geometry.

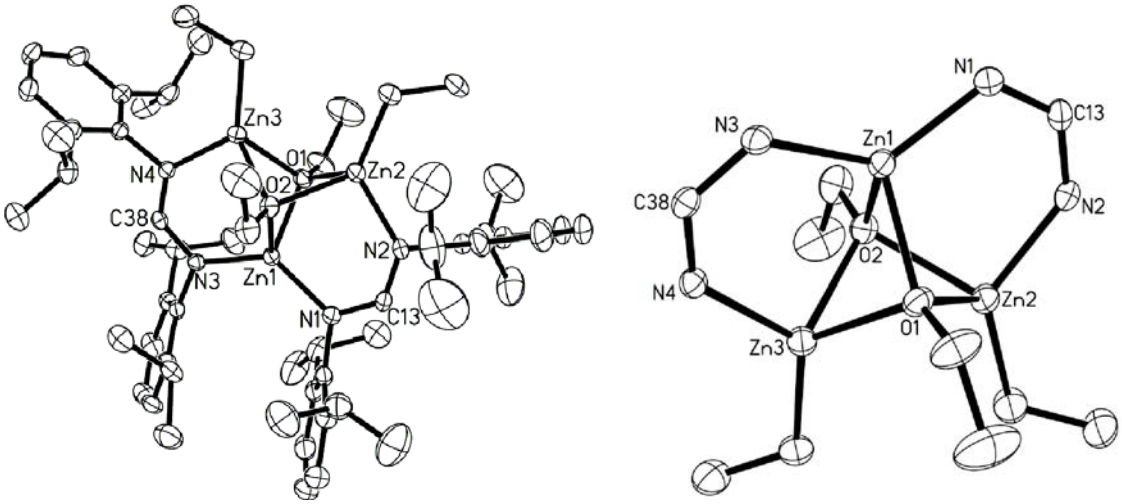

Figure 54. Molecular structure of $[\{HC(NDipp)_2\}_2Zn_3Et_2](OEt)_2$, **30**. On the left hand side is the asymmetric unit and on the right hand side is the Zn_3O_2 core of the molecule. Thermal ellipsoids at 30% probability level, hydrogen atoms have been omitted for clarity. Selected bond lengths(Å) and angles(°): Zn1-N1 1.984(3), Zn1-N3 1.984(3), Zn2-N2 1.969(4), Zn3-N4 2.026(3), Zn1-O1 2.042(3), Zn1-O2 2.036(3), Zn2-O1 2.112(3), Zn2-O2 2.178(3), Zn3-O1 2.176(3), Zn3-O2 2.178(3), Zn1-Zn2 2.990(7), Zn1-Zn3 2.999(7), Zn2-Zn3 2.945(7), N1-C13 1.332(5), N4-C38 1.305(5), Zn2-O1-Zn3 86.74(10), C51-O1-Zn1 126.0(3), Zn3-O2-Zn2 86.71(10), C53-O2-Zn2 128.3(3), N3-Zn1-O2 110.8(12), N1-Zn1-O1 113.1(12), N2-Zn2-O1 103.2(12), C57-Zn2-O1 119.7(19), N4-Zn3-O1 101.2(11), C55-Zn3-O2 122.6(16).

The coordination sites around each oxygen atom are occupied by 3 zinc atoms and 1 ethyl group. Examples of a four coordinate oxygen center with bonds to three zinc atoms and one ethyl group are rare but not unprecendented.[203] The ethyl group attached to the oxygen (O–Et) is likely a result from the elimination of ethane and subsequent coordination to the oxygen. Each zinc atom in **30** displays distorted tetrahedral

geometry. The Zn···Zn separations fall within the range of 2.945(7)–2.999(7) Å, which correspond closely to the Zn···Zn distances of complex **29** and afore mentioned examples.[181,182] However, only three zinc atoms are present in complex **30** with one zinc atom attached to both formamidinate ligands via N,N'-chelation. Additionally, the bond lengths Zn–N (1.965(2)–2.026(3) Å), Zn–O (1.948(2)–2.178(3) Å), and N–C (1.305(5)–1.332(5) Å) for complexes **29** and **30** are similar to those observed for related amidinate analogues, examples include $[\{HC(NPh)_2\}_6Zn_4]O$,[181] $[\{HC(N\text{-}p\text{-}CH_3C_6H_4)_2\}_6Zn_4]O$,[182] and $[\{MeC(NDipp)_2\}_2Zn_4]O$.[183] The source of the oxygen contamination in both complexes **29** and **30** is not confirmed, but likely from atmospheric oxygen/water moisture during the reaction. Tetranuclear zinc amidinate clusters containing an oxygen have been previously reported and are known to be highly oxophilic.[182,183] Infrared spectroscopy confirmed the structures of **30** exhibiting distinctive peaks for C=N, C=C, and C–N at 1665, 1597, 1561, 1287 cm^{-1}, respectively.

5.3 Summary

The reactions of the neutral formamidinate, DippN(H)C(H)NDipp, with aluminum and zinc alkyls have produced a variety of complexes **25**–**30** featuring different coordination modes. The chelating binding mode is observed which is in accordance with the sterically large 'Dipp' substituents attached to the nitrogen atoms of the NCN backbone. Yet, X-ray crystallographic analysis revealed that steric constraints do not govern coordination modes entirely. Through manipulation of reaction stoichiometry a variety of coordination compounds that feature monodentate and η^2-bridging coordination as well as cluster complexes were observed. The monomeric complexes and aluminum are adducts, as previously seen with AlX_3 due to their vacant orbital. However, the η^2-bridging and cluster type zinc complexes are likely the result of the lack of steric protection on the carbon of the NCN backbone. Overall, this work has focused on investigating the steric influence of the formamidinate ligand and stoichiometric conditions in metal complex formation.

5.4 Experimental

5.4.1 General Procedures

Hexane and toluene were dried using an MBraun-SPS solvent purification system. All manipulations were performed under anaerobic conditions using standard Schlenk techniques. The reagents $ZnEt_2$ (1.0 M in hexanes), $AlMe_3$ (2.0 M in hexanes), $AlMe_2Cl$ (1.0 M in hexanes), and I_2 sublimed were purchased from Aldrich and used as received. The amidinate ligand, L^H = (Dipp)N(H)C(H)N(Dipp), was prepared according to published procedures.[66]

5.4.2 Spectroscopy Measurements

The ^1H and ^{13}C NMR spectra were recorded on a Varian Mercury 300 spectrometer (^1H 300.05 MHz and ^{13}C 75.45 MHz). IR analysis was conducted as Nujol Mulls with NaCl plates on a MIDAC M4000 Fourier transform infrared (FT IR) spectrometer. Ultraviolet-visible absorption spectra were recorded on an Agilent 8453 UV/Vis spectrometer. Mass spectrometry analysis was carried out using a Bruker Esquire 6000 Mass Spectrometer. Melting points were determined in capillaries under a nitrogen atmosphere and are uncorrected.

5.4.3 Experimental Procedures and Spectroscopic Data

Preparation of [{HC(NDipp)$_2$}$_2$AlMe], 25: $AlMe_3$ (0.17 mL, 0.34 mmol)) was added dropwise to 2 equiv. of L^H (0.25 g, 0.69 mmol) in 25 mL of toluene at 25 ^oC. Evolution of a gas was observed. Stirring was maintained for 30 minutes after which time the solvent was removed *in vacuo* and the solid was extracted into hexane. The reaction

mixture was concentrated, filtered and stored at room temperature to afford **25** as colorless needles. Yield: 0.13 g, 25%. M.p. >250 ^{o}C. ^{1}H NMR (C_6D_6, 25 ^{o}C): δ (ppm) –0.36 (s, 3H, AlCH_3), 0.57–1.15 (m, 48H, CH(CH_3)$_2$), 2.33 (septet, 8H, $^{1}J_{H\text{-}H}$ = 6.9 Hz, CH(CH$_3$)$_2$), 6.58–6.98 (m, 12H, H$_{aryl}$), 7.33 (s, 2H, NCHN); ^{13}C NMR (C_6D_6, 25 ^{o}C): δ (ppm) 12.9 (AlCH$_3$), 21.1 (CH(CH$_3$)$_2$), 22.3 (CH(CH$_3$)$_2$), 26.9 (CH(CH$_3$)$_2$), 117.5 (*m*–ArC), 121.7 (*m*–ArC), 122.0 (*p*–ArC), 122.3 (*p*–ArC), 124.5 (*o*–ArC), 130.8 (*o*–ArC), 139.1 (ArC–N), 143.0 (ArC–N), 166.4 (NCN); IR (υ cm^{-1}, Nujol mull): 1666 (m), 1635 (w), 1553 (m), 1324 (w), 1292 (w), 1179 (m), 966 (m), 934 (m), 755 (m), 664 (w), 636 (w); MS (*m/z*; found (calcd)): 769.4 (769.1) M^{+}, 365.3 (364.5) L^{H}, 176.1 (176.2) L^{H} – (Dipp)NC(H), 160.3 (159.4) M – AlMe – (DippN)$_2$C(H) – Dipp – ^{i}Pr.

Preparation of [{HC(NDipp)$_2$H}AlMeCl$_2$], 26: To a 25 ^{o}C toluene (25 mL) solution of L^{H} (0.25 g, 0.69 mmol) was added 1.2 equiv. of AlMe$_2$Cl (0.82 mL, 0.82 mmol)) dropwise. Evolution of gas was observed. Stirring was maintained for 30 minutes after which time the solvent was removed *in vacuo* and the solid was extracted into hexane. The reaction mixture was concentrated, filtered and stored at room temperature to afford crystalline colorless needles of **26**. Yield (based on ligand): 0.15 g, 46%. M.p. 243–249 ^{o}C (decomp). ^{1}H NMR (C_6D_6, 25 ^{o}C): δ (ppm) –0.85 (s, 3H, AlCH_3), 1.15–1.28 (m, 24H, CH(CH_3)$_2$), 2.82–3.23 (m, 4H, CH(CH$_3$)$_2$), 7.09–7.25 (m, 6H, H$_{aryl}$), 7.33 (s, 1H, NCHN), 8.46 (s, 1H, NH); ^{13}C NMR (C_6D_6, 25 ^{o}C): δ (ppm) –2.0 (AlCH$_3$), 19.1 (CH(CH$_3$)$_2$), 19.6 (CH(CH$_3$)$_2$), 20.7 (CH(CH$_3$)$_2$), 21.1 (CH(CH$_3$)$_2$), 22.8 (CH(CH$_3$)$_2$), 27.3 (CH(CH$_3$)$_2$), 120.5 (*m*–ArC), 121.2 (*m*–ArC), 121.8 (*p*–ArC), 123.5 (*p*–ArC), 133.8 (*o*–ArC), 135.8 (*o*–ArC), 141.4 (ArC–N), 143.3 (ArC–N), 166.5 (NCN); IR (υ cm^{-1},

Nujol mull): 3067 (shoulder, N–H stretch), 1680 (m), 1639 (m), 1596 (m), 1556 (s), 1528 (m), 1335 (m), 1199 (m), 934 (m), 854 (m), 776 (m), 682 (m); MS (*m/z*; found (calcd)): 478.5 (477.5) M^+, 365.3 (364.5) M – $AlCl_2Me$, 176.2 (176.3) M – $AlCl_2Me$ – (Dipp)NC(H).

Preparation of [{HC(NDipp)$_2$H}AlCl$_{1.4}$I$_{1.6}$], 27: To a 25 ^oC toluene (25 mL) solution of L^H (0.35 g, 0.96 mmol) was added 1.2 equiv. of $AlMe_2Cl$ (1.2 mL, 1.2 mmol)) dropwise. Evolution of gas was observed. Stirring was maintained for 3 h, after which time sublimed I_2 (0.24 g, 0.96 mmol) was added quickly to the reaction mixture. The dark purple reaction was then allowed to stir for 4 days until the reaction mixture became a clear pale tan color. The toluene was then removed *in vacuo* and the pale tan solid was extracted into hexane, concentrated, and filtered. Storage at room temperature afforded colorless crystalline plates of **27**. Yield (based on ligand): 0.36 g, 58%. M.p. 231–235 ^oC (decomp). ^1H NMR (C_6D_6, 25 ^oC): δ (ppm) 0.80 (d, 24H, $^1J_{H\text{-}H}$ = 7.2 Hz, CH(CH_3)$_2$), 2.87 (septet, 4H, $^1J_{H\text{-}H}$ = 6.8 Hz, CH(CH$_3$)$_2$), 6.60 (d, 4H, $^1J_{H\text{-}H}$ = 7.5 Hz, *m*–H$_{aryl}$), 6.78 (t, 2H, $^1J_{H\text{-}H}$ = 7.8 Hz, *p*–H$_{aryl}$), 6.86 (s, 1H, NCHN), 12.05 (s, 1H, NH); ^{13}C NMR (C_6D_6, 25 ^oC): δ (ppm) 22.2 (CH(CH_3)$_2$), 27.7 (CH(CH$_3$)$_2$), 122.9 (*m*–ArC), 128.8 (*p*–ArC), 130.0 (*o*–ArC), 144.4 (ArC–N), 157.7 (NCN); IR (υ cm^{-1}, Nujol mull): 3302 (shoulder, N–H stretch), 1682 (m), 1638 (m), 1595 (m), 1557 (m), 1337 (m), 935 (s), 670 (m); MS (*m/z*; found (calcd)): 716.6 (716.2) M, 365.4 (364.5) M – $AlCl_2I_2$.

Preparation of [{HC(NDipp)$_2$}$_2$Zn], 28: $ZnEt_2$ (0.34 mL, 0.34 mmol) was added dropwise to 2 equiv. of L^H (0.25 g, 0.69 mmol) in 25 mL of toluene at 25 ^oC. Evolution

of gas was observed. Stirring was maintained for 30 minutes after which time the solvent was removed *in vacuo* and the solid was extracted into hexane. The reaction mixture was concentrated, filtered and stored at room temperature to afford colorless crystals of **28**. Yield: 0.18 g, 33%. M.p. 209–211 ^{o}C. ^{1}H NMR (C_6D_6, 25 ^{o}C): δ (ppm) 0.75 (d, $^{1}J_{H\text{-}H}$ = 6.9 Hz, 12H, CH(CH_3)$_2$), 0.84 (d, $^{1}J_{H\text{-}H}$ = 6.6 Hz, 36H, CH(CH_3)$_2$), 3.12 (br, 8H, CH(CH$_3$)$_2$), 6.60–6.90 (m, 12H, H$_{aryl}$), 6.96 (s, 2H, NCHN); ^{13}C NMR (C_6D_6, 25 ^{o}C): δ (ppm) 21.1 (CH(*C*H$_3$)$_2$), 22.2 (CH(*C*H$_3$)$_2$), 27.2 (*C*H(CH$_3$)$_2$), 121.8 (*m*–ArC), 123.7 (*p*–ArC), 140.0 (*o*–ArC), 142.3 (ArC–N), 165.9 (NCN); IR (υ cm^{-1}, Nujol mull): 1667 (w), 1634 (w), 1597 (m), 1557 (m), 1319 (m), 1177 (m), 934 (m), 865 (m), 756 (m), 722 (m); MS (*m/z*; found (calcd)): 793.4 (792.5) M^{+}, 365.3 (364.5) L^{H}, 176.1 (176.2) L^{H} – (Dipp)NC(H).

Preparation of [{HC(NDipp)$_2$}Zn$_2$Et$_2$]$_2$O, 29: To a 25 ^{o}C toluene (25 mL) solution of L^{H} (0.25 g, 0.69 mmol) was added 1 equiv. of ZnEt$_2$ (0.69 mL, 0.69 mmol) dropwise. Evolution of gas was observed. Stirring was maintained for 30 minutes after which time the solvent was removed *in vacuo* and the solid was extracted into hexane. The reaction mixture was concentrated, filtered and stored at room temperature to afford colorless crystals of **29**. Yield: 0.18 g, 23%. M.p. 210–213 ^{o}C. ^{1}H NMR (C_6D_6, 25 ^{o}C): δ (ppm) 0.52–0.57 (m, 8H, ZnCH_2CH$_3$), 0.74–0.96 (m, 48H, CH(CH_3)$_2$), 1.06 (t, $^{1}J_{H\text{-}H}$ = 6.5 Hz, 12H, ZnCH$_2$CH_3), 3.03–3.23 (br. m, 8H, CH(CH$_3$)$_2$), 6.60–6.86 (m, 12H, H$_{aryl}$), 7.02 (s, 2H, NCHN); ^{13}C NMR (C_6D_6, 25 ^{o}C): δ (ppm) 9.7 (Zn*C*H$_2$CH$_3$), 22.3 (CH(*C*H$_3$)$_2$), 26.9 (ZnCH$_2$*C*H$_3$), 37.7 (*C*H(CH$_3$)$_2$), 122.0 (*m*–ArC), 122.3 (*p*–ArC), 141.9 (*o*–ArC), 144.6 (ArC–N), 153.9 (NCN); IR (υ cm^{-1}, Nujol mull): 1667 (m), 1597 (m), 1557 (m), 1320

(w), 934 (m); MS (*m/z*; found (calcd)): M^+ not observed, 1004.8 (1005.1) M – 4Et, 365.3 (364.5) L^H.

Preparation of [{HC(NDipp)$_2$}$_2$Zn$_3$Et$_2$](OEt)$_2$, 30: To a 25 ^{o}C toluene (25 mL) solution of L^H (0.25 g, 0.69 mmol) was added 1 equiv. of $ZnEt_2$ (0.69 mL, 0.69 mmol) dropwise. Evolution of gas was observed. Stirring was maintained for 30 minutes after which time the solvent was removed *in vacuo* and the solid was extracted into hexane. The reaction mixture was concentrated, filtered and stored at room temperature to afford **30** as colorless crystalline needles. Yield: 0.25 g, 35%. M.p. 232–235 ^{o}C. ^{1}H NMR (C_6D_6, 25 ^{o}C): δ (ppm) 0.23 (q, $^1J_{H\text{-}H}$ = 8.1 Hz, 4H, ZnCH_2CH$_3$), 0.62 (d, $^1J_{H\text{-}H}$ = 6.6 Hz, 12H, CH(CH_3)$_2$), 0.72 (d, $^1J_{H\text{-}H}$ = 7.2 Hz, 12H, CH(CH_3)$_2$), 0.83 (t, $^1J_{H\text{-}H}$ = 6.3 Hz, 6H, OCH$_2$CH_3), 0.89 (d, $^1J_{H\text{-}H}$ = 7.2 Hz, 12H, CH(CH_3)$_2$), 1.11 (d, $^1J_{H\text{-}H}$ = 6.9 Hz, 12H, CH(CH_3)$_2$), 1.32 (t, $^1J_{H\text{-}H}$ = 6.9 Hz, 6H, ZnCH$_2$CH_3), 2.82–2.98 (m, 4H, CH(CH$_3$)$_2$), 3.20–3.33 (m, 4H, CH(CH$_3$)$_2$), 4.16 (q, $^1J_{H\text{-}H}$ = 6.8 Hz, 4H, OCH_2CH$_3$), 6.60–6.86 (m, 12H, H_{aryl}), 7.00 (s, 2H, NCHN); ^{13}C NMR (C_6D_6, 25 ^{o}C): δ (ppm) 5.5 (ZnCH$_2$CH$_3$), 9.7 (ZnCH$_2$CH$_3$), 12.8 (OCH$_2$$CH_3$), 21.1 (CH($CH_3$)$_2$), 21.5 (CH($CH_3$)$_2$), 22.3 (CH($CH_3$)$_2$), 23.2 (CH($CH_3$)$_2$), 26.9 (ZnCH$_2$$CH_3$), 27.8 (ZnCH$_2$$CH_3$), 28.8 ($C$H(CH$_3$)$_2$), 29.4 ($C$H(CH$_3$)$_2$), 33.3 ($C$H(CH$_3$)$_2$), 37.7 ($C$H(CH$_3$)$_2$), 66.6 (O$CH_2CH_3$), 121.7 (*m*–ArC), 122.0 (*m*–ArC), 122.3 (*p*–ArC), 122.6 (*p*–ArC), 129.3 (*o*–ArC), 137.5 (*o*–ArC), 144.6 (ArC–N), 145.4 (ArC–N), 166.1 (NCN); IR (υ cm^{-1}, Nujol mull): 1665 (m), 1597 (m), 1561 (m), 1287 (m), 1180 (m), 756 (m); MS (*m/z*; found (calcd)): M^+ not observed, 1042.6 (1042.4) M – Et, 447.2 (447.1) M – 2OEt – 2Et – Zn – 2Dipp – 2^{i}Pr – 2H, 365.3 (364.5) L^H.

CHAPTER VI

The reactions of Ga(III), In(III), and Tl(III) Halides with Pyridineselenolate and Pyrazinamide Ligands

6.1 Introduction

Beginning in the 1990's, the pyridineselenolate complexes consisting of transition, main group, and lanthanide metals became a topic for exploration.[68,70-86] In 1994, Brennan and co-workers reported the synthesis and structural characterization of the first transition metal pyridineselenolate complexes.[72] These complexes feature ligands in both chelating and bridging coordination modes (Figure 55).

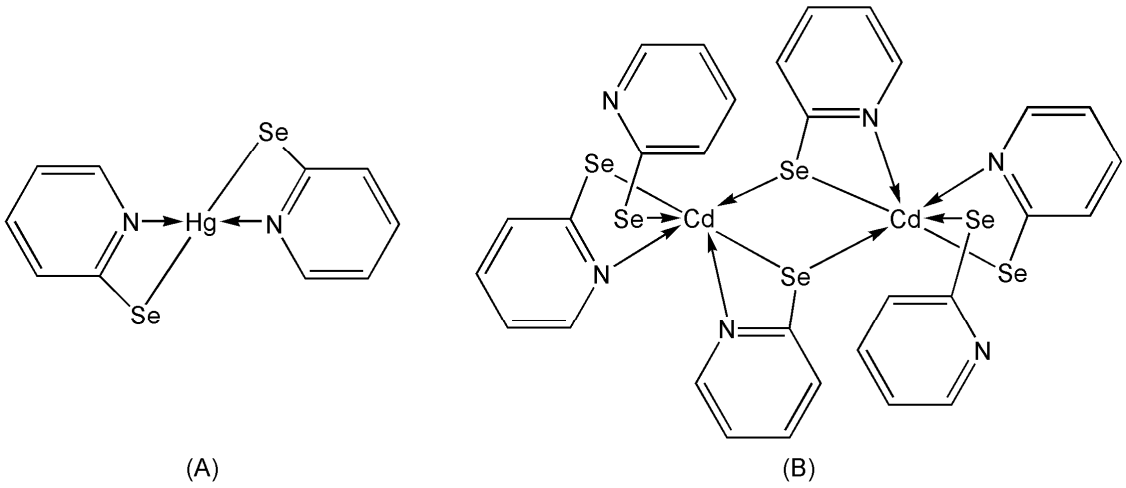

Figure 55. (A) $Hg(Se\text{-}2\text{-}NC_5H_4)$ (B) $Cd(Se\text{-}2\text{-}NC_5H_4)$

Shortly after their initial reports, Brennan and co-workers reported pyridine-2-selenol complexes with the main group elements; lithium, tin and lead.[68,73] The resulting lithium pyridineselenolate complex was dimeric, consisting of two lithium ions.[73] The nitrogen and selenium of each ligand coordinated to different lithium atoms, thus forming an eight membered ring (Figure 56).

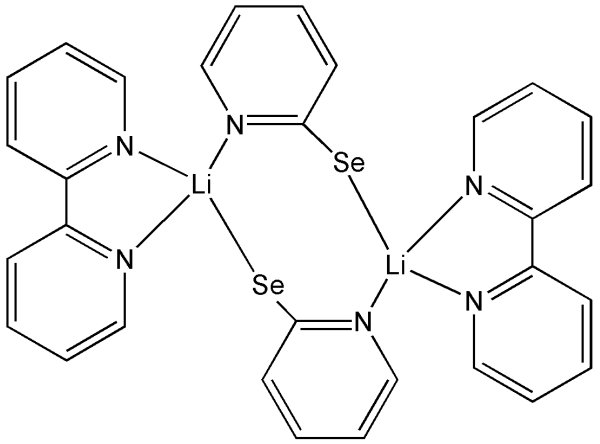

Figure 56. Li(Se-2-NC_5H_4)

Among the tin(II), tin(IV), and lead(II) complexes formed, only the tin(II) pyridineselenolate complex was determined by single-crystal X-ray diffraction. Similarly to the Li complex, the tin(II) pyridineselenolate complex was dimeric, with each tin center consisting of one chelating pyridineselenolate and a pair of pyridineselenolate ligands with the nitrogen and selenium coordinated to a different tin atom, thus forming an eight membered ring.[68] The homoleptic tin(II) complex was prepared by a metathesis reaction (Eq. 6.1) or insertion of the metal into the Se–Se bond of dipyridyl diselenide (Eq. 6.2).

$$SnCl_2 + NaSePy \xrightarrow{thf} Sn(SePy)_2 + 2NaCl \qquad \text{(Eq. 6.1)}$$

$$Sn + PySe{-}SePy \xrightarrow{toluene} Sn(SePy)_2 \qquad \text{(Eq. 6.2)}$$

Only a handful of main group metal pyridineselenolate complexes have been reported but include indium, tin, and phosphorus metal centers.[71,74,83-85] For example, in 1996, Brennan and co-workers reported the structures of two indium complexes both

containing three chelating pyridineselenolate ligands (Scheme 38).[74] The direct insertion of the indium metal into the diselenide bond proved to be the best means of preparation.

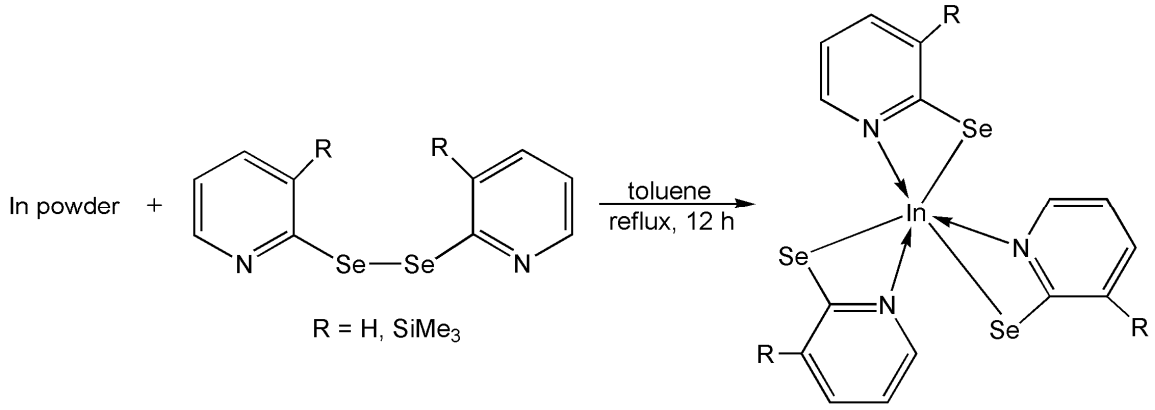

Scheme 38. Synthesis of $In(SePy)_3$

Soon after, in 1997, Sousa and co-workers reported and characterized the same indium pyridineselenolate complex, $[In(pySe)_3]$, by an electrochemical procedure.[84] The difference lied in the absence of the acetone molecule of solvation that was found in the asymmetric unit of the structure reported by Brennan.

Similarly to the pyridineselenolate ligands, pyrazinamide complexes consisting of main group, transition, lanthanide, and actinide metals have been extensively explored.[102-109,111,204-219] The most numerous complexes of pyrazinecarboxamide are with transition metals spanning the entire d-block with the most common examples including cobalt, nickel, copper, and zinc.[102,104-107,111,205-217,219] Several examples of lanthanide[103,108,109] and actinide[218] complexes have also been reported. However, it appears that main group complexes supported by the pyrazinamide ligand are lagging with only a few complexes reported, including Be(II), Mg(II), and Sn(IV).[102,220] Both group 2 elements formed five membered chelate ring compounds by means of the oxygen of the carbonyl and the nitrogen of the ring (Figure 57).[220]

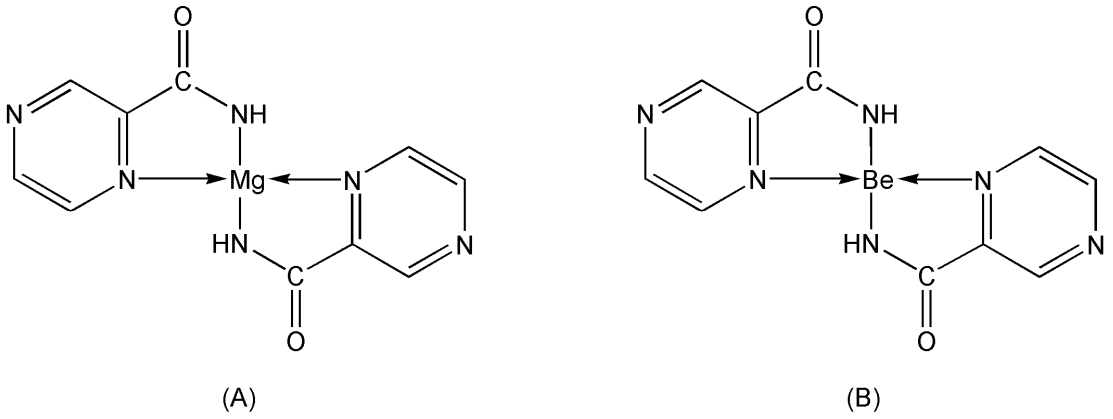

Figure 57. (A) Magnesium pyrazinamide complex (B) Beryllium pyrazinamide complex

In 1976, Jain, Gill, and Rao reported the main group complex of tin(IV) pyrazinamide that was synthesized by reacting an excess amount of the ligand with $SnCl_4$ in dichloromethane.[102] The reaction was stirred at room temperature for 2 days, after which time characterization by infrared spectroscopy implied the formation of a five membered chelate through the oxygen atom of the carbonyl and the nitrogen atom of the heterocycle (Figure 58).

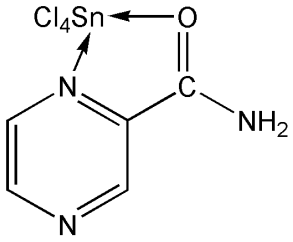

Figure 58. Pyrazinamide Sn(IV) complex

In addition, Jain and co-workers reported another unique example of a titanium pyrazinamide complex incorporating two binding modes.[102] The complex was synthesized by reacting $TiCl_4$ and the ligand, in a 1:3 amount respectively, in

dichloromethane. Coordination occurred at both nitrogen atoms of the heterocycle, thus forming two five membered chelates and a bridged titanium(IV) molecule (Figure 59).

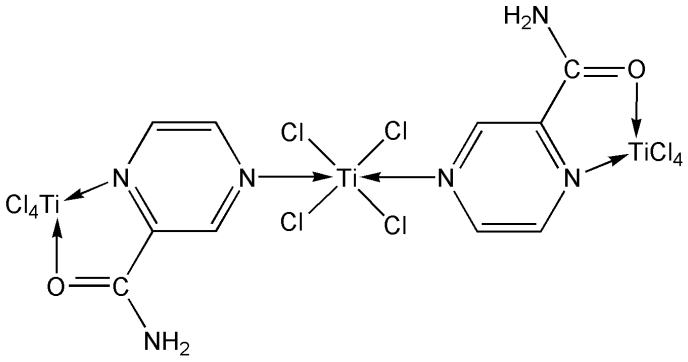

Figure 59. Pyrazinamide Ti(IV) complex

Several other examples have been reported observing coordination of the metal with two pyrazinecarboxamide ligands through the nitrogen atom of the ring (Figure 60) including, but limited to, transition metals[111,205,207,209,211,217] and lanthanides.[103,108,218]

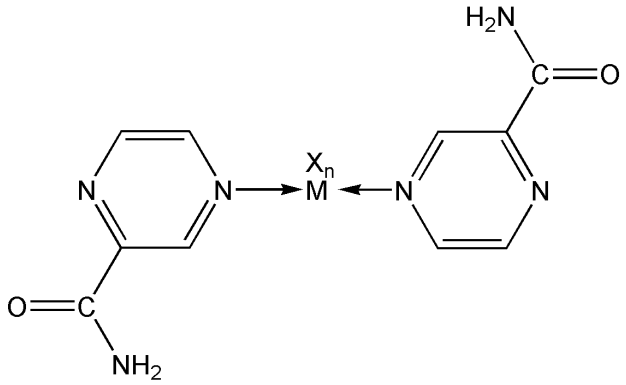

Figure 60. Nitrogen coordinated metal complexes

In this chapter, the coordination chemistry of pyridineselenolate and pyrazinecarboxamide ligands are explored with group 13 metal halides. We report the synthesis of gallium, indium, and thallium pyridineselenolate and pyrazinecarboxamide complexes, and the chemistry and reactivity of these complexes is explored. The

preparation of these complexes offers further insight into their potential catalytic, technological, and electronic applications that have been observed by other related group 13 compounds.[39,221-224] For example, indium metal complexes have success in MOCVD growth,[218,222] specifically the synthesis of InSe thin films which are active III-VI semiconductors.[223] The research focuses on the individual synthetic methods for the preparation of indium and thallium complexes **32**–**39**. Structural data were acquired by single-crystal X-ray diffraction experiments for each complex and as well as other spectroscopic techniques.

6.2 Results and Discussion

6.2.1 Discussion of $[(PyO)_2SeCl_2]$, 31

The pyridineselenolate ligand was synthesized following a previous literature procedure,[72] however upon completion a mixture of products were obtained including 2-selenopyridine, 2,2'-selenodipyridine, and 2,2'-dipyridyl diselenide as confirmed by mass spectroscopy (Refer to Figure 9). We continued performing reactions based on the expected major product and therefore used an excess of metal salt. To examine the coordination preferences with group 13 metal halides, $InCl_3$ was initially selected. The reaction of the ligand with $InCl_3$ in a 1:1 ratio was performed in anhydrous dichloromethane at room temperature (Scheme 39).

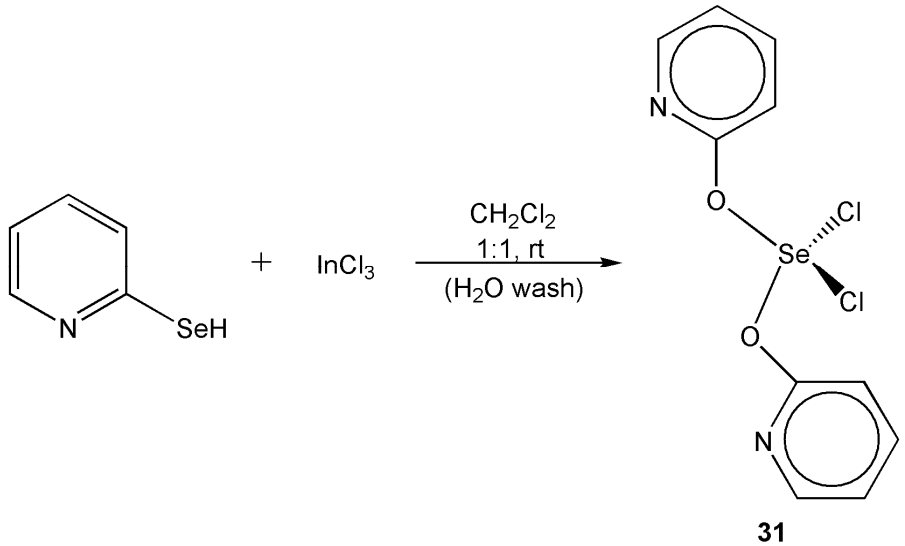

Scheme 39. Synthesis of compound **31**.

Colorless crystalline blocks of **31** were isolated and the molecular structure determined by X-ray crystallography (Figure 61). Complex **31** crystallizes in the

monoclinic space group C_2/c where [(PyO)SeCl] is observed in the asymmetric unit, and a mirror center exists at the selenium atom.

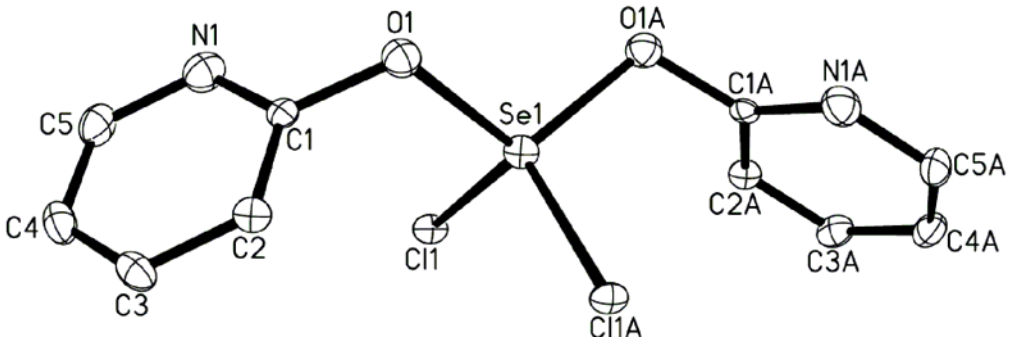

Figure 61. Molecular structure of $[(PyO)_2SeCl_2]$, **31**. Thermal ellipsoids at 30% probability level, hydrogen atoms have been omitted for clarity. Selected bond lengths(Å) and angles(°): Se1-O1 2.053(2), Se1-Cl1 2.252(7), O1-C1 1.450(4), O1-Se1-Cl1 108.6(7), Cl1#1-Se1-Cl1 108.7(4), O1-Se1-Cl1#1 109.3(7), O1-Se1-O1#1 112.0(14).

The solid-state analysis does not show the expected coordination, but rather oxygen insertion between the pyridine ring and selenium, as well as attachment of two chloride atoms to the selenium center in the full structure. The insertion of oxygen atoms are likely a result of moisture contamination of the anhydrous CH_2Cl_2 solvent. Most interestingly is the chloride atom rearrangement to the selenium center of the ligand. Halogenating the selenium is probably the result of the CH_2Cl_2 solvent as well as an excess of $InCl_3$ during the reaction. The concept of the halogen rearrangement has been previously observed in the formation of selenium heterocycles employing the β-diketiminato ligands, where halogenating the ligand backbone was confirmed by excess $SeCl_4$.[121] In complex **31**, the Se–Cl bond length 2.252(7) Å is considerably shorter than the Se–Cl bond length observed for [MesnacnacHCl$_2$SeCl] where the bond length is 2.579(7) Å,[121] but is within the appropriate values for normal bonds,[225] where the

covalent radii for Se–Cl is 2.21 Å.[162] The Se center has undergone oxidation from Se(II) to Se(IV) and can be viewed as having a slightly distorted tetrahedral geometry which is observed by bond angles of 108.6(7)°, 108.7(4)°, 109.3(7)°, and 112.0(14)° for O(1)-Se(1)-Cl(1), Cl(1)#1-Se(1)-Cl(1), O(1)-Se(1)-Cl(1)#1, O(1)-Se(1)-O(1)#1, respectively. Solution ^{1}H and ^{13}C NMR data in CD_2Cl_2 was attempted for compound **31**. The proton peaks were observed ranging from 7.60–8.62 ppm which are similar to those observed for other transition metal complexes with 2-selenopyridine and 2,2'-dipyridyl diselenide ranging from 5.89–8.46 ppm.[70] Attempts in other solvents failed due to the limited solubility of the complex.

6.2.2 Discussion of $[(Py)_2Se]InCl_3$, 32

In keeping with our original goal of targeting the indium coordination complex with pyridineselenolate, the equimolar reaction of the ligand with $InCl_3$ was performed in anhydrous ethanol at room temperature (Scheme 40).

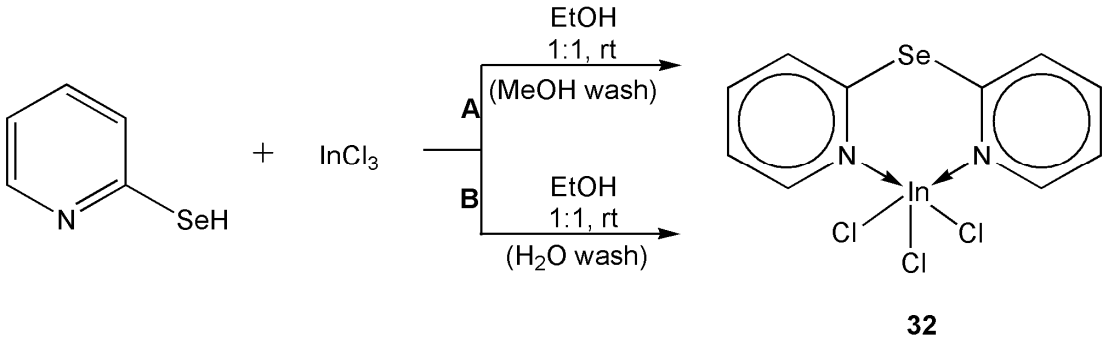

32

Scheme 40. Synthesis of compound **32**.

After stirring overnight, the solution was concentrated under reduced pressure and pale yellow needles of compound **32** were obtained. Crystals of **32** could be obtained employing the ligand acquired from either the MeOH or H_2O washes, with the MeOH

wash resulting in a slightly higher yield of 85%. Structural analysis revealed that compound **32** had in fact formed a coordination complex with the metal halide (Figure 62).

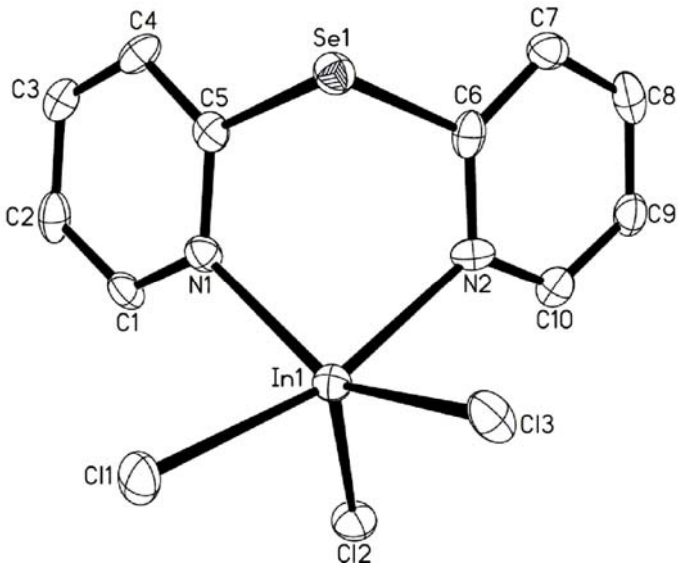

Figure 62. Molecular structure of $[(Py)_2Se]InCl_3$, **32**. Thermal ellipsoids at 30% probability level, hydrogen atoms have been omitted for clarity. Selected bond lengths(Å) and angles(°): In1-N1 2.263(7), In1-N2 2.305(7), In1-Cl1 2.421(2), In1-Cl2 2.394(2), In1-Cl3 2.413(2), Se1-C5 1.941(9), Se1-C6 1.946(9), N1-In1-N2 82.60(2), N1-In1-Cl2 99.40(18), N2-In1-Cl2 92.88(18), N2-In1-Cl3 86.45(18), Cl2-In1-Cl3 114.0(9), N1-In1-Cl1 86.49(18), N2-In1-Cl1 164.6(18), Cl3-In1-Cl1 96.58(8), C5-Se1-C6 94.20(4).

The solid-state analysis revealed that **32** crystallizes in the monoclinic space group $P2_1/c$ where the geometry around the indium center is distorted trigonal bipyramidal. The actual product corresponds to the expected outcome, as the preferred hard–hard interactions between the nitrogen and indium(III) are observed rather than the hard–soft interaction between the selenium and indium(III). The In–N bond distances, 2.263(7) Å and 2.305(7) Å, are within the appropriate range and similar to the

tris(pyridine-2-selenolato)indium(III) structure, [In(PySe)$_3$], where In–N bond lengths range from 2.297(10)–2.370(11) Å.[84] Additionally, the In–Cl bond lengths of 2.421(2) Å, 2.394(2) Å, and 2.413(2) Å fall in the expected range of In(III)Cl distances, for example the pyrazine indium complexes [(L)$_3$InCl$_3$] and [LInCl$_3$(OH)$_2$], where L = pyrazine and pyrazine-2-carboxylic acid, respectively, exhibit In–Cl bond distances ranging from 2.388(3)–2.445(4) Å.[225] Infrared spectroscopy and solution NMR in CD_2Cl_2 was obtained to confirm the solid-state analysis of compound **32**, where ^{1}H NMR showed peaks ranging from 7.75–8.79 ppm which are similar to those observed for **31** as well as other examples.[70] Attempts in other solvents failed due to the limited solubility of the complex.

6.2.3 Discussion of $[Py_4Se]^{2+}2[InBr_4]^{-}2[CH_2Cl_2]$, 33

In addition to the formation of complex **32**, we also aimed to synthesize the analogues indium complex with $InBr_3$. The equimolar reaction of the pyridineselenolate ligand with $InBr_3$ was performed in anhydrous CH_2Cl_2 at room temperature (Scheme 41).

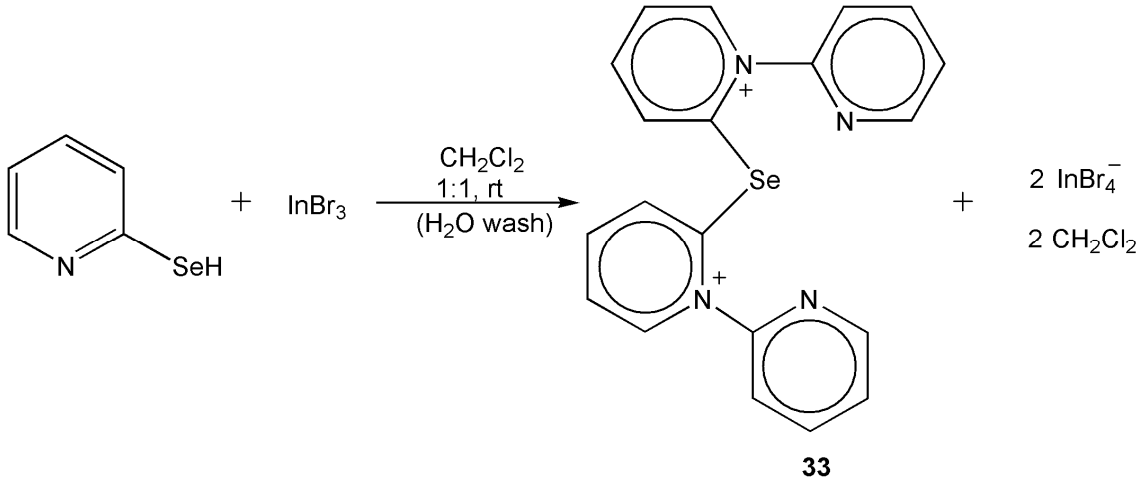

Scheme 41. Synthesis of compound **33**.

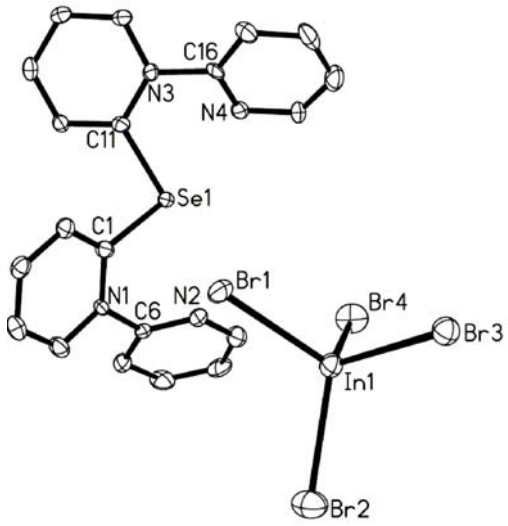

Figure 63. Molecular structure of $[Py_4Se]^{2+}2[InBr_4]^{-}2[CH_2Cl_2]$, **33**. Thermal ellipsoids at 30% probability level, two CH_2Cl_2 molecules, one $[InBr_4]^{-}$, and hydrogen atoms have been omitted for clarity. Selected bond lengths(Å) and angles(°): Se1-C1 1.933(7), Se1-C11 1.937(7), N1-C6 1.460(9), N3-C16 1.447(9), In1-Br1 2.469(11), In1-Br2 2.482(13), In1-Br3 2.545(14), In1-Br4 2.476(7), C1-Se1-C11 96.20(3).

Despite employing identical reaction conditions as for the synthesis of **31**, no oxygen insertion or halide coordination was observed in the crystallographic analysis. Colorless needles were obtained from the reaction in low yield and determined by X-ray crystallography as compound **33** which crystallizes in the monoclinic space group $P2_1/c$ (Figure 63). The solid-state analysis of complex **33** exhibits the 2,2'-selenodipyridine ligand, as observed for complexes **31** and **32**, where the pyridine rings are further coordinated to an additional pyridine. The molecule is balanced by two anionic $[InBr_4]^{-}$ molecules present in the asymmetric unit, along with two dichloromethane solvent molecules. The Se–C bond lengths 1.933(7) Å and 1.937(7) Å for Se(1)–C(1) and Se(1)–

C(11), respectively, are nearly identical to **32** and within the appropriate values. The N–C bond lengths of 1.460(9) Å and 1.447(9) Å observed between the two pyridine rings exhibit single bonds. Due to the particularly low yield of **33**, no further characterization was conducted.

6.2.4 Discussion of $[(Py)_2SeCl]^+[Cl]^-[H_2O]$, 34

To further examine the coordination preferences of the pyridineselenolate ligand with group 13 metal halides, thallium(III) chloride tetrahydrate was selected for the reaction. Since thallium halides have shown to be successful in coordination to nitrogen based ligands, for example the thallium(III) chloride pyrazine polymer, $[TlCl_3(pyz)]_\infty$,[224] we deemed that the pyridineselenolate ligand might also prove a useful precursor. The ethanol reaction of 2,2'-selenodipyridine with $TlCl_3 \cdot 4H_2O$ in a 1:1 ratio was performed in aerobic conditions at room temperature (Scheme 42).

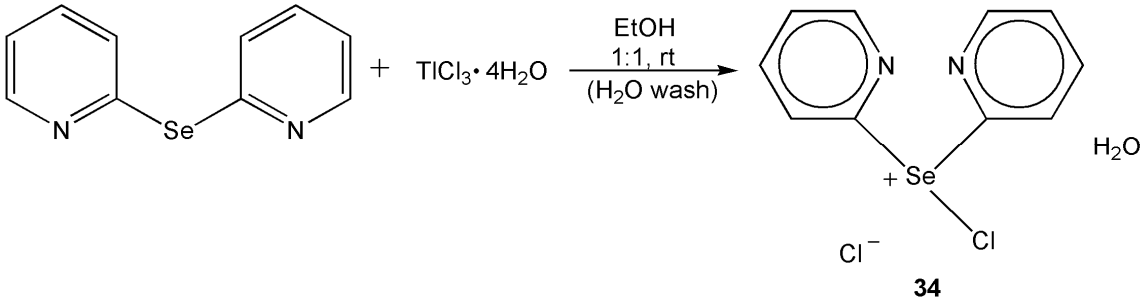

Scheme 42. Synthesis of compound **34**.

Pale yellow crystals of **34** were isolated in low yield and the molecular structure was determined by X-ray crystallography (Figure 64). Structural analysis revealed that no thallium coordination occurs, but rather, attachment of a chloride atom to the selenium center. The cationic charge is counterbalanced by a free chloride ion. Complex **34** is

structurally related to compound **31**, $[(PyO)_2SeCl_2]$. The major difference between the two compounds is that **34** only has one chloride atom attached while the chloride counter-ion sits ~3.1 Å from the cationic selenium center. Within the asymmetric unit a water molecule is also present, which is the result of the hydrated thallium(III) chloride. The Se(1)–Cl(1) bond distance of 2.451(11) Å is slightly longer than the covalent radii but lies within the appropriate range, for example $[MesnacnacHCl_2SeCl]$ exhibits the Se–Cl bond length at 2.579(7) Å.[121] The solid-state analysis of **34** is confirmed by infrared spectra which exhibits characteristic peaks[68,70,72] and by solution CD_2Cl_2 NMR which additionally confirms the presence of the water molecule exhibiting a distinctive characteristic singlet peak at 1.18 ppm.[226]

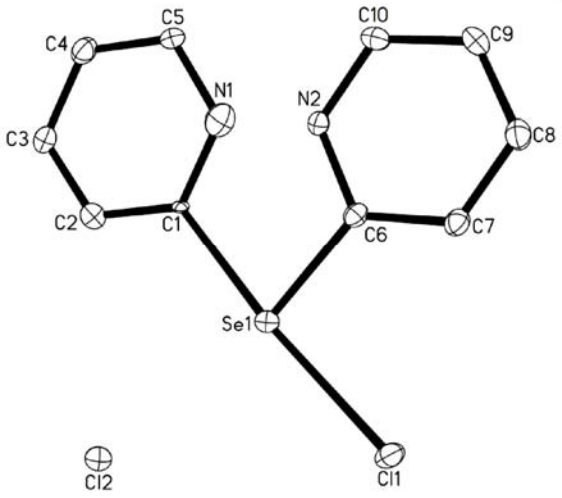

Figure 64. Molecular structure of $[(Py)_2SeCl]^+[Cl]^-[H_2O]$, **34**. Thermal ellipsoids at 30% probability level, hydrogen atoms and water molecule have been omitted for clarity. Selected bond lengths(Å) and angles(°): Se1-C1 2.060(3), Se1-C6 1.904(4), Se1-Cl1 2.451(11), C6-Se1-C1 79.86(14), C6-Se1-Cl1 94.28(11), C1-Se1-Cl1 174.1(9).

6.2.5 Discussion of $[(PySe)C_3H_5OH]^+[TlCl_4]^-$, 35

Continuing with our goal of targeting thallium coordination complexes with pyridineselenolate, the equimolar reaction of PySeH with $TlCl_3 \cdot 4H_2O$ was performed in acetone at room temperature. Complex **35** was isolated as yellow crystalline chunks in low yield (Scheme 43).

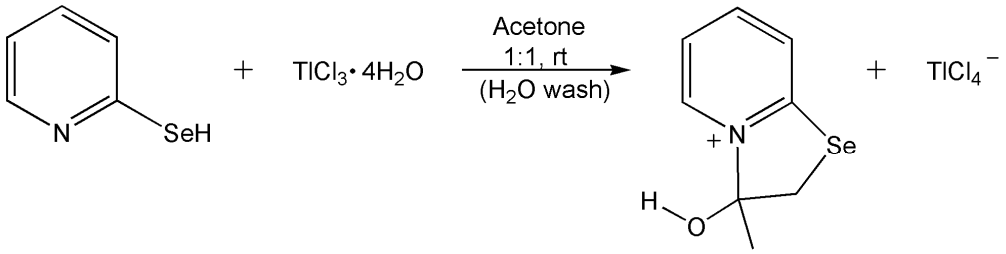

35

Scheme 43. Synthesis of compound **35**.

From the X-ray analysis of **35** it can be seen that once again no thallium coordination occurred, instead the 2-selenopyridine ligand is coordinated to a molecule of acetone (Figure 65). The oxygen atom has been protonated and the cationic 2-selenopyridine structure is counterbalanced by an anionic $[TlCl_4]^-$. The selenium center exhibits a bent geometry with C(5)–Se(1)–C(6) bond angle at 88.00(1)°. The hydrogen atom attached to the oxygen atom is confirmed by the electron density in the difference map. However, due to the poor quality X-ray data and low yield of **35**, no further characterization was performed.

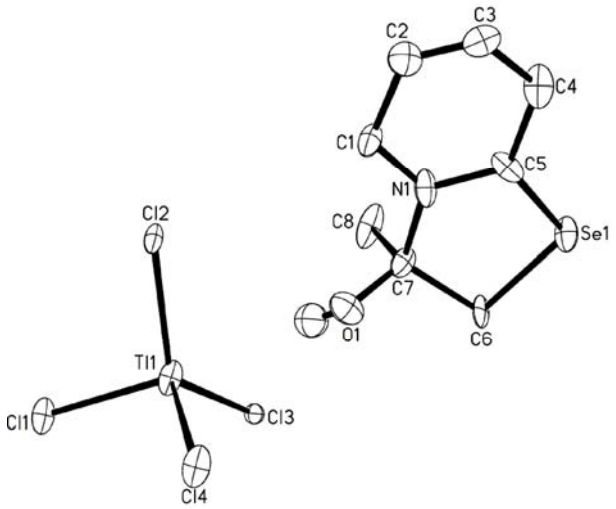

Figure 65. Molecular structure of $[(PySe)C_3H_5OH]^+[TlCl_4]^-$, **35**. Thermal ellipsoids at 30% probability level, except for oxygen all hydrogen atoms have been omitted for clarity. Selected bond lengths(Å) and angles(°): Se1-C5 1.880(3), Se1-C6 1.950(3), N1-C7 1.540(3), O1-C7 1.380(4), C6-C7 1.600(4), C7-C8 1.550(4), Tl1-Cl1 2.493(7), Tl1-Cl2 2.416(7), Tl1-Cl3 2.455(6), Tl1-Cl4 2.417(6), C5-Se1-C6 88.00(1), C7-C6-Se1 105.4(19), O1-C7-N1 108.0(2), O1-C7-C6 111.0(2), N1-C7-C6 108.0(2), C8-C7-C6 112.0(2).

6.2.6 Discussion of $[(PySe)_2H]^+[GaCl_4]^-$, 36

To complete our investigation of the group 13 metals with pyridineselenolate, the reaction of $GaCl_3$ with the ligand in a 1:1 ratio was performed in anhydrous ethanol at room temperature (Scheme 44).

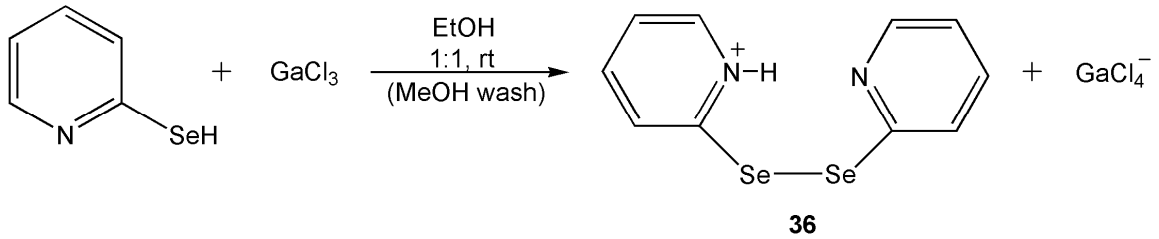

Scheme 44. Synthesis of compound **36**.

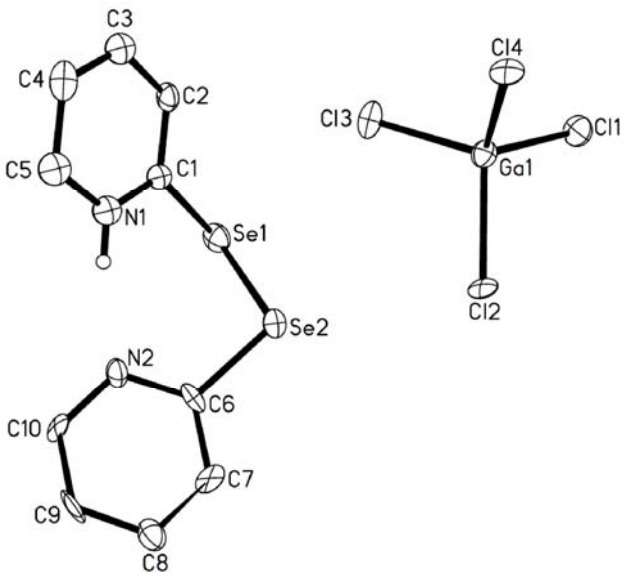

Figure 66. Molecular structure of $[(PySe)_2H]^+[GaCl_4]^-$, **36**. Thermal ellipsoids at 30% probability level, hydrogen atoms have been omitted for clarity. Selected bond lengths(Å) and angles(°): Se1-C1 1.923(6), Se2-C6 1.900(2), Se1-Se2 2.308(2), Ga1-Cl1 2.164(5), Ga1-Cl2 2.226(4), Ga1-Cl3 2.178(3), Ga1-Cl4 2.196(4), C1-Se1-Se2 98.60(4), C6-Se2-Se1 100.9(4).

Complex **36** was determined by X-ray crystallography to crystallize in the triclinic space group $P\bar{1}$. Structural analysis revealed that no gallium coordination occurred and the 2,2'-dipyridyl diselenide ligand resulted (Figure 66). Examination of the electron density in the difference map confirmed the presence of a hydrogen present on N(1). The cationic 2,2'-dipyridyl diselenide is counterbalanced by an anionic $[GaCl_4]^-$.

6.2.7 Discussion of $[(Pyza)_2InCl_3]$, 37

In addition to observing the coordination preferences of the group 13 metal halides with pyridineselenolate, we also aimed to synthesize indium and thallium

coordination complexes with the pyrazinecarboxamide ligand and to further observe the coordination preferences. The reaction of $InCl_3 \cdot 4H_2O$ with pyrazinamide in a 1:1 ratio was stirred overnight at 65 ^oC in methanol (Scheme 45). Following slow evaporation of the solvent, colorless plate crystals were isolated in moderate yield and crystallize in the triclinic space group $P\bar{1}$.

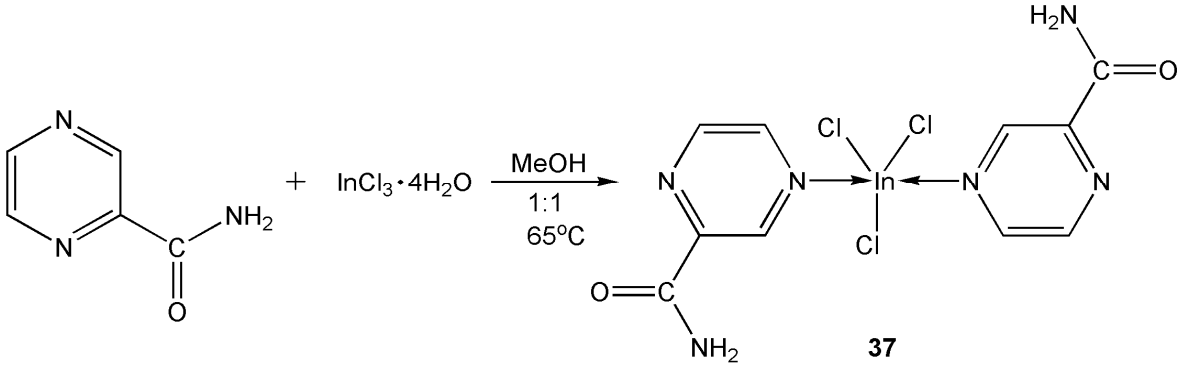

Scheme 45. Synthesis of compound **37**.

The molecular structure of **37** was determined by X-ray crystallography (Figure 67). In the asymmetric unit of **37**, there are five molecules present, each of which differs very slightly in bond lengths and angles. No higher symmetry space group could be determined. Each indium atom is coordinated to two ligands by the nitrogen in the 4 position, as is commonly observed for transition metals,[111,205,207,209-210,215] for example $[Cu(pyza)_2X]$ where X = Cl, Br, I, NO_3, ClO_4.[111] The indium center adopts a trigonal bipyramidal geometry, which is typical for five coordinate indium derivatives[166] and was previously observed in complexes **20** and **21** namely, $[DippN\{C(Me)\}_2C(Me)O]_2InCl$ and $[(Et_2)NC_2H_4NC(Me)CHC(Me)O]\ InCl_2$.[160]

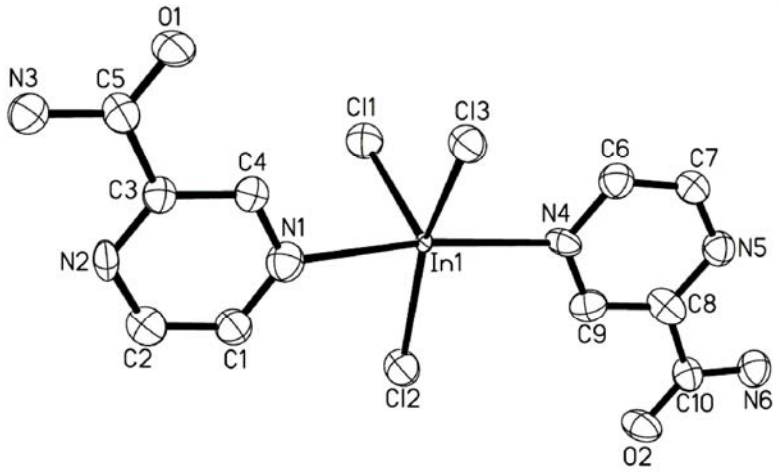

Figure 67. Molecular structure of $[(Pyza)_2InCl_3]$, **37**. Thermal ellipsoids at 30% probability level, hydrogen atoms have been omitted for clarity. Selected bond lengths(Å) and angles(°): In1-N1 2.460(2), In1-N4 2.430(2), In1-Cl1 2.446(9), In1-Cl2 2.388(8), In1-Cl3 2.472(18), O1-C5 1.240(3), O2-C10 1.220(3), N3-C5 1.330(3), N6-C10 1.320(3), N1-In1-Cl3 88.00(6), N4-In1-Cl3 88.50(5), Cl2-In1-N1 87.60(6), Cl2-In1-N4 90.70(5), N4-In1-Cl1 102.5(5), Cl2-In1-Cl1 107.6(3), N4-In1-N1 167.8(7).

In **37**, the In–N and In–Cl bond lengths range from 2.410(2)–2.480(2) Å and 2.384(8)–2.483(7) Å, respectively, where the In–N lengths are slightly longer than the In–N bond lengths observed in complex **32**, $[(Py)_2Se]InCl_3$**,** of 2.263(7) and 2.305(7) Å as well as other examples of In–N bond lengths.[84] The In–Cl lengths fall in the expected range of In(III)Cl distances.[227] The distorted trigonal bipyramidal geometry around the In(III) center can be observed from the bond angles which range from 87.30(6)° to 168.9(9)°. The solid-state analysis additionally reveals that **37** packs in order to maximize the hydrogen bonding (Figure 68). As a result, a system of alternating rows is formed where the molecules within each row are oriented in the same direction, and the adjacent rows are at ~79°. Infrared spectroscopy and solution NMR in CD_3CN was obtained to

confirm the solid-state analysis of compound **37**, where ^{1}H NMR showed peaks ranging from 7.12–9.40 ppm which are similar to the peaks reported of the parent ligand.[211]

Figure 68. Packing diagram for compound **37**.

6.2.8 Discussion of $[(Pyza)_2TlCl_3]$, 38

The 1:1 reaction of $TlCl_3 \cdot 4H_2O$ with pyrazinecarboxamide was performed in H_2O and stirred overnight at 90°C (Scheme 46). Following slow evaporation of the solvent, complex **38** was isolated as colorless plate crystals and was determined by X-ray crystallography to crystallize in the triclinic space group $P\bar{1}$.

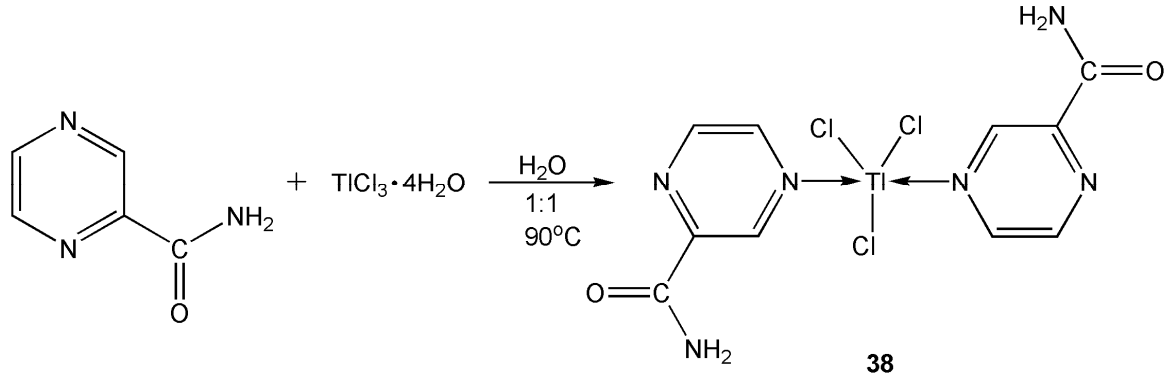

Scheme 46. Synthesis of compound **38**.

Structural analysis revealed that the thallium coordination to the ligand occurred in an analogous manner as complex **37**, where the Tl center was coordinated to two

pyrazinamide ligands at the nitrogen atoms in the 4 position (Figure 69). Within the asymmetric unit of **38** there are two neutral ligands and one molecule of the thallium pyrazinecarboxamide coordination complex.

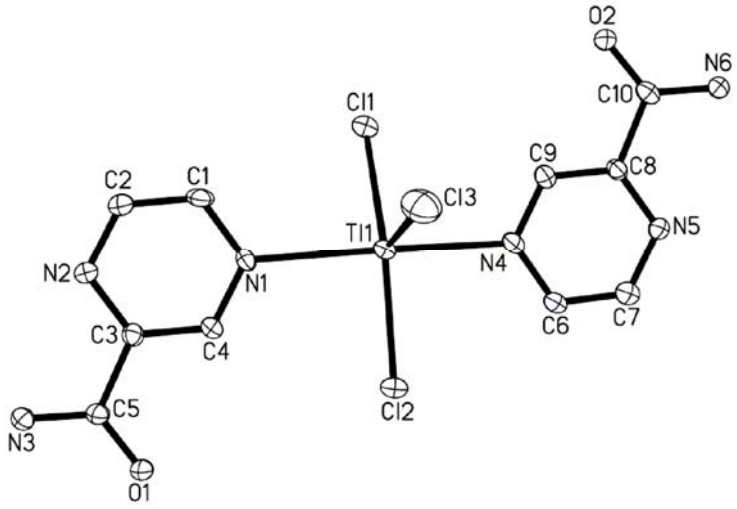

Figure 69. Molecular structure of $[(Pyza)_2TlCl_3]$, **38**. Thermal ellipsoids at 30% probability level, hydrogen atoms and neutral ligands have been omitted for clarity. Selected bond lengths(Å) and angles(°): Tl1-N1 2.442(5), Tl1-N4 2.446(5), Tl1-Cl1 2.477(17), Tl1-Cl2 2.411(17), Tl1-Cl3 2.421(2), N1-Tl1-Cl1 86.25(12), N4-Tl1-Cl1 87.64(12), Cl2-Tl1-N1 89.55(12), Cl3-Tl1-N4 92.51(13), Cl3-Tl1-N1 104.2(13), Cl2-Tl1-Cl3 106.8(7).

The thallium center adopts a distorted trigonal bipyramidal geometry which is exhibited by selected bond angles ranging from 86.25(12)° to 106.8(7)°. The Tl–N bonds at 2.442(5) Å and 2.446(5) Å for Tl(1)–N(1) and Tl(1)–N(4), respectively, are slightly longer than the covalent radii of 2.23 Å,[162] but comparable to other pyrazine thallium coordinated complexes, for example 2.462(5) Å for $[TlCl_3(pyz)]_\infty$.[228] Additionally, the Tl–Cl bonds at 2.477(17) Å, 2.411(17) Å, and 2.421(2) Å for Tl(1)–Cl(1), Tl(1)–Cl(2),

and Tl(1)–Cl(3), respectively, are comparable to other Tl(III) chloride bond lengths.[228] Moreover, the solid-state analysis reveals that like **37**, compound **38** packs in order to maximize the hydrogen bonding and results in alternating rows where the molecules are oriented in the same direction. The solid-state analysis is confirmed by IR and solution NMR where the ^{1}H NMR spectrum exhibits characteristic peaks similar to those reported[212] as well as those seen for complex **37**.

6.3 Summary

The reactions of group 13 halides have been studied with two nitrogen based ligands including pyridineselenolate and pyrazinecarboxamide. The reported pyridineselenolate structures **31**–**36** verify the mixture of products obtained from the different washes including 2-selenopyridine, 2,2'-selenodipyridine, and 2,2'-dipyridyl diselenide. Furthermore, the indium and thallium pyrazinamide complexes, **37**–**38**, are observed forming N–monodentate structures as coordination occurs through the nitrogen atom in the 4 position. The series of complexes highlight that reaction outcomes are dependent on temperature, solvent, and metal halide employed. The X-ray crystallographic analysis of the pyridineselenol complexes **31** and **34** revealed chloride transfer to the selenium metal center occurred concurrent with oxidation of the selenium from Se(II) to Se(IV). The choice of solvent appears to play a substantial role in the 2-PySeH reactions, as in **35** where the 2-selenopyridine prefers coordination to the acetone rather than the Tl center, thus preventing coordination to the thallium metal. However, solid-state analysis does show that the hard-hard interaction preference is favored over the soft-hard alternative in compound **32**. The hard-hard coordination preference is further highlighted by complexes **37** and **38** where nitrogen coordinates to the metal center. The pyrazinecarboxamide main group complexes are rare, but typically exhibit N,N' coordination forming a 5 membered ring.[102] These results further exhibit nitrogen coordination complexes employing nitrogen based aromatic ligands.

6.4 Experimental

6.4.1 General Procedures

All manipulations were performed under anaerobic conditions using standard Schlenk techniques unless stated otherwise. Anhydrous solvents, including dichloromethane and ethanol, were purchased from Aldrich and used as received. The reagents $InCl_3$, $InBr_3$, $GaCl_3$, $InCl_3 \cdot 4H_2O$, $TlCl_3 \cdot 4H_2O$, and pyrazinecarboxamide were purchased from Aldrich and used as received. The pyridineselenolate ligand, PySeH, was prepared according to published procedures.[72]

6.4.2 Spectroscopy Measurements

The ^1H and ^{13}C NMR spectra were recorded on a Varian Mercury 300 spectrometer (^1H 300.05 MHz and ^{13}C 75.45 MHz). IR analysis was conducted as Nujol Mulls with NaCl plates on a MIDAC M4000 Fourier transform infrared (FT IR) spectrometer. Melting points were determined in capillaries under a nitrogen atmosphere and are uncorrected.

6.4.3 Experimental Procedures and Spectroscopic Data

Preparation of $[(PyO)_2SeCl_2]$, 31: $InCl_3$ (0.20 g, 0.90 mmol) and 2-selenopyridine (0.14 g, 0.90 mmol, H_2O wash) were dissolved in 5 mL of anhydrous CH_2Cl_2 under dry oxygen-free conditions using standard Schlenk techniques. The dark yellow solution was allowed to stir overnight at room temperature. The resulting cloudy neon yellow solution mixture was allowed to settle, after which time was filtered, concentrated under reduced pressure, and stored at –30 ^oC affording colorless crystalline blocks of **31** in low yield.

Yield: 0.08 g, 26%. M.p. 207–210 ^{o}C (decomp). ^{1}H NMR (CD_2Cl_2, 25^{o}C): δ (ppm) 7.60 (t, 2H, $^{1}J_{H\text{-}H}$ = 6.8 Hz), 7.90 (t, 2H, $^{1}J_{H\text{-}H}$ = 8.5 Hz), 8.45 (d, 2H, $^{1}J_{H\text{-}H}$ = 6.0 Hz), 8.62 (d, 2H, $^{1}J_{H\text{-}H}$ = 6.3 Hz); ^{13}C NMR (CD_2Cl_2, 25^{o}C): δ (ppm) 97.74, 125.3, 129.4, 141.5, 146.6.

Preparation of [(Py_2Se)$InCl_3$], 32: Method **A**: $InCl_3$ (0.20 g, 0.90 mmol) and 2-selenopyridine (0.14 g, 0.90 mmol, MeOH wash) were dissolved in 5 mL of anhydrous ethanol under dry oxygen-free conditions using standard Schlenk techniques. The pale yellow solution was allowed to stir overnight at room temperature. The resulting cloudy yellow solution mixture was allowed to settle, after which time was filtered, concentrated under reduced pressure, and stored at room temperature for 1 week affording crystalline yellow needles of **32** in high yield. Yield: 0.35 g, 85%. M.p. 198–200 ^{o}C (decomp). ^{1}H NMR (CD_2Cl_2, 25^{o}C): δ (ppm) 7.75 (t, 2H, $^{1}J_{H\text{-}H}$ = 6.0 Hz), 8.04 (m, 4H), 8.79 (d, 2H, $^{1}J_{H\text{-}H}$ = 4.8 Hz); ^{13}C NMR (CD_2Cl_2, 25^{o}C): δ (ppm) 91.37, 125.4, 129.4, 141.5, 146.7; IR (Nujol Mull): ν (cm^{-1}) 1569 (w), 868 (m).

Method **B**: $InCl_3$ (0.18 g, 0.81 mmol) and 2-selenopyridine (0.13 g, 0.81 mmol, H_2O wash) were dissolved in 5 mL of anhydrous ethanol under dry oxygen-free conditions using standard Schlenk techniques. The yellow solution was allowed to stir overnight at room temperature, after which time the solution was filtered from a large yellow precipitate. Concentration under reduced pressure and storage at room temperature for 2 weeks afforded yellow crystalline needles of **32** in moderate yield. Yield: 0.27 g, 73%. M.p. and characterization refer to Method A.

Preparation of $[Py_4Se]^{2+}2[InBr_4]^{-}2[CH_2Cl_2]$, 33: $InBr_3$ (0.22 g, 0.63 mmol) and 2-selenopyridine (0.10 g, 0.63 mmol, H_2O wash) were dissolved in 10 mL of anhydrous CH_2Cl_2 under dry oxygen-free conditions using standard Schlenk techniques. The pale yellow solution was allowed to stir overnight at room temperature. The resulting yellow solution was filtered, concentrated under reduced pressure, and stored at room temperature affording colorless crystalline needles of **33** in low yield. Yield: 0.06 g, 8.4%. While complex **33** is unambiguous, due to low yield no further characterization was performed.

Preparation of $[(Py_2Se)Cl]^{+}[Cl]^{-}[H_2O]$, 34: $TlCl_3 \cdot 4H_2O$ (0.98 g, 0.64 mmol) and 2,2'-selenodipyridine (0.15 g, 0.64 mmol, H_2O wash) were dissolved in 5 mL of EtOH in a vial and stirred at room temperature overnight. The cloudy bright yellow reaction mixture was then filtered into a clean beaker. Yellow crystals suitable for X-ray diffraction were obtained by slow evaporation of the solution at room temperature. Yield: 0.10 g, 21%. M.p. 211–213 ^{o}C. ^{1}H NMR (CD_2Cl_2, 25^{o}C): δ (ppm) 1.18 (s, 2H, H_2O), 7.61 (t, 2H, $^{1}J_{H\text{-}H}$ = 6.0 Hz), 7.97 (t, 2H, $^{1}J_{H\text{-}H}$ = 7.3 Hz), 8.73 (d, 2H, $^{1}J_{H\text{-}H}$ = 5.1 Hz), 8.81 (d, 2H, $^{1}J_{H\text{-}H}$ = 5.4 Hz); ^{13}C NMR (CD_2Cl_2, 25^{o}C): δ (ppm) 117.9, 125.4, 129.2, 141.6, 147.9; IR (KBr pellet): ν (cm^{-1}) 1579 (m), 1546 (m), 1470 (m), 1447 (m), 1430 (m), 1336 (m), 1267 (s), 1156 (s), 1110 (w), 1070 (m), 1048 (m), 1017 (m), 762 (s), 729 (m), 697 (m), 647 (m).

Preparation of $[(PySe)C_3H_5OH]^{+}[TlCl_4]^{-}$, 35: $TlCl_3 \cdot 4H_2O$ (0.19 g, 0.63 mmol) and 2-selenopyridine (0.10 g, 0.63 mmol, H_2O wash) were dissolved in ~10 mL of acetone in a vial and stirred at room temperature for 3 h. The cloudy bright yellow reaction mixture

was then filtered into a clean beaker. Yellow chunk crystals suitable for X-ray diffraction were obtained by slow evaporation of the solution at room temperature. Yield: 0.09 g, 25%. Due to the unambiguous structure of complex **35**, no further characterization was performed.

Preparation of $[(PySe)_2H]^+[GaCl_4]^-$, 36: $GaCl_3$ (0.11 g, 0.63 mmol) and 2-selenopyridine (0.10 g, 0.63 mmol, MeOH wash) were dissolved in 5 mL of anhydrous ethanol under dry oxygen-free conditions using standard Schlenk techniques. The bright yellow solution was allowed to stir overnight at room temperature, after which time the solution was filtered, concentrated under reduced pressure, and stored at room temperature for 1 week affording yellow crystalline needles of **36**. Yield: 0.13 g, 39%. While complex **36** is unambiguous, poor quality x-ray data resulted in crystal data that is not publishable and after numerous attempts better quality crystals could not be achieved, therefore no further characterization was performed.

Preparation of $[(Pyza)_2InCl_3]$, 37: A methanol solution (5 mL) of $InCl_3 \cdot 4H_2O$ (0.20 g, 0.68 mmol) and pyrazinecarboxamide (0.08 g, 0.68 mmol) were stirred and heated in a vial at 65 ^oC for 24 h. After 24 h, the solution was filtered into a clean beaker for further crystallization. Colorless plate crystals suitable for X-ray diffraction were obtained by slow evaporation of the solution at room temperature. Yield: 0.16 g, 50%. M.p. 158–160 ^oC. ^1H NMR (CD_3CN, 25^oC): δ (ppm) 7.12 (s, 2H, NH_2) and 8.09 (s, 2H, NH_2) (equilibrium exchange), 8.92 (s, 2H, H_{ring}), 9.03 (s, 2H, H_{ring}), 9.40 (s, 2H, H_{ring}); ^{13}C NMR (CD_3CN, 25^oC): δ (ppm) 143.6 (C_{ring}), 144.9 (C_{ring}), 146.8 (C_{ring}), 150.5 (C_{ring}),

165.5 ($C(O)NH_2$); IR (KBr pellet): ν (cm^{-1}) 3404 (w), 1687 (s), 1610 (m), 1584 (m), 1524 (w), 1471 (w), 1435 (m), 1377 (s), 1261 (m), 1171 (s), 1088 (m), 1054 (m), 1023 (m), 868 (m), 820 (m, br), 776 (m), 670 (m), 560 (m), 448 (m).

Preparation of $[(Pyza)_2TlCl_3]$, 38: $TlCl_3 \cdot 4H_2O$ (0.20 g, 0.64 mmol) and pyrazinecarboxamide (0.08 g, 0.69 mmol) were dissolved in 5 mL of H_2O in a vial and stirred overnight at ~90 ^oC. The colorless solution was then filtered from a yellow precipitate into a clean beaker for further crystallization. Colorless plate crystals suitable for X-ray diffraction were obtained by slow evaporation of the solution at room temperature. Yield: 0.12 g, 23%. M.p. 149–152 ^oC. ^1H NMR (D_2O, 25^oC): δ (ppm) 7.58 (s, 2H, NH_2) and 8.35 (s, 2H, NH_2) (equilibrium exchange), 8.81 (s, 2H, H_{ring}), 8.75 (s, 2H, H_{ring}), 9.18 (s, 2H, H_{ring}); ^{13}C NMR (D_2O, 25^oC): δ (ppm) 141.3 (C_{ring}), 145.2 (C_{ring}), 146.9 (C_{ring}), 149.9 (C_{ring}), 165.3 ($C(O)NH_2$); IR (KBr pellet): ν (cm^{-1}) 3411 (m), 3162 (m, br), 1687 (m), 1606 (w), 1529 (w), 1403 (m), 1377 (m), 1171 (m), 1089 (m), 1052 (m), 1021 (m), 872 (m), 791 (m, br), 751 (w), 668 (m), 612 (m), 540 (m), 449 (m).

REFERENCES

1. Lee, A. V.; Schafer, L. L. *Eur. J. Inorg. Chem.* **2007**, 2243.

2. Bourget-Merle, L.; Lappert, M. F.; Severn, J. R. *Chem. Rev*. **2002**, *102*, 3031 and references cited therein.

3. (a) Gilroy, J. B.; Patrick, B. O.; McDonald, R.; Hicks, R. G. *Inorg. Chem.* **2008**, *47*, 1287.

   (b) Gilroy, J. B.; Ferguson, M. J.; McDonald, R.; Patrick, B. O.; Hicks, R. G. *Chem. Commun.* **2007**, 126.

4. (a) Hitchcock, P. B.; Lappert, M. F.; Layh, M. *Chem. Commun.* **1998**, 2179.

   (b) Farwell, J. D.; Hitchcock, P. B.; Fernandes, M. A.; Lappert, M. F.; Layh, M.; Omondi, B. *Dalton Trans.* **2003**, 1719.

   (c) Farwell, J. D.; Hitchcock, P. B.; Lappert, M. F.; Protchenko, A. V. *J. Organomet. Chem.* **2007**, *692*, 4953.

5. For examples of transition metal complexes, see:

   (a) Lappert, M. F.; Liu, D.-S. *J. Organomet. Chem.* **1995**, *500*, 203.

   (b) Rahim, M.; Taylor, N. J.; Xin, S.; Collins, S. *Organometallics*, **1998**, *17*, 1315.

   (c) Gibson, V. C.; Maddox, P. J.; Newton, C.; Redshaw, C.; Solan, G. A.; White, A. J. P.; Williams, D. J. *Chem. Commun.* **1998**, 1651.

   (d) Kim, W.-H.; Fevola, M. J.; Liable-Sands, L. M.; Rheingold, A. L.; Theopold, K. H. *Organometallics* **1998**, *17*, 4541.

   (e) Budzelaar, P. H. M.; de Gelder, R.; Gal, A. W. *Organometallics* **1998**, *17*, 4121.

(f) Budzelaar, P. H. M.; van Oort, A. B.; Orpen, A. G. *Eur. J. Inorg.* **1998**, 1485.

(g) Budzelaar, P. H. M.; Moonen, N. N. P.; de Gelder, R.; Smits, J. M. M.; Gal, A. W. *Eur. J. Inorg.* **2000**, 753.

(h) Cheng, M.; Lobkovsky, E. B.; Coates, G. W. *J. Am. Chem. Soc.* **1998**, *120*, 11018.

(i) Lee, L. W. M.; Piers, W. E.; Elsegood, M. R. J.; Clegg, W.; Parvez, M. *Organometallics* **1999**, *18*, 2947.

(j) Qian, B.; Scanlon IV, W. J.; Smith, M. R., III.; Motry, D. H. *Organometallics* **1999**, *18*, 1693.

(k) Kakaliou, L.; Scanlon IV, W. J.; Qian, B.; Baek, S. W.; Smith, M. R., III.; Motry, D. H. *Inorg. Chem.* **1999**, *38*, 5964.

(l) Holland, P. L.; Tolman, W. B. *J. Am. Chem. Soc.* **1999**, *121*, 7270.

(m) Holland, P. L.; Tolman, W. B. *J. Am. Chem. Soc.* **2000**, *122*, 6331.

(n) Ding, Y.; Ma, Q.; Roesky, H. W.; Herbst-Irmer, R.; Uson, I.; Noltemeyer, M.; Schmidt, H.-G. *Organometallics* **2002**, *21*, 5216.

(o) Hamaki, H.; Takeda, N.; Tokitoh, N. *Organometallics* **2006**, *25*, 2457.

(p) Bercaw, J. E.; Davies, D. L.; Wolczanski, P. T. *Organometallics* **1986**, *5*, 443.

6. For examples of main group complexes, see:

(a) Qian, B.; Ward, D. L.; Smith, M. R., III. *Organometallics* **1998**, *17*, 3070.

(b) Radzewich, C. E.; Coles, M. P.; Jordan, R. F. *J. Am. Chem. Soc.* **1998**, *120*, 9384.

(c) Radzewich, C. E.; Guzei, I. A.; Jordan, R. F. *J. Am. Chem. Soc.* **1999**, *121*, 8673.

(d) Kuchta, M. C.; Parkin, G. T. *New. J. Chem.* **1998**, *22*, 523.

(e) Qian, B.; Baek, S. W.; Smith, M. R., III. *Polyhedron* **1999**, *18*, 2405.

(f) Cui, C.; Roesky, H. W.; Hao, H.; Schmidt, H.-G.; Noltemeyer, M. *Angew. Chem. Int. Ed.* **2000**, *39*, 1815.

(g) Bailey, P. J.; Dick, C. M. E.; Fabre, S.; Parsons, S. *J. Chem. Soc., Dalton Trans.* **2000**, 1655.

(h) Gibson, V. C.; Segal, J. A.; White, A. J. P.; Williams, D. J. *J. Am. Chem. Soc.* **2000**, *122*, 7120.

(i) Cui, C.; Roesky, H. W.; Schmidt, H.-G.; Noltemeyer, M.; Hao, H.; Cimpoesu, F. *Angew. Chem. Int. Ed.* **2000**, *39*, 4274.

(j) Bailey, P. J.; Coxhall, R. A.; Dick, C. M.; Fabre, S.; Parsons, S. *Organometallics* **2001**, *20*, 798.

(k) Avent, A. G.; Crimmin, M. R.; Hill, M. S.; Hitchcock, P. B.; *Organometallics* **2005**, *24*, 1184.

(l) Dove, A. P.; Gibson, V. C.; Marshall, E. L.; White, A. J. P.; Williams, D. J. *Dalton Trans.* **2004**, 570.

(m) Avent, A. G.; Caro, C. F.; Hitchcock, P. B.; Lappert, M. F.; Li, Z.; Wei, X.-H. *Dalton Trans.* **2004**, 1567.

(n) El-Kaderi, H. M.; Xia, A.; Heeg, M. J.; Winter, C. H. *Organometallics* **2004**, *23*, 3488.

(o) Harder, S. *Organometallics* **2002**, *21*, 3782.

(p) Hitchcock, P. B.; Lappert, M. F.; Liu, D.-S.; Sablong, R. *Chem. Commun.* **2002**, 1920.

(q) Ding, Y.; Hao, H.; Roesky, H. W.; Noltemeyer, M.; Schmidt, H.-G. *Organometallics* **2001**, *20*, 4806.

(r) Cowley, A. H.; Lu, Z.; Jones, J. N.; Moore, J. A. *J. Organomet. Chem.* **2004**, *689*, 2562.

(s) Ding, Y.; Roesky, H. W.; Noltemeyer, M.; Schmidt, H. G.; Power, P. P. *Organometallics* **2001**, *20*, 1190.

(t) Harder, S. *Angew. Chem. Int. Ed. Engl*. **2003**, 3430.

(u) Vidovic, D.; Findlater, M.; Cowley, A. H. *J. Am. Chem. Soc.* **2007**, *129*, 8436.

(v) Vidovic, D.; Findlater, M.; Cowley, A. H. *J. Am. Chem. Soc.* **2007**, *129*, 11296.

(w) Vidovic, D.; Reeske, G.; Findlater, M.; Cowley, A. H. *Dalton Trans.* **2008**, 2293.

7. For examples of lanthanide complexes, see:

(a) Driess, D.; Magull, J. *Z. Anorg. Allg. Chem.* **1994**, *620*, 814.

(b) Hitchcock, P. B.; Lappert, M. F.; Protchenko, A. V. *Chem. Commun.* **2005**, 951.

(c) Neculai, D.; Roesky, H. W.; Neculai, A. M.; Magull, J.; Herbst-Irmer, R.; Walfort, B.; Stalke, D. *Organometallics* **2003**, *22*, 2279.

(d) Zhang, Y.; Yao, Y.-M.; Luo, Y.-J.; Shen, Q.; Cui, Y.; Yu, K.-B. *Polyhedron* **2003**, *22*, 1241.

(e) Hitchcock, P. B.; Lappert, M. F.; Tian, S. *Dalton Trans.* **1997**, 1945.

(f) Hitchcock, P. B.; Holmes, S. A.; Lappert, M. F.; Tian, S. J. *J. Chem. Soc., Chem. Commun.* **1994**, 2691.

8. (a) Cowley, R. E.; Elhaik, J.; Eckert, N. A.; Brennessel, W. W.; Eckard, B.; Holland, P. L. *J. Am. Chem. Soc*. **2008**, *130*, 6074.

(b) Smith, J. M.; Sadique, A. R.; Cundari, T. R.; Rodgers, K. R.; Lukat-Rodgers, G.; Lachicotte, R. J.; Flaschenriem, C. J.; Vela, J.; Holland, P. L. *J. Am. Chem. Soc.* **2006**, *128*, 756.

(c) Holland, P. L. *Can. J. Chem.* **2005**, *83*, 296.

(d) Eckert, N. A.; Vaddadi, S.; Stoian, S.; Lachicotte, R. J.; Cundari, T. R.; Holland, P. L. *Angew. Chem. Int. Ed.* **2005**, *45*, 6868.

(e) Smith, J. M.; Lachicotte, R. J.; Pittard, K. A.; Cundari, T. R.; Lukat-Rodgers, G.; Rodgers, K. R.; Holland, P. L. *J. Am. Chem. Soc.* **2001**, *123*, 9222.

(f) Yang, Y.; Schulz, T.; John, M.; Ringe, A.; Roesky, H. W.; Stalke, D.; Magull, J.; Ye, H. *Inorg. Chem*. **2008**, *47*, 2585.

(g) Wei, X.-H.; Farwell, J. D.; Hitchcock, P. B.; Lappert, M. F. *Dalton. Trans*. **2008**, *8*, 1073.

(h) Cui, C.; Roesky, H. W.; Noltemeyer, M.; Lappert, M. F.; Schmidt, H. G.; Hao, H. *Organometallics* **1999**, *18*, 2256.

(i) Hardman, N. J.; Cui, C.; Roesky, H. W.; Fink, W. H.; Power, P. P. *Angew. Chem. Int. Ed.* **2001**, *40*, 2172.

(j) Stender, M.; Phillips, A. D.; Power, P. P. *Inorg. Chem.* **2001**, *40*, 5314.

(k) Hardman, N. J.; Eichler, B. E.; Power, P. P. *Chem. Commun.* **2000**, 1991.

(l) Green, S. P.; Jones, C.; Stasch, A. *Science* **2007**, *318*, 1754.

(m) Liddle, S. T.; Arnold, P. L. *Dalton Trans*. **2007**, *30*, 3305.

(n) Bai, G.; Wei, P.; Das, A.; Stephan, D. W. *Organometallics* **2006**, *5*, 5870.

9. Hitchcock, P.B.; Hu, J.; Lappert, M. F.; Layh, M.; Liu, S. S.; Severn J. R.; Shun, T. *An. Quin. Int. Ed.* **1996**, *92*, 186.

10. Feldman, J.; McLain, S. J.; Parthasarathy, A.; Marshall, W. J.; Calabrese, J. C.; Arthur, S. D. *Organometallics* **1997**, *16*, 1514.

11. Chamberlain, B. M.; Cheng, M.; Moore, D. R.; Ovitt, T. M.; Lobkovsky, E. B.; Coates, G. W. *J. Am. Chem. Soc.* **2001**, *123*, 3229.

12. Cheng, M.; Moore, D. R.; Reczek, J. J.; Chamberlin, B. M.; Lobkovsky, E. B.; Coates, G. W. *J. Am. Chem. Soc.* **2001**, *123*, 8738.

13. For some examples, see:

    (a) Randall, D. W.; George, S. D.; Holland, P. L.; Hedman, B.; Hodgson, K. O.; Tolman, W. B.; Solomon, E. I. *J. Am. Chem. Soc.* **2000**, *122*, 11632.

    (b) Brown, E. C.; York, J. T.; Antholine, W. E.; Ruiz, E.; Alvarez, S.; Tolman, W. B. *J. Am. Chem. Soc.* **2005**, *127*, 13752.

    (c) Aboelella, N. W.; Gherman, B. F.; Hill, L. M. R.; York, J. T.; Holm, N.; Young Jr., V. G.; Cramer, C. J.; Tolman, W. B. *J. Am. Chem. Soc.* **2006**, *128*, 3445.

    (d) Vela, J.; Stoian, S.; Flaschenriem, C. J.; Munck, E.; Holland, P. L. *J. Am. Chem. Soc.* **2004**, *126*, 4522.

14. Basuli, F.; Huffman, J. C.; Mindiola, D. J. *Inorg. Chim. Acta.* **2007**, *360*, 246 and references cited therein.

15. McGeachin, S. G. *Can. J. Chem.* **1968**, *46*, 1903.

16. Dorman, L. C. *Tetrahedron Lett.* **1966**, *4*, 459.

17. Stender, M.; Wright, R. J.; Eichler, B. E.; Prust, J.; Olmstead, M.; Roesky, H. W.; Power, P. P. *J. Chem. Soc., Dalton Trans.* **2001**, *23*, 3465 and references cited therein.

18. Barry, W. J.; Finar, I.; Mooney, E. F. *Spectrochim. Acta* **1965**, *21*, 1095.

19. Hitchcock, P. B.; Lappert, M. F.; Liu, D.-S. *J. Chem. Soc., Chem. Commun.* **1994**, 1699.

20. Hamaki, H.; Takeda, N.; Yamasaki, T.; Sasamori, T.; Tokitoh, N. *J. Organomet. Chem.* **2007**, *692*, 44.

21. Sasamori, T.; Matsumoto, T.; Takeda, N.; Tokitoh, N. *Organometallics* **2007**, *26*, 3621.

22. Cromwell, N. H.; Miller, F. A.; Johnson, A. R.; Frank, R. L.; Wallace, D. J. *J. Am. Chem. Soc.* **1949**, *71*, 3337.

23. Witkop, B. *J. Am. Chem. Soc.* **1956**, *78*, 2873.

24. (a) Holtzclaw, H. F., Jr.; Johnson, K. W. R.; Hengeveld, F. W. *J. Am. Chem. Soc.* **1952**, *74*, 3776.

(b) Holtzclaw, H. F., Jr.; Carlson, A. H.; Collman, J. P. *J. Am. Chem. Soc.* **1956**, *78*, 1838.

(c) Holtzclaw, H. F., Jr.; Collman, J. P. *J. Am. Chem. Soc.* **1957**, *79*, 3318.

(d) Holtzclaw, H. F., Jr.; Collman, J. P.; Alire, R. M. *J. Am. Chem. Soc.* **1958**, *80*, 1100.

25. Weinstein, J.; Wyman, G. M. *J. Org. Chem.* **1958**, *23*, 1618.

26. (a) Dudek, G. O.; Holm, R. H. *J. Am. Chem. Soc.* **1961**, *83*, 2099.

(b) Dudek, G. O.; Holm, R. H. *J. Am. Chem. Soc.* **1962**, *84*, 2691.

(c) Dudek, G. O.; Volpp, G. P. *J. Am. Chem. Soc.* **1963**, *85*, 2697.

27. (a) Everett, G. W., Jr.; Holm, R. H. *J. Am. Chem. Soc.* **1965**, *87*, 2117.

(b) Jäger, V. E.-G. *Z. Anorg. Allg. Chem.* **1965**, *337*, 80.

(c) Yamada, S.; Nishikawa, H.; Yoshida, E. *Bull. Chem. Soc. Jpn.* **1966**, *39*, 994.

(d) Everett, G. W., Jr.; Holm, R. H. *J. Am. Chem. Soc.* **1966**, *88*, 2442.

(e) Yamada, S.; Yoshida, E. *Bull. Chem. Soc. Jpn.* **1967**, *40*, 1854.

(f) Everett, G. W., Jr.; Holm, R. H. *Inorg. Chem.* **1968**, *7*, 776.

(g) Ernst, R. E.; O'Conner, M. J.; Holm, R. H. *J. Am. Chem. Soc.* **1967**, *89*, 6104.

28. Li, X.-F.; Dai, K.; Ye, W.-P.; Pan, L.; Li, Y.-S. *Organometallics* **2004**, *23*, 1223.

29. Zhang, D.; Jin, G.-X.; Weng, L.-H.; Wang, F. *Organometallics* **2004**, *23*, 3270.

30. Liu, B.; Tian, C.; Zhang, L.; Yan, W.; Zhang, W. *J. Polym. Sci., Part A: Polym. Chem.* **2006**, *44*, 6243 and references therein.

31. Parks, J. E.; Holm, R. H. *Inorg. Chem.* **1968**, *7*, 1408.

32. Zhang, L.; Brookhart, M.; White, P. S. *Organometallics* **2006**, *25*, 1868.

33. He, X.; Wu, Q. *J. Appl. Polym. Sci.* **2006**, *101*, 4172.

34. Yu, R.-C.; Hung, C.-H.; Huang, J.-H.; Lee, H.-Y.; Chen, J.-T. *Inorg. Chem.* **2002**, *41*, 6450.

35. Pang, X.; Chen, X.; Zhuang, X.; Jing, X. *J. Polym. Sci., Part A: Polym. Chem.* **2008**, *46*, 643.

36. Tang, H.-Y.; Chen, H.-Y.; Huang, J.-H.; Lin, C.-C. *Macromolecules* **2007**, *40*, 8855.

37. He, X.; Wu, Q. *Appl. Organomet. Chem.* **2006**, *20*, 264.

38. Sachse, A.; Mösch-Zanetti, N. C.; Lyashenko, G.; Wielandt, J. W.; Most, K.;

Magull, J.; Dall'Antonia, F.; Pal, A.; Herbst-Irmer, R. *Inorg. Chem.* **2007**, *46*, 7129.

39. Chou, T.-Y.; Chi, Y.; Huang, S.-F.; Liu, C.-S. Carty, A. J.; Scoles, L.; Udachin, K. A. *Inorg. Chem.* **2003**, *42*, 6041.

40. Tung, Y.-L.;Tseng, W.-C.; Lee, C.-Y.; Hsu, P.-F.; Chi, Y.; Peng, S.-M.; Lee, G.-H. *Organometallics* **1999**, *18*, 864.

41. (a) Costes, J.-P.; Cros, G.; Darbieu, M.-H.; Laurent, J.-P. *Inorg. Chim. Acta.* **1982**, *60*, 111.

(b) Costes, J.-P.; Cros, G.; Darbieu, M.-H.; Laurent, J.-P. *Trans. Met. Chem.* **1982**, *7*, 219.

(c) Coombes, R. C.; Costes, J.-P., Fenton, D. E. *Inorg. Chim. Acta* **1983**, *77*, L173.

(d) Adams, H.; Bailey, N. A.; Baird, I. S.; Fenton, D. E.; Costes, J.-P.; Cros, G.; Laurent, J.-P. *Inorg. Chim. Acta* **1985**, *101*, 7.

(e) Costes, J.-P.; Cros, G.; Laurent, J.-P. *Inorg. Chim. Acta* **1985**, *97*, 211.

(f) Costes, J.-P. *Inorg. Chim. Acta.* **1987**, *130*, 17.

42. Costes, J.-P. *Polyhedron* **1987**, *6*, 2169 and references therein.

43. (a) Morgan, G.; Smith, H. *J. Chem. Soc.* **1925**, 2030.

(b) Morgan, G.; Smith, H. *J. Chem. Soc.* **1926**, 912.

(c) McCarthy, P. J.; Hovey, R. J.; Ueno, K.; Martell, A. E. *J. Am. Chem. Soc.* **1955**, *77*, 5820.

44. (a) Olson, D. C.; Vasilevskis, J. *Inorg. Chem.* **1969**, *8*, 1611.

(b) Elfring, W. H., Jr.; Rose, N. J. *Inorg. Chem.* **1975**, *14*, 2759.

45. Neculai, D.; Roesky, H. W.; Neculai, A. M.; Magull, J.; Schmidt, H.-G.; Noltemeyer, M. *J. Organomet. Chem.* **2002**, *643-644*, 47.

46. (a) Neculai, A. M.; Roesky, H. W.; Neculai, D.; Magull, J. *Organometallics*, **2001**, *20*, 5501.

(b) Neculai, A. M.; Neculai, D.; Roesky, H. W.; Magull, J. *Polyhedron* **2004**, *23*, 183.

(c) Nikiforov, G. B.; Roesky, H. W.; Vidovic, D.; Magull, J. *J. Mol. Struct.* **2003**, *656*, 155.

(d) Pineda, L. W.; Jancik, V.; Nembenna, S.; Roesky, H. W. *Z. Anorg. Allg. Chem.* **2007**, *633*, 2205.

47. Talukder, P.; Datta, A.; Mitra, S.; Rosair, G.; El Fallah, M. S.; Ribas, J. *Dalton Trans.* **2004**, 4161.

48. Pasko, S.; Hubert-Pfalzgraf, L. G.; Richard, P.; Abrutis, A. *Inorg. Chem. Commun.* **2005**, *8*, 483.

49. Aronica, C.; Jeanneau, E.; El Moll, H.; Luneau, D.; Gillon, B.; Goujon, A.; Cousson, A.; Carvajal, M. A.; Robert, V. *Chem. Eur. J.* **2007**, *13*, 3666.

50. Sarkar, B.; Ray, M. S.; Li, Y.-Z.; Song, Y.; Figuerola, A.; Ruiz, E.; Cirera, J.; Cano, J.; Ghosh, A. *Chem. Eur. J.* **2007**, *13*, 9297.

51. Sarkar, B.; Ray, M. S.; Drew, M. G. G.; Lu, C.-Z.; Ghosh, A. *J. Coord. Chem.* **2007**, *60*, 2165.

52. Schmidt, J. A. R.; Arnold, J. *J. Chem. Soc., Dalton Trans.* **2002**, 3454 and references cited therein.

53. (a) Edelmann, F. T. *Coord. Chem. Rev.* **1994**, *137*, 403.

(b) Barker, J.; Kilner, M. *Coord. Chem. Rev.* **1994**, *133*, 219 and references cited therein.

54. Coles, M. P. *Dalton Trans.*, **2006**, 985.

55. Mansfield, N. E.; Coles, M. P.; Hitchcock, P. B. *Dalton Trans.* **2005**, 2833.

56. Nijhuis, C. A.; Jellema, E.; Sciarone, T. J. J.; Meetsma, A.; Budzelaar, P. H. M.; Hessen, B. *Eur. J. Inorg. Chem.* **2005**, 2089.

57. Kissounko, D. A.; Zabalov, M. V.; Brusova, G. P.; Lemenovskii, D. A. *Russ. Chem. Rev.* **2006**, *75*, 351.

58. (a) Volkis, V.; Nelkenbaum, E.; Lisovskii, A.; Hasson, G.; Semiat, R.; Kapon, M.; Botoshansky, M.; Eishen, Y.; Eisen, M. S. *J. Am. Chem. Soc.* **2003**, *125*, 2179.

(b) Gibson, V. C.; Spitzmesser, S. K. *Chem. Rev.* **2003**, *103*, 283.

(c) Keaton, R. J.; Koterwas, L. A.; Fettinger, J. C.; Sita, L. R. *J. Am. Chem. Soc.* **2002**, *124*, 5932.

(d) Decker, J. M.; Geib, S. J.; Meyer, T. Y. *Organometallics* **1999**, *18*, 4417.

(e) Talarico, G.; Budzelaar, P. H. M. *Organometallics* **2000**, *19*, 5691.

(f) Dagorne, S.; Guzei, I. A.; Coles, M. P.; Jordan, R. F. *J. Am. Chem. Soc.* **2000**, *122*, 274.

(g) Dagorne, S.; Jordan, R. F.; Young, V. G. *Organometallics* **1999**, *18*, 4619.

(h) Coles, M. P.; Swenson, D. C.; Jordan, R. F.; Young, V. G. *Organometallics* **1998**, *17*, 4042.

(i) Coles, M. P.; Swenson, D. C.; Jordan, R. F.; Young, V. G. *Organometallics* **1997**, *16*, 5183.

(j) Coles, M. P.; Jordan, R. F. *J. Am. Chem. Soc.* **1997**, *119*, 8125.

(k) Brazeau, A. L.; Wang, Z.; Rowley, C. N.; Barry, S. T. *Inorg. Chem.* **2006**, *45*, 2276.

(l) Duchateau, R.; Meetsma, A.; Teuben, J. H. *Chem. Commun.* **1996**, 223.

59. (a) Barker, J.; Blacker, N. C.; Phillips, P. R.; Alcock, N. W.; Errington, W.; Wallbridge, M. G. H. *J. Chem. Soc., Dalton Trans.* **1996**, 431.

(b) Kenney, A. P.; Yap, G. P. A.; Richeson, D. S.; Barry, S. T. *Inorg. Chem.* **2005**, *44*, 2926.

60. (a) Lim, B. S.; Rahtu, A.; Park, J.; Gordon, R. G. *Inorg. Chem.* **2003**, *42*, 7951.

(b) Lim, B. S.; Rahtu, A.; Gordon, R. G. *Nat. Mater.* **2003**, *2*, 749.

(c) Li, Z.; Barry, S. T.; Gordon, R. G. *Inorg. Chem.* **2005**, *44*, 1728.

(d) Li, Z.; Rahtu, A.; Gordon, R. G. *J. Electrochem. Soc.* **2006**, *153*, 787.

61. Cole, M. L.; Davies, A. J.; Jones, C.; Junk, P. C. *New. J. Chem.* **2005**, *29*, 1404.

62. (a) Kondo, H.; Matsubara, K.; Nagashima, H. *J. Am. Chem. Soc.* **2002**, *124*, 534.

(b) Kondo, H.; Yamaguchi, Y.; Nagashima, H. *J. Am. Chem. Soc.* **2001**, *123*, 500.

63. Boeré, R. T.; Klassen, V.; Wolmershäuser, G. *J. Chem. Soc., Dalton Trans.* **1998**, 4147.

64. Boeré, R. T.; Klassen, V.; Wolmershäuser, G. *Can. J. Chem.* **2000**, *78*, 583.

65. Sanger, A. R. *Inorg. Nucl. Chem. Lett.*, **1973**, *9*, 351.

66. Krahulic, K. E.; Enright, G. D.; Parvez, M.; Roesler, R. *J. Am. Chem. Soc.* **2005**, *127*, 4142.

67. (a) Clive, D. L. J. *Tetrahedron* **1978**, *34*, 1049.

(b) Reich, H. J. *Acc. Chem. Res.* **1979**, *12*, 22.

(c) *The Chemistry of Organic Selenium and Tellurium Compounds*; Patai, P., Rappoport, Z., Eds.; Wiley-Interscience: New York, 1986; Vol. 1-2.

68. Cheng, Y.; Emge, T. J.; Brennan, J. G. *Inorg. Chem.* **1996**, *35*, 342 and references therein.
69. (a) Mautner, H. G.; Chu, S. H.; Lee, C. M. *J. Org. Chem.* **1962**, *27*, 3671. (b) Colonna, F. P.; Distefano, G.; Galasso, V.; Irgolic, K.; Pappalarardo, G. C.; Pope, L. *J. Chem. Soc., Perkin Trans.* **1981**, *2*, 281.
70. Kienitz, C. O.; Thöone, C.; Jones, P. G. *Inorg. Chem.* **1996**, *35*, 3990.
71. Chopra, N.; Damude, L. C.; Dean, P. A. W.; Vittal, J. J. *Can. J. Chem.* **1996**, *74*, 2095.
72. Cheng, Y.; Emge, T. J.; Brennan, J. G. *Inorg. Chem.* **1994**, *33*, 3711.
73. Khasnis, D. V.; Buretea, M.; Emge, T. J.; Brennan, J. G. *J. Chem. Soc., Dalton Trans.* **1995**, 45.
74. Cheng, Y.; Emge, T. J.; Brennan, J. G. *Inorg. Chem.* **1996**, *35*, 7339.
75. Jung, O.-S.; Jo, D. H.; Lee, Y.-A.; Conklin, B. J.; Pierpont, C. G. *Inorg. Chem.* **1997**, *36*, 19.
76. Narayan, S.; Jain, V. K.; Varghese, B. *J. Chem. Soc., Dalton Trans.* **1998**, 2359.
77. Narayan, S.; Jain, V. K. *Transition Met. Chem.* **1999**, *24*, 409.
78. Narayan, S.; Jain, V. K.; Panneerselvam, K.; Lu, T. H.; Tung, S.-F. *Polyhedron* **1999**, *18*, 1253.
79. Kita, M.; Tamai, H.; Ueta, F.; Fuyuhiro, A.; Yamanari, K.; Nakajima, K.; Kojima, M.; Murata, K.; Yamashita, S. *Inorg. Chim. Acta* **2001**, *314*, 139.
80. Sousa-Pedrares, A.; Durán, M. L.; Romero, J.; García-Vásquez, J. A.;

Monteagudo, J. C.; Sousa, A.; Dilworth, J. R. *Inorg. Chim. Acta* **2006**, *359*, 863.

81. Ma, X.; Schulzke, C.; Yang, Z.; Ringe, A.; Magull, J. *Polyhedron* **2007**, *26*, 5497.
82. Kienitz, C. O.; Thone, C.; Jones, P. G. *Z. Naturforsch., B: Chem. Sci.* **2000**, *55*, 587.
83. Laube, J.; Thone, C. *Phosphorus, Sulfur Silicon Relat. Elem.* **2001**, *168-169*, 497.
84. Romero, J.; Durán, M. L.; García-Vázquez, J. A.; Castiñeiras, A.; Sousa, A.; Christiaens, L.; Zubieta, J. *Inorg. Chim. Acta* **1997**, *255*, 307.
85. Laube, J.; Jäger, S.; Thöne, C. *Eur. J. Inorg. Chem.* **2001**, 1983.
86. Lopes, I.; Hillier, A. C.; Liu, S. Y.; Domingos, A.; Ascenso, J.; Galvão, A.; Sella, A.; Marques, N. *Inorg. Chem.* **2001**, *40*, 1116.
87. Kamiyama, T.; Enomoto, S.; Inoue, M. *Chem. Pharm. Bull.* **1985**, 5184.
88. Klayman, D. L.; Griffin, T. S. *J. Am. Chem. Soc.* **1973**, *95*, 197.
89. Toshimitsu, A.; Owada, H.; Terao, K.; Uemura, S.; Okano, M. *J. Org. Chem.* **1984**, *49*, 3796.
90. Syper, L.; Mlochowski, J. *Tetrahedron* **1988**, *44*, 6119.
91. Grant, H. G.; Summers, L. A. *Z. Naturforsch., B: Chem. Sci.* **1978**, *33B*, 118.
92. Pierini, A. B.; Peñéñory, A. B.; Rossi, R. A. *J. Org. Chem.* **1984**, *49*, 486.
93. Bhasin, K. K.; Arora, V.; Sharma, S. K.; Venugopalan, P. *Appl. Organomet. Chem.* **2005**, *19*, 161.
94. Dunne, S. J.; Von Nagy-Felsobuki, E. I. *Acta Cryst.* **1995**, *C51*, 1454.
95. Tiecco, M.; Testaferri, L.; Tingoli, M.; Chianelli, D.; Bartoli, D.; Balducci, R. *Tetrahedron* **1988**, *44*, 4883.

96. Bernatowicz, P.; Stefaniak, L.; Giurg, M.; Syper, L.; Webb, G. A. *Polish J. Chem.*, **1997**, *71*, 441.

97. Bhasin, K. K.; Bhandal, B. S.; Singh, J.; Singh, N.; Singh, K. N.; Singh, P. *Synth. Commun.* **2002**, *32*, 1319.

98. Bhasin, K. K.; Jain, V. K.; Kumar, H.; Sharma, S.; Mehta, S. K.; Singh, J. *Synth. Commun.* **2003**, *33*, 977.

99. (a) Staedel, W.; Rügheimer, L. *Chem. Ber.* **1876**, *9*, 563.
(b) Gutknecht, H. *Chem. Ber.* **1879**, *12*, 2290.

100. Woolfson, A.; Rothschild, M. *Proc. R. Soc. Lond. B.* **1990**, *242*, 113.

101. Munakata, M.; Wu, L.-P.; Kuroda-Sowa, T.; Maekawa, M.; Moriwaki, K.; Kitagawa, S. *Inorg. Chem.* **1997**, *36*, 5416 and references therein.

102. Jain, S. C.; Gill, M. S.; Rao, G. S. *J. Indian Chem. Soc.* **1976**, *53*, 537.

103. Rao, T. R.; Kumar, P. A. *Bull. Chem. Soc. Jpn.* **1994**, *67*, 96.

104. Kaur, J.; Marwaha, S. S.; Sodhi, G. S. *Rev. Latinoam. Quim.* **1998**, *26*, 37 and references therein.

105. Simon, V.; Jurca, T.; Simon, S. *Int. J. Mod. Phys. B* **2004**, *18*, 63.

106. Allan, J. R.; Paton, A. D.; Turvey, K.; Bowley, H. J.; Gerrard, D. L. *J. Coord. Chem.* **1998**, *17*, 255.

107. Ramadan, R. M.; El-Medani, S. M.; Ali, O. A. M.; Mohamed, H. A. *J. Coord. Chem.* **2004**, *57*, 373.

108. Lavini, V.; de Souza Maia, A.; Paulino, I. S.; Schuchardt, U.; de Oliveira W. *Inorg. Chem. Commun.* **2001**, *4*, 582.

109. Miotti, R. D.; de Souza Maia, A.; de Oliveira, W.; Paulino, I. S.; Schuchardt, U. *Quim. Nova* **2002**, *25*, 762.

110. (a) Soini, J.; Backman, A. *Acta Chem. Scand. Ser. B* **1975**, *B29*, 710.

(b) Sato, N. *J. Hetercycl. Chem.* **1983**, *20*, 169.

(c) Minisci, F.; Citterio, A.; Vismara, E.; Giordano, C. *Tetrahedron* **1985**, *41*, 4157.

(d) Hirota, T.; Namba, T.; Sasaki, K. *J. Hetercycl. Chem.* **1987**, *24*, 949.

(e) Kagarlitsky, A. D.; Krichevsky, L. A.; Suvorov, B. V. *Khim.-Farm. Zh.* **1993**, *27*, 45.

(f) Kagarlitskii, A. D.; Krichevskii, L. A.; Amirkhanova, A. K. *Pharm. Chem. J.* **1999**, *33*, 381.

(g) Bendale, P. M.; Khadilkar, B. M. *Synth. Commun.* **2000**, *30*, 1713.

(h) Katritzky, A. R.; He, H.-Y.; Suzuki, K. *J. Org. Chem.* **2000**, *65*, 8210.

(i) Minisci, F.; Recupero, F.; Punta, C.; Gambarotti, C.; Antonietti, F.; Fontana, F.; Pedulli, G. F. *Chem. Commun.* **2002**, *21*, 2496.

(j) Bondareva, V. M.; Andrushkevich, T. V.; Lapina, O. B.; Vlasov, A. A.; Dovlitova, L. S. *React. Kinet. Catal. Lett.* **2003**, *79*, 165.

(k) Bondareva, V. M.; Andrushkevich, T. V.; Lapina, O. B.; Khabibulin, D. F.; Vlasov, A. A.; Dovlitova, L. S.; Burgina, E. B. *Kinet. Catal.* **2004**, *45*, 104.

(l) Khadilkar, B. M.; Madyar, V. R. *Indian J. Chem., Sect B* **2003**, *42B*, 2814.

111. Goher, M. A. S.; Mautner, F. A. *Polyhedron* **2000**, *19*, 601.

112. Maraval, A.; Arquier, D.; Igau, A.; Coppel, Y.; Donnadieu, B.; Majoral, J.-P. *Organometallics* **2001**, *20*, 1716.

113. Schiffer, M.; Scheer, M. *Angew. Chem. Int. Ed.* **2001**, *40*, 3413.

114. (a) Ragogna, P. J.; Burford, N.; D'eon, M.; McDonald, R. *Chem. Commun.* **2003**, 1052.

(b) Burford, N.; D'eon, M.; Ragogna, P. J.; McDonald, R.; Ferguson, M. J. *Inorg. Chem.* **2004**, *43*, 734.

115. Hitchcock, P. B.; Lappert, M. F.; Nycz, J. E. *Chem. Commun.* **2003**, 1142.

116. Twamley, B.; Hardman, N. J.; Power, P. P. *Acta Crystallogr., Sect. E* **2001**, *57*, m227.

117. (a) Jones, C. *Coord. Chem. Rev.* **2001**, *215*, 151 and references therein.

(b) Opris, L. M.; Silvestru, A.; Silvestru, C.; Breuning, H. J.; Lork, E. *Dalton Trans.* **2003**, 4367.

(c) Opris, L. M.; Silvestru, A.; Silvestru, C.; Breuning, H. J.; Lork, E. *Dalton Trans.* **2004**, 3575.

(d) Ferguson, G.; Harris, G. S.; Khan, A. *Acta Crystallogr., Sect. C* **1987**, *43*, 2078.

(e) Balázs, L.; Breuning, H. J.; Ghesner, I.; Lork, E. *J. Organomet. Chem.* **2002**, *648*, 33.

118. (a) Weber, L. *Angew. Chem., Int. Ed.* **2002**, *41*, 563.

(b) Nyulászi, L. *Chem. Rev.* **2001**, *101*, 1229.

(c) van Assema, S. G. A.; Ehlers, A. W.; de Kanter, F. J. J.; Schakel, M.; Spek, A. L.; Lutz, M.; Lammertsma, K. *Chem. Eur. J.* **2006**, *12*, 4333.

119. Lesikar, L. A.; Richards, A. F. *J. Organomet. Chem.* **2006**, *691*, 4250.

120. (a) Bai, G.; Wei, P.; Stephan, D. W. *Organometallics* **2006**, *25*, 2649.

(b) Bulls, A. R.; Schaefer, W. P.; Serfas, M.; Bercaw, J. E. *Organometallics* **1987**, *6*, 1219.

(c) Riley, P. N.; Parker, J. R.; Fanwick, P. E.; Rothwell, I. P. *Organometallics* **1999**, *18*, 3579.

(d) Bai, G.; Wei, P.; Stephan, D. W. *Organometallics* **2005**, *24*, 5901.

121. Gushwa, A. F.; Richards, A. F. *Eur. J. Inorg. Chem.* **2008**, 728.

122. Clegg, W.; Elsegood, M. R. J.; Graham, V.; Norman, N. C.; Pickett, N. L.; Tavakkoli, K. *J. Chem. Soc., Dalton Trans.* **1994**, 1743.

123. (a) Survey of CCDC, 2006.

(b) Genge, A. R. J.; Hill, N. J.; Levason, W.; Reid, G. *J. Chem. Soc., Dalton Trans.* **2001**, 1007.

124. Vidović, D. *The Chemistry of β-Diketiminate-Supported Boron, Aluminum, Gallium, and Phosphorus Compounds*, Ph.D. Dissertation, University of Texas Austin, **2007**.

125. (a) Gushwa, A. F.; Karlin, J. G.; Fleischer, R. A.; Richards, A. F. *J. Organomet. Chem.* **2006**, *691*, 5069.

(b) Gushwa, A. F.; Karlin, J. G.; Fleischer, R. A.; Richards, A. F. *J. Organomet. Chem.* **2007**, *692*, 1173.

126. Reeske, G.; Cowley, A. H. *Chem. Commun.* **2006**, 1784.

127. Reeske, G.; Hoberg, C. R.; Hill, N. J.; Cowley, A. H. *J. Am. Chem. Soc.* **2006**, *128*, 2800.

128. Vidovic, D.; Lu, Z.; Reeske, G.; Moore, J. A.; Cowley, A. H. *Chem. Commun.* **2006**, 3501.

129. Green, M. L. H.; Mountford, P.; Smout, G. J.; Speel, S. R. *Polyhedron* **1990**, *9*, 2763.

130. a) G. M. Sheldrick, SHELXS-97, Program for the solution of crystal structures; University of Göttingen: Germany, 1997.

b) G. M. Sheldrick, SHELXL-97, Program for the refinement of crystal structures.

131. Cowley, A. H. *J. Organomet. Chem.* **2004**, *689*, 3866.

132. Burford, N.; Macdonald, C. L. B.; Parks, T. M.; Wu, G.; Borecka, B.; Kwiatkowski, W.; Cameron, T. S. *Can. J. Chem.* **1996**, *74*, 2209.

133. Lesikar, L. A.; Woodul, W. D.; Richards, A. F. *Polyhedron* **2007**, *26*, 3242.

134. Lu, Z.; Reeske, G.; Moore, J. A.; Cowley, A. H. *Chem. Commun.* **2006**, 5060.

135. Lu, Z.; Findlater, M.; Cowley, A. H. *Chem. Commun.* **2007**, 2873.

136. Lu, Z.; Findlater, M.; Cowley, A. H. *Chem. Commun.* **2008**, 184.

137. Hitchcock, P. B.; Lappert, M. F.; Li, G.; Protchenko, A. V. *Chem. Commun.* **2007**, 846.

138. (a) Zouari, F.; Ben Salah, A. *Phase Transitions* **2005**, *78*, 317.

(b) Bigoli, F.; Lanfranchi, M.; Pellinghelli, M. A. *Inorg. Chim. Acta* **1984**, *90*, 215.

139. Boardman, B. M.; Valderrama, J. M.; Muñoz, F.; Wu, G.; Bazan, G. C.; Rojas, R. *Organometallics* **2008**, *27*, 1671.

140. Allen, S. D.; Moore, D. R.; Lobkovsky, E. B.; Coates, G. W. *J. Organomet. Chem.* **2003**, *683*, 137.

141. Hsu, S.-H.; Chang, J.-C.; Lai, C.-L.; Hu, C.-H.; Lee, H. M.; Lee, G.-H.; Peng, S.-M.; Huang, J.-H. *Inorg. Chem.* **2004**, *43*, 6786.

142. Hsu, S.-H.; Li, C.-Y.; Chiu, Y.-W.; Chiu, M.-C.; Lien, Y.-L.; Kuo, P.-C.; Lee, H. M.; Huang, J.-H.; Cheng, C.-P. *J. Organomet. Chem.* **2007**, *692*, 5421.

143. Lyashenko, G.; Saischek, G.; Pal, A.; Herbst-Irmer, R.; Mösch-Zanetti, N. C. *Chem. Commun.* **2007**, 701.

144. Gussenhoven, E. M.; Olmstead, M. M.; Fettinger, J. C.; Balch, A. L. *Inorg. Chem.* **2008**, *47*, 4570.

145. Kuo, P.-C.; Chen, I.-C.; Chang, J.-C.; Lee, M.-T.; Hu, C.-H.; Hung, C.-H.; Lee, H. M.; Huang, J.-H. *Eur. J. Inorg. Chem.* **2004**, 4898.

146. Kuo, P.-C.; Chen, I.-C.; Lee, H. M.; Hung, C.-H.; Huang, J.-H. *Inorg. Chim. Acta* **2005**, *358*, 3761.

147. Lee, W.-Y.; Hsieh, H.-H.; Hsieh, C.-C.; Lee, H. M.; Lee, G.-H.; Huang, J.-H.; Wu, T.-C.; Chuang, S.-H. *J. Organomet. Chem.* **2007**, *692*, 1131.

148. Macedo, F. P.; Gwengo, C.; Lindeman, S. V.; Smith, M. D.; Gardinier, J. R. *Eur. J. Inorg. Chem.* **2008**, 3200.

149. Kao, J.-M.; Ho, S.-M.; Chen, I.-C.; Kuo, P.-C.; Lin, C.-Y.; Tu, C.-Y.; Hu, C.-H.; Huang, J.-H.; Lee, G.-H. *Inorg. Chim. Acta* **2008**, *361*, 2792.

150. Wu, J.; Yu, T.-L.; Chen, C.-T.; Lin, C.-C. *Coord. Chem. Rev.* **2006**, *250*, 602.

151. (a) Orita, A.; Mitsutome, A.; Otera, J. *J. Org. Chem.* **1998**, *63*, 2420.

(b) Orita, A.; Sakamoto, A.; Hamada, Y.; Mitsutome, A.; Otera, J. *Tetrahedron* **1999**, *55*, 2899.

(c) Espinet, P.; Echavarren, A. M. *Angew. Chem., Int. Ed.* **2004**, *43*, 4704.

(d) Gielen, M. *Coord. Chem. Rev.* **1996**, *151*, 41.

(e) Willem, R.; Dalil, H.; Broekaert, P.; Biesemans, M.; Gyhs, L.; Nooter, K.; de Vos, D.; Ribot, F.; Gielen, M. *Main Group Met. Chem.* **1997**, *20*, 535.

(f) Höti, N.; Ma, J.; Tabassum, S.; Wang, Y.; Wu, M. *J. Biochem.* **2003**, *134*, 521.

(g) Tabassum, S.; Pettinari, C. *J. Organomet. Chem.* **2006**, *691*, 1761.

152. Dudek, G. O.; Dudek, E. P. *Inorg. Chim. Acta* **1974**, *8*, 219.
153. Costes, J.-P.; Serra, J.-F.; Dahan, F.; Laurent, J.-P. *Inorg. Chem.* **1986**, *25*, 2790.
154. Costes, J.-P.; Dahan, F.; Laurent, J.-P. *Inorg. Chem.* **1991**, *30*, 1887.
155. Bonnet, M.-L.; Aronica, C.; Chastanet, G.; Pilet, G.; Luneau, D.; Mathonière, C.; Clérac, R.; Robert, V. *Inorg. Chem.* **2008**, *47*, 1127.
156. Becht, M.; Gerfin, T.; Dahmen, K.-H. *Helv. Chim. Acta* **1994**, *77*, 1288.
157. Sato, T.; Takeda, H.; Sakai, K.; Tsubomura, T. *Inorg. Chim. Acta* **1996**, *246*, 413.
158. Zhao, Q.; Cao, W.-L.; Yang, Z.-Y.; Zhang, J.-C. *Beijing Huagong Daxue Xuebao, Ziran Kexueban* **2005**, *32*, 68-71, 93.
159. (a) Sadique, A. R.; Brennessel, W. W.; Holland, P. L. *Inorg. Chem.* **2008**, *47*, 784.

(b) Spielmann, J.; Harder, S. *Chem. Eur. J.* **2007**, *13*, 8928.

(c) Bai, G.; Wei, P.; Das, A. K.; Stephan, D. W. *Dalton Trans.* **2006**, *9*, 1141.

(d) MacAdams, L. A.; Buffone, G. P.; Incarvito, C. D.; Rheingold, A. L.; Theopold, K. H. *J. Am. Chem. Soc.* **2005**, *127*, 1082.

160. Lesikar, L. A.; Gushwa, A. F.; Richards, A. F. *J. Organomet. Chem.* **2008**, *693*, 3245.
161. (a) di Bianca, F.; Rivarola, E.; Spek, A. L.; Meinema, H. A.; Noltes, J. G. *J. Organomet. Chem.* **1973**, *63*, 293.

(b) Turner, L. E.; Davidson, M. G.; Jones, M. D.; Ott, H.; Schulz, V. S.; Wilson, P. J. *Inorg. Chem.* **2006**, *45*, 6123.

162. Cambridge Crystallographic Database Centre elemental radii table.

163. (a) Neumayer, D. A.; Cowley, A. H.; Decken, A.; Jones, R. A.; Lakhotia, V.; Ekedrt, J. G. *J. Am. Chem. Soc.* **1995**, *117*, 5893.

(b) Fischer, R. A.; Sussek, H.; Miehr, A.; Pritzkow, H.; Herdtweck, E.; *J. Organomet. Chem.* **1997**, *548*, 73.

(c) Kim, J.; Bott, S. G.; Hoffmann, D. M. *J. Chem. Soc., Dalton Trans.* **1999**, 141.

164. (a) Avaritsiotis, J. N.; Howson, R. P. *Thin Solid Films* **1980**, *80*, 63.

(b) Wang, A.; Dai, J.; Cheng, J.; Chudzik, M. P.; Marks, T. J.; Chang, R. P. H.; Kannewurf, C. R. *Appl. Physics Letters* **1998**, *73*, 327.

165. (a) Nomura, R.; Inazawa, S.; Matsuda, H.; Saieki, S. *Polyhedron* **1987**, *6*, 507.

(b) Maruyama, T.; Fukui, K. J. *J. Appl. Phys.* **1991**, *70*, 3848.

(c) Reich, S.; Suhr, H.; Waimer, B. *Thin Solid Films* **1990**, *189*, 293.

166. (a) Lewiński, J.; Zachara, J.; Starowieyski, K. B. *J. Chem. Soc., Dalton Trans.* **1997**, 4217.

(b) Lewiński, J.; Zachara, J.; Kopeć, T.; Starowieyski, K. B.; Lipowski, J.; Justyniak, I.; Kolodziejczyk, E. *Eur. J. Inorg. Chem.* **2001**, 1123.

(c) Lewiński, J.; Zachara, J.; Justyniak, I. *Organometallics* **1997**, *16*, 4597.

167. Khan, M.; Steevensz, R. C.; Tuck, D. G.; Noltes, J. G.; Corfield, P. W. R. *Inorg. Chem.* **1980**, *19*, 3407.

168. (a) Hill, M. S.; Hitchcock, P. B. *Chem. Commun.* **2004**, 1818.

(b) Stender, M.; Power, P. P. *Polyhedron* **2002**, *21*, 525.

(c) Hill, M. S.; Hitchcock, P. B.; Pongtavornpinyo, P. *Dalton Trans.* **2007**, 731.

169. Su, Q.; Wu, Q.-L.; Li, G.-H.; Liu, X.-M.; Mu, Y. *Polyhedron* **2007**, *26*, 5053.
170. Ambrosi, G.; Boggioni, A.; Formica, M.; Fusi, V.; Giorgi, L.; Lucarini, S.; Micheloni, M.; Secco, F.; Venturini, M.; Zappia, G. *Dalton Trans.* **2005**, 485.
171. (a) Farwell, J. D.; Hitchcock, P. B.; Lappert, M. F.; Luintra, G. A.; Protechenko, A. V.; Wei, X.-H. *J. Organomet. Chem.* **2008**, *693*, 1861.

(b) Doyle, D. J.; Gibson, V. C.; White, A. J. P. *Dalton Trans.* **2007**, 358.

(c) Hunger, J.; Blaurock, S.; Sieler, J. *Z. Anorg. Allg. Chem.* **2005**, *631*, 472.

172. Basuli, F.; Huffmann, J. C.; Mindiola, D. J. *Inorg. Chem.* **2003**, *42*, 8003.
173. van der Steen, F. H.; Boersma, J.; Speak, A. L.; von Koten, G. *Organometallics* **1991**, *10*, 2467.
174. Haaland, A. *Angew. Chem. Int. Ed. Engl.* **1989**, *28*, 992.
175. Geerts, R. L.; Huffman, J. C.; Caulton, K. G. *Inorg. Chem.* **1986**, *25*, 590.
176. (a) Vela, J.; Zhu, L.; Flaschenriem, C. J.; Brennessel, W. W.; Lachicotte, R. J.; Holland, P. L. *Organometallics* **2007**, *26*, 3416.

(b) Prust, J.; Stasch, A.; Zheng, W.; Roesky, H. W.; Alexopoulos, E.; Uson, I.; Boehler, D.; Schuchardt, T. *Organometallics* **2001**, *20*, 3825.

177. (a) Shearer, H. M. M.; Spencer, C. B. *J. Chem. Soc. Chem. Commun.* **1966**, 194a.

(b) Shearer, H. M. M.; Spencer, C. B. *Acta Cryst. Sect. B.* **1980**, *B36*, 2046.

(c) Noltes, J. G.; Boerma, J. J. *J. Organomet. Chem.* **1968**, *12*, 425.

(d) Olmstead, M. M.; Power, P. P.; Shoner, S. C. *J. Am. Chem. Soc.* **1991**, *113*, 3379.

178. He, Z.; He, C.; Wang, Z.-M.; Gao, E.-Q.; Liu, Y.; Yan, C.-H. *Dalton Trans.* **2004**, 502.

179. van der Sluis, P.; Spek, A. L. *Acta Cryst. Sect. A*. **1990**, *46*, 194.

180. Gottlieb, H. E.; Kotlyar, V.; Nudelman, A. *J. Org. Chem.* **1997**, *62*, 7512.

181. Cotton, F. A.; Daniels, L. M.; Falvello, L. R.; Matonic, J. H.; Murillo, C. A.; Wang, X.; Zhou, H. *Inorg. Chim. Acta* **1997**, *266*, 91.

182. Cole, M. L.; Evans, D. J.; Junk, P. C.; Louis, L. M. *New J. Chem.* **2002**, *26*, 1015.

183. Nimitsiriwat, N.; Gibson, V. C.; Marshall, E. L.; Takolpuckdee, P.; Tomov, A. K.; White, A. J. P.; Williams, D. J.; Elsegood, M. R. J.; Dale, S. H. *Inorg. Chem.* **2007**, *46*, 9988.

184. (a) Beck, W. F.; Brudvig, G. W. *J. Am. Chem. Soc.* **1988**, *110*, 1517.

(b) Wieghardt, K. *Angew. Chem. Int. Ed. Engl.* **1989**, *28*, 1153.

(c) Beyer, W. F.; Fridovich, I. *Biochemistry* **1985**, *24*, 6460.

185. Jacobsen, H.; Cavallo, L. *Chem. Eur. J.* **2001**, *7*, 800.

186. (a) Wang, S.; Li, H.-W.; Xiem, Z. *Organometallics* **2004**, *23*, 2469.

(b) Eckert, N. A.; Smith, J. M.; Lachicotte, R. J.; Holland, P. L. *Inorg. Chem.* **2004**, *43*, 3306.

(c) Langley, S.; Helliwell, M.; Raftery, J.; Tolis, E. I.; Winpenny, R. E. P. *Chem. Commun.* **2004**, 142.

(d) Roesky, P. W. *Organometallics* **2002**, *21*, 4756.

187. (a) Wang, D.; Wang, M.; Wang, X.; Zhang, R.; Ma, J.; Sun, L. *J. Mol. Catal. A: Chem.* **2007**, *270*, 278.

(b) Panda, A.; Stender, M.; Wright, R. J.; Olmstead, M. M.; Klavins, P.; Power, P. P. *Inorg. Chem.* **2002**, *41*, 3909.

188. Cole, M. L.; Jones, C.; Junk, P. C.; Kloth, M.; Stasch, A. *Chem. Eur. J.* **2005**, *11*, 4482.
189. Brazeau, A. L.; DiLabio, G. A.; Kreisel, K. A.; Monillas, W.; Yap, G. P. A.; Barry, S. T. *Dalton Trans.* **2007**, 3297.
190. Rowley, C. N.; DiLabio, G. A.; Barry, S. T. *Inorg. Chem.* **2005**, *44*, 1983.
191. Abeysekera, D.; Robertson, K. N.; Cameron, T. S.; Clyburne, J. A. C. *Organometallics* **2001**, *20*, 5532.
192. Münch, M.; Flörke, U.; Bolte, M.; Schulz, S.; Gudat, D. *Angew. Chem. Int. Ed.* **2008**, *47*, 1512 and references cited therein.
193. Schmidt, J. A. R.; Arnold, J. *Organometallics* **2002**, *21*, 2306 and references cited therein.
194. Coles, M. P.; Hitchcock, P. B. *Eur. J. Inorg. Chem.* **2004**, 2662.
195. Minghetti, G.; Banditelli, G.; Bonati, F. *Inorg. Chim. Acta* **1975**, *12*, 85.
196. Bond, A. D.; Linton, D. J.; Schooler, P.; Wheatley, A. E. H. *J. Chem. Soc., Dalton Trans.* **2001**, 3173.
197. Lesikar, L. A.; Richards, A. F. **2008**, Submitted Article.
198. Jones, C.; Junk, P. C.; Kloth, M.; Proctor, K. M.; Stasch, A. *Polyhedron* **2006**, *25*, 1592.
199. Selected examples include:

(a) Stender, M.; Eichler, B. E.; Hardman, N. J.; Power, P. P.; Prust, J.; Noltemeyer, M.; Roesky, H. W. *Inorg. Chem.* **2001**, *40*, 2794.

(b) Wright, R. J.; Phillips, A. D.; Power, P. P. *J. Am. Chem. Soc.* **2003**, *125*, 10784.

(c) Wright, R. J.; Brynda, M.; Power, P. P. *Angew. Chem. Int. Ed.* **2006**, *45*, 5953.

200. Buijink, J.-K.; Noltemeyer, M.; Edelmann, F. T. *Z. Naturforsch. B* **1991**, *46*, 1328.

201. (a) Resa, I.; Carmona, E.; Cutierrez-Puebla, E.; Monge, A. *Science* **2004**, *305*, 1136.

(b) del Río, D.; Galindo, A.; Resa, I.; Carmona, E. *Angew. Chem. Int Ed.* **2005**, *44*, 1244.

202. Wang, Y.; Quillion, B.; Wei, P.; Wang, H.; Yang, X.-J.; Xie, Y.; King, R. B.; Schleyer, P. v. R.; Schaefer III, H. F.; Robinson, G. H. *J. Am. Chem. Soc.* **2005**, *127*, 11944.

203. Sekizaki, M.; Yamasaki, K. *Rev.Chim. Miner.* **1969**, *6*, 255.

204. (a) Sekizaki, M. *Acta Cryst.* **1973**, *B29*, 327.

(b) Sekizaki, M. *Acta Cryst.* **1974**, *B30*, 253.

205. Tenhunen, A.; Bergman, M. *Finn. Chem. Lett.* **1974**, *1*, 31.

206. Singh, P. P.; Shukla, U. P.; Seth, J. N. *Indian J. Chem., Sect. A* **1975**, *14A*, 158.

207. Singh, P. P.; Seth, J. N. *Inorg. Nucl. Chem. Lett.* **1975**, *11*, 525.

208. Singh, P. P.; Seth, J. N. *J. Inorg. Nucl. Chem.* **1975**, *37*, 593.

209. Eckberg, R. P.; Hatfield, W. E. *J. Chem. Soc., Dalton Trans.* **1975**, 616.

210. Sanyal, G. S.; Modak, A. B.; Mudi, A. K. *Indian J. Chem., Sect. A* **1982**, *21A*, 1044.

211. Sileo, E. E.; García Posse, M. G.; Morando, P. J.; Blesa, M. A. *Polyhedron* **1987**, *6*, 1757.

212. Segl'a, P.; Palicová, M. *Synth. React. Inorg. Met.-Org. Chem.* **1999**, *29*, 1843.

213. Tanase, S.; Gallego, P. M.; Bouwman, E.; de Gelder, R.; Reedijk, J. *Inorg. Chem. Commun.* **2005**, *8*, 680.

214. You, Y.; Park, S. Y. *J. Am. Chem. Soc.* **2005**, *127*, 12438.

215. Akyuz, S.; Andreeva, L.; Minceva-Sukarova, B.; Basar, G. *J. Mol. Struct.* **2007**, *834*, 399.

216. Miotti, R. D.; de Souza Maia, A.; Rodrigues, J. G.; de Oliveira, W. *Inorg. Chem. Commun.* **2006**, *9*, 228.

217. Ahuja, I. S.; Yadava, C. L.; Tripathi, S. *Indian J. Chem., Sect. A* **1988**, *27A*, 171.

218. O'Brian, P.; Haggata, S. *Adv. Mater. Optics Electron.* **1995**, *5*, 117.

219. Ellsworth, J. M.; zur Loye, H.-C. *Dalton Trans.* **2008**, 5823.

220. Shrivastava, S.; Gupta, P. K. *Asian J. Chem.* **1999**, *11*, 424.

221. (a) Gysling, H. J.; Wernberg, A. A. *Chem. Mater.* **1992**, *4*, 900.

(b) Cheon, J.; Arnold, J.; Yu, K.-M.; Bourret, E. D. *Chem. Mater.* **1995**, *7*, 2273.

222. Stoll, S. L.; Bott, S. G.; Barron, A. R. *Dalton Trans.* **1997**, 1315.

223. Zhou, Y.; Richeson, D. S. *Inorg. Chem.* **1996**, *35*, 2448.

224. Singh, S.; Ahn, H.-J.; Stasch, A.; Jancik, V.; Roesky, H. W.; Pal, A.; Biadene, M.; Herbst-Irmer, R.; Noltemeyer, M.; Schmidt, H.-G. *Inorg. Chem.* **2006**, *45*, 1853.

225. Dutton, J. L.; Tabeshi, R.; Jennings, M. C.; Lough, A. J.; Ragogna, P. J. *Inorg. Chem.* **2007**, *46*, 8594.

226. Otter, A. NMR Spectroscopy: NMR News 2005–03. http://nmr.chem.ualberta.ca/ (September 8, 2008).

227. Samanamú, C. R.; Richards, A. F. *Polyhedron* **2007**, *26*, 923.

228. Samanamú, C. R.; Lococo, P. M.; Richards, A. F. *Inorg. Chim. Acta* **2007**, *360*, 4037.

VITA

Leslie Lesikar was born October 1, 1982 in Fort Worth, Texas. She is the daughter of Lyn and Harriet Lesikar. In 2001, she graduated with honors from Western Hills High School in Fort Worth, Texas. She then went to receive a Bachelor of Science degree in chemistry from Texas Christian University, in 2005, graduating *magna cum laude* and was awarded the Senior Scholar Award in chemistry.

In August 2005, she enrolled in Texas Christian University to pursue her doctorate in Inorganic Chemistry under the direction of Dr. Anne F. Richards. During this time, she worked as a Graduate Teaching Assistant for four semesters and was awarded the Graduate Student Teaching Award from the Department of Chemistry in the fall of 2006.

ABSTRACT

THE SYNTHESIS AND STRUCTURAL CHARACTERIZATION OF MAIN GROUP AND TRANSITION METAL COMPLEXES SUPPORTED BY NITROGEN BASED LIGANDS

by

Leslie A. Lesikar, Ph.D., 2008
Department of Chemistry
Texas Christian University

Dissertation Advisor: Anne F. Richards, Assistant Professor

Nitrogen based monodentate and bidentate chelating ligands have captured a significant interest due to their ability to coordinate to a wide variety of elements. The β-diketimine, β-ketoiminato, formamidine, pyridineselenolate, and pyrazinecarboxamide ligands have all been employed in this study to further investigate the coordination preferences among main group and transition metals. Steric and electronic properties of these ligands can easily be altered by manipulating the substituents attached, thus leading to predictable structures with potential for many useful and significant applications. Investigations have shown that temperature, solvent, and metal halide employed are all key factors in the reaction outcomes. All of the complexes obtained throughout these studies have been characterized by X-ray crystallography along with other spectroscopic techniques, including NMR, IR, UV/Vis, and M/S.

β-diketiminato ligands, $[\{N(R)C(Me)\}_2C(H)]^-$ where R = Dipp, Mes, commonly referred to as nacnac, have played an important role in the synthesis of novel pnictogenium complexes. Results show that through manipulation of the halide precursor,

reaction stoichiometry, and the R substituent on the nacnac both N,N'- and N,C'-metal chelated complexes can be achieved.

Additionally, β-ketiminato ligands, [RN(H)(C(Me))$_2$C(Me)=O] where R = Dipp, and [RN(H)C(Me)CHC(Me)=O] where R = $C_2H_4NEt_2$, have been studied. Both ligands were investigated with a range of d and p block metal halides and alkyls in order to compare and contrast the bulky, flexible, and even multi-dentate nature of each ligand. The preferred metal geometry remains constant for products with either ligand, but the steric protection offered by the individual ligands governs the nuclearity of the products, ranging from tetrameric cages to simple adducts.

The formamidinate ligand, [RN(H)C(H)NR] where R = Dipp, was employed in synthesizing several aluminum and zinc complexes. In addition to their numerous applications as catalysts, the smaller ligand backbone is capable of N,N'-chelation analogously to the β-diketiminates and β-ketiminato ligands, as well as a variety of other coordination modes. The stoichiometric ratio of ligand to the metal alkyl was emphasized for these reactions affording aluminum and zinc formamidinate complexes exhibiting monodentate, bidentate, and bridging coordination modes.

Lastly, the coordination of group 13 metal halides was investigated employing the pyridineselenolate, [HSe-2-NC_5H_4], and pyrazinecarboxamide, [($C_4H_3N_2$)$CONH_2$], ligands. The research focused on the individual synthetic methods in the preparation of group 13 complexes.